17th International Conference on Ternary and Multinary Compounds

ICTMC-17

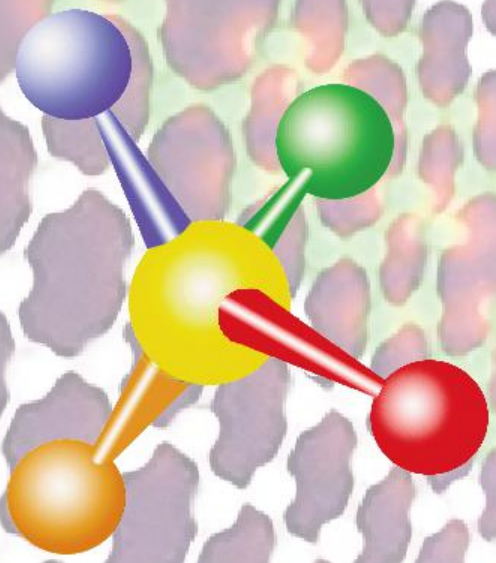

www.science.gov.az/physics

27-30 September, 2010

Institute of Physics
Azerbaijan National Academy of Sciences
Baku

ICTMC17
Baku 2010

17th International Conference on Ternary and Multinary Compounds

ABSTRACTS

27-30 September, 2010

Institute of Physics
Azerbaijan National Academy of Sciences
Baku

SPONSOR:

H. A. Aliyev Foundation

CO-SPONSORS:

Azerbaijan Ministry of Communications and Information Technologies

Japan Society of Applied Physics

Azerbaijan Ministry of Education

Azerbaijan National Academy of Sciences

Bruker Corporation

ICTMC HISTORY



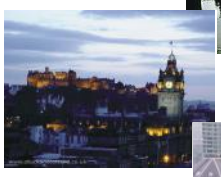




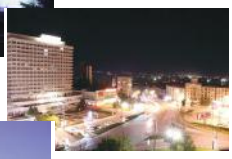



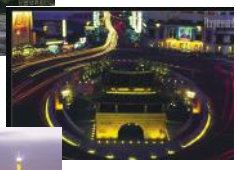
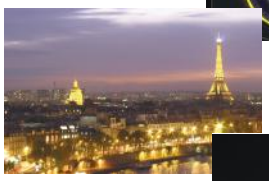
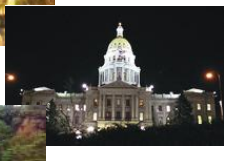


1973 Bath (United Kingdom)

1975 Strasbourg (France)

1977 Edinburgh (United Kingdom)

1980 Tokyo (Japan)

1982 Cagliari (Italy)

1984 Caracas (Venezuela)

1986 Snowmass, Colorado (USA)

1990 Kishinev (Former Soviet Union)

1993 Yokohama (Japan)

1995 Stuttgart (Germany)

1997 Salford (United Kingdom)

2000 Hsin-chu (Taiwan)

2002 Paris (France)

2004 Denver, Colorado (USA)

2006 Kyoto (Japan)

2008 Berlin (Germany)

2010 Baku (Azerbaijan)

International Advisory Committee (IAC)

S. Schorr (Germany), chair
T. Wada (Japan)
S. Deb (USA)
J. F. Guillemoles (France)
H. L. Hwang (Taiwan)
S. Iida (Japan)
N. Joshi Venezuela)
L. Kazmerski (USA)
C. D. Kim (Korea)
M. Leon (Spain)
D. Lincot (France)
E. Rogatcheva (Ukrain)
K. Sato (Japan)
H. W. Schock (Germany)
C. Schwab (France)
I. Tiginyanu (Moldova)
A. N. Tiwari (Switzerland and UK)
A. Zunger (USA)
D. Abou-Ras (Germany)
T. Matsumoto (Japan)

Honorary IAC Members

T. Arai (Japan)
D. Cahen (Israel)
R. Feigelson (USA)
K. Masumoto (Japan)
F. Meloni (Italy)
Xu Xu Rong (China)
R. D. Tomlinson (UK)
H. Y. Park (Korea)

Chairs

Arif Pashaev (Azerbaijan)
Nazim Mamedov (Azerbaijan)

Organizing Committee

Oktay Alekperov (Azerbaijan)
Ayaz Bayramov (Azerbaijan)
Emil Huseynov (Azerbaijan)
Daniel Lincot (France)
Nazim Mamedov (Azerbaijan)
Tofiq Q. Mammadov (Azerbaijan)
Talat Mehdiyev (Azerbaijan)
Sener Oktik (Turkey)
Elena Rogacheva (Ukraine)
Katsuaki Sato (Japan)
Sho Shirakata (Japan)
Kazuki Wakita (Japan)
Conference Secretaris: Eldar Mammadov (Azerbaijan)
Ismail Yusifov (Azerbaijan)

Program Committee

Chingiz Qajar (chair), Nadir Abdullayev, Sevda Abdullayeva, Seiji Akita, Kerim Allakhverdiev, Oktay Alekperov, Bahram Askerov, Gregory Belenky, Satyen Deb, Norifumi Fujimura, Jean F. Guillemoles, Firudin Hashimzade, Rauf Huseynov, Hiromichi Horinaka, Hajime Ishihara, Takekazu Ishida, Yosuke Kayanuma, Maximo Leon, Nazim Mamedov, Takashi Matsumoto, Arzu Najafov, Sener Oktik, Huseyn Orujev, Susan Schorr, Claude Schwab, Nozomu Tsuboi, Hisao Uchiki, Naotaka Uchitomi, Takahiro Wada, Kazuki Wakita, Nobuyuki Yamamoto, and Kenji Yoshino

6 Invited Speakers

Tutorial Session

Superconductor-insulator transition and localized electron pairs
Vsevolod F. Gantmakher (Institute of Solid State Physics, Chernogolovka, Russia)

Introduction to nanotechnology based on carbon nanotubes
Yoshikazu Nakayama (Osaka University, Japan)

Opto-electronic devices fabricated by printing technology: light emitting diodes, thin film transistors and solar cells
Hiroyoshi Naito (Osaka Prefecture University, Japan)

Spintronics for next generation innovative devices
Katsuaki Sato (Japan Science and Technology Agency, Japan.)

Neutrons and photons in photovoltaic materials research
Susan Schorr (Free University Berlin, Germany)

Regular Sessions

Anisotropic physical properties in sulfosalt structures
Herbert Dittrich (University Salzburg, Austria)

Raman and X-ray diffraction studies of ternary chalcogenides at ambient and high pressure
Hans D. Hochheimer (Colorado University, USA)

Ab initio design of new generation superalloys
Eyvaz Isaev (Linkoping University, Sweden)

Radiative properties of halogen intercalated transition metal dichalcogenide layered crystals
Leonid Kulyuk (Institute of Applied Physics, Moldova)

Pressure dependence of the bandgap, lattice parameters, and pressure-induced phase transitions in AIIB2IIIC4VI compounds
Francisco Javier Manjon (Universidad Politecnica de Valencia, Spain)

Electronic structure of ternary chain Tl chalcogenides studied by photoemission spectroscopy
Kojiro Mimura (Osaka Prefecture University, Japan)

Interplay of spin-orbital interactions in a quasi-two-dimensional electron gas with finite thickness under in-plane magnetic field
Enver Nakhmedov (Universitat Wurzburg, Germany; Insitute of Physics, Azerbaijan)

The phonon percolation scheme for alloys: Pressure-dependence and extension to the whole lattice dynamics
Olivier Pages (Universite de Metz, France)

Mechanism of "controlled atomic defects": Extension to the ternary systems
Elena Rogacheva (National Technical University, Kharkov, Ukraine)

Thermoelectric Functions in Clathrates
Peter Rogl (Vienna University, Austria)

Chalcopyrite solar cells: Formation of the buffer / absorber interface and related transport mechanisms
Marin Rusu (Helmholtz Center for Materials and Energy, Berlin, Germany)

High-pressure studies of iron-based superconductors
Hiroki Takahashi (Nihon University, Japan)

Effect of REE co-doping on the Mn red emission in Ca and Sr Thiogallates
Takeo Takizawa (Nihon University, Japan)

Microwave surface impedance and complex conductivity of organic and multizone superconductors
Mikhail Trunin (Institute of Solid State Physics, Chernogolovka, Russia)

Epitaxial graphene on SiC
Thomas Seyller (Friedrich-Alexander-Universitut, Erlangen-Nurnberg, Germany)

Self-consistent GW and Bethe-Salpeter equation: applications to optoelectronic properties of multinary compounds
Julien Vidal (Ecole Polytechnique, France)

Theoretical investigation of quaternary chacogenides for solar cell
Su-Huai Wei (NREL,USA)

TOPICS

Growth and preparation techniques; bulk materials, thin films, nanostructured materials, nanoscale structures

Characterization techniques, including large scale facilities

Temperature and pressure induced phase transitions, superconductivity

Electron and phonon spectra :
ab-initio calculations and experiment

Computational material design and modeling at the nanoscale

Light emitting materials and devices

Photovoltaic, thermoelectric and multiferroic materials and applications

Misscellaneous

SECTION ONE

Growth and preparation techniques; bulk materials, thin films, nanostructured materials, nanoscale structures

I1-1

Epitaxial graphene on SiC(0001): growth, electronic structure, and interface engineering

Thomas Seyller

Friedrich-Alexander-Universität Erlangen-Nürnberg, Lehrstuhl für Technische Physik, Erwin-Rommel-Str. 1, 91058 Erlangen, Germany
Phone: +49-9131-8528335; FAX: +49-9131-8527889; Email: thomas.seyller@physik.uni-erlangen.de
Thomas.Seyller@physik.uni-erlangen.de

Graphene is a two-dimensional crystal comprised of carbon atoms in a honeycomb structure. Since the observation of the half-integer, chiral quantum Hall effect [1] in graphene, many researcher have been inspired to study the fascinating properties of this material, which also promises new applications [2].
Epitaxial growth of graphene on SiC surfaces by solid state decomposition is most promising for the development of graphene-based electronic devices [3]. Graphene can be grown the Si-terminated SiC(0001) surface and the C-terminated SiC(000-1) surface. The resulting layers are different in several aspects [4] as shown in fig. 1. The SiC(0001) yields monolayers and bilayers which are aligned with respect to the substrate and with respect to each other. Growth on SiC(000-1) results in many graphene layers which are rotated against each other. The mutual rotation restores the linear dispersion at the K-point for each layer [5].
In the first part of my talk I will discuss the electronic structure and structural properties of graphene on SiC(0001) grown in the traditional way in UHV [6]. In the second part I will show how the growth of graphene can be improved by going from the traditional growth environment to an environment with an Argon atmosphere [7]. Finally I will demonstrate, how epitaxial graphene can be manipulated by transfer doping using molecular adsorbates [8] or by the intercalation of hydrogen [9].

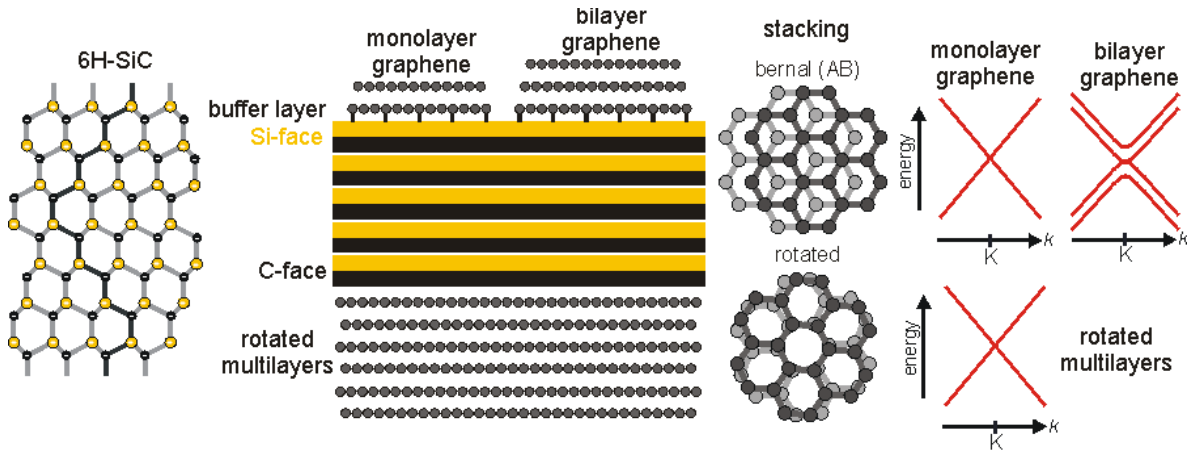

Figure 1. Some properties of epitaxial graphene (EG) on SiC(0001) and SiC(000-1). EG on the Si-face is aligned with respect to the substrate and is situated on a buffer layer. Bilayer graphene exhibits AB stacking with parabolic bands. On the C-face multilayers are formed in which the graphene sheets are rotated against each other which restores the linear dispersion at the K-point.

[1]. K. S. Novoselov, et al., Nature **438** (2005) p. 197; Y. B. Zhang, et al., Nature **438** (2005) p. 201.
[2]. A. K. Geim and K.S. Novoselov, Nat. Mater. **6** (2007) p. 183; A. K. Geim, Science **324** (2009) p. 1530.
[3]. C. Berger, et al., J. Phys. Chem. B **108** (2004) p. 19912; C. Berger, et al., Science **312** (2006) p. 1191.
[4]. P.N. First, et al., MRS Bulletin **35** (2010) p. 296; K. V. Emtsev, et al., Phys. Rev. B **77** (2008) 155303.
[5]. S. Shallcross, Phys. rev. Lett. 101 (2008) 056803; S. Shallcross, Phys. Rev. B **81** (2010) 165105;
[6]. A. Bostwick, et al., Nat. Phys. **3** (2007) p. 36; T. Ohta, et al., Science **313** (2006) p. 951.
[7]. K. V. Emtsev, et al., Nat. Mater. **8** (2009) p. 203.
[8]. D. Waldmann, et al., Phys. Rev. B **81** (2010) 195434.
[9]. C. Riedl, et al., Phys. Rev. Lett. **103** (2009) 246804; F. Speck, et al., Mater. Sci. Forum, **645-648** (2010) p. 629; A. Bostwick, et al., Science 328 (2010) p. 999.

I1-2

Mechanism of "controlled atomic defects": extension to the ternary systems

E.I. Rogacheva

National Technical University "Kharkov Polytechnic Institute", 21 Frunze Str., 61002 Kharkov, Ukraine
E.I. Rogacheva: e-mail: rogacheva@kpi.kharkov.ua, telephone: +38 057 7076092

To establish the influence of native and impurity defects on physical properties of ternary crystals and to predict those properties, it is necessary to find the ways of controlled introduction of defects into a crystal.

Two types of ternary phases important from the practical point of view are considered: 1) solid solutions based on a ternary compound where atoms of constituents play the role of impurity components; 2) solid solutions based on binary compounds. In both cases it is assumed that initial compounds have certain homogeneity regions, i.e. have certain concentrations of native defects, which depend on the degree of deviation from stoichiometry.

The method of "controlled atomic defects" realized by changing the alloy composition along a definite section in the Gibbs concentration triangle that determines mechanism of impurity solution, number and type of impurity and native atomic defects introduced into the crystal, is applied and developed for ternary phases of such types. Using the above indicated method, one can differentiate the influence of native and impurity defects. For example, studying physical properties of IV – X – VI alloys based on IV-VI compounds (X is impurity component) along VI isoconcentrates, it is possible to establish the influence of impurity defects at a fixed deviation from stoichiometry, whereas studying properties along X isoconcentrates one can establish the influence of the deviation from stoichiometry at a fixed impurity concentration. Analyzing properties along radial sections, one can investigate the joint influence of both types of defects.

To predict the defect structure and properties of alloys, it is very useful to apply crystallochemical approach taking into consideration electrochemical properties of components, size effects, the most probable mechanisms of solution, the possibility of chemical interaction, manifestation of variable valence and other factors. Comparing formation energies for different types of defects, it is possible to predict the most probable defect structure for a certain scheme of substitution and deviation from stoichiometry.

The overview of extensive experimental material, which we obtained when studying ternary phases IV – X – VI (IV – Pb, Sn, Ge; VI – Se, Te; X – Cu, Ag, Cd, In, Ga, Sb, Bi, Mn, V) based on IV-VI binary compounds and ternary phases based on I–III–VI_2 compounds (I – Cu; III – In, Ga; VI – Se, Te) will be given. In these studies, the controlled introduction of non-stoichiometric and impurity defects of different types into I-III-VI_2 ternary compounds and IV-VI binary compounds was realized by changing the alloy composition along different sections of the concentration triangle. The types of predominant defects corresponding to different schemes of doping and deviation from stoichiometry were identified. It was shown that there is a distinct correlation between the composition, type and concentration of impurity and non-stoichiometric defects, on the one side, and the crystal structure, mechanical, electrophysical, galvanomagnetic, and thermoelectric properties on the other side.

The application of the method of "controlled atomic defects" to binary and ternary compounds gives a possibility to vary the defect structure in different ways and to establish the influence of defects of different types on the structure and properties.

The results obtained prove the fruitfulness of using the "controlled atomic defects" method for the development of physical foundations of controlling properties of complex semiconductor phases by introducing impurity and non-stoichiometric defects.

O1-1

Ultrathin CIGS solar cells from controlled chemical etching of state of the art co-evaporated absorbers

N. Naghavi[1] , Z. Jehl[1] , F. Erfurth[1], , L. Lombez[1], I. Gerard [2], M. Bouttemy[2], P. Tran-Van[2], A. Etcheberry[2] , G. Voorwinden[3], B. Dimmler [3], W. Wischmann[4] , M. Powalla[4], J.F.Guillemoles[1], D. Lincot[1]

[1] Institut de Recherche et Développement sur l´Energie Photovoltaïque (IRDEP-UMR 7174 EDF-CNRS-ENSCP), 6 quai Watier, 78401Chatou Cedex, France
[2]ILV - UMR 8180, Université de Versailles St Quentin, 45 Av. des Etats Unis, 78035 Versailles CEDEX
[3] Wuerth Elektronik Research GmbH, Industriestr. 4, 70565 Stuttgart, Germany
[4] Zentrum für Sonnenenergie- und Wasserstoff-Forschung (ZSW), Industriestr. 6, 70565 Stuttgart, Germany

daniel-lincot@chimie-paristech.fr

This presentation will present the influence of reducing the CIGSe absorber layer thickness by highly controlled bromine etching on the electrical and optical solar cell properties. When going from the standard 2.5 micron thickness to 500 nm films we observe a decrease in efficiency which is mainly caused by a reduced short circuit current. Even without deliberate light trapping or anti-reflection coating, an efficiency of 10.3% has been obtained for a 0.5 micron thick CIGSe absorber. A smoothing of the absorber surface was observed during the etching, its influence on the cell parameters will be discussed. Furthermore we monitored the increase of the surface band-gap, induced by the etching, which causes a slight increase of the open circuit voltage for thin absorber layers. Besides fundamental interest, ultrathin CIGS layers represents a key option to reduce the consumption of indium for large scale development.

Acknowlegements : This study is carried out with the ULTRACIS project supported by the French National Research Agency (ANR).

O1-2

Room-temperature ferromagnetism in (Zn,Mn,Sn)As_2 thin films applicable to InP-based spintronics devices

N. Uchitomi, J. T. Asubar, H.Oomae, H.Endoh and Y. Jinbo

Department of Electrical Engineering, Nagaoka University of Technology
1603-1, Kamitomioka, Nagaoka, Niigata, Japan 940-2188
uchitomi@nagaokaut.ac.jp, +81-258-47-9505

III-V compound-based diluted semiconductors (DMS's) such as (Ga,Mn)As, capable of being epitaxially grown on GaAs substrates with high-quality interface, are important for the implementation of a variety of spintronics devices [1]. However, the applicability of ferromagnetic semiconductors in spintronic devices requires increasing Curie temperature from around 180 K in (Ga,Mn)As to above room temperature [2-3]. Recently, II-IV-V_2 compounds crystallizing in the chalcopyrite structure have attracted growing interest as semiconductor hosts for magnetic impurities such as Manganese. The synthesis of $CdGeP_2$:Mn with Tc=320 K and $ZnSnAs_2$:Mn with Tc=329 K marked the emergence of novel spintronic materials exhibiting above-room-temperature ferromagnetism [4-5]. Furthermore, an important step towards practical applications would be to find high-quality thin films showing ferromagnetism at room temperature.

In this work, we report on some results obtained from our efforts to develop Mn-doped $ZnSnAs_2$ thin films as a ferromagnetic building block for InP-based semiconductor spintronics. This work is dedicated to furthering our knowledge of the magnetic properties of Mn-doped $ZnSnAs_2$ epitaxial thin films.

The Mn-doped $ZnSnAs_2$ thin films were grown on semi-insulating InP (001) substrates in an MBE growth chamber using all elemental solid sources at a substrate temperature of 300ºC. A 50-nm-thick *un-doped* $ZnSnAs_2$ buffer layer was grown prior to the growth of the Mn-doped $ZnSnAs_2$ epitaxial films with different doping concentration (2-7 at%). *In-situ* reflection high-energy electron diffraction (RHEED) patterns exhibited streaky features during the entire buffer layer growth process, indicating that the $ZnSnAs_2$ films were epitaxially grown on InP (001) substrates. The detailed growth process has been described elsewhere [6].

The crystalline structures were characterized using high-resolution x-ray diffraction and high-resolution transmission electron microscopy. Superconducting quantum interference device magnetometry was used to investigate the magnetic properties of the Mn-doped $ZnSnAs_2$ thin films. The high-resolution reciprocal space mapping (RSM) of the Mn-doped $ZnSnAs_2$ epitaxial film around the (224) Bragg peak of the underlying InP substrate was also carried out. The values of the in-plane lattice parameter *a* of the Mn-doped $ZnSnAs_2$ thin films were estimated from the RSM to be 0.5869 nm corresponding to the lattice constant *a* of the InP substrate.

The figure shows the temperature dependence of the magnetization along the in-plane [110] direction of the 8mm × 8mm square specimens of the Mn-doped samples. The 4% and 7% Mn-doped samples have respectively in-plane magnetization of 1.5× and 4.3×10^{-5} emu and almost the same values of Tc of 333 K and 325 K. These results reveal that the magnetization of thin films is controllable by adjusting the Mn doping concentration, thereby demonstrating its applicability as a building block for InP-based spintronics devices such as Datta-Das type spin transistors and spin light -emitting diodes.

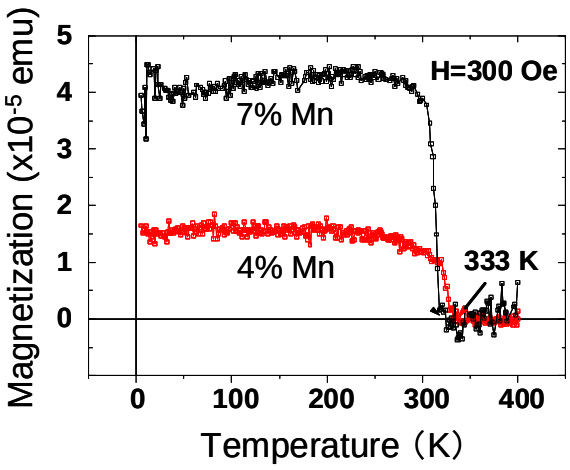

[1]. H.Ohno Science 281 (1998) p.951
[2]. K.Olejnik *et al.* Phys.Rev. B 72 (2008) p.054403
[3]. S.Ohya *et al.* Appl.Phys Lett. 90 (2007) p.112503
[4]. G.A.Medvedkin *et al*. Jpn. J. Appl.Phys. Part2 39 (2000) L949
[5]. S.Choi *et al*. Sol.Stat.Commun. 122 (2002) p.165
[6]. J.T.Asubar *et al.* J.Crystal Growth 311 (2009) p.929

O1-3

$Sn_{1-x}Pb_xS$ nanorods on isochemical substrates for thermoelectric and photovoltaic application

K. Bente[1], V. Lazenka[1], D. Unuchak[1], G. Wagner[1], R. Kaden[1], V. Gremenok[2] and V. Ivanov[2]

[1] Institut für Mineralogie, Kristallographie und Materialwissenschaft, University of Leipzig, Scharnhorststr. 20, 04275 Leipzig, Germany
[2] State Scientific and Production Association «Scientific-Practical Materials Research Centre of the National Academy of Sciences of Belarus», P. Brovka str., 19, 220072 Minsk, Belarus

bente@rz.uni-leipzig.de, +49 341 9736 251 / 299

Ternary IV-VI orthorhombic SnS (Herzenbergite) – $SnPbS_2$ (Teallite) mixed crystals are promising candidates as a light-absorbing medium of next-generation solar cells because they have direct band gap energies in the range of 1.1-1.65 eV, a high absorption coefficient of 10^5 cm^{-1} and large Seebeck coefficients [1]. Hot wall vacuum deposition method (HWVD) is concerned with the epitaxial growth of layers under conditions close to thermodynamic equilibrium and with a minimum loss of material. IV-VI thin films of high quality with carrier concentrations with one or two orders of magnitude less than those of the bulk can be produced by HWVD under relatively low vacuum (about 10^{-4} Pa) [2]. Based on $Sn_{1-x}Pb_xS$ mixed crystal targets, thin films and lawns of $Sn_{1-x}Pb_xS$ nanorods (Figure 1) were produced using HWVD method. The lawn was formed onto the surface of an underlying thin $Sn_{1-x}Pb_xS$ film being built by oriented blocks on glass.

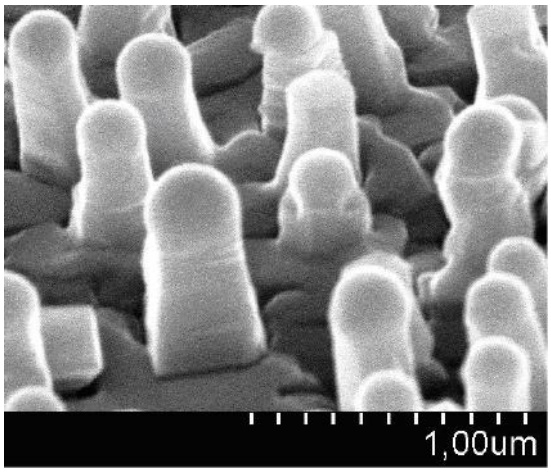

Figure 1. SEM image of $Sn_{1-x}Pb_xS$ nanorods

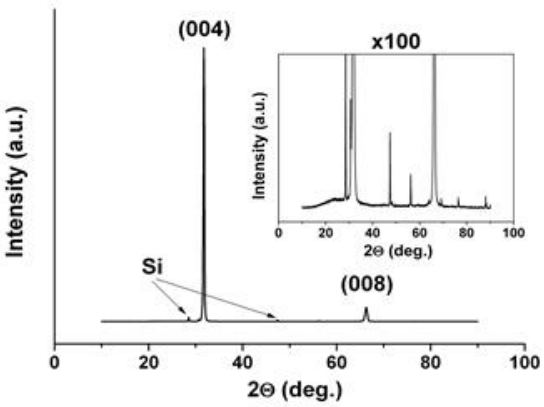

Figure 2. XRD of epitaxial $Sn_{1-x}Pb_xS$

The density of rods arranged like a lawn depends on the metal ratio and substrate temperature. X-ray (Figure 2) and TEM analysis of the epitaxial material showed preferential (001) orientation perpendicular to the surface of the glass substrate. The roughness of the films measured by atomic force microscopy was in the range of R_q = 49.5–86.3 nm depending on lead concentration The rods were maximally 600 nm high and < 300 nm in diameter. As revealed by TEM-EDX experiments the droplet at the tip of rods consists of tin. Therefore it is assumed the rods grew via a self-consuming vapor–liquid–solid (VLS) mechanism [3-7].
First measurements of physical properties of corresponding SnS thin films reveal electrical conductivities about 8 $S*cm^{-1}$ and Seebeck coefficients of 800 – 1000 μV/K.

[1]. D.M. Unuchak, K. Bente, G. Kloess, W. Schmitz, V.F. Gremenok, V.A. Ivanov and V. Ukhov, *Phys. Stat. Sol. C* **6** (2009), p. 1191.
[2]. A.Lopez-Otero, *Thin Solid Films* **49**, (1978) p. 3.
[3]. D.F. Pridmore and R.T. Shuey, *Am. Mineral.* **61** (1976), p. 248.
[4]. M. Paic and V. Paic, *J. Mater. Sci.* **7** (1972), p. 1260.
[5]. G.F. McLane and K.J. Sleger, *J. Electron. Mater.* **4** (1975), p. 465.
[6]. M.S. Gudiksen and C.M. Lieber, *J. Am. Chem. Soc.* **122** (2000), p. 8801.
[7]. A.Yella, E. Mugnaioli, M. Panthofer, H.A. Therese, U. Kolb and W. Tremel, *Angew. Chem. Int. Ed.* **48** (2009), p. 6426.

O1-4

Preparation and electrical properties of ZnO/CdS/Cu(In,Zn)Se_2 (ZCIS) heterojunctions

V.A. Ivanov[1], V.F. Gremenok[1], V.B. Zalesski[2], V.I. Kovalevski[2], K. Bente[3]

[1] State Scientific and Production Association «Scientific-Practical Materials Research Centre of the National Academy of Sciences of Belarus», P. Brovka str., 19, 220072 Minsk, Belarus
[2] Institute of Physics, National Academy of Sciences of Belarus, Logoiski trakt 22, 220090, Minsk, Belarus
[3] Institut für Mineralogie, Kristallographie und Materialwissenschaft, University of Leipzig, Scharnhorststr. 20, 04275 Leipzig, Germany

vasil@ifttp.bas-net.by. Tel.: +375 172 84 12 49, FAX: +375 172 84 08 88

Cu(In,Zn)Se_2 (ZCIS) is one of the most promising materials for commercial photovoltaic applications. This is due to the high absorption coefficient of approximately 10^5 cm^{-1} in a wide spectral region and a band gap that is in principle adjustable between 1.05 eV for $CuInSe_2$ and 2.60 eV for ZnSe [1]. Therefore they are suggested to be used in thin film solar cells as absorber as well a wide-gap window layers [2]. The Cu/(In+Zn) ratio of the ZCIS layers is the important parameter for the physical properties of the semiconductor material as well for the solar cell applications.
The presented results consider the preparation as well as the chemical, structural and physical characterization of the electrical properties of the ZnO/CdS/$CuIn_{0,94}Zn_{0,06}Se_2$ thin films heterojunctions.
The ZCIS films were prepared by two-step selenization of Cu-In-ZnSe layers under N_2 flow by evaporating a solid Se source close to samples [3]. Such technology is especially suited for developments of industrial processing of large area ZCIS films suitable for solar cells. Cu-In-ZnSe layers were deposited onto Mo-coated soda lime glass substrates by thermal evaporation or rf-sputtering. The Zn content in the ZCIS films was controlled by choise of In/ZnSe ratio in the initial alloy.
The thin films microstructure consisted of densely packed grains with dimensions of 1 - 2 μm and crystallite growth direction perpendicular to substrate plane. The films were polycrystalline and their phase composition and structural characteristics were determined by Cu/In/ZnSe ratio in the starting layer. The as-prepared films show *p*-type electrical conductivity, which is confirmed by the thermoelectric probe measurement. All the obtained films had thicknesses of 1.1 – 1.8 μm. The films showed absorption coefficients > $1 \cdot 10^5$ cm^{-1} above the fundamental absorption edge with an optical band gap in the range of 1.20 - 1.25 eV, indicating that these films adequate to be used as absorber material in thin film solar cells.
Buffer layers of CdS were deposited onto the ZCIS films in the chemical bath. The ZnO films were deposited onto CdS by thermal evaporation. The ZnO and CdS films were detected to be polycrystalline with thicknesses of 0.4 μm and 0.06 μm respectively and revealed n-type conductivity. The “Leit-C” conductive glue was used as electrical contacts. The effective area of each cell was about 0.8 cm^2.
Under non-illuminated conditions, $I - V$ characteristics of the heterojunctions were approximately exponential at low voltages according to the standard diode equation $I=I_o[\exp(eV/nkT)-1]$, with a slight deviation from this behaviour at high voltages due to a series of resistance effects. The capacitance of the heterojunctions versus reverse bias voltage was carried out at room temperature with a frequency of 1 MHz. Plots of C^{-2} versus V were found to be linear indicating that the fabricated junctions were abrupt. The values of the built-in voltage data calculated from the slope of the $C–V$ plot were 1.2 V and were comparable with values due to the electrical measurements.

[1]. V.G. Lambrecht, *Mater. Res. Bull*. **8** (1973), p. 1383.
[2]. V.F. Gremenok, E.P. Zaretskaya, K. Bente, W. Schmitz, V.B. Zalesski and H.J. Moller, *Thin Solid Films*, **487** (2005), p. 193.
[3]. V.F. Gremenok, E.P. Zaretskaya, V.B. Zalesski, K. Bente, W. Schmitz, R.W. Martin and H.J. Moller, *Sol. Energy Mat. & Sol. Cells* **89** (2005), p. 129.

O1-5

Epitaxial Growth of Chalcopyrite $CuInS_2$ Films on GaAs(001) Substrates by Evaporation Method with Elemental Sources

Nozomu Tsuboi[1,2], Takashi Tamogami[3] and Satoshi Kobayash[1]

[1] Faculty of Engineering, Niigata University, 2-8050 Ikarashi, Nishi-ku, Niigata 950-2181, Japan
[2] Center for Transdisciplinary Research, Niigata Univ., 2-8050 Ikarashi, Nishi-ku, Niigata 950-2181, Japan
[3] Graduate School of Sci. and Tech., Niigata Univ., 2-8050 Ikarashi, Nishi-ku, Niigata 950-2181 Japan

E-mail: tsuboi@eng.niigata-u.ac.jp, Tel/Fax: +81-25-262-7261

Ternary chalcopyrite semiconductor $CuInS_2$ is one of the potential candidates for absorber layers in high-efficiency thin film solar cells due to its direct bandgap E_g of 1.5 eV, which matches with solar spectrum. However, $CuInS_2$ solar cells face the problem of lower solar conversion efficiency compared with $Cu(InGa)Se_2$ (E_g≈1.2 eV) solar cells. Investigation of fundamental properties of $CuInS_2$ films is necessary to understand key issues for solar cell performance.

Although in bulk $CuInS_2$ is known to crystallize into chalcopyrite (CH) structure, in thin film other structures such as Cu-Au (CA) and sphalerite (SP) structures may coexist. We had reported epitaxial growth of slightly Cu-rich $CuInS_2$ films with *c*-axis orientated CA only and/or with a mixture of *a*- and *c*-axes orientated CH structures on GaP(001) at substrate temperature of 500 °C using the conventional evaporation method with three elemental sources.[1] Successful growth of epitaxial CH structured $CuInS_2$ were observed for films grown on GaP(001) at 570 °C with slightly Cu-rich composition.[2] Film thicknesses of the films were 0.2~0.4 μm and the compressive strain due to the lattice mismatch of −1.3% were almost relaxed. In this paper, $CuInS_2$ films with various [Cu]/[In] ratios are grown on GaAs(001) substrates, and the composition range in terms of the [Cu]/[In] ratio where epitaxial films with CH structure grow and the structural qualities of the films are discussed in comparison with those on GaP(001) substrates.

Films with various ratios of [Cu]/[In]=0.8~1.9 are grown at 500 °C and 570 °C using the evaporation system described in our previous reports.[1, 2]. Film thicknesses are 0.2~0.3 μm. Regardless of the substrate temperature, noticeable X-ray diffraction (XRD) peaks of CH structured $CuInS_2$ phase are observed in slightly Cu-rich films ([Cu]/[In]≈1.2~1.4) and those of $CuIn_5S_8$ phase are observed in In-rich and almost stoichometric films ([Cu]/[In]<1.1). Noticeable XRD peaks of CA structured $CuInS_2$ phase are observed in all films grown at 500 °C and In-rich and almost stoichometric films ([Cu]/[In]≥1.2) grown at 570 °C, *i.e.*, slightly Cu-rich and Cu-rich films grown at 570 °C exhibit no noticeable XRD peaks of the CA structured $CuInS_2$ phase. Figure 1 shows typical XRD patterns around $2\theta \approx 32^o$ of the films grown at 570 °C. The XRD peak due to the *c*-axis oriented CH structure of $CuInS_2$ phase is dominant in the slightly Cu rich films and the tensile strain due to the lattice mismatch of 2.4 % seems to be almost relaxed. However, reflection high energy electron diffraction (RHEED) patterns of the slightly Cu-rich films grown at 570 °C exhibit noticeable spots not only due to the CH structure but also due to the CA structure. The amount of the CA structure is considered to be small because of the absence of the XRD peaks of the CA structure. Taking account of the previous report that the slightly Cu-rich films grown on GaP(001) at 570 °C had only the c-axis oriented CH structure patterns even in RHEED, the slight appearance of the Cu-Au structure is possibly related the larger lattice mismatch for GaAs.

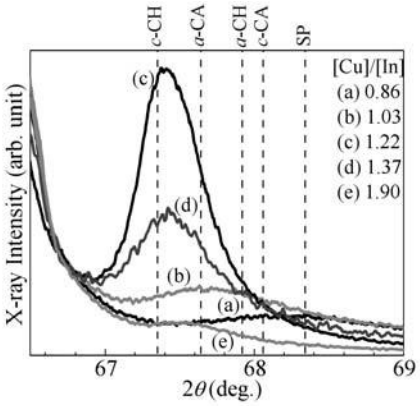

Figure 1. XRD patterns of films grown at 570°C with various [Cu]/[In] ratios. The dashed lines show estimated 2θ values of the XRD peaks corresponding to *a*-axis oriented CH, *c*-axis oriented CH, *a*-axis oriented CA, *c*-axis oriented CA and SP structures.

[1]. R. M. Vequizo, S. Kobayashi, N. Tsuboi, K. Oishi and F. Kaneko: Jpn. J. Appl. Phys. **46** (2007) 716.
[2]. R. M. Vequizo, S. Kobayashi, N. Tsuboi, K. Oishi and F. Kaneko: Phys. Status Solidi C **6** (2009) 1019.

O1-6

Influence of the preparation conditions on the properties of $Cu(In,Ga)(S,Se)_2$ thin films obtained by two-step growth

E.P. Zaretskaya[1], V.F. Gremenok[1], N.N. Mursakulov[2], N.N. Abdulzade[2], Ch.E. Sabzaliyeva[2]

[1] State Scientific and Production Association "Scientific-Practical Materials Research Centre of the National Academy of Sciences of Belarus", National Academy of Sciences of Belarus, P. Brovka 19, 220072 Minsk, Belarus. Tel: +375 172 841249; FAX: +375 172 840888;
[2] Institute of Physics, Azerbaijan National Academy of Sciences, H. Cavid ave., 33, Baky, Az-1143
email: ezaret@ifttp.bas-net.by

$CuInSe_2$ (CIS) and $CuIn_{1-x}Ga_x(S,Se)_2$ (CIGSS) are considered as the most promising materials for low cost and high-efficiency solar cells due to of their high optical absorption ($>10^5$ cm $^{-1}$) and stability against photo-degradation. The optical band gap (E_g) of CIS is 1.05 eV, which is lower than the optimum value for solar cells. An advantage of the CIGSS material is that E_g easily can be changed from 1.04eV up to 2.4 eV. Furthermore, the use of compositional variations through the depth of the absorber allows the design of a band gap engineering which leads to an improved module performance.

In this paper, we present a growth process developed to form single-phase CIGSS films with reduced grading in the [Ga]/([Ga]+[In]) ratio. The technology is based on sequential deposition of the Cu-In-Ga precursors followed by their two-step annealing in S/Se-containing atmosphere under N_2 flow [1]. Reaction time, temperature and S/Se weight ratio in reaction system were used to control the reaction kinetics. Full characterizations have been carried out using XRD, SEM, AES, electrical and optical absorption measurements.

X-ray diffraction and EDS studies have shown that the temperature of high-stage (T_s) affects the composition and crystalline structure of the grown material. The samples obtained at T_s of 400 ^{0}C contain two $CuInSe_2$ and $CuInS_2$ phases. There is no evidence for other ternary or binary phases (CuS or $Cu_{2-x}Se$) in these samples. In case of this reaction process, all films were morphologically rough and non-uniform but did not show distinct layers and significant difference in the grain size in the surface-near region and in the bottom-near region. The increase in the recrystallization temperature to 500 ^{0}C resulted in a high intermixing of the material and in a change in morphology. Single-phase pentenary CIGSS thin films of the chalcopyrite structure with [112] preferred orientation were formed under these conditions. These films were relatively uniform and dense and consisted of interconnected grains approximately 1.5-2.5μm in size. The most important feature of the films obtained at temperatures of 500 ^{0}C is a remarkable constant Cu/In/Ga atomic ratio through the depth, which is a precondition to form the single-phase CIGSS material.

An obvious improvement in the crystal structure of CIGSS films was noticed with the increasing the high-stage temperature to 540 ^{0}C. The improvement of long-range ordering in the lattice was evidenced from the increase of the degree of preferred orientation $I_{112}/I_{220/204}$ from 2 to 4.

The AES depth profile was used to study the concentration of elements present in the bulk of the grown CIGSS films. The measured AES compositions as a function of depth were used to calculate the $Cu(In_{1-x}Ga_x)(S_ySe_{1-y})_2$ band gap profiles [2].

Determination of the optical band gap by optical transmission measurements and its correlation to the values estimated from AES shows that the minimum band gap E_g^{min} defines the absorption edge in the graded structure. These values deviation did not exceed 0.1 eV.

It was shown that single-phase CIGSS thin films with a larger band gap can be produced at relatively low temperatures (400 – 460 ^{0}C). This enables to employ the described method in the developing of the technology of CIGSS- based solar cells on flexible polyimide substrates.

Acknowledgements: This work has been supported by the Belarusian Republican Foundation for Fundamental Research and Azerbaijan National Academy of Sciences (NASA).

[1]. E. Zaretskaya, V. Gremenok, V. Zalesski, S. Schorr, V. Rud, Y. Rud. Preparation and properties of In/p-$Cu(In_{1-x}Ga_x)(S_{1-y}Se_y)_2$ surface-barrier structures // Physica Status Solidi (c), Vol. 6, № 5, p. 1278-1281.
[2]. I.L. Repins, B.J. Stanbery, D.L. Young, S.S. Li, W.K. Metzger, C.L. Perkins, W.S. Safarman, M.E. Beck, L. Chen, V.K. Kapur, D. Tarrant, M.D. Gonzalez, D.G. Jensen, T.J. Anderson, X.Wang, L.L. Kerr, B. Keyes, S. Asher, A.

Delanoy, B.Von Roedern, Prog. Photovolt: Res. Appl. 14 (2006) 25.

O1-7

Ternary compounds in Fe-Mo-C spinning films and e quilibrium alloys: experiment and thermodynamic modelling at high-temperatures

T.A. Velikanova[1], M.V. Karpets[1], P.G. Agraval[2], M.A. Turchanin[2]

[1] Institute for Problems of Materials Sience NASU, 3, Krzhyzhanovsky str., Kyiv-142, 03680, Ukraine
[2] Donbass State Engineering Academy, Shkadinova Street 72, UA–84313 Kramatorsk, Ukraine
e-mail: tavel@ipms.kiev.ua

As was early shown [1] metastable ternary **π**-phase (*cP*20, $P4_132$, β-Mn), which was detected in 78,4Fe10,8Mo10,8C (% at.) spinning films (~50 μm thickness and coherence area ~60 nm), decomposes at heating in the range of 873…973 K under *in situ* high-temperature (from 973 to 1473 K, when Liquid phase appearances) X-Ray diffractometry (HT XRD) conditions.

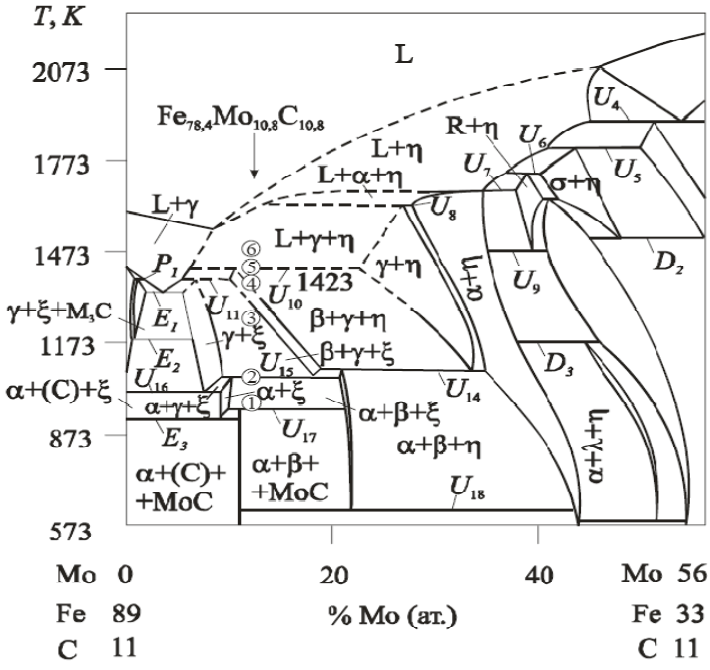

Figure. Politherm section of the Fe–Mo–C system at 11 % at. carbon :- - - - - - – supposed phase boundaries

Comparison of the phase composition of 78,4Fe10,8Mo10,8C alloy at each HT XRD curing temperature, and its phase composition under conditions of thermodynamic equilibrium at the same temperatures has been carried out in order to estimate the degree of phase transformations completeness under *in situ* HT XRD-experiment. For this aim the politherm section of the Fe–Mo–C system at 11 % at. carbon was calculated (see **Figure**) by CALPHAD-method using Andersson`s thermodynamic model of the system.

In the result of the comparative analysis it was shown that Fe–Mo–C spinning alloys reach the state of thermodynamic equilibrium under *in situ* HT XRD-experiment (see **Table**).

Table. Phase composition of 78,4Fe10,8Mo10,8C spinning ribbons according *in situ* HT XRD-experiment and phase composition of 78,4Fe10,8Mo10,8C equilibrium alloy according thermodynamic modelling (TM)

T, K	designation at Figure	phase composition on HT XRD data	phase composition on TM data	crystal structure and designation of phases in this paper
973	①	α + β + ξ	α + β + ξ	α=α-Fe: *cI*2, *Im*-3*m*, W β= β-Mo_2C: *hP*3, $P6_3/mmc$, Fe_2N ξ=$M_{34}C_{10}$: *mC*44, *C*2/*m*, $Mo_6Fe_{11}C_5$ γ=γ-Fe: *cF*4, *Fm*-3*m*, Cu η=M_6C: *cF*112, *Fd*-3*m*, W_3Fe_3C L=liquid phase
1073	②	α + ξ + β + γ	ξ + β + γ	
1273	③	γ + β	γ + β	
1373	④	γ + β + η	γ + β + η	
1423	⑤	γ + β + η	γ + β + η	
1473	⑥	L + γ + η	L + γ + η	

[1]. Velikanova T.A., Karpets M.V. Turchanin M.A. “Perspective technologies, materials and equipment in foundry” (DSMA, Kramatorsk, Ukraine, 2009), P. 50-52.

O1-8

Peculiarities of linear thermal expansion of $CuInS_2$ single crystal

Akira Nagaoka[1], Kenji Yoshino[1] and Hideto Miyake[2]

[1] Department of Electrical and Electric Engineering, University of Miyazaki,
1-1 Gakuen Kibanadai-nishi 889-2192, Japan
[2] Department of Electrical and Electric Engineering, Mie University,
Kamihama-cho 1515 Tsu, Mie 514-8507, Japan

t0b114u@ccmiyazaki-u.acjp, phone/ fax +81-985-58-7396

I–III–VI_2 chalcopyrire semiconductors have made rapid progress in recent years. In addition chalcopyrite semiconductors show unique thermal properties. Usually, liner thermal expansion in semiconductors increases with increasing temperature. However, liner thermal expansion of most chalcopyrite semiconductors decreases at low temperature. For example, $AgGaSe_2$ shows decreasing the liner thermal expansion below 100 K[1, 2].

It is well known that high-quality single crystals of the I–III–VI_2 compounds are difficult to grow because most of the compounds grow through a peritectic reaction or a solid state transition during the cooling process. $CuInS_2$ single crystal can be grown by traveling heater method (THM), which is one of the solution growth techniques. Advantages of the THM growth are following that growth temperature is low compared with that of the other melt growth and larger crystals can be grown compared with a conventional solution growth. In a previous study, $CuGaS_2$, $CuGaSe_2$, $CuGaTe_2$, $CuInSe_2$ ternary compounds have been obtained by the THM technique[3].

In this work, we investigated a liner thermal expansion of single crystal $CuInS_2$ by using X-ray diffraction (XRD). Measurement temperature was changed from 10 K to 300 K. From results of XRD measurement, we calculates lattice constants of *a* and *c* axes and the liner thermal expansion. As a result, lattice constants of *a* axis increase with increasing temperature, that of *c* axis decreases with increasing temperature. The liner thermal expansion decreases for T < 150 K. We can show experimentally anomalous behavior of $CuInS_2$ single crystal at low temperature.

[1]. S. Ozaki, M. Sasaki and S. Adachi, Phys. Stat. Sol. (a) **203** 2648 (2006).
[2]. I. V. Bodnar and N. S. Orlova, Inorg. Mater. **23** 680 (1987).
[3]. H. Miyake, K. Sugiyama and K. Hiramatsu. Res. Rep. Fac. Eng. Mie Univ. **24** 31 (1999).

P1-1

Effects of Y_2O_3/CuO co-doping on microstructure and dielectric properties of $BaTiO_3$-based ceramics

T. V. Tarasevich and S. A. Lebedev

SSPA "Sci.-Pract. Materials Research Centre of NAS of Belarus", P. Brovki Str., 19. 220072, Minsk, Belarus
e-mail: tarasevich@physics.by

$BaTiO_3$ with the perovskite structure is well-known material for capacitors. $BaTiO_3$-based X7R dielectric materials have attracted considerable attention because of their temperature change of capacitance less then ±15 % over the temperature range from -55 to 125°C. It has been established that X7R temperature stability is achieved by formation the so-called grain core-shell structure in $BaTiO_3$-based ceramics. This structure includes reacted $BaTiO_3$ with dopants (shell) and unreacted $BaTiO_3$ (core). With the recent tendency in miniaturization of electronic components capacitor materials are required to have a high permittivity and a grain size as small as possible. Therefore Y_2O_3 and CuO co-doping ceramics can be examined in producing fine-grained $BaTiO_3$ ceramics with high dielectric properties.

In this work $BaTiO_3$-based ceramics with CeO_2, SnO_2, $MgNb_2O_6$, Y_2O_3 and CuO dopants were sintered at 1240 ^{0}C in air. The microstructure and dielectric properties of Y_2O_3/CuO co-doped $BaTiO_3$-based ceramics were investigated. It was found that all samples containing Y_2O_3 and CuO from 0.25 to 0.5wt.% show a tetragonal structure of $BaTiO_3$ as the main phase. Addition of Y_2O_3 more than 0.3wt. % results in formation pyrochlore phase $Y_2Ti_2O_7$, indicating that the solubility limit of Y_2O_3 less than 0.3wt.%. This result is in agreement with Bo Li et al. for $BaTiO_3$-Y_2O_3-ZnO system [1]. Additions of Y_2O_3 and CuO lead to improving the temperature change of capacitance (TCC) around Curie point. It is known that Cu addition shifts the Curie point toward lower temperatures [2]. Therefore the increasing of the Curie point value is connected with the presence of Y_2O_3. Y_2O_3 addition restrains the diffusion of other dopants into $BaTiO_3$ grains due to its solubility limit, maintaining Curie point close to 125^{0}C. As a result the TCC around 125^{0}C decreases and samples satisfy the X7R material characteristics (fig. 1).

Microstructures of samples with different Y_2O_3 and CuO content point out to production fine-dense grained ceramics with average grain size less 1 μm (fig. 2). CuO acts as flux and facilitates sintering of ceramics. Increasing of CuO content to 0,5 wt. % causes dielectric loss rising up to 1,3 % at 25^{0}C. Y_2O_3/CuO co-doping in the ratio 0,25/0,25wt. % or 0,25/0,3wt. % is effective for obtaining X7R material at sintering temperature 1240°C with high dielectric properties at 25^{0}C: dielectric constant - 2260-2285; dielectric loss-0,007-0,009; TCC=9,3%.

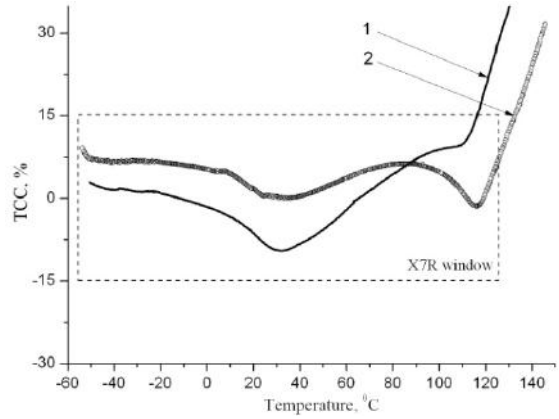

Figure 1. Temperature dependence of capacitance change for $BaTiO_3$ ceramics without Y_2O_3/CuO (1) and with Y_2O_3/CuO in the ratio 0,25/0,25wt.%(2).

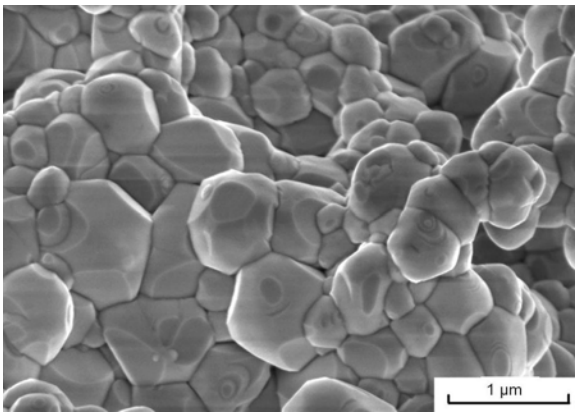

Figure 2. Microstructure $BaTiO_3$ ceramics doped Y_2O_3/CuO in the ratio 0,25/0,25wt.%

[1]. B. Li, S. Zhang, X. Zhou, Z. Chen. *J. Mater Sci*. **42** (2007), p. 5223-5228.
[2]. H. T. Langhammer, T. Muller, R. Bottcher. *Solid State Sciences*. **5** (2003), p. 965-971.

P1-2

Initial growth process in the electrochemical deposition of ZnO

Atsushi Ashida, Naoya Nouzu, and Norifumi Fujimura

[1]Graduate School of Engineering, Osaka Prefecture University,
1-1 Gakuen-cho, Naka-ku, Sakai, Osaka 599-8531, Japan
E-mail address: ashida@pe.osakafu-u.ac.jp; Tel. & Fax: +81-72254-9327

ZnO is well-known as a wide bandgap semiconductor applicable to UV devices, sensors, and transparent conductive films. In general, ZnO thin films are prepared under vacuum or reduced pressure. In this study, ZnO films, as well as nano- and micro-crystals, were prepared by electrochemical deposition (ECD) from aqueous solutions. ZnO crystallizes in ECD at ambient pressure and at temperatures below 100 °C; ECD therefore consumes less energy than conventional vapor-phase deposition. Furthermore, the raw material efficiency is high because the substance is deposited only on the electrode. However, the mechanism and process of crystal growth in ECD have not yet been clarified. We focused on the initial crystal growth process in ECD.

Using a conventional three-electrode electrochemical cell, we grew ZnO crystals from 0.1 M zinc nitrate aqueous solution at 60 °C. The working electrode was epitaxial (111)Pt grown on c-sapphire by rf sputtering. The reference and counter electrodes were Ag/AgCl and Zn, respectively. Constant current densities in the range of 25–150 μA/cm^2 were applied to the Pt electrode, and the total charge for the deposition was fixed at 0.50 coulomb/cm^2. [1, 2]

Figure 1 shows an SEM image of ZnO prepared at 100 μA/cm^2. Hexagonal grains with sharp edges are aligned in the same direction, thus signifying epitaxial growth on (111)Pt. Some grains however are slightly rotated, as indicated by the two lines in Fig. 1. The full width at half-maximum of the ϕ-scan XRD peaks is as large as 5.0°. Such loosely bound epitaxial growth is not observed in the case of other growth methods. Figure 2 shows the time course of potential for deposition at various electrolytic current densities. The broken line at −0.1 V shows the upper limit of potential for ZnO growth. The potential was initially higher than −0.1 V, and then abruptly decreased to the ZnO growth region. After that, the potential was nearly constant. Crystals were expected to nucleate in the region of decreasing potential and to grow in the region of constant potential. To confirm the nucleation of ZnO, the deposition was stopped immediately after the abrupt decrease in cathodic potentialreached zero. For this sample, discrete grains were observed by AFM. However, no XRD peaks from the grains were observed because of the extremely small amount of material. To identify the substance, the sample was evaluated by reflection high-energy electron diffraction (RHEED). The obtained pattern is shown in Fig. 3. This analysis revealed that the substance generated in the initial process was not ZnO but rather $Zn(OH)_2$. The in-plane fluctuation of epitaxial ZnO prepared by ECD may arise from this initial growth of $Zn(OH)_2$.

Acknowledgments: This study was supported in part by a Grant-in-Aid for Scientific Research (C) #22550164 from the Ministry of Education, Culture, Sports, Science and Technology, a research grant from the Murata Science Foundation, and a research grant from the Iwatani Naoji Foundation.

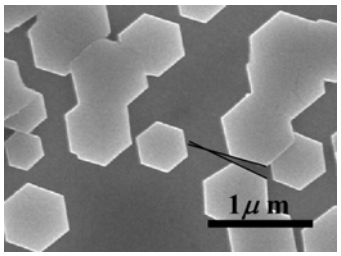

Figure 1. SEM image of ZnO crystals epitaxially grown on (111)Pt by the galvanostatic electrochemical method.

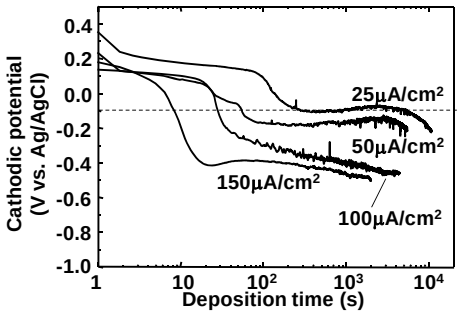

Figure 2. Time course of ZnO crystal growth at various constant current densities.

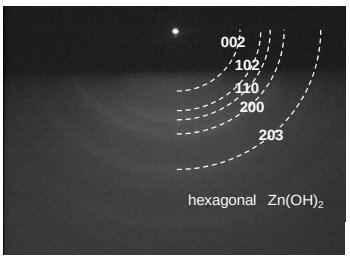

Figure 3. RHEED pattern for deposit obtained immediately after the abrupt decrease in cathodic potential.

[1]. A. Ashida, A. Fujita, Y. Shim, K. Wakita, and A. Nakahira, Thin Solid Films **517** (2008), p.1461.
[2]. N. Nouzu, A. Ashida, T. Yoshimura, and N. Fujimura, Thin Solid Films **518** (2010), p. 2957.

P1-3

Growth of multicomponent solid solutions A3B5 containing antimony by metal-organic chemical vapor deposition

G. S. Gagis[1], V. I. Vasil'ev[1], and N.N. Mursakulov[2]

[1] [1]Ioffe Physico-Technical Institute of the Russian Academy of Sciences,
26 Polytekhnicheskaya st., St Petersburg 194021, Russian Federation ,
Fax: (812) 297 1017, Phone: (812) 292 7914 giman@mail.ioffe.ru
[2] Institute of Physics, Azerbaijan National Academy of Sciences, H. Cavid ave., 33, Baku, Az-1143,
Fax: (99412) 4395961, Phone: (99450) 6138667 e-mail: nmursakulov@physics.ab.az

The wavelength range 1.7-5 μm is of considerable interest in gas analysis and optical communications, because of absorption lines of several gases (including toxic), atmosphere transparency windows and minimum of loses in optical fibers based on fluoride glasses.
Semiconductor optoelectronic devices of this range can be produced with A^3B^5 solid solutions containing antimony and lattice-matched with InAs or GaSb substrates [1].
Theoretical and experimental investigations showed that the multicomponent solid solutions GaInAsSb, InAsPSb, GaInAsPSb for active regions and pentanary solid solutions AlGaInAsSb for cladding layers providing effective optical and carrier confinement are needed for properties optimization of 3-5 μm optoelectronic devices. In present, such materials commonly are obtained by liquid phase epitaxy or molecular beam epitaxy methods. However, for fabrication of such devices in industrial scales, the technologies of obtaining of such materials by metal-organic chemical vapor deposition (MOCVD) are needed.
Our previous researches showed thatch narrow-bandgap solid solutions obtained on InAs substrates has more good properties than analogs obtained on GaSb substrates [2].
In present work the technological conditions of MOCVD of A3B5 solid solutions containing antimony were investigated and epitaxial procedures suitable for A3B5 with compositions close to InAs were selected. The examples of obtained samples are listed in **Table 1**.
The epitaxial growth was carried out on AIX200 setup with horizontal reactor. The growth temperature was 600ºC, the pressure was 100 mbar. The sources of chemical elements of III group were trimethylaluminum (TMAl), triethylgallium (TEGa) and trimethylindium (TMIn), V group – trimethylantimony (TMSb), arsine (AsH3) deluted to 10% in H_2 and phosphine (PH3). PH3 was not pyrolized prior to mixing to other source gases. The total H_2 flow was kept constant at 5.5 liter/min. Growth rate was 3 – 4 μm per hour.

Table I. Solid solutions, grown by MOCVD on InAs(100) substrates

Solid solution	composition range	Lattice mismatch	Wavelength, μm
$Ga_{1-x}In_xAs_ySb_{1-y}$	$0.86 < x < 0.93$, $0.89 < y < 0.92$	$-2.0\cdot10^{-3} – 3.8\cdot10^{-3}$	3.5 – 3.9 (300 K)
$InAs_yP_zSb_{1-y-z}$	$0.63 < y < 0.68$, $0.17 < z < 0.26$	$8.29\cdot10^{-4} – 6.36\cdot10^{-3}$	2.9 – 4.0 (300 K)
$Al_uGa_{1-u-x}In_xAs_ySb_{1-y}$	$0.11 < u < 0.20$, $0.88 < x < 0.94$, $0.90 < y < 0.98$	$-8.8\cdot10^{-3} – 5.5\cdot10^{-3}$	2.4 – 2.5 (4 K)

[1]. N. N. Mursakulov. Features of the growth of epitaxial layers of solid solutions $InAs_{1-x-y}Sb_yP_z$ lattic-matched the substrate InAs. *Inst/ Phys. Conf. Ser. No 152: Section B: Thin Film growth and Characterization. 11th Int. Conf. on Ternary and Multinary Compounds, ICTMC-11, Salford, 8-12 September (1997), pp: 341-344, 1998 IOP Publishing LTD*

[2]. G. S. Gagis, V. I. Vasil'ev, A. G. Deryagin, V. V. Dudelev, A. S. Maslov, R. V. Levin, B. V. Pushnyi, V. M. Smirnov, G. S. Sokolovskii, G. G. Zegrya and V. I. Kuchinskii. *Semicond. Sci. Technol.* ***23*** *(2008) p125026 (6pp)*

P1-4

Physical properties of SnS thin films grown by hot wall deposition

V. Gremenok[1], D. Unuchak[2], V. Lazenka[2], K. Bente[2], V. Ivanov[1], S. Bashkirov[1], I. Tashlykov[3], A. Turovets[3]

[1] State Scientific and Production Association «Scientific-Practical Materials Research Centre of the National Academy of Sciences of Belarus», P. Brovka str., 19, 220072 Minsk, Belarus
[2] Institut für Mineralogie, Kristallographie und Materialwissenschaft, University of Leipzig, Scharnhorststr. 20, 04275 Leipzig, Germany
[3] Belarusian State Pedagogical University, Sovetskaja str. 18, 220050 Minsk, Belarus

gremenok@ifttp.bas-net.by. Tel.: +375 172 84 12 49, FAX: +375 172 84 08 88

Recently, considerable effort has been invested to gain a better and deeper knowledge of structural and physical properties of metal chalcogenide semiconductors because of their potential application in electrical and photonic devices. Among them, tin sulphide (SnS) has attracted attention because of band gap of 1.3 eV and an absorption coefficient greater than 10^4 cm^{-1} [1-3]. Additionally, by using tin sulfide compounds for photovoltaic devices, the production costs are decreased, because these materials are cheap and abundant in nature [4].

For the sythesis of SnS thin films by hot wall deposition, SnS ingots were used as the source materials synthesized from high purity elements (99.999%) [5]. The thin films were grown onto glass at substrate temperatures between 220 and 380 °C. The thickness of the films was in the range of 1.0 - 2.5 μm. The crystal structure and crystalline phases of the materials were studied by XRD using a Siemens D-5000 diffractometer with CuK_α (λ = 1.5418 Å) radiation. In order to consider instrumental error, the samples were coated by Si powder suspended in acetone. The composition and surface morphology of thin films were investigated by electron probe microanalysis (EPMA) using a CAMECA SX-100, a scanning electron microscope JEOL 6400 and an atomic force microscope (AFM, Model: NT 206), respectively. Depth profiling was performed by Auger electron spectroscopy (AES) using a Perkin Elmer Physical Electronics 590. The electrical resistivity was studied by van der Pauw four-probe technique using silver paste contact. The optical transmittance was carried out using a Varian Cary 50 UV–VIS spectrophotometer in the range 500 – 2000 nm.

The as-grown films exhibited a composition with a Sn/S at. % ratio of 1.06. The AES depth profiles revealed relatively uniform composition through the film thickness. The XRD analysis of the SnS films showed that they were monophase (JCPDS 39-0354), polycrystalline with orthorhombic crystal structure and preferential orientations (010) plane parallel to the substrate. The SEM analysis of the films showed densely packed crystallites of up to 1.5 μm long. The AFM studies revealed the formation of cluster of crystallites and improvement in grain size with growth temperature. The as-grown films were p-type conductivity and exhibited an electrical resistivity of (2 - 6) Ω·cm. The values of the activation energy (ΔE) were 0.12 - 0.13 eV. The thermopower value of SnS films varied from 240 $\mu v \cdot K^{-1}$ to 950 $\mu v \cdot K^{-1}$ depending on deposition parameters. The films showed absorption coefficients > $6 \cdot 10^4$ cm^{-1} above the fundamental absorption edge with an optical band gap in the range of 1.15 - 1.28 eV, indicating that these films adequate to be used as absorber material in thin film solar cells.

Acknowledgments: This work has been supported by the Deutsches Zentrum für Luft - und Raumfahrt e.V. (project DLR08/003) and DAAD (A/08/78852 and A/07/99716).

[1]. .M.G. Bawendi, W.L. Wilson, L. Rothberg, P.L. Carroll, T.M. Jedju, M.L. Teigerwald and L.E. Brus, *Phys. Rev. Lett.* **65** (1990), p. 623.
[2]. C.B. Murray, C.R. Kagan and M.G. Bawendi, *Science* **270** (1995), p. 1335
[3]. B. Ghosh, M. Das, P. Banerjee, S. Das, *Solar Energy Materials & Solar Cells* **92** (2008), p. 1099.
[4]. Jonathan J. Scragg, Philip J. Dale, Laurence M. Peter, Guillaume Zoppi and Ian Forbes, *Phys. Stat. Sol. B* **245** (2008), p. 1772.
[5]. D.M. Unuchak, K. Bente, G. Kloess, W. Schmitz, V.F. Gremenok, V.A. Ivanov and V. Ukhov, *Phys. Stat. Sol. C* **6** (2009), p. 1191.

P1-5

Growth features of HgCdTe LPE layers

Huseynov E.K., Eminov Sh.O, Ibragimov T.I., Ismaylov N.J, Rajabli A.A.

Institute of Physics of National Academy of Science, *H.Javid ave.33,* Az-1143, Baku, Azerbaijan

emil@azeuro.net; phone/fax (99-412)-432-4336

The results of growth of $Hg_{1-x}Cd_xTe$ (MCT) layers by liquid phase epitaxy (LPE) from Te-rich solutions (molar fraction $(Hg_{1-z}Cd_z)_{(1-y)}Te_y$, z=0.054, y=0.805 for T_L=501ºC) obtained by the tipping method in closed system is presented. Epitaxial layers with different compositions (x=0.20-0.22) and thicknesses (10-20 μm) suitable for manufacturing the photodiode structures operable at 8-14 μm spectrum range were grown on (111)B oriented $Cd_{0.96}Zn_{0,04}Te$ polished and repolished substrates. The growth was carried out in the temperature range 500-480°C with cooling rates 0.05-0.1°C/min in a sealed quartz ampoule using the original apparatus for LPE. The attention was paid mainly to the surface morphological quality, good decantation from the layers, uniformity of composition and thickness of films.

One of the limitations of the most LPE growth apparatus (cassettes) with slider or tipping system is their impossibility to wipe the last drop of growth solution from the surface of just-grown epilayer. Some remnant or residual of the growth solution tends to adhere to the surface of the epilayer after growth in such apparatus and strongly affect the surface quality. The novel apparatus for LPE providing the surface without unwanted residual drops of melt solution of Hg, Cd and Te was developed with the aim of solving such a problem.

The effect of different steps of LPE growth on morphology and composition of epitaxial layers was studied. By holding the CdZnTe substrate inside the growth ampoule at the melt homogenization temperature during of 15-50 min without contact with the melt resulted in visually (using the Leitz-orthoplan microscopes x 500-1000) observed surface roughness.

Using the expressions for the Te-angle of Hg-Cd-Te phase diagram the effect of the preliminary synthesis of the source on liquidus temperature and composition of the epilayers was numerically evaluated.

HgCdTe layers were characterized using different methods: microscopic examinations, optical transmission at 300K, X-ray diffraction and scanning electron microscopy measurements. The electrical properties of the layer at 77 K were measured by Van Der Pauw technique using a Bio-Rad system. Typical layers show that the as grown layers are *p*-type conductivity with a carrier concentration $1.4 \cdot 10^{17}$ cm^{-3} and mobility 260 cm^2 $V^{-1}s^{-1}$. Under thermal annealing at 200°C for 10 h in the presence of Hg overpressure, point defects, such as Cd, Te precipitates are annealed out and their size and density are reduced considerably causing improved transmission that is increased in 5-6 times. Redistribution of constituents Hg, Cd and Te takes place upon annealing that improves the homogeneity of the epilayer leading to the sharpening of absorption edge. The annealed layers display charge carriers concentration $9 \cdot 10^{16}$ cm^{-3} and a mobility $1.1 \cdot 10^4$ cm^2 $V^{-1}s^{-1}$.

P1-6
Structural and Optical Properties of Cobalt Doped Sprayed ZnO Films

V. Supriya[1], T. Sato[2], M. Sugiyama[2] and K.T. R. Reddy[1a]

[1]Thin Film Laboratory, Department of Physics, Sri Venkateswara University, Tirupati – 517 502, India.
[2]Department of Electrical Engineering, Tokyo University of Science, Noda 278-8510, Japan.

[1a]Corresponding author: Email: ktrkreddy@rediffmail.com Tel: +918772289472; Fax: +91 877 2289555

The dilute magnetic semiconductors (DMS) are promising materials for many device applications that include spintronics as they have charge and spin degrees of freedom in a single substance [1]. The $A^{II}_{1-x}TM_xB^{VI}$ materials are widely studied materials due to the higher solubility of magnetic atoms in them. Among the II–VI oxide based DMS, transition-metal-doped ZnO is currently attracting much attention due to its wide band gap and exhibits ferromagnetism at room temperature [2, 3]. In recent years, $Zn_{1-x}Co_xO$ has attracted special attention due to the highest solubility of Co in ZnO matrix and is expected to behave as a dilute magnetic semiconductor which exhibits ferromagnetic properties. In our earlier study, the effect of Co-composition on the physical properties of $Zn_{1-x}Co_xO$ films have been investigated [4]. In the present study, thin films of cobalt doped ZnO were deposited on glass substrates by chemical spray pyrolysis at various deposition temperatures that vary in the range, 260 - 350 ° C. 0.1M aqueous solutions of zinc acetate (Zn $(CH_3COO)_2.2H_2O$) and cobalt acetate (Co $(CH_3COO)_2 .4H_2O$) were taken as precursors. The as-grown layers were characterized by different techniques to know their physical properties. The X-ray diffraction studies revealed that all the layers exhibited wurtzite structure with the (002) plane as the preferred orientation and the incorporation of cobalt into ZnO host matrix was found to be uniform without the of secondary phases. The grain size of the films was varied in the range, 20 - 40 nm. The average optical transmittance of the films was found to be > 75% in the visible region and the evaluated optical band gap of the films decreased from 3.22 eV to 3.37 eV with the increase of substrate temperature. The details of these results were reported and discussed.

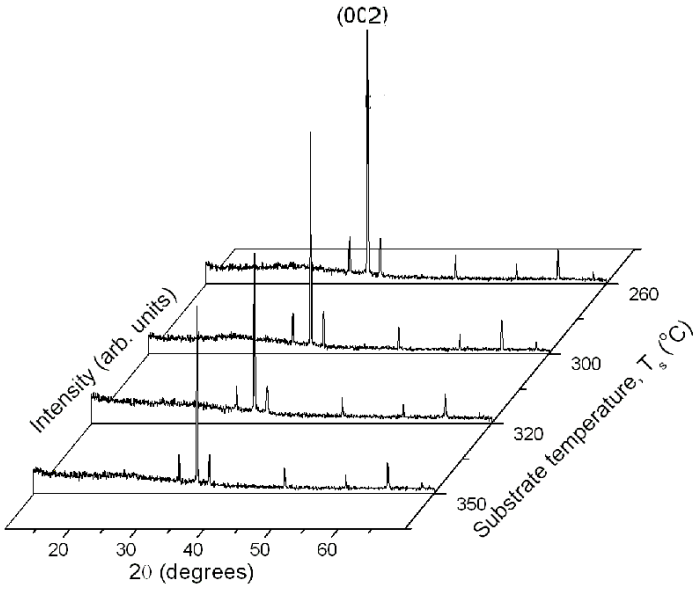

Figure 1: XRD spectra of $Zn_{1-x}Co_xO$ films as a function of T_s.

[1]. A. Dinia, G. Schmerber, V. P. Bohnes, C. Meny, P. Panissod, E. Beaurepaire, J. Magn. Magn. Mater., 286 (2005) 37
[2]. K. Sato, H. Katayama-Yoshida, Physica B, 308 (2001) 904.
[3]. K. Sato, H. Katayama-Yoshida, Jpn. J. Appl. Phy., 40 (2001) L334.
[4]. V. Supriya, P. Prathap, M. Sugiyama and K.T. Ramakrishna Reddy, E-MRS Spring Meeting, 7 – 11 June 2010, Strasbourg, France.

P1-7

Investigations on Al-doped ZnMnO films deposited by chemical spray

L.Rajamohan Reddy[1], P. Prathap[2], N. Revathi[1], T. Sato[3], M. Sugiyama[3] and K.T.R.Reddy[1a]

[1]Thin Film Laboratory, Department of Physics, Sri Venkateswara University, Tirupati – 517 502, India.
[2]InESS-CNRS, F-67037 Strasbourg Cedex-2, France
[3]Department of Electrical Engineering, Tokyo University of Sciences, Noda, Japan.

[1a]Corresponding author: Email: ktrkreddy@rediffmail.com, Tel: +918772289472; Fax: +91 877 2289555,

Recently various oxide based dilute magnetic semiconductors (DMS) are being investigated for their potential application in different fields [1]. Among these, $Zn_{1-x}Mn_xO$ is one of the prominent materials that has an attractive fundamental properties suitable for device applications that includes spintronics as they have charge and spin degrees of freedom in a single substance [2]. In our earlier work, the effect of Mn-composition and deposition temperature on the physical and magnetic properties of the $Zn_{1-x}Mn_xO$ films have been investigated [3, 4]. From these studies, we have observed that the presence of Mn^{2+} substitution for Zn^{2+} is simply not sufficient for observation of good ferromagnetic behavior at room temperature and creation of more free carriers is necessary for the improvement of the ferromagnetic property in this material. Hence in this study, aluminum doped $Zn_{1-x}Mn_xO$ thin films have been synthesized by chemical spray pyrolysis on Corning 7059 glass substrates at a constant temperature of 400 ^oC. The 'Al' composition in the layers was varied in the range, 0.0-0.07 and 'Mn' composition in the layers was fixed at x = 0.15. The compositional analysis shows the presence of zinc, manganese, oxygen and aluminum without any other impurities. All the films were polycrystalline and showed the hexagonal wurtzite structure of ZnO with (002) crystal plane as the predominant orientation. From the Raman analysis an intense E_2 mode was observed in all samples, which is attributed to the non-polar optical phonon mode of ZnO. The film exhibited a maximum optical transmittance of > 60% and the evaluated band gap was 3.22 eV at a Al-doping level of 0.07. The highest remanent magnetization of $3.14x10^{-4}$ emu and coercive field of 464.8 Oe was observed in this study for a Al-doping of 0.07. The crystallite size, morphology, optical band gap and electrical resistivity were found to be significantly affected by changing the 'Al' concentration.

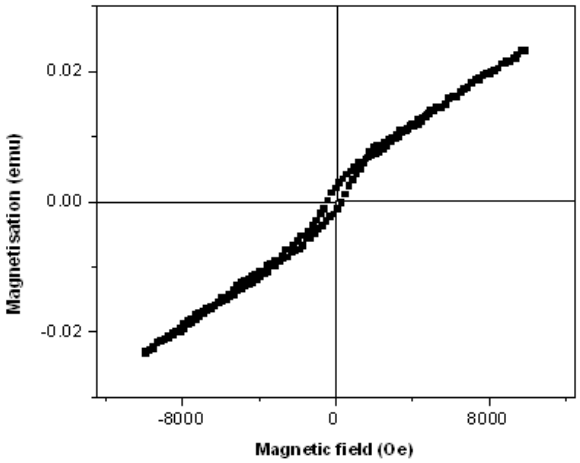

Figure 1. M-H curve of $Zn_{0.78}Mn_{0.15}Al_{0.07}O$ film recorded at 10 K.

[1]. H.Ndilimabaka, S.Colis, G.Schmerber, D.Muller, J.J.Grob, L.Gravier, C.Jan, E.Beaurepaire, A.Dinia, Chem. Phys. Lett., 421 (2006) 184.
[2]. A.Dinia, G.Schmerber, V.Pierron-bohnes, C.Meny, P.Panissod, E.Beaurepaire, J. Magn, Magn. Mater. 286 (2005) 37.
[3]. L. Rajamohan Reddy, P. Prathap and K.T. Ramakrishna Reddy, Current Appl. Phys., 9 (2009) 667.
[4]. L. Rajamohan Reddy, P. Prathap and K.T. Ramakrishna Reddy, Solid State Sci., 9(2007) 718.

P1-8

Annealing temperature dependence of properties of Cu_2ZnSnS_4 thin films prepared by sol-gel sulfurizing method

Kazuya Maeda, Kunihiko Tanaka and Hisao Uchiki

Department of Electrical Engineering, Nagaoka University of Technology, 1603-1 Kamitomioka, Nagaoka, Niigata 940 2188, Japan

maeda@stn.nagaokaut.ac.jp, +81-258-47-9527/+81-258-47-9500

Cu_2ZnSnS_4 (CZTS) has a direct band gap of ~1.4 eV which is very close to an ideal band gap for photovoltaic devices and high absorption coefficient of the order of 10^4 cm^{-1}.[1)] In addition, CZTS is a low environmental lode because of not containing toxic and rare materials. Therefore, CZTS is a promising candidate as a new type absorption layer for thin film photovoltaic devices. In our laboratory, CZTS thin films are deposited by sulfurizing oxyhydroxide precursors which are prepared by sol-gel method. This process is named "sol-gel sulfurizing method". We have reported that a CZTS thin film solar cell was fabricated and demonstrated a 1.61% efficiency with V_{OC} = 554 mV, I_{SC} = 6.70 mA/cm^2 and $F.F$ = 0.434.[2)] In this report, in order to improve grain size of the CZTS, the influence of sulfurizing temperature was investigated.

CZTS thin films were deposited by sol-gel sulfurization method. Solution for CZTS precursors was prepared from copper (II) acetate monohydrate, zinc acetate dehydrate, tin (II) chloride dehydrate, 2-methoxyethanol (2-metho) and monoethanolamine (MEA). The solution was spin coated onto a soda lime glass substrate and dried in the air at 300°C. These precursors were sulfurized in a N_2 + H_2S(5%) atmosphere for 60 min at different temperatures from 500°C to 600°C after the samples were preheated at 250°C for 60 min in order to prevent CZTS thin films from detaching from the soda lime glass substrate. The rate of temperature increase was kept at constant of 100°C/min.

Figure 1 shows the XRD pattern of the thin film sulfurized at 580°C. XRD studies showed that the thin film had the kesterite structure and the preferred orientation to the (112). Figure 2 shows the transmission and reflection spectra of the thin film sulfurized at 580°C. The transmittance in the infrared region is ~50% which indicated the existence of S defects and organic compounds in the thin film.

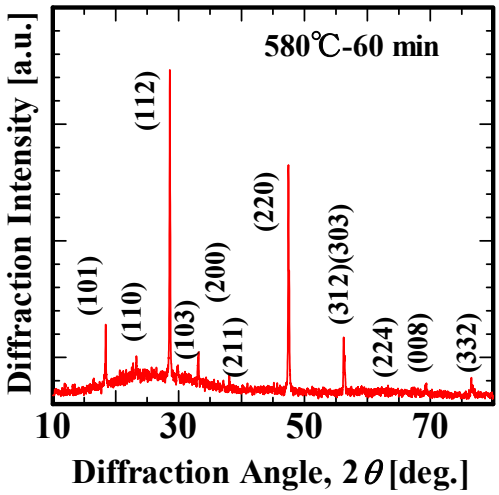

Figure 1. XRD pattern of the thin film annealed at 580°C for 60 min.

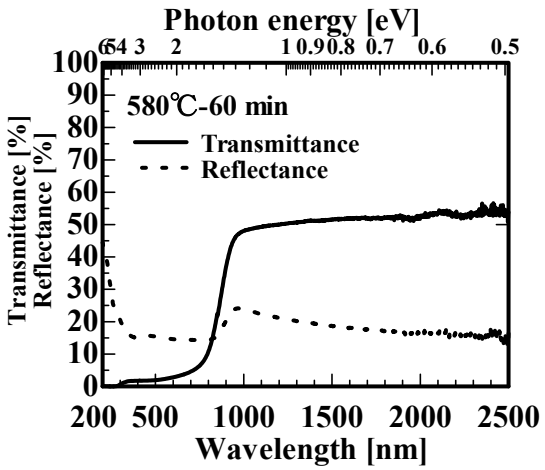

Figure 2. Transmission and reflection spectra of the thin film annealed at 580°C for 60 min.

[1]. Kunihiko Tanaka *et al.*: Sol. Energy Mater. Sol. Cells **91**, 1199 (2007).
[2]. Noriko Moritake *et al.*: Phys. Stat. Sol. **C6**(5), 1233 (2009).

P1-9

H_2S concentration dependence of properties of Cu_2ZnSnS_4 thin film prepared under non-vacuum condition

Kazuya Maeda, Kunihiko Tanaka and Hisao Uchiki

Department of Electrical Engineering, Nagaoka University of Technology, 1603-1 Kamitomioka-machi, Nagaoka, Niigata 940-2188, Japan

e:mail maeda@stn.nagaokaut.ac.jp, phone +81-258-47-9527/fax +81-258-47-9500

Cu_2ZnSnS_4 (CZTS) is one of promising materials as an absorber layer of thin film solar cells because of its optimal band gap of 1.5 eV and large absorption coefficient of larger than 10^4 cm^{-1}. Furthermore all constituent elements of CZTS are abundant in the crust of the earth and non-toxic.
In our previous reports, CZTS absorber layer was prepared under non-vacuum condition by sol-gel sulfurizing method to reduce cost [1,2]. By the sol-gel sulfurizing method, precursors of the CZTS absorber layer were prepared by coating aqueous sol-gel solution containing Cu, Zn and Sn ions and then the precursors were sulfurized in N_2+ H_2S (5%) atmosphere. Since the chemical composition of sulfur in the CZTS absorber layer affects the properties of the CZTS solar cell, in this report dependence of properties of CZTS thin film and CZTS solar cell on H_2S concentration in the sulfurizing process was investigated.

In this study chemical compositions of starting material were Cu/(Zn+Sn) = 0.87 and Zn/Sn =1.15. The precursors were sulfurized at 500ºC for 1 hour. H_2S concentrations of sulfurizing process were 3, 5, 10 and 20%.

Table 1. H_2S concentration dependence of CZTS chemical composition.

H_2S	Cu/(Zn + Sn)	Zn/Sn	S/metal
3%	0.898	1.327	0.881
5%	0.968	1.158	0.810
10%	0.939	1.215	0.851
20%	0.917	1.311	0.909

Table 1 shows that the chemical composition of CZTS thin films depends on H_2S gas concentration. The chemical composition of the CZTS films showed the same relation to that of the sol-gel solution, Cu poor and Zn rich tendency. The chemical composition of S decreases from 20% to 5% as H_2S concentration decreases, but at 3%, S concentration increases again.

Figure 1 shows H_2S concentration dependence of surface images of CZTS. The grain size of CZTS decreases from 20% to 5% as H_2S concentration deceases, but at 3%, the grain size increases again. CZTS films of 3% and 20% are constructed with packed large grains and the size of grains is larger than 1 μm. The CZTS film of 5% is composed of ~100nm sized grains and the CZTS film of 10% is composed of a few 100nm sized grains and there are void more than 5%.

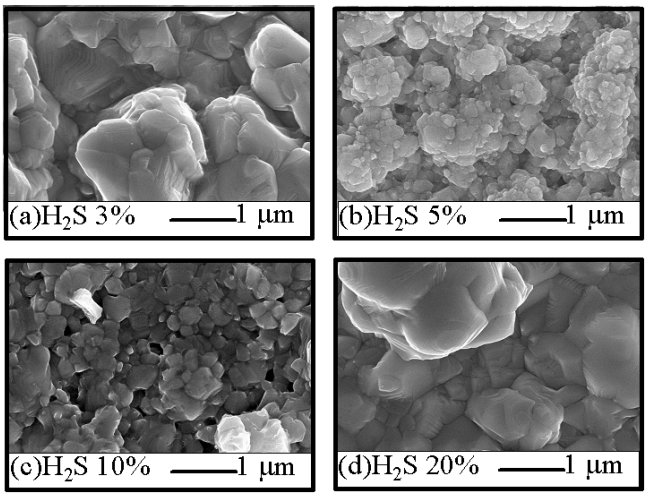

Fig. 1 H_2S dependence of surface images of CZTS

Acknowledgments: A part of this research receives help from the Grants-in-Aid for Scientific Research (No. 21760231) and The Uchida Energy Science Promotion Foundation.

[1]. K. Tanaka, N. Moritake, and H. Uchiki, *Sol. Energy Mater. Sol. Cells* **91** (2007), 1199.
[2]. N. Moritake, Y. Fukui, M. Oonuki, K. Tanaka, and H. Uchiki, *Phys. Status Solidi* **C 6** (2009), 1233.

P1-10

Electrical properties of Ga-doped ZnO transparent conducting films prepared at temperatures close to room temperature

T. Matsumoto[*1], K. Mizuguchi[1], T. Horii[1], S. Sano[1], T. Muranaka[1], Y. Nabetani[1], S. Hiraki[2], H. Furukawa[2], A. Fukasawa[2], S. Sakamoto[2], S. Hagihara[3], Y. Kono[3], K. Kijima[3], O. Abe[3] and K. Yashiro[3]

[1] Department of Electrical Engineering, University of Yamanashi, Takeda 4, Kofu 400-8511 Japan
[2] Nakaya Corporation, Showacho, Nakakoma, Yamanashi 409-3853 Japan
[3] Yamanashi Industrial Technology Center, Otsu, Kofu 400-0055 Japan

[*]Corresponding author: e-mail:matumoto@es.yamanashi.ac.jp, phone:+81-55-220-8459, fax:+81-55-220-8777

Transparent conducting films (TCF) are key components of opt-electronic devices such as solar cells, image sensors, light emitting diodes and flat panel displays. Indium thin oxide (ITO) has been the most commonly used material for TCF. Ga-doped ZnO (GZO) is a promising alternative to ITO because of its low resistivity, high transparency, nontoxicity and resource abundance. Recent ZnO TCF studies have aimed two goals. One is to lower deposition temperatures close to room temperature for depositing on flexible plastic sheets. The other is to achieve damage-free deposition. The deposition technique widely used in industry is sputtering. During sputtering, high energy particles may damage TCF itself and also devices such as solar cells underlying the TCF.

In this study we have grown GZO TCF on glass and flexible plastic substrates at temperatures close to room temperature, and resistivities as low as 3×10^{-4} Ωcm have been achieved on plastic sheets. The effects of substrate temperature (T_{sub}) and Ga doping on the electrical properties and crystalline structure of the GZO films are discussed.

Ga-doped and undoped ZnO films of thickness of ~200 nm were grown by using plasma assisted deposition technique [1] at temperatures of 50 ~ 300°C. Zinc and gallium vapours were supplied by heating metallic sources. Oxygen was excited in a microwave cavity and neutral atomic radicals were supplied onto the substrate. The oxygen plasma was confined in the plasma cell and therefore the growing film was isolated from the plasma and not attacked by ions. Grown films were characterized by Hall measurements, X-ray diffraction, optical transmittance, SEM and AFM.

With increasing the Ga cell temperature, the carrier concentration (n) in GZO films increased from the mid 10^{18} cm^{-3} of undoped ZnO to around 9×10^{20} cm^{-3} both for T_{sub} = 300°C and 50°C. The carrier concentration increased nearly proportional to Ga/Zn supply ratio up to $n \approx 4\times10^{20}$ cm^{-3}, and after that the increasing rate became smaller. Ga-doping effect on carrier mobility (μ) was quite different between the high- and low-temperature growth. For high-temperature growth, the carrier mobility slightly increased from 22 to 25 cm^2/Vs with the increase in n. Contrarily, for 50°C growth, the carrier mobility decreased from 28 cm^2/Vs of undoped ZnO to 8 cm^2/Vs for $n = 9\times10^{20}$ cm^{-3}. All GZO films showed a single XRD peak at around 2θ = 34.4°, suggesting that the GZO films had the wurtzite structure with their c-axes perpendicular to the substrate surface. The FWHM of the (0002) diffraction peak was almost independent of T_{sub} and Ga doping. The FWHM was determined by grain size, not by the crystallinity in each grain. The peak position of the (0002) peak varied with T_{sub} and Ga doping. The lattice constant c of films grown at 300°C was smaller than that of bulk ZnO crystal, which indicated that the GZO films included in-plane tensile strains due to thermal expansion mismatch between the film and the substrate, but was independent of Ga doping. When T_{sub} was 50°C, the lattice constant c was almost same as that of bulk ZnO crystal for films with n less than mid 10^{19} cm^{-3} because of small effect of the thermal expansion mismatch for low T_{sub}. However, as n increased over 10^{20} cm^{-3}, the lattice constant c and a became larger. The observation suggested that Ga atoms were introduced into interstitial sites at high doping levels and degraded the crystallinity in each individual grain.

The slight increase in μ with Ga doping of the high-temperature grown GZO was explained as screening effect of the scattering potentials due to ionized impurities and grain boundaries. The decrease in μ of 50°C-grown GZO with high doping levels was explained due to defect scattering in each individual grains.

[1]. A.Nishii, T.Uehara, T.Sakano, Y.Nabetani, T.Akitsu, T.Kato, T.Matsumoto, S.Hagihara, O.Abe, S.Hiraki, and Y.Fujikawa, *Phys. Status Solidi. (a)* **203**(2006), p.2887.

P1-11

Growth and characterization of GaInAsSb solid solutions with composition near the miscibility gap boundary

N. Mursakulov[1], I.A. Andreev[2], E.V. Kunitsyna[2], Yu.P. Yakovlev[2], M. Ahmetoglu[3] (Afrailov), G. Kaynak[3]

[1] Institute of Physics ANAS, G. Javid ave. 33, AZ1143 Baku, Azerbaijan
[2] Ioffe Physical-Technical Institute RAS, 26 Politekhnicheskaya st., 194021 St Petersburg, Russia
[3] Department of Physics, Uludag University, 16059 Gorukle, Bursa, Turkey

nmursakulov@physics.ab.az

The materials based on GaSb have been attracting much interest because of their importance in semiconductor device technology. These semiconductors are the most promising for the fabrication of optoelectronic devices in mid infrared spectral range. Unfortunately, a solid phase miscibility gap limits the working wavelength domain of GaInAsSb solid solutions.

In this paper we present the important aspects of growth by LPE and characterization of the GaInAsSb solid solutions with composition in the vicinity of the miscibility gap boundary. The main drawback of a near-equilibrium technique such as LPE is lack of exact data on a thermodynamic description of the coexisting phases – melt and solid solution – that makes difficulties for obtaining materials. The original thermodynamical model [1] based on the third order virial descending for mean free mole Gibbs energy of the melt onto the mole portion of each component has been used for phase equilibrium diagram calculating. The use of Pb as a neutral solvent [2] in growth of the GaInAsSb solid solutions offered to obtain the undoped material with low concentration of defects and impurities, as well as high carrier mobility. The effect of the influence of the GaSb substrate crystallographic orientation on composition of the GaInAsSb solid solutions was investigated. The chemical composition of the obtained GaInAsSb solid solutions was determined by the method of quantitative x-ray spectral analysis using a JXA-5 CAMEBAX microanalyzer. It was found that using a GaSb substrate with (111)B orientation makes it possible to increase the indium content in the solid phase and to obtain the material with narrower band gap.

Based on the GaInAsSb solid solutions with composition near the miscibility gap boundary the long-wavelength photodiodes (λ_{th}=2.55 μm) have been created. The monochromatic current sensitivity for the fabricated photodiodes at the λ_{max}=2.2-2.4 μm is S_λ=1.1-1.2 A/W, which corresponds to a quantum efficiency of 0.6-0.7 without anti-reflection coatings. The estimated temperature coefficient of the $\lambda_{50\%}$ shift is 1.6 nm×K^{-1}. The capacitance of the photodiode with the sensitive element diameter of 1.0 mm is 450 pF at the zero bias.

The proposed technique shows a great potential for creating the GaInAsSb-based light emitting diodes, photodiodes, thermophotovoltaic devices, optical sensors [2] for 1.8-3.0 μm spectral range.

The work is supported in part by the Russian Foundation of Basic Research (RFBR) through Grant No. 09-08-91224, and of the Scientific and Technological Research Council of Turkey (TÜBİTAK) under Grant No: 108T325.

[1]. A.M. Litvak, and N.A. Charykov, Zh. of Inorganic Materials, **27** (1990) p. 225.
[2]. M.Mikhailova, N.Stoyanov, I.Andreev, B.Zhurtanov, S.Kizhaev, E.Kunitsyna, K.Salikhov and Yu.Yakovlev. SPIE **6585** (2007), p.658526-1.

P1-12

Mechanochemical synthesis of Ce-doped $CaGa_2S_4$

Takumi Ohta, Kunihiko Tanaka and Hisao Uchiki

Department of Electrical Engineering, Nagaoka University of Technology, 1603-1 Kamitomioka, Nagaoka, Niigata 940-2188, Japan

takumio@stn.nagaokaut.ac.jp, +81-258-47-9527/+81-258-47-9500

One of the alkaline thiogallates, $CaGa_2S_4$, has a wide band gap of 4.2 eV. $CaGa_2S_4$ is regarded as promising host to rare earth Ce and Eu to apply in flat panel displays and lasers.[1] Many studies on the growth of its bulk and film forms have been reported so far. The mechanochemical method is a simple method and it would be suited to the mass production. Mechanochemical synthesis of powders has been reported for a variety of materials, e.g., for sulfides, As_2S_3[2] and CaS[3], but not for alkaline-earth metal thiogallates.

In this study $CaGa_2S_4$:Ce was synthesized by mechanochemical reaction of CaS, Ga_2S_3 and Ce_2S_3 source powders with use of a planetary ball milling apparatus. The growth process was studied by observing XRD patterns and Raman scattering spectra of the milled powder as a parameter of milling time as shown in Figs. 1 and 2.

Within 2.5-h milling the diffraction lines from the source powders become weak gradually and any diffractions from $CaGa_2S_4$ did not appear. In this reaction stage the crystalline source powders become amorphous and/or were broken by high-energy milling and no $CaGa_2S_4$ crystallites were generated, whereas the mechanochemical reaction started to take place because Raman scattering from $CaGa_2S_4$ was observed in the powder milled for 2.5 h as shown in Fig. 2 . After 3-h milling the X-ray diffractions from $CaGa_2S_4$ appeared and grew as milling while the diffractions from the source powders become weak gradually. For 5-h milling the reaction completed and no distinct change in the patterns after 5-h milling was observed.

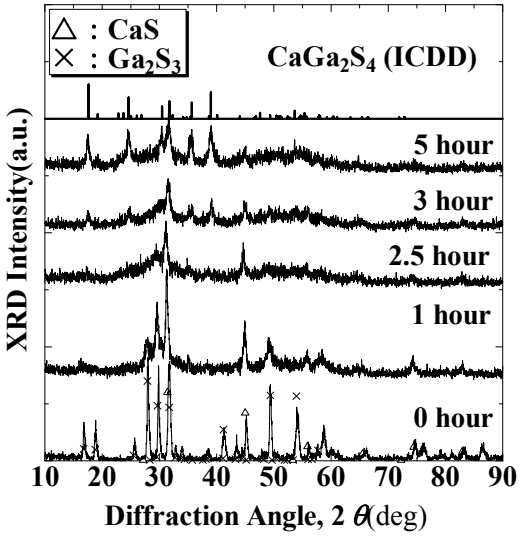

Figure 1. X-ray diffraction patterns of the starting materials and mechanically-milled samples at several milling times.

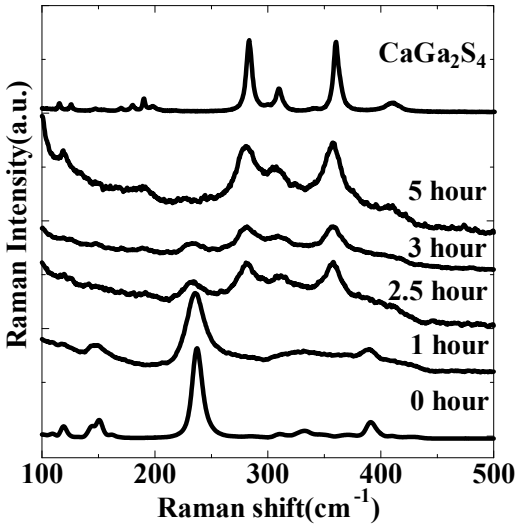

Figure 2. Raman scattering spectra of the starting materials and mechanically-milled samples at several milling times.

[1]. Y. Shim, N. Mamedov, N. Yamamoto, Thin Solid Films **244–247** (2004) 455.
[2]. T. Tsuzuki, J. Ding, P.G. McCormick, Physica **B 239** (1997) 378.
[3]. T. Tsuzuki, P.G. McCormick, Nanostructured Materials **12** (1999) 75.

P1-13

Fabrication of $Cu(In,Ga)Se_2$ thin films by sputtering and selenization using diethylselenide

T. Sato[1], Y. Kawasaki[1], M. Sugiyama[1] and S. F. Chichibu[2]
[1] Department of Electrical Engineering, Tokyo University of Science, 2641 Yamazaki, Noda 278-8510, Japan
[2] CANTech, Institute of Multidisciplinary Research for Advanced Materials, Tohoku University, 2-1-1 Katahira, Aoba, Sendai 980-8577, Japan

Presenting author optoelec@rs.noda.tus.ac.jp, phone/ fax number +81-4-7121-1585 (T. Sato)

Chalcopyrite structure $CuIn_{1-x}Ga_xSe_2$ (CIGS) alloys are used as light-absorbing medium in high conversion efficiency, low cost, lightweight, and radiation-resistant solar cells. The ideal band gap energy for solar cells is known to be 1.4 eV, which corresponds to the band gap of $CuIn_{0.4}Ga_{0.6}Se_2$. However, growing $CuIn_{0.4}Ga_{0.6}Se_2$ alloys or CIGS solid solutions of high $CuGaSe_2$ (CGS) molar faction is difficult because of unwanted compositional separation caused by the difference in reaction rates of the two end-point compounds.

The morphology and crystal structure of the CIGS thin films strongly depend on the heating profile and the time of each step during the selenization process. However, few experimental results have been reported. In this presentation, we will introduce fabrication of CIGS thin films by selenization using diethylselenide [$(C_2H_5)_2Se$: DESe] as a selenization source.

Cu-In-Ga precursors were deposited on Mo by RF magnetron sputtering. The precursors were selenized using DESe [1] under atmospheric pressure [2]. As shown in the inset of Fig 1, the selenization process was performed by two sequential stages. First, the precursors were selenized at 300 °C for 20 min (first step). Then, the precursors were heated to 515 °C and selenized for 60 min (second step).

The XRD patterns of CIGS thin films by selenization are shown in Fig. 1. The precursor consisted of $Cu_{11}In_9$ alloy before selenization (Fig.1(a)). The film selenized at 300 °C for 10 min had binary compounds such as Cu-Se, In-Se, Cu-In except CIGS (Fig.1(b)). After the first step selenization at 300 °C for 20 min, the Cu-Se alloy was not observed (Fig.1(c)). The film selenized at 515 °C for 60 min had only a CIGS chalcopyrite phase without an extra phase (Fig.1(d)). These results indicate that the films selenized at 300 °C are due to insufficient of CIGS growth, and phase transformation occurred during the selenization process when using H_2Se or elemental Se as a selenization source.

Acknowledgments: This work was supported in part by the Advanced Device Laboratories, Research Institute for Science and Technology, Tokyo University of Science.

[1]. S. F. Chichibu *et al.*, J. Cryst Growth, 243 (2002) 404.
[2]. M. Sugiyama *et al.,* Thin Solid Films, 515 (2007) 5867.

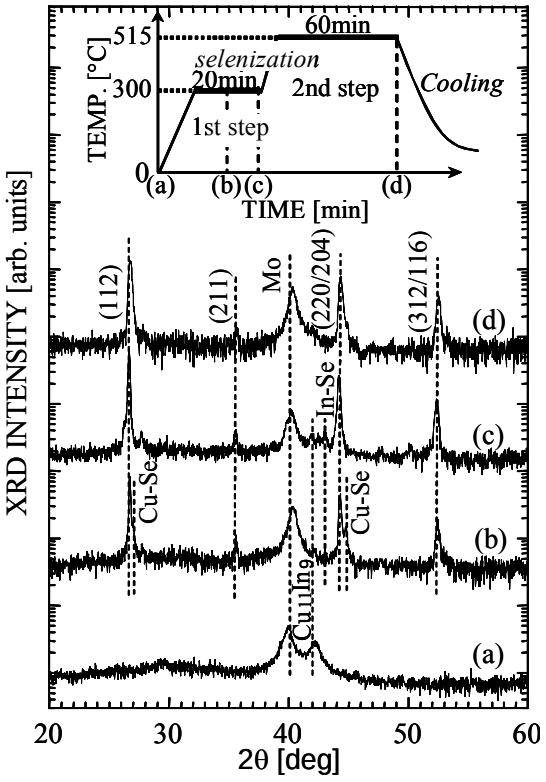

Fig. 1 XRD patterns of CIGS thin film by selenization. The insert shows growth sequence of selenization.

P1-14
Growth of γ-In_2Se_3 thin films by electrostatic spray pyrolysis deposition

Takamasa Kato[1], Toshitaka Hiramatsu[1] and Norio Onojima[1]

[1] Interdisciplinary Graduate School of Medicine and Engineering, University of Yamanashi, Takeda 4, Kofu 400-8511, Japan

kato@yamanashi.ac.jp, +81-55-220-8460

The electrostatic spray pyrolysis deposition (ESPD) growth technique has the advantages that the crystal growth is carried out in a non-vacuum atmosphere, the sizes of the droplets are very small below an order of micrometer and the growth rate is slow compared with the conventional spray pyrolysis deposition (SPD) technique. Therefore, it is expected to grow good crystalline thin films at a low cost. The γ-In_2Se_3 is an attractive material for a top cell of tandem-type solar cells because of its energy gap value of 1.9eV [1,2]. However, the In_2Se_3 system has usually been grown under a vacuum such as an MBE or a vacuum evaporation technique [1-3]. There are few reports about the SPD growth [4] or ESPD growth of In_2Se_3. In this abstract, we report the growth and the characterization of γ-In_2Se_3 films by the ESPD growth technique.

$InCl_3$ and N,N-Dimethyl selenourea were used as source materials and they were dissolved in ethanol. The typical concentration of $InCl_3$ was 6×10^{-3} mol/l and the Se/In atomic ratio ranged from 1.2 to 5. The film thickness was about 1 μm after a 3 h growth period under an applied voltage of 25kV between the source solution and the glass substrates.

Figure 1 shows the XRD spectra of films grown at a constant Se/In ratio of 2.0 and various substrate temperatures (T_s). The γ-In_2Se_3 peaks were observed at the substrate temperature (T_s) range from 235 to 280 °C. The growth of γ-In_2Se_3 was also confirmed by the Raman spectrum peak located at 151cm^{-1}, which was known as a γ-In_2Se_3 mode peak [5]. The InSe was grown below 215 °C as shown in Fig.1. The γ-In_2Se_3 (0006) diffraction peak becomes dominant around T_s =250 °C. The full width at half maximum of this peak had a minimum value at around T_s=250 °C. The diffraction intensity ratio of (11-20) /(0006) also had a minimum value of about 0.02 at this T_s. This shows that the grown films are strongly oriented to [0001] direction. The film thickness decreases with decreasing In concentration of the solution. Hexagonal shape grains with diameters of 0.4-0.5μm were observed in the surface morphology and their sizes also decrease with decreasing In concentration. The films were oriented to the [0001] direction for higher Se/In ratios up to 5.0. On the other hand, weak (11-20) and (30-30) diffraction peaks appeared and the (0006) peak disappeared for the low Se/In ratio of 1.3. When the Se/In ratio was 1.0, only InSe was grown. α-In_2Se_3 crystal was not observed in this study. This is favorable for the growth of the top cell of tandem type solar cells, because the energy gap of the α-In_2Se_3 is about 1.3eV. The optical band gaps, which were estimated from the plots of $(\alpha h\nu)^2$ vs. hν, were about 1.94eV for the films grown at T_s ≥235 °C. This value is in good agreement with the estimation by the CL measurement [1]. The resistivity of the films was an order of 10^2 Ωcm.

In summary, γ-In_2Se_3 can be grown by the ESPD technique. The films were strongly oriented to [0001] direction and the band gap was about 1.94eV.

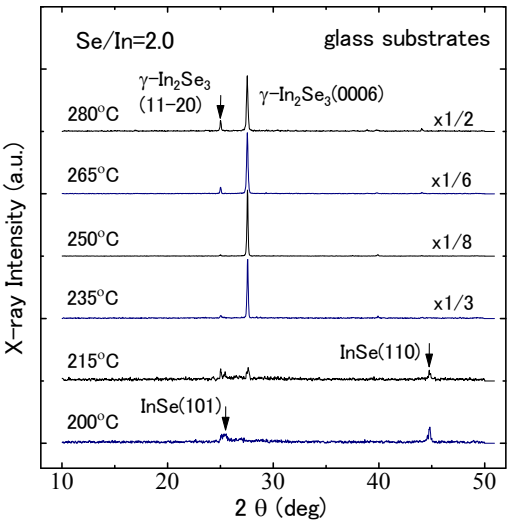

Figure 1. XRD spectra of grown films.

[1]. T. Ohtsuka, T. Okamoto, A. Yamada and M. konagai, J. of Luminescence **87-89** (2000), p.293.
[2]. C. H. de Groot and J. S. Moodera, J. Appl. Phys. **89** (2001), p.4336.
[3]. T. Kato, Y. Utsugi, T. Ohara, T. Muranaka, Y. Nabetani and T. Matsumoto, J. Crystal Growth **311** (2009), p.847.
[4]. H. Bouzouita, N. Bouguila, S. Duchemin, S. Fiechter and A. Dhouib, Renewable Energy **25** (2002), p.131.
[5]. K. Kambas, C. Julien, M. Jouanne, A. Likforman and M. Guittard, Phys. Status Solidi (b) **124** (1984), p. K105.

P1-15

Analysis of barrier height inhomogeneity for bismuth Schottky contacts on the layered *p*-GaTe compound

B. ABAY[1] and Y. K. YOĞURTÇU[2]

[1] Atatürk University, Faculty of Science, Physics Department, 25240, Erzurum, TURKEY
[2] İstanbul Aydın University, Faculty of Science and Arts, Sefaköy-Küçükçekmece, İstanbul, TURKEY

e-mail: babay@atauni.edu.tr, Tlf: 90 442 231 4181, Fax: 90 442 236 0948

The Metal-Semiconductor (MS) structures are important research tools for the characterization of new semiconductor materials and the fabrication of these structures plays a crucial role in constructing some useful devices in technology. This highly productive characteristic of the MS structures can be merged with the unique feature of the layered crystals, which have covalently bonded two-dimensional sandwich layers that are separated from each other along the third dimension *c* by only weak interlayer interactions and often referred to as van der Waals-like [1], to obtain some useful knowledge for this area of the semiconductor technology. Layered chalcogenides such as GaTe, GaSe and InSe can easily be cleaved across their van der Waals gap between the layers which leads to the outer surfaces closely resembling the inner ones. This cleavage planes have been found to be free of dangling bonds and proved to be very inert to chemical reactions, and these features leads us to consider them as idealized substrates for the investigation of fundamental aspects of surface or interface reactions [2].

Single crystals of GaTe binary compound were grown by the directional freezing method from a stoichiometric melt in a carbon coated and vacuum sealed quartz ampoules. Ohmic contacts of low resistance on the backside of the freshly cleaved samples were formed by evaporating of indium followed by a temperature treatment at 220 ^{o}C for 3 minutes in nitrogen atmosphere. The Schottky contacts were formed on the other face of the sample by evaporating Bi as dots with diameters of 1.0 mm. The current-voltage (*I-V*) and capacitance-voltage (*C-V*) measurements of the devices were measured by using a computer controlled Keithley 487 Picoammeter/Voltage Source and HP4280A capacitance meter at 1 MHz modulation frequency, respectively.

The effective barrier heights (BHs) ideality factors (*n*) and serial resistances of identically fabricated Bi/*p*-GaTe Schottky Barrier Diodes (SBDs) (25 dots) have been calculated from their experimental *I-V* and *C-V* characteristics. A statistical study related to the experimental BHs and ideality factors of the diodes has been made. The BHs obtained from the *I-V* and *C-V* characteristics varied from 0.668 to 0.724 eV and 0.726 to 0.787 eV, respectively. The values of *n* varied from 1.079 to 1.245 and the serial resistances varied from 66.82 to 72.39 Ω. The results showed that all parameters of SBDs differ from one diode to another even if they are identically prepared. The experimental BH, ideality factor and serial resistance distributions are fitted by a Gaussian function, and their mean values were found to be 0.699±0.015 eV, 0.759±0.016 eV, 1.147±0.040 and 69.88±1.39 Ω, respectively. The lateral homogeneous SBH ($\varphi_{\text{hom.}}$) value of 0.760 eV for the Bi/*p*-GaTe contacts has been obtained from the $\varphi_{\text{eff.}}$ vs. *n* plot by using $n_{\text{imf.}} = 1.018$ and $\Delta\varphi_{\text{imf.}} = 32.3$ meV. It has been seen that the mean effective BH obtained from the *C-V* measurements is correlate well with the $\varphi_{\text{hom.}}$. The good agreement of these parameters indicates that the SBH inhomogeneity of Bi/*p*-GaTe SBDs can be well described by spatial distributions of BH, that is, electron transport at the MS interface is significantly affected by nanoscale spatial variations [3].

[1]. Lee P A (Editor), "Optical and Electrical Properties of Layered Materials" (Dordrecht: Reidel 1976), p. 1
[2]. O. Lang, R. Schlaf, C. Pettenkofer and W. Jaegermann *J. Appl. Phys.* **75** (1994), p. 7805.
[3]. R.T.Tung, *Mater.Sci.Eng.***35** (2001)p. 1.

P1-16

Ionic conductivity and twin structure configuration change in LSGM

T. Tataryn[1], D. Savytskii[1], E. Schmidbauer[2], C. Paulmann[3], U. Bismayer[4]

[1] Lviv Polytechnic National University, 12 Bandera Str., 79013, Lviv, Ukraine
[2] Geophysics, Munich University, Theresienstr. 41, D-80333 Munich, Germany
[3] HASYLAB, DESY, Notkestr. 85, D-22603 Hamburg, Germany
[4] Min.-Petrogr. Institut, Universität Hamburg, Grindelallee 48, D-20146 Hamburg, Germany

tataryn.taras@gmail.com

The aim of our investigations was to study the arrangement and distribution of twin boundaries during mechanical and thermal treatment in order to examine reversibility phenomena in larger ferroelastic crystal plates (5x6x0.87 mm^3) as well as the influence of the domain structure on ionic conductivity. In a selected $La_{0.95}Sr_{0.05}Ga_{0.9}Mg_{0.1}O_{3-x}$ (LSGM) - crystal plate the submicron twin structure was studied using white synchrotron radiation at the Kappa-diffractometer F1 equipped with a MAR CCD-detector (HASYLAB, DESY). Scanning of the sample under the beam ($0.05x0.05mm^2$) and collecting diffraction data at each step with 45 micron spatial resolution was used to map the domain pattern in the LSGM-plate after mechanical and thermal treatment. Conductivity measurements were done between ~ 70 ^oC and 710 ^oC in air. Impedance spectroscopy was applied using a HP4284 LCR-meter in the range 20 Hz – 1 MHz. Data were recorded applying AC amplitudes of 80 mV and 1V to the electrode.

It was shown that before mechanical treatment mainly twin walls normal to the largest surface of the plate occurred. The observed domain structure was partially switched to another twin configuration with domain walls parallel to the surface or to certain domain states during polishing. After annealing the domain configuration with prevalent domain walls normal to the largest plate surface was fully restored.

Impedance plots show two semicircular arcs. The first high frequency arc corresponds to the bulk conductivity while the second low frequency one corresponds to the conductivity on domain boundaries.

Our results show that strain can relax completely by forming phase-specific domain wall configurations [1], and hence, reorientations occur during thermal cycling. This feature may be of practical use as the preparation of electrolyte and electrode ceramics for SOFC includes compaction during one of the synthesis stages. Ceramics of LSGM can be approximated by an ensemble of small crystallites. Mechanical pressure imposed to such an electrolyte pellet causes the rearrangement of the twin structure of “chevron cells” in ceramic grains along the direction parallel or nearly parallel to the imposed pressure. Hence, such pressure will cause memory texturing of twin “chevrons” in electrolyte layers along the direction of oxygen diffusion in the SOFC structure. Keeping in mind the influence of twin walls on the conductivity and the high density of twin walls in LSGM solid solutions, it is supposed that texturing of the twins, e.g. reorientation of “chevron cells” increases the conductivity of the perovskite-type electrolyte LSGM along the cathode-anode direction.

Acknowledgments. The work was supported by WTZ (UKR 07/009) and the Ukrainian Ministry of Education and Science (project “Tern”). T. Tataryn acknowledges financial support of the Deutscher Akademischer Austauschdienst (Leonhard-Euler program).

[1]. D. Savytskii, U. Bismayer, *Phase Transitions* **81 (**2008), p. 431.

P1-17

Effect of substitution of Ga and In atoms by Yb on physical properties of $TlGa(In)S_2$ layered crystals

E.M.Kerimova, N.Z.Gasanov, A.I.Gasanov and K.M.Huseynova
Institute of Physics, Azerbaijan National Academy of Sciences, Az-1143, Baku, Azerbaijan
e-mail: ekerimova@physics.ab.az, tel. +99412 4395913

Equilibrium in the $TlGaS_2$-$TlYbS_2$ system was investigated. According to the results of differential-thermal analysis in the system of $TlGaS_2$-$TlYbS_2$ with the relationship of components 1:1 the compound of Tl_2GaYbS_4 is formed with the congruent melting at a temperature of 1380K. On the basis of $TlGaS_2$, solid solutions up to 8mol% of $TlYbS_2$ are formed at room temperature. Nonvariant eutectic point relates to the composition of $(TlGaS_2)_{0.84}(TlYbS_2)_{0.16}$ and the temperature of 1085K.

$TlGaS_2$ single crystals, in which Ga atoms are replaced by rare-earth element Yb in quantities of 0.1÷1%, are grown by Bridgeman method. Over a wide range of temperatures (300 - 900 K) the electro-physical properties of the ternary compound of $TlYbS_2$ are investigated. It has been found that the prevailing mechanism of current carriers scattering is the scattering on the lattice acoustic phonons. Effective masses, carriers state densities, mobility proportions, temperature coefficients of the forbidden gap are determined. From studies of the heat transport phenomena at temperatures of 77-650K in the above-mentioned single crystals it has been found that the three-phonon processes are the basic mechanisms of phonon scattering.

The absorption edge of $TlGa_{1-x}Yb_xS_2$ single crystals was also investigated. In $TlGa_{0.995}Yb_{0.005}S_2$ the temperature shear coefficient of the exciton peak in the range of temperatures 77÷200K was $\Delta E_{ex}/\Delta T=1.5\cdot10^{-4}$eV/K, i.e., has positive sign, as for the $TlGaS_2$. Partial substitution Ga→Yb leads to the small red shift of absorption edge.

It is also established, that the partial (0.1-0.5%) substitution of Ga by Yb in layered $TlGaS_2$ single crystals leads to the shift of the maximum of photocurrent to the long-wave region, considerable expansion of the region of spectral sensitivity, a 3 times increase in the amplitude of contaminant photocurrent and coefficient of X-ray sensitivity, which is promising for creation on the basis of $TlGaS_2$<Yb> single crystals photo receivers with spectral range in extended IR region and sensitive X-ray detectors.

Phase equilibrium in the system $TlInS_2$ - $TlYbS_2$ was studied. It was discovered that in solid solutions of $(TlInS_2)_{1-x}(TlYbS_2)_x$ (x=0÷0,12) in the $TlInS_2$ crystal lattice trivalent In ions are substituted by Yb ions, which have larger radius. Parameters of crystal lattice and space symmetry group for several compositions of the given system were determined.

Temperature dependence of electrical conductivity and Hall coefficient of $(TlInS_2)_{1-x}(TlYbS_2)_x$ (x=0÷0,12) solid solutions were studied. Value of the band gap width determined from $lg\sigma = f(10^3/T)$ and $lg(R_xT^{3/2}) = f(10^3/T)$ curves is decreasing from 2.2eV to 1.85eV under partial substitution of In atoms with Yb atoms. Change of carrier mobility with temperature corresponds to scattering on acoustic vibration of the lattice.

Thermal properties of $(TlInS_2)_{1-x}(TlYbS_2)_x$ (x=0÷0,12) crystals were also studied and it was determined that measured thermal conductivity is caused by lattice contribution, since its electron component, determined by Wiedemann-Franz ratio, is negligible.

It is determined that the optical absorption edge of $TlIn_{1-x}Yb_xS_2$ single crystals is formed by direct exciton and is shifted towards long wavelength side as compared to $TlInS_2$ (at 77K this shift is around 50meV for $TlIn_{0,995}Yb_{0,005}S_2$). Coefficient of temperature shift of exciton peak is also decreased, in 77-200K interval it is equal to $-5,1\cdot10^{-4}$eV/K for $TlInS_2$ and to $-2,0\cdot10^{-4}$eV/K for $TlIn_{0,995}Yb_{0,005}S_2$. If we assume that exciton binding energy varies only slightly, then partial substitution of In atoms with rare earth element Yb considerably reduces width of the band gap of $TlInS_2$ single crystal.

P1-18

Quaternary nonvariant reactions in Fe-rich corner of the Fe-Mo-C system at high temperatures

T.A. Velikanova[1], M.V. Karpets[1], P.G. Agraval[2], M.A. Turchanin[2]

[1] Institute for Problems of Materials Sience NASU, 3, Krzhyzhanovsky str., Kyiv-142, 03680, Ukraine
[2] Donbass State Engineering Academy, Shkadinova Street 72, UA–84313 Kramatorsk, Ukraine

e-mail: tavel@ipms.kiev.ua

It was early shown that 78,4Fe10,8Mo10,8C and 75,5Fe10Mo14,5C spinning ribbons, which contain ~90 % mass. of metastable ternary **π**-phase (*cP*20, $P4_132$, β-Mn, a = 0,6327 − 0,6370 nm), reach the state of thermodynamic equilibrium under *in situ* high-temperature X-Ray diffractometry (HT XRD) conditions [1, 2].

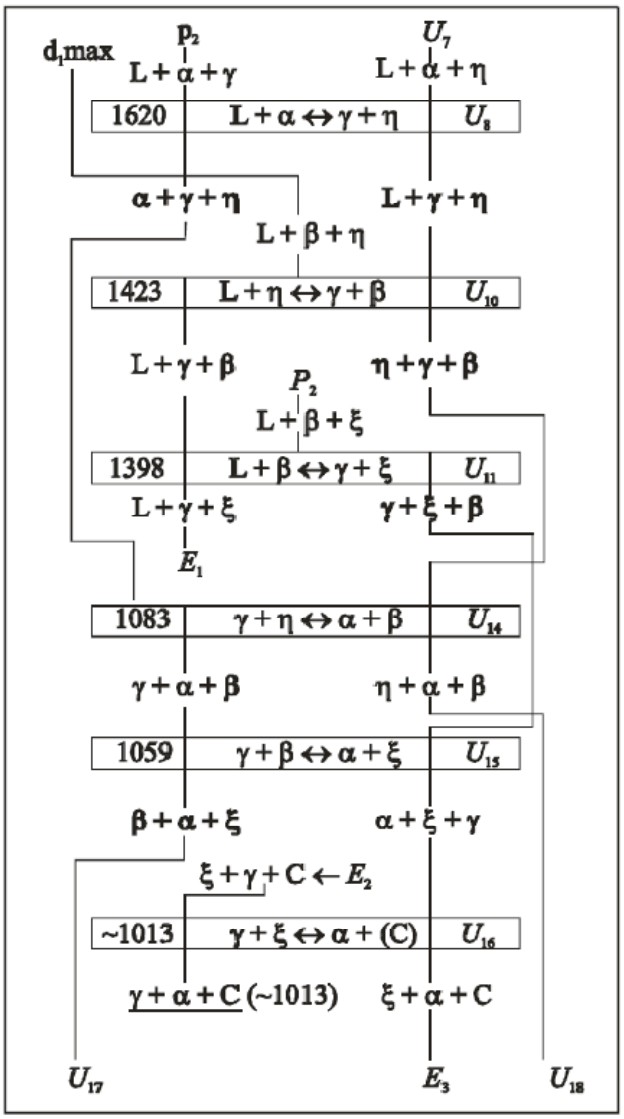

Figure. The fragment of the reactions scheme of the iron rich part of the Fe–Mo–C system; T, K

According HT XRD data three-phase equilibrium fields η + β + γ, α + γ + η , β + γ + ξ exist among others on the solidus surface of the Fe–Mo–C system.

This experimental result corroborated completely data of thermodynamic modelling [3], which have been obtained by CALPHAD-method on the base of Andersson`s model of Fe-Mo-C system with using of Thermo-Calc applications modules. The fragment of the reactions scheme of the iron rich part of the Fe–Mo–C system in the temperature range of ~1000…1600 K is shown at the **Figure,** where **α**=α-Fe: *cI*2, *Im*-3*m*, W; **β**= β-Mo_2C: *hP*3, $P6_3/mmc$, Fe_2N; **ξ**=$M_{34}C_{10}$: *mC*44, *C*2/*m*, $Mo_6Fe_{11}C_5$; **γ**=γ-Fe: *cF*4, *Fm*-3*m*, Cu; **η**=M_6C: *cF*112, *Fd*-3*m*, W_3Fe_3C; **L**=liquid phase.

[1]. T.A. Velikanova, M.V. Karpets, M.A. Turchanin “Perspective technologies, materials and equipment in foundry” (DSMA, Kramatorsk, Ukraine, 2009), pp. 50-52.

[2]. T.A. Velikanova, M.V. Karpets, P.G. Agraval, M.A. Turchanin (Ternary compounds in Fe-Mo-C spinning films and equilibrium alloys: experiment and thermodynamic modelling at high-temperatures. - this conference, topic 1).

[3]. T.Ya. Velikanova, M. Turchanin, T. Dobatkina, T.A. Velikanova “Carbon-Iron-Molybdenum” Landolt-Börnstein, Numerical Data and Functional Relationships in Science and Technology, New Series, Group IV: Physical Chemistry. Ed. W. Martinsen, “Ternary Alloy Systems. Phase Diagrams, Crystallographic and Thermodynamic Data Critically Evaluated by MSIT”, G. Effenberg, S. Ilyenko (Eds.). Vol. 11D2, (Berlin Heidelberg: Springer-Verlag, 2008), pp. 124—172.

P1-19

Preparation of $Cu_2ZnSnSe_4$ thin films by selenization of stacked Cu/Sn/Zn precursor

Toshiyuki Yamaguchi[1], Shinsuke Ooura[1], Shigetoshi Niiyama[2] and Toshito Imanishi[2]

[1] Wakayama National College of Technology, 77 Noshima, Nada-cho, Gobo-shi 644-0023, Japan
[2] Industrial Technology Center of Wakayama Prefecture, 60 Ogura, Wakayama-shi 649-6261, Japan
yamaguchi@wakayama-nct.ac.jp, +81-738-29-8367/+81-738-29-8216

Thin film solar cells based on $Cu(In,Ga)Se_2$ technologies have demonstrated significant improvements [1]. However, indium and gallium is considered to be an expensive component for solar cell. Earth-abundant copper-zinc-tin-chalcogenide kesterites, Cu_2ZnSnS_4 and $Cu_2ZnSnSe_4$, have been examined as potential alternatives for the leading technology. Cu_2ZnSnS_4 thin film solar cells by annealing of the co-sputtered SnS/Cu/ZnS precursor in the atmosphere of N_2+H_2S gases showed an efficiency of 6.67% [2]. Only limited studies have been done on $Cu_2ZnSnSe_4$, and devices have been reported on a few occasions [3, 4]. In this study, we fabricated $Cu_2ZnSnSe_4$ thin films by selenization of the stacked precursor which was evaporated from Zn, Sn and Cu elements on Mo/soda lime glass substrate and their properties were investigated.

Our selenization process had two stages which consisted of a precursor preparation stage by using vacuum deposition apparatus and subsequently a selenization stage by using electric heating furnace. In the first stage for preparation of precursor, the Cu/Sn/Zn layers were prepared on Mo/soda lime glass substrate by evaporation of each element without intentional substrate heating. The stacked Cu/Sn/Zn precursor was set in a vacuum-sealed quartz ampoule with selenium shots. The precursor was crystallized by annealing for 2 hours in the atmosphere of selenium. The annealing temperature was varied from 350°C to 580°C.

EPMA analysis demonstrated that the thin films crystallized over 450°C had nearly the stoichiometric composition of $Cu_2ZnSnSe_4$. From XRD studies, these prepared thin film had a kesterite $Cu_2ZnSnSe_4$ structure and the preferred orientation to the 112 plane. From SEM micrograph, the grains became larger with increasing the annealing temperature. $Cu_2ZnSnSe_4$ thin film solar cell showed the open circuit voltage of 212mV.

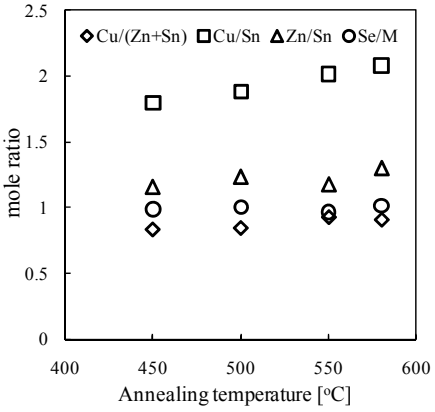

Figure 1. Dependence of mole ratio of components on annealing temperature.

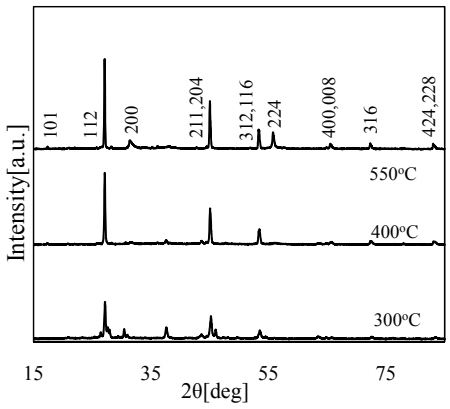

Figure 2. X-ray diffraction patterns for crystallized thin films.

[1]. I.Repins, M. A. Contreras, B. Egaas, C. DeHart, J. Scharf, C.L. Perkins, B. To and R. Noufi: Prog. Photovolt. Res. Appl. 16 (2008), p.235.
[2]. Hironori. Katagiri Kazuo. Jimbo, Satoru. Yamada, Tsuyoshi. Kamimura, Win Shwe Maw, Tatsuo Fukano, Tadashi Ito, and Tomoyoshi Motohiro, App. Phys. Express 1 (2008), p.041201.
[3]. Th. Magorian Friedlmeier, N. Wieser, Th. Walter, H. Dittrich, and H-W. Schock, Proceedings of the 14th European Photovoltaic Specilists Conference (Barcelona, 30 June-4 July, 1997), p.1242.
[4]. G.Zoppi, I.Forbes, R.W.Miles, P.J.Gale, J.J.Scragg and L.M.Peter, Prog. Photovolt: Res. Appl. 17 (2009), p.315.

P1-20

Growth of $CuInGaSe_2$ films on Mo substrate by RF sputtering and their characterization

Takahiro Tokuda[1], Kenji Yoshino[1],
Ken-ichiro Miseki[2], Rie Mori[2], Shoubin Zhang[2], Shigeo Doutyoku[2]

[1] Department of Electrical and Electric Engineering, University of Miyazaki,
1-1 Gakuen Kibanadai-nishi 889-2192, JAPAN
[2]Sanda Plant, Mitsubishi Materials Corporation, 12-6 Technopark, Sanda, Hyogo, 669-1339 JAPAN

t0b114u@ccmiyazaki-u.acjp, phone/ fax +81-985-58-7396

I-III-VI_2 chalcopyrite-type semiconductors have large absorption coefficient because of their direct band gap structure. Band gap energies of these materials range from the 0.8 eV of $CuInTe_2$ to the 3.5 eV of $CaAlS_2$. Therefore, the chalcopyrite-type semiconductors have been used in solar cell technologies, for example a solar cell based on a $CuInGaSe_2$ (CIGS) polycrystalline thin film is reported to have a conversion efficiency of 19.9% [1]. CIGS polycrystalline thin film absorption layers are produced either in a three-stage sputtering method or a selenization method. In general, the three-stage method is an evaporation or sputtering method using three kinds of alloys, e.g. In-Ga-Se, Cu-Se and In-Ga-Se, whereas the selenization method is a sputtering method using Cu-Ga and In (or Cu-Ga-In) targets before annealing in H_2Se gas. We are developing selenization process without H_2Se, which is a poisonous gas. In the present study, we propose a sputtering method using a CIGS single phase target for developing superstrate-type CIGS-based solar cell.
The CIGS films on Mo substrate were prepared by RF sputtering under argon gas. The target used in the sputtering experiments consisted of single phase $CuIn_{0.8}Ga_{0.2}Se_2$. The deposition pressure was between 0.1 and 5 Pa and the sputtering power was between 20 and 50 W. The substrate temperature was varied from room temperature (RT) to 550 °C and soda-lime glass was used as the substrate. The samples were evaluated by X-ray diffraction (XRD), SEM, EPMA, Hall, thermo probe and optical absorption measurements.
$CuIn_{0.8}Ga_{0.2}Se_2$ powder was used as the target source. No secondary phases such as selenide materials can be observed in the patterns. The (112) diffraction peak is strong in comparison with ICDD of $CuInSe_2$ and $CuGaSe_2$. All samples indicate a (112) orientation. The lattice constants of the *a* and *c* axes become close to those calculated by Vegard's law with increasing substrate temperature. Furthermore, thermoprobe and Hall measurements indicate p-type conductivity in all samples. EPMA results indicate that Se vacancy concentration is low in all samples.

[1]. I. Repins et al., Prog. Photovol. Res. Appl. **16** (2008), 235

P1-21
Non-vacuum Process of $AgInSe_2$ Crystal Growth by Hot-press Method

Kenji Yoshino[1], Hiroyuki Tsuru[1] and Akira Nagaoka[1]

[1] Department of Electrical and Electric Engineering, University of Miyazaki,
1-1 Gakuen Kibanadai-nishi 889-2192, Japan

t0b114u@ccmiyazaki-u.acjp, phone/ fax +81-985-58-7396

Chalcopyrite semiconductors of moderate bandgap have been studied. Because of direct bandgap and high optical absorption, these semiconductors are particularly attractive for solar cell applications. Indeed, $CuInGaSe_2$ solar cell energy conversion efficiencies of more than 19.5 % have been reported [1]. On the other hand, Ag-III-VI_2 materials, such as $AgInSe_2$, are also promising candidate materials for solar cells. $AgInSe_2$ has a bandgap of 1.20 eV [2] and a melting point of 780 °C, which are even better than $CuInSe_2$ for solar cell applications. An efficiency of 7.5% was reported for a solar cell used $AgInSe_2$ absorber on p-$AgInSe_2$/n-CdS [3]. Furthermore, an efficiency of energy conversion of more than 8 % [4] has been reported recently on $AgInGaSe_2$. However, few papers are known about the properties of $AgInSe_2$ in comparison to those of $CuInSe_2$.
The successful hot-press (HP) growth of $CuInS_2$, $AgInS_2$ and $AgGaSe_2$ crystals was reported in our previous work [5-7]. One of the advantages of the HP method is that a crystal can be grown without a vacuum condition and at low temperature. In this work, undoped $AgInSe_2$ crystals were grown by the HP method at 400 - 700 °C for 1 h under high pressure (25 MPa) from stoichiometric Ag_2Se and In_2Se_3 powders.
$AgInSe_2$ crystals were grown by the HP method at low temperatures (400 - 700 ˚C) under high pressure. X-ray diffraction measurements indicate that growth of the $AgInSe_2$ crystal begins at 400°C and that single phase $AgInSe_2$ could be observed at 650 ˚C. This temperature is much lower than the melting point of crystalline $AgInSe_2$. The center of this sample was found to be close to stoichiometry. However, the sample exhibited a slightly Ag-rich, Ga-poor and Se-rich composition at 650 ˚C. This suggests that donor-type defects, namely interstitial Ag atoms are present, which may lead to an enhancement in electrical conductivity. This is supported by Hall measurement which indicates n-type conductivity in the sample. The $AgInSe_2$ crystals grown at 650 ˚C has a resistivity of 2.2 Ωcm, a carrier concentration of 2.5×10^{18} cm^{-3} and a mobility of 70 $cm^2V^{-1}s^{-1}$ at RT. Furthermore, a bandgap energy of 1.172 eV can be obtained from optical transmittance at RT.

[1]. I. Repins, M. A. Contreras, B. Egaas, C. Dehart, J. Scharf, C. L. Perkins, B. To, R. Noufi, Prog. Photovol. Res. Appl. **16** (2008) 235.
[2]. B. Tell, J. T. Shary and H. M. Kasper, J. Appl. Phys. **43**, 2469 (1972).
[3]. P. P. Ramesh, O. M. Hussain, S. Uthanna, B. S. Naidu and P. J, Reddy, Mater. Lett. **34**, 27 (1997).
[4]. K.Yamada, N. Hoshino and T. Nakada, Sci. Tecnol Advanced Mater. **7**, 42 (2006).
[5]. H. Komaki, K. Yoshino, S. Seto, M. Yoneta, Y. Akaki and T. Ikari, J Crystal Growth **236**, 253 (2002).
[6]. K.Yoshino, H. Komaki, T. Kakeno, Y. Akaki and T. Ikari, J. Phys. Chem. Sol. **64**, 1839 (2002).
[7]. A. Kinoshita, H. Matsuo, K. Yoshino, T. Ikari and K. Kakimoto, Phys. Stat. Sol. (c) **8**, 2903 (2006).

P1-22
Effect of annealing for $CuInS_2$ thin films prepared from In-rich ternary compound

Yoji Akaki[*,1], Yu Kawano[1], Shigeyuki Nakamura[2], Takahiro Tokuda[3] and Kenji Yoshino[3]

[1] Department of Electrical and Computer Engineering, Miyakonojo National College of Technology
473-1 Yoshio, Miyakonojo, Miyazaki 885-8567, Japan
[2] Department of Electrical and Electronics Engineering, Tsuyama National College of Technology
624-1 Numa, Tsuyama, Okayama 708-8509, Japan
[3] Department of Electrical and Electronics Engineering, University of Miyazaki
1-1 Gakuen Kibanadai-nishi, Miyazaki 889-2192, Japan

*Corresponding author: e-mail akaki@cc.miyakonojo-nct.ac.jp, Phone: +81-986-47-1197, Fax: +81-986-47-1208,

Among ternary chalcopyrite semiconductors, $CuInS_2$ may be the most promising material for photovoltaic applications due to the band gap energy of 1.53 eV [1], which perfectly matches the solar spectrum for energy conversion. Furthermore, since the material does not contain toxic Se atom, these may have an advantage in comparison with the frequently studied $CuInSe_2$ and Cu(In,Ga)Se.

In our previous papers [2], Cu-rich $CuInS_2$ films have been prepared on glass substrates using the single-source thermal evaporation method, and the films were subsequently annealed from 250 to 500 ˚C in air or H_2S atmosphere. We reported that the polycrystalline $CuInS_2$ thin films with other phases were grown above 250 ˚C by X-ray diffraction (XRD) measurement, and the films annealed at 400 ˚C exhibited the single phase. In this paper, we report on effect of annealing for In-rich $CuInS_2$ thin films prepared by the single-source thermal evaporation method using In-rich $CuInS_2$ powder.

Cu-In-S thin films were deposited on glass substrates by the single-source thermal evaporation using In-rich ternary compound as starting materials. Polycrystalline In-rich $CuInS_2$ powder grown at 700 ˚C for 1 hour under high pressure at 25 MPa by HP method from the mixed Cu_2S and In_2S_3 powders was employed as a starting material [3]. Cu/In ratios of $CuInS_2$ powder were from 0.67 to 1. After the evaporation, the films were annealed in air or H_2S gas from 250 to 500 ˚C for 60 min. The thickness of the films was about 1.4~2.0 μm. Figure 1 shows X-ray diffraction (XRD) patterns of the films annealed in H_2S prepared from the starting material of the Cu/In ratio of 0.67. XRD patterns indicated that the In-rich films appeared $CuIn_5S_8$ phase with $CuInS_2$ phase by annealing above 350 ˚C. The composition ratios of Cu, In and S atoms of the In-rich films become close to Cu, In and S composition ratio of the starting material with increasing the annealing temperature. The measured Cu/In ratios of the films are close to the ratio of the starting materials. The grain sizes of the crystals in the In-rich films is more than 0.4 μm, the surface morphology of the In-rich films is smooth in comparison with the Cu-rich films.

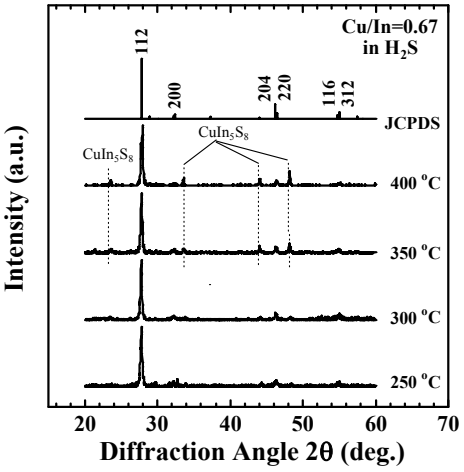

Fig. 1 XRD patterns of the films annealed in H_2S prepared from the starting material of the Cu/In ratio of 0.67.

[1]. J. L. Shay, B. Tell, H. M. Kasper and L. M. Schiavone, Phys. Rev. B 5 (1972) 5003.
[2]. Y. Akaki, S. Nakamura, K. Nomoto, T. Yoshitake and K Yoshino, Phys. Status Solidi (c) 6 (2009) 1030.
[3]. H. Komaki, K. Yoshino, S. Seto, M. Yoneta, Y. Akaki and T. Ikari, J. Cryst. Growth 236 (2002) 256.

P1-23

Effect of H_2S annealing for Sb-doped $CuInS_2$ thin films prepared from ternary compound

Yoji Akaki[*,1], Noriyuki Yamazumi[1], Shigeyuki Nakamura[2], Takahiro Tokuda[3] and Kenji Yoshino[3]

[1] Department of Electrical and Computer Engineering, Miyakonojo National College of Technology
473-1 Yoshio, Miyakonojo, Miyazaki 885-8567, Japan
[2] Department of Electrical and Electronics Engineering, Tsuyama National College of Technology
624-1 Numa, Tsuyama, Okayama 708-8509, Japan
[3] Department of Electrical and Electronics Engineering, University of Miyazaki
1-1 Gakuen Kibanadai-nishi, Miyazaki 889-2192, Japan

*Corresponding author: e-mail akaki@cc.miyakonojo-nct.ac.jp, Phone: +81-986-47-1197, Fax: +81-986-47-1208,

Among ternary chalcopyrite semiconductors, $CuInS_2$ may be the most promising material for photovoltaic applications due to the band gap energy of 1.53 eV [1], which perfectly matches the solar spectrum for energy conversion. Furthermore, since the material does not contain toxic Se atom, these may have an advantage in comparison with the frequently studied $CuInSe_2$ and Cu(In,Ga)Se.

In our previous papers [2], Sb-doped $CuInS_2$ films have been prepared on glass substrates using the single-source thermal evaporation method, and the films were subsequently annealed from 250 to 500 ˚C in air atmosphere. We reported that the polycrystalline $CuInS_2$ thin films were successfully grown at annealing of 400 ˚C by X-ray diffraction (XRD) measurement and the $CuInS_2$ thin films was stable for annealing at high temperature. In this paper, we report on effect of H_2S annealing for Sb-doped $CuInS_2$ thin films prepared by the single-source thermal evaporation method using Sb-doped $CuInS_2$ powder.

Cu-In-S thin films were deposited on glass substrates by the single-source thermal evaporation using Sb-doped ternary compound as starting materials. Polycrystalline Sb-doped $CuInS_2$ powder that were grown at 700 ˚C for 1 hour under high pressure at 25 MPa by HP method from the mixed Cu_2S and In_2S_3 powders with Sb powder was employed as a starting material [3]. After the evaporation, the films were annealed in H_2S atmosphere from 250 to 500 ˚C for 60 min. The thickness of the films was about 1.4~2.0 μm. Figure 1 shows X-ray diffraction (XRD) patterns of the Sb-doped films annealed in H_2S. XRD patterns indicated that these films appeared CuS phase with $CuInS_2$ phase by annealing at 250 ˚C as same as the undoped films [4]. The composition ratios of Cu, In and S atoms of the Sb-doped films are close to stoichiometry at the lower temperature than those of the undoped films [4]. The grain size of the crystals in the Sb-doped films annealed at 400 ˚C is approximately 1.0 μm. The grain size of the crystals in the Sb-doped films becomes large with increasing the temperature.

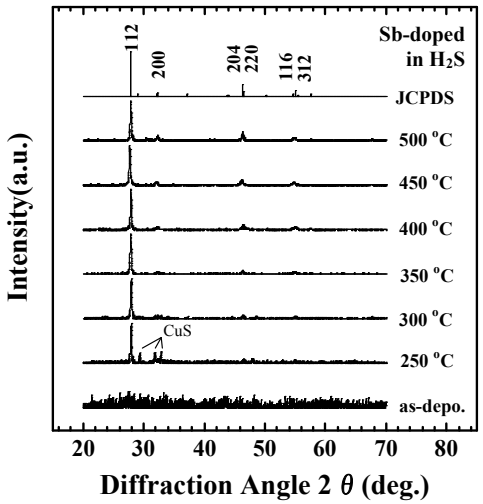

Fig. 1 XRD patterns of the Sb-doped films annealed in H_2S.

[1]. J. L. Shay, B. Tell, H. M. Kasper and L. M. Schiavone, Phys. Rev. B **5** (1972) 5003.
[2]. Y. Akaki, H. Komaki, H. Yokoyama, K. Yoshino, K. Maeda and T. Ikari, J. Phys. Chem. Solids, **64** (2003) 1863.
[3]. H. Komaki, K. Yoshino, Y. Akaki, M. Yoneta and T. Ikari, Phys. Status Solidi (c) **0** (2003) 759.
[4]. Y. Akaki, K. Nomoto, S. Nakamura, T. Yoshitake and K. Yoshino, J. Phys. **100** (2008) 082022.

P1-24

Effect of annealing for Ag-rich $AgInS_2$ thin films prepared by a vacuum evaporation method

Yoji Akaki[*,1], Kyohei Yamashita[2], Tsuyoshi Yoshitake[2], Shigeyuki Nakamura[3], Takahiro Tokuda[4] and Kenji Yoshino[4]

[1] Department of Electrical and Computer Engineering, Miyakonojo National College of Technology 473-1 Yoshio, Miyakonojo, Miyazaki 885-8567, Japan
[2] Department of Applied Science for Electronics and Materials, University of Kyushu, Fukuoka, 816-8580, Japan
[3] Department of Electrical and Electronics Engineering, Tsuyama National College of Technology 624-1 Numa, Tsuyama, Okayama 708-8509, Japan
[4] Department of Electrical and Electronics Engineering, University of Miyazaki 1-1 Gakuen Kibanadai-nishi, Miyazaki 889-2192, Japan

*Corresponding author: e-mail akaki@cc.miyakonojo-nct.ac.jp, Phone: +81-986-47-1197, Fax: +81-986-47-1208,

I-III-VI_2 compounds are direct energy-gap semiconductors showing very interesting electrical and optical properties, solar cell technologies using I-III-VI_2 compounds have been extensively reported. Conversion efficiency for polycrystalline Cu(In,Ga)Se_2 based solar cells have achieved at 19.9 % [1]. One way of improving the higher conversion efficiency is stacking different cells in series, so-called a tandem structure. Because $AgInS_2$ crystals of the chalcopyrite structure have band gap energy of 1.9 eV [2], $AgInS_2$-based materials are promised absorbers of the shorter wavelength. However, there are few reports on $AgInS_2$ films. Therefore, the accurate material characterization of the $AgInS_2$ films is not well understood.

In our previous paper [3], we investigated the effect of H_2S annealing for Ag-In-S thin films deposited by a single-source thermal evaporation method. All the films annealed above 300 ˚C were obtained chalcopyrite $AgInS_2$ crystal phase. The composition of the $AgInS_2$ thin films annealed above 350 ˚C became slightly Ag-rich and In-poor. The composition ratios of Ag, In and S atoms become close to stoichiometry with increasing the annealing temperature. The grain size of the $AgInS_2$ crystals increases with increasing the annealing temperature. The grain size of the $AgInS_2$ crystal in the films annealed at 400 °C are approximately 1.5~4 μm.

Ag-In-S thin films were deposited on glass substrates by the single-source thermal evaporation using Ag-rich ternary compound as starting materials. Polycrystalline Ag-rich $AgInS_2$ powder grown at 700 ˚C for 1 hour under high pressure at 25 MPa by HP method was employed as a starting material [4]. Ag/In ratios of $AgInS_2$ powder were from 1.0 to 1.5. After the evaporation, the films were annealed in H_2S gas from 250 to 500 ˚C for 60 min. The thickness of the films was about 1.0~2.0 μm. Figure 1 shows X-ray diffraction (XRD) patterns of the films annealed in H_2S prepared from the starting material of the Cu/In ratio of 1.5. From the XRD patterns, the chalcopyrite $AgInS_2$ phase with Ag, Ag_2S and orthorhombic $AgInS_2$ phase appeared from the films annealed above 250 ˚C. The composition ratios of Ag, In and S atoms of the Ag-rich films become close to Ag, In and S composition ratio of the starting material with increasing the annealing temperature. The measured Ag/In ratios of the films are also close to the ratio of the starting materials.

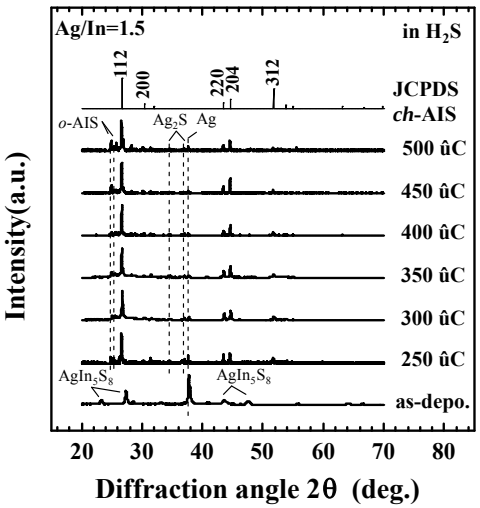

Fig. 1 XRD patterns of the films annealed in H_2S prepared from the starting material of the Ag/In ratio of 1.5.

[1]. I. Repins *et al.*, Prog. Photovolt.: Res. Appl. 16 (2008) 235.
[2]. J. L. Shay *et al.*, Phys. Rev. B 5 (1972) 5003.
[3]. Y. Akaki *et al.*, Proc. of 35th IEEE PVSC (2010).
[4]. K. Yoshino *et al.*, J. Phys. Chem. Solids, 64 (2003) 1839.

P1-25
Glass-crystals materials of B_2O_3-Bi_2O_3-Me_2O_3 (Me =Yb, Lu) systems

Asadov M.M., Akhmedova N.A.

Institute of Chemical Problems, National Academy of Sciences of Azerbaijan
G. Javid pr., 29, AZ 1143, Baku, Azerbaijan
E-mail: mirasadov@gmail.com

Bi_2O_3-B_2O_3-Yb_2O_3 system was investigated to determine the conditions of creation, melting character of ternary oxide phases and to find out the regions of glass-formation on the base of initial components. The investigations were carried out by the methods of physico-chemical analysis, DTA, RFA, IR-spectroscopy and density-measurements of $Bi_2O_3 \cdot 3B_2O_3$–$Yb_2O_3 \cdot B_2O_3$; $3Bi_2O_3 \cdot 5B_2O_3$–$Yb_2O_3 \cdot B_2O_3$; $Bi_2O_3 \cdot B_2O_3$ – $Yb_2O_3 \cdot B_2O_3$; $2Bi_2O_3 \cdot B_2O_3$ – $Yb_2O_3 \cdot B_2O_3$ cuts. The chemically pure reactive: H_3BO_3; Yb_2O_3 and Bi_2O_3 were used as initial materials. The glasses of Bi_2O_3–B_2O_3–Yb_2O_3 system were boiled at 1000-1150^{0}C during 6-7 hours. After boiling the melt was poured out on titanium plate, which had room temperature. In dependence on composition the melt was cooled in form of transparent glasses, glass-crystals and crystals. On the base of these data about the character of specimens and by means of roentgen-study of obtained samples we determined the boundaries of glass-formation regions in Bi_2O_3–B_2O_3–Yb_2O_3 system. In Bi_2O_3–B_2O_3–Yb_2O_3 system the glass-formation region is tapered in $Bi_2O_3 \cdot B_2O_3$–$Yb_2O_3 \cdot B_2O_3$ cut, but in 2 $Bi_2O_3 \cdot B_2O_3$–$Yb_2O_3 \cdot B_2O_3$ cut at compositions from 10 mol % Bi_2O_3 to 40 mol % Bi_2O_3 the glasses with decreased thermal characteristics were revealed (T_{melt}=380 ^{0}C; T_{cr}=440 ^{0}C).

The synthesis of $Bi_2O_3 \cdot B_2O_3$–$Lu_2O_3 \cdot B_2O_3$, $Lu_2O_3 \cdot B_2O_3$–Bi_2O_3, $Lu_2O_3 \cdot B_2O_3$–$Lu_2O_3 \cdot Bi_2O_3$, $Bi_2O_3 \cdot B_2O_3$–$Lu_2O_3 \cdot Bi_2O_3$ systems was carried out by solid-state-phase method. Weighed according to calculation oxides were mixed, powdered and pressed to tablets. Obtained tablets were conglomerated at 900 ^{0}C and then were thermally treated at 730-1000 ^{0}C in dependence on the composition. Prepared specimens were investigated by the methods of roentgenographyc analysis, IR-spectroscopy and density-measurements. The color of specimens was varied from brightly-yellow to brown. In Lu_2O_3–B_2O_3–Bi_2O_3 system three regions were revealed: homogenous glasses, crystal compounds and un-mixed phases. The boundaries of regions of glass-formation were determined by visually and from rentgenographyc study of obtained specimens. Homogeneous glasses were obtained in follow cuts: $Bi_2O_3 \cdot B_2O_3$ – $Lu_2O_3 \cdot B_2O_3$ up to 15 mol % Lu_2O_3; $Lu_2O_3 \cdot B_2O_3$–Bi_2O_3 up to 10 mol % Lu_2O_3; $Bi_2O_3 \cdot B_2O_3$ – $Lu_2O_3 \cdot Bi_2O_3$ up to 15 mol % Lu_2O_3.

Polymorphic modifications are characteristical for the compounds of $LnBO_3$-type (Ln = La, Ce, Pr, Nd, Sm, Eu, Gd, Dy, Ho, Er, Yb, Lu). Thermodynamical properties and heat capacity of these compounds are unstudied.

Data about limits of solubility of components in Ln′BO_3–Ln′′BO_3 systems (where Ln′ and Ln′′ are various lantanoides) were not found.

Variety of approximated equations C_p = f(T) have been determined by us for low-temperature modifications of L-$LnBO_3$- type compounds. Maer-Kelli correlations: C_p= a+bT+cT^{-2} and values of heat capacity of B_2O_3, Ln_2O_3 binary oxides have been used for calculations.

P1-26

Growth of $Cu(In,Al)(Se,S)_2$ thin films by selenization and sulfurization for a wide bandgap absorber

C. Fujiwara[1], Y. Kawasaki[1], T. Sato[1], M. Sugiyama[1] and S. F. Chichibu[2]
[1] Department of Electrical Engineering, Tokyo University of Science, 2641 Yamazaki, Noda 278-8510, Japan
[2] CANTech, Institute of Multidisciplinary Research for Advanced Materials, Tohoku University, 2-1-1 Katahira, Aoba, Sendai 980-8577, Japan

Presenting author optoelec@rs.noda.tus.ac.jp, phone/ fax number +81-4-7121-1585 (C. Fujiwara)

Chalcopyrite structure $Cu(In_{1-x}Al_x)(S_ySe_{1-y})_2$ (CIASS) alloys are attracting attention as promising candidates for the light-absorbing medium of high conversion efficiency (η), low cost, and lightweight solar cells. In addition, according to the wide variation in the band-gap energy (1.0–3.5eV), multiple-junction or tandem solar cells able to be fabricated using CIASS films of different compositions, x and y. In fact, several research groups have recently fabricated $Cu(In,Al)Se_2$-based solar cells [1], and a high η of 16.9% has been demonstrated.

The sulfurization following selenization of $Cu(In,Ga)Se_2$ (CIGS) films is believed to be promising for bandgap engineering of absorber material. Furthermore, it has been reported that the controlled incorporation of sulfur into CIGS films reduces the carrier recombination in the space charge region due to the deep trap states. Therefore, the sulfurization following selenization is expected to be used as a method of growth of CIASS films. However, sulfurization condition following selenization for obtaining CIASS films has not been clarified. The crystal growth of CIASS must be studied for solar cell applications. In this study, the advantages of using sulfurization for the growth of CIASS will be presented.

Cu-In-Al precursors were selenized using diethylselenide (DESe) [2] at 515–570 °C for 60–90 min under atmospheric pressure. The flow rates of DESe and N_2 carrier gases were 35 μmol/min and 2 L/min, respectively [3]. The films were then sulfurized at 550°C using S vapor. These films were characterized by SEM, EDX, XRD, and PL measurements.

Using the selenization and sulfurization technique, polycrystalline $Cu(In,Al)Se_2$, $CuIn(Se,S)_2$, $CuInS_2$ films with thickness of approximately 2.0 μm were formed without additional annealing. The films adhered well to the Mo/SLG substrate, which was confirmed by the peeling test. Representative XRD patterns of CIASS films are shown in Fig. 1. Phase separations, i.e. distinct peaks corresponding to $CuInSe_2$, $CuAlSe_2$ $CuInS_2$, or binary compounds were not observed. These results represent a step toward realizing a tandem solar cell using CIASS film grown by selenization and sulfurization that use conventional and large-scale equipment.

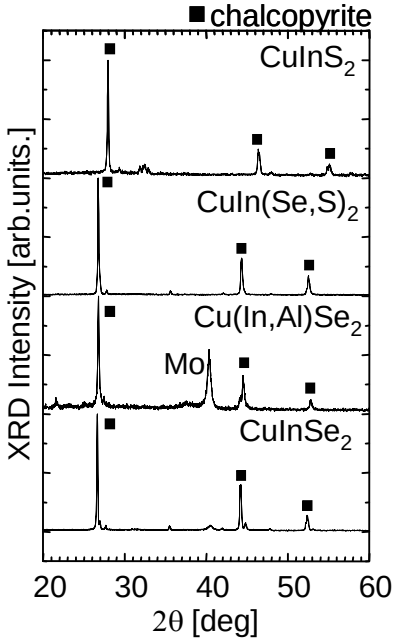

Fig. 1. Representative XRD patterns of CIASS films.

Acknowledgments: This work was supported in part by the Advanced Device Laboratories, Research Institute for Science and Technology, Tokyo University of Science.

[1]. S. Marsillac *et al.*, Appl. Phys. Lett, 81 (2002) 1350.
[2]. S. F. Chichibu *et al.*, J. Cryst Growth, 243 (2002) 404.
[3]. M. .Sugiyama *et al.*, Thin Solid Films, 515 (2007) 5867.

P1-27

Growth and Electrochemical property of DC and RF sputter deposited IrO_x-SnO_x Films

S. Harada[1] and S. Yoshino[1]

[1]*Department of Electrical and Electric Engineering, University of Miyazaki, 1-1 Gakuen Kibanadai, Miyazaki, 889-2192 Japan.*

Corresponding author: t0b114u@cc.miyazaki-u.ac.jp

Ion insertion materials that change colour when a voltage is applied across them are called electrochromic (EC) and are found in transition metal oxides of tungsten, vanadium, nickel, and iridium among others, as well as for mixed nickel-based oxides. The change of colour in an EC layer is caused by the intercalation of ions together with electrons. A typical EC device is either built up by five layers on one substrate, or by two coated substrates. Normally, the substrate is glass, but flexible polymer foils may be used to increase the range of applications. The substrates are coated with transparent conductor films, which have to be transparent in the visible wavelength interval and electronically conducting. The most common transparent conductor is tin doped indium oxide (ITO) [1]. Mixed with iridium is often used because of high cost of iridium oxide. However, there are few reports on mixed crystal iridium–tin oxide ($IrSnO_x$).

In this work, iridium oxide (IrO_x) and $IrSnO_x$ thin films were prepared by DC and RF magnetron sputtering using a carousel type. Obtained samples were examined by X-ray diffraction (XRD), Scanning electron microscopy (SEM), X-ray photoelectron spectroscopy (XPS), electrical resistivity, optical transmittance and refractive index, Cyclicvoltammetry (CV).

$IrSnO_x$ thin films on glass and ITO substrate were obtained at RT with changing base pressure (1.0 ~4.1 Pa) using 2 kinds of SnO_2 and Ir targets. All samples indicate amorphous by XRD spectra. Thickness of the samples decreases slightly with increasing base pressure. Optical transmittance decreases with increasing the pressure. EDX indicate that iridium ratio in the film decrease with increasing the pressure. This corresponds to the results of the XPS. An electrical resistivity decreases with increasing the pressure. This means that the electrical resistivity decreasing with increasing iridium concentration. It is assumed that one of this increasing of the electrical resistivity may be due to increasing an oxygen vacancy from XPS results.

[1]. J. Backholm, E. Avendano, A. Azens, G. de M Azevedo, E. Coronel, G.A. Niklasson, C.G. Granqvist, Sol. Energy Mater. & Sol. Cells **92** (2008) 91.

P1-28

Low-temperature preparation of ZnO films by electrostatic spray pyrolysis deposition for transparent conductive oxide

Norio Onojima[1], Shin-ichi Fukui[1], Umi Horimoto[1] and Takamasa Kato[1]

[1] Interdisciplinary Graduate School of Medicine and Engineering, University of Yamanashi, Takeda 4, Kofu 400-8511, Japan
nonojima@yamanashi.ac.jp, +81-55-220-8503

Zinc oxide (ZnO) has received great interest as transparent conductive oxide (TCO) because ZnO is non-poisonous and consists of abundant materials [1-5]. Transparent conducting films of ZnO have been prepared by several techniques such as sputtering, reactive evaporation, chemical vapour deposition, and spray pyrolysis deposition (SPD). The SPD technique is cheaper, simpler and more versatile than other techniques, and gives the possibility to obtain films with suitable properties for optoelectronic applications. Compared to conventional SPD techniques, electrostatic SPD (ESPD) has the advantage of high deposition efficiency (up to 80%) as the droplets are transported by electrical forces and does not need a carrier gas [6]. In the present work we study ESPD of ZnO films onto glass substrates. Despite atmospheric conditions, we achieved sufficiently transparent ZnO films deposited at the substrate temperature of as low as 200ºC.

The precursor solution used in this study contained zinc acetylacetonate monohydrate ($Zn(CH_3COCHCOCH_3)_2 \cdot H_2O$ or $Zn(acac)_2 \cdot H_2O$) diluted in methanol and deionized water (4:1) at 3.0×10^{-3} mol/l, and was sprayed onto heated substrates. The substrate temperature was maintained at between 200 and 300ºC. The applied potential difference between the nozzle and the substrates was 25 kV. The thickness of deposited films was in a range of 200 to 400 nm.

Optical transmittance spectra of the films deposited at 200 and 300ºC are shown in Fig. 1. It can be noticed that the transmittance in the visible region is larger than 80% for the film deposited at 200ºC. To solve whether the film has a direct or indirect band gap, plots of $(\alpha hv)^2$ versus hv and $(\alpha hv)^{1/2}$ versus hv were analyzed. Better linearity was observed in the former case (see Fig. 2). Optical energy gap is obtained by extrapolating the linear portion of the absorption spectrum to $\alpha hv = 0$, and an energy gap of $E_g = 3.29$ eV was deduced.

In summary, sufficiently transparent ZnO films have been deposited by ESPD at a low temperature of 200ºC. EPSD might be a suitable method to fabricate transparent conducting films based on ZnO with sufficient quality and at low cost. Structural and electrical properties of ZnO films deposited by EPSD are now under investigation.

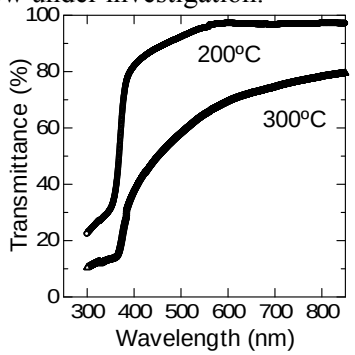

Fig. 1 Optical transmittance spectra of ZnO films deposited at 200 and 300ºC.

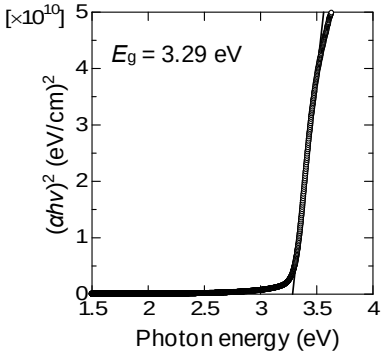

Fig. 2 Plots of $(\alpha hv)^2$ as a function of photon energy, from which an optical energy gap of $E_g = 3.29$ eV was deduced.

[1]. A.J.C. Fiddes, K.Durose, A.W.Brinkman, J.Woods, P.D.Coates, A.J. Banister, J. Cryst. Growth **159** (1996), p.210.
[2]. A. T. Silver, A. S. Juarez, and A. A. Garcia, Solar Energy Mater. **55** (1998), p. 3.
[3]. F.Paraguay D, D.W.Estrada L, D.R.Acosta N,E.Andrade, and M. M. Yoshida, Thin Solid Films **350** (1999), p.192.
[4]. K. Haga, P. S. Wijesena, and H. Watanabe, Appl. Surf. Sci. **169-170** (2001), p.504.
[5]. P. Nunes, E. Fortunato, P. Tonello, F. B. Fernandes, P. Vilarinho, and R. Martins, Vacuum **64** (2002), p.281.
[6]. O. Wilhelm, L. Mädler, and S. E. Pratsinis, J. Aero. Sci. **34** (2003), p.815.

P1-29

Effects of Sb on the film formation of $CuInSe_2$

Huey-Liang Hwang[1], Yu-Yang Ho[2], Yu-Han Kuo[2], Bae-Heng Tseng[2]

[1] Department of Electrical Engineering, National Tsing-Hua University, Hsinchu 30013, Taiwan.
[2] Department of Materials and Optoelectronic Science, National Sun Yat-Sen University, Kaohsiung 80424, Taiwan.

Presenting author's e-mail address: hlhwang@ee.nthu.edu.tw, phone number: +886-3-5715131 ext. 34056

Thin films of $CuInSe_2$ (CIS) for high-efficiency photovoltaic application can be prepared by co-evaporation or selenization. In this work, we demonstrate that the addition of Sb to both film formation processes may result in highly compact grain structure and smooth surface. Figure 1(a) shows surface morphology observed by SEM and Fig. 1(b) is a TEM micrograph revealed the grain structure without any pore at the grain intersections. This film was prepared by co-evaporation with the addition of Sb during the film deposition process at a substrate temperature of 450°C. The Sb-beam flux was as high as that of Se, but only trace of Sb in the film was detected by SIMS. Electrical characterization indicated that the incorporation of Sb in the CIS lattice acted as an acceptor. We also prepared the CIS films using the rapid thermal selenization technique. A thin Sb layer with the thickness of 15nm was inserted between Cu and In, which could prohibit the formation of Cu-In alloy during the precursor deposition processes. Namely, the precursor films with the Cu/Sb/In/Se stacking sequence were deposited on a soda-lime glass substrate. A suitable annealing condition could obtain a CIS film with large grain and smooth surface, see Fig. 2a. Composition analysis using EPMA indicated that the CIS:Sb film prepared by rapid thermal selenization had a fairly uniform composition as shown in Fig. 2b. Though the mechanisms of the film formation are different for the evaporated and selenized films, the effect of Sb seems to benefit the grain growth and leads to large grain and compact grain structure.

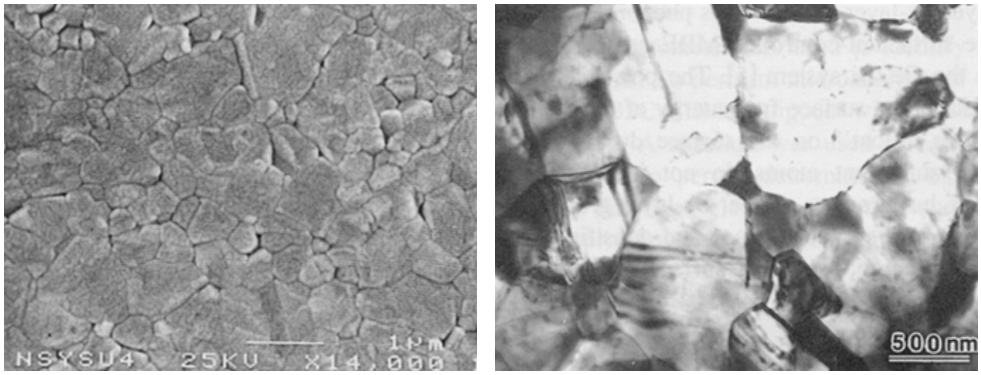

Figure 1. A CIS:Sb film prepared by co-evaporation: (a) surface morphology observed by SEM (b) grain structure revealed by TEM.

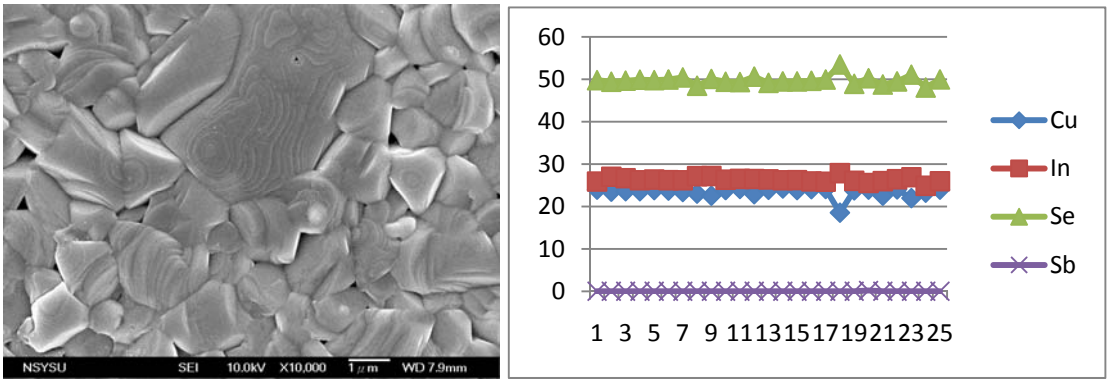

Figure 2. A CIS:Sb film prepared by rapid thermal selenization: (a) surface morphology (b) composition data measured by EPMA.

P1-30

Growth and dielectric properties of novel $TlGaS_2$ <Ni> single crystals in alternate electric fields

A.M. Pashaev, S.N. Mustafaeva, E.M. Kerimova, R.N. Kerimov

Institute of Physics, National Academy of Sciences of Azerbaijan, Baku
G. Javid pr., 33, AZ 1143, Baku, Azerbaijan
E-mail: solmust@gmail.com

$TlGaS_2$ single crystals are high resistive layered semiconductors. Layered crystals usually contain structural defects, such as vacancies and dislocations. The presence of these defects results in a high density of localized states near the Fermi level. Doping of these crystals allows one to tune their physical properties.

The present work was undertaken to study the effect of partial substitution of gallium for Ni in $TlGaS_2$ single crystals on their electric and dielectric properties.

Homogeneous $TlGaS_2$ <Ni> samples were obtained by the method of direct synthesis, i.e. by the reaction between the starting components (Tl, Ga, Ni, S) of high purity degree. $TlGa_{1-x}Ni_xS_2$ (x = 0.01) single crystals were grown by the Bridgman method.

Investigated samples formed flat capacitors whose plane was perpendicular to the crystalline C-axis. Ohmic contacts of samples are made by Ag paste.

Measurements of the dielectric coefficients of studied single crystals were performed by the resonant method using a TESLA BM 560 Qmeter.

The electrical properties (loss tangent, real (ε) and imaginary ($\varepsilon^{//}$) parts of complex dielectric permittivity, and ac conductivity across the layers of $TlGa_{0.99}Ni_{0.01}S_2$ layered single crystals have been studied in the frequency range $f = 5 \cdot 10^4$ to $3.5 \cdot 10^7$ Hz. The results demonstrate that the dielectric dispersion in the $TlGaS_2$ <Ni> crystals has a relaxation nature. Partial substitution of Ni for gallium increases the dielectric permittivity of $TlGaS_2$ and changes the shape of the $\varepsilon^{//}(f)$ curve.

The experimental frequency dependence of the dissipation factor tan δ for $TlGaS_2$ <Ni> single crystal is characterized with a monotonic descending. The hyperbolic decrease of tan δ with frequency is evidence of the fact, that conductivity loss becomes the main dielectric loss mechanism at studied frequency range.

Over the entire frequency range studied, the *ac* conductivity of the $TlGaS_2$ <Ni> crystals varies as $f^{0.8}$, characteristic of hopping conduction through localized states near the Fermi level. The Fermi-level density of states ($N_F = 1.1 \cdot 10^{19}$ $eV^{-1} \cdot cm^{-3}$), the spread of their energies ($\Delta E = 6.6 \cdot 10^{-2}$ eV), and the mean hop distance ($R = 86$ Å) and time ($\tau = 0.2$ μs) have been estimated.

Partial substitution of Ni for Ga in $TlGaS_2$ increases the density of localized states N_F, hop distance and time.

Thus, the replacement of Ga on Ni in $TlGaS_2$ allows us to operate its dielectric properties.

P1-31

Structural evolutions of the mechanically alloyed $Al_{70}Cu_{20}Fe_{10}$ powders

Musa Göğebakan[1] and Barış Avar[1]

[1] Department of Physics, Faculty of Art and Science, Kahramanmaras Sutcu Imam University, Kahramanmaras, 46100, Turkey

barisavar@ksu.edu.tr, +903442191069/ +903442191042

Elemental mixtures of Al, Cu, Fe powders with the nominal composition of $Al_{70}Cu_{20}Fe_{10}$ was mechanically alloyed in planetary ball mills for times up to 80 h. Subsequent annealing of the as-milled powders were performed at different temperatures in the ranges 600-800 °C for 4 h. Structural characteristics of the mechanically alloyed $Al_{70}Cu_{20}Fe_{10}$ powders with the milling time and the heat treatment were investigated by X-ray diffraction (XRD), differential scanning calorimeter (DSC), and differential thermal analysis (DTA). Mechanical alloying of the $Al_{70}Cu_{20}Fe_{10}$ did not result in the quasicrystalline (QC) icosahedral phase (i-phase) formation, and a long time milling resulted in the formation of an β-Al(Cu, Fe) solid solution phase (β-phase). The QC i-phase was only observed for short-time milled powders after heat treatment above 600 °C. The β-phase is observed to be present as one of the major phase in the $Al_{70}Cu_{20}Fe_{10}$ alloy. The w-$Al_7Cu_2Fe_1$ phase (w-phase) was obtained only after heat treatment of the short-time milled and un-milled samples. The present investigation indicated that a suitable technique to obtain a large amount of QC powders is by using a combination of short-time milling and subsequent annealing.

P1-32

Characteristic of low resistivity FTO thin film grown by spray method

Minoru Oshima and Kenji Yoshino
Department of Electrical & Electronic Engineering, Universisty of Miyazaki,
1-1 Gakuen Kibanadai-nishi Miyazaki, 889-2192 JAPAN
swc3900@student.miyazaki-u.ac.jp

Transparent conductive oxide (TCO) films has both transparent and electroically conduction. TCO films have been widely used in applications as optical devices, liquid crystal displays and solar cells. Especially, indium tin oxide (ITO) is known as a good TCO material. On the other hand, tin oxide (SnO_2) is genarally n-type semiconductor material with wide band gap energy, high carrier concentration and large mobility. The material is transparent in the visible and reflective in the infrared regions. Therefore, the SnO_2 thin films have been utilized as transparent electrode.

In the present study, fluorine-doped SnO_2 (FTO) films on glass substrate were grown by spray pyrolysis method at 500 ˚C under air atmosphere. Fluorine concentration varied between 0 and 33 mol% in SnO_2. N_2 gas was used as carrier gas and the flow rate was 6 l/min and the solution flux was kept at 5 ml/min. The substrate size was used microslide glass plates was 25 × 25 mm. The spray solution was containing stannic chloride ($SnCl_4$) and alcohol. In order to dope fluorine into SnO_2 films, NH_3F was used as a source. The samples were examined by XRD and SEM for structural characterization. Hall measurement was carried out at room temperature using the Van der Pauw method for electrical characterization such as carrier concentration, resistivity and mobility. Indium metal was used as ohmic contact. Optical transmittance was also measured at room temperature.

FTO films were deposited on glass substrates by spray pyrolysis technique in order to find out the effect of solution concentration. Figure 1 shows the XRD patterns of FTO films with various fluorine concentration at substrate temperature of 500 ˚C. An ICDD file of SnO_2 is also included as a reference [1]. Peak positions of all XRD patterns correspond well to those of the ICDD. Therefore, the SnO_2 film obtained indicates a tetoragonal structure. A (200) orientation is strongly observed in the all SnO_2 film. A tetragonal structure remains by F-doping. This result corresponds to other paper [2]. The best electrical and optical properties, average transmittance of 82 % and resistivity of 4.0×10^{-4} Ω cm, carrier concentration of 4.7×10^{20} cm^{-3}, mobility of 34 cm^2/Vs, were achieved with fluorine doing concentration of 17 mol% at substrate temperature of 500 °C.

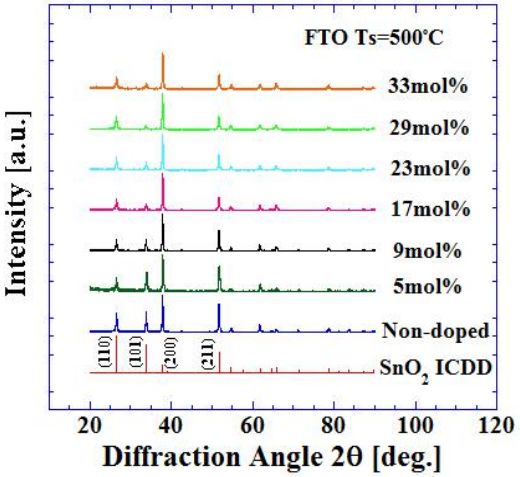

Fig.1 XRD patterns of F-doped SnO_2 films in various fluorine concentration.

[1]. ICDD No.00-041-1445.
[2]. H. Haitjema, J. J. Ph. Elich, C. J. Hoogendoorn, Solar Energy Materials **18** (1989) 283-297.

P1-33

Characterization of n and p-type ZnO thin films grown by pulsed filtered cathodic vacuum arc system

H. Kavak,[1] N. H. Erdogan, I. Ozsahin, R. Esen
Physics Department, Cukurova University, 01330, Adana, Turkey
[1]e-mail: hkavak@cu.edu.tr, Tel: 90 322 3386081 fax: 90 322 3386070

Semiconductor ZnO thin films with wide band gap attract much interest due to their properties such as chemical stability in hydrogen plasma, high optical transparency in the visible and near-infrared region. Due to these properties ZnO oxide is a promising materials for electronic or optoelectronic applications such as solar cell (as an antireflecting coating and a transparent conducting material), gas sensors, surface acoustic wave devices[1,2]. The purpose of this research is to improve the properties of n and p-type ZnO thin films for device applications. Polycrystalline ZnO is naturally n-type and very difficult to dope to make p-type. Therefore nowadays hardly produced p-type ZnO attracts a lot of attention. Nitrogen considered as the best dopant for p-type ZnO thin films.The transparent, conductive and very precise thickness controlled n and p-type semiconducting nanocrystalline ZnO thin films were prepared by pulsed filtered cathodic vacuum arc deposition (PFCVAD) method. Structural, optical and electrical properties of these films were investigated. And also photoluminescence properties of these films were investigated.

Transparent p-type ZnO thin films were produced by oxidation of PFCVAD deposited zinc nitride. Zinc nitride thin films were deposited with various thicknesses and under different oxygen pressures on glass substrates. Zinc nitride thin films, which were deposited at room temperatures, were amorphous and the optical transmission was below 70%. For oxidation zinc nitride, the sample was annealed in air starting from 350 °C up to 550 °C for one hour duration[3]. XRD pattern of these films have diffraction peaks with (100), (101) and (110) orientations. These XRD patterns imply that zinc nitride thin films converted to zinc oxide thin films with the same hexagonal crystalline structures of ZnO. The optical measurements were made for each annealing temperature and the optical transmissions of ZnO thin films were found better than 90% in visible range after annealing over 350 °C. By oxidation zinc nitride the film converted to p-type zinc oxide and the film became more transparent. During the oxidation process at each temperature Hall measurements were made to determine carrier type, carrier concentration, mobility and resistivity. Hall effect measurements indicated that ZnO films were p-type, the reliable results obtained for carrier concentration and mobility. Hall effect measurements proved that after annealing at 350 °C up to 500 °C the film was p-type. By increasing the oxidation temperature over 550 °C the ZnO thin films turned into n-type due to the loss of N atoms in the film[4]. Room temperature photoluminescence measurements were performed to investigate doping and impurity level of these films.

The deposited best quality n and p type ZnO thin films were used to produce hetero and homo-junctions. p-type ZnO deposited on the n-type Si substrate and aluminum or indium was evaporated as metal contacts (n-p). On the other hand n-type ZnO deposited on p-type Si substrate for p-n structure[5]. In the case of homo-junction both n and p-type ZnO thin films were deposited on glass substrates with Al contacts. Current-Voltage characteristics of these devices were determined and the typical result for p-n hetero-junction was shown in the Figure1.

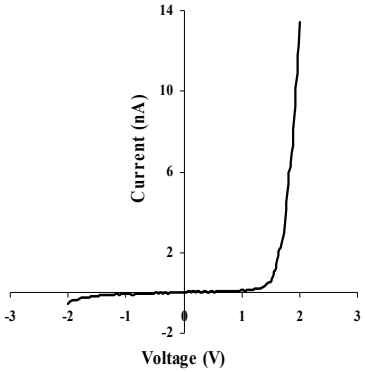

Figure 1. The Output Characteristics of p-n junction

[1]. Look D.C.,*Materials Science and Engineering*,**B80**,383–387 (2001).
[2]. Zhang, Z.Z., Wei, Z.P., Lu, Y.M., Shen, D.Z., Yao, B., Li, B.H., Zhao, D.X., Zhang, J.Y., Fan, X.W., Tang,, Z.K., *J. of Cystal Growth*, **301-301**, 362-365, (2007).
[3]. Kambilafka, V., Voulgaropoulou, P., Dounis, S., Ilioupoulos, E., Androulidaki, M., Saly, Y. V., Ruzinsky, Y. M., Aperathitis, E. *Superlattices and Microstructures* **42**, 55-61 (2007).
[4]. Wang, X., Lu Y.M., Shen, D.Z., Zhang, Z.Z., Li, B.H., Yao, B., Zhang, J.Y., Zhao, D.X., Fan, X.W., Tang, Z.K., *Semicond. Sci. Technol*. **22**, 65-69, (2007).
[5]. S.K. Hazra and Basu,S., *Solid-State Electronics*, **49**, 1158–1162, (2005).

P1-34

Athermal Nonvacuum Creation of new Polydisalicylidene Azometines/Si(GaAs) Heterojunctions

N.M. Mehdiev[1], Yu.A. Nikolaev[2], V.Yu. Rud'[3], Yu.V.Rud'[2], E.I. Terukov[2], T.N. Ushakova[2], N.M. Heller[4], A.G. Ivanov[4], and V.V. Shamanin[4]

[1]Azerbaidzhan State Oil Academy, Azadlig Av.20,Baku,Az1010,Azerbaijan Republic, e-mail: nizami-mehdiyev@rambler.ru
[2]Ioffe Physico-Technical Institute Russian Academy of Sciences, ul. Polytekhnicheskaya 26, St. Petersburg, 194021 Russia
[3]St. Petersburg State Polytechnical University, ul. Polytekhnicheskaya 29, St Petersburg, 195251 Russia
[4]Institute of Macromolecular Compounds, Russian Academy of Sciences, Bolshoi pr. 31, St. Petersburg, 199004 Russia

The creation of new heterojunctions (HJs) on inorganic semiconductors is accompanied widening of the functional range of existing semiconductor devices and offers the possibility of simplifying and, hence, reducing the cost of materials and technology [1, 2]. Currently, interest has grown in the photoelectric properties of direct contact of diamond-like semiconductors with materials of organic nature [3]. In this paper, we consider the main results of the pioneer studies of electrical properties of nonclassically polyconjugated polydisalicylidene azomethines (PSAs), the developed new athermal nonvacuum technique for creation of photosensitive HJs on the new polymers, and comprehensive studies of their photoelectrical properties.

The measured conductivities σ for different polymers are in the range of $10^{-7} \div 10^{-8}$ $\Omega^{-1} \cdot cm^{-1}$ at 300 K. The main feature of temperature dependences of these polymers is the detection of the activation mechanism of charge transport in thin films of new polymers. The activation energies for PSAs are in the range of 0.2÷0.4 eV, there is reason to believe that the conductivity of new polymers is of semiconductor type. In this study, we also attamped to develop fundamentals of the method for controlling the value σ of polymer films. Thus, films of PSAs exhibit the doping effect, which appears upon dissolution of an impurity element (iodine) introduced into them.

The HJs obtained by the nonvacuum athermal method of bringing drops of initially liquid PSAs polymer solution into direct contact with inorganic semiconductor. The rectification factor in the first HJs is small and varies from 1.5 to 5.

The HJs obtained by bringing semiconductors Si(GaAs) without vacuum into direct contact with in initially liquid and then solid polymer exhibited the photovoltaic effect. The main features photovoltaic effect of new HJs is mainly controlled by the energy barrier appearing at the polymer/semiconductor contact. The longwavelength edge of photoconversion η of these HJs is entirely controlled by interband photoabsorption on incident radiation Si or GaAs. Therefore, an increase in η in Si-based HJs appear at $\hbar\omega$>1 eV, while the onset of the increase in η on GaAs-based HJs begins at $\hbar\omega$>1.2 eV, which is caused by difference in energy gap E_G. Extrapolation of the dependences $(\eta\hbar\omega)^{1/2} \rightarrow 0$ and $(\eta\hbar\omega)^2 \rightarrow 0$ yields values corresponding to the known for Si and GaAs band gaps and interband absorption mechanisms, Si — $E_G^{ind} \approx 1{,}07$ eV and GaAs — $E_G^{d} \approx 1{,}41$ eV, respectively, which is in agreement with well-known analysis for these semiconductors.

So, based on the contact of diamond-like inorganic semiconductors (by the example of Si and GaAs), new type photoconversion HJs was suggested and created. The HJs here created for the first time may find application in optoelectronics in developing low-cost broadband potoconvertors of the next generations.

[1]. N.A. Goryunova, "Chemistry of diamond-like Semiconductors" (Leningrad State University, Leningrad, 1963).
[2]. Zh.I. Alferov, *Semiconductor*s **32** (1998), p. 1.
[3]. V.Yu. Rud',Yu.V. Rud', and V.Kh. Shpunt *J. Techn. Phys*. **45** (2000), p. 255.

P1-35

About one feature of interface of the heterojunctions made by a method of landing to optical contact

Kyazym-zade A.G., Salmanov V.M., Axmedov S.F.

Baku State University, Az1148, 23, Z.Khalilov str., Baku, Azerbaijan
E-mail: bsu_aydin@yahoo.com

In work one important feature of heterojunctions (HJ), made by a method of landing to optical contact is discussed.

In simple model of the Anderson it is supposed that electronic balance between adjoining bodies in HJ is established only after one component which electrochemical potential is called as Fermi's level. However such approach is possible only in that specific case when the crystal lattice of adjoining bodies possesses an identical chemical compound and structure. Actually at removal from a firm body valence electrons together with it one of structural knots of a lattice with characteristic for the given body type of a chemical bond disappears and there is positively charged rest with new type of communication generally from the thermodynamic point of view the system cannot be considered as the unicomponent. The specified process is formally similar to a separation electrons from free atom and can be written symbolically down in a kind $a = e + g$, where a – a symbol of neutral knot of a lattice of atom, e – a symbol of a free electron, g – a symbol of a free hole. As generally all three particles (a, e, g) have independent degrees of freedom they should be considered in the statistician as independent particles with own electrochemical potentials μ_a, μ_e, μ_g. Therefore full thermodynamic balance between adjoining bodies A and B, will be established at performance of two conditions, for example: $\mu_{aA} = \mu_{aB}, \mu_{eA} = \mu_{eB}$. Differently, the considered system should be considered as the two-componential. In semiconductor heterojunctions when the basic crystal lattices of adjoining bodies A and B are various, in an initial condition $\mu_{aA} \neq \mu_{aB}$. As almost in all methods of manufacturing of heterojunctions boundary atoms of bodies A and B incorporate among themselves valence communications there comes balance $\mu_{aA} = \mu_{aB}$, and full of electronegativity of boundary atoms get identical values. It occurs at the expense of redistribution of clouds of the general valence electrons and is accompanied by occurrence of interphase jump of potential ΔU_f and the double charged layer with a thickness d, equal 1-4 internuclear distances. Thereof the total bend of zones is defined by expression $\Delta\varphi - q\Delta U_f$ and differs from a difference of works of an exit of adjoining bodies $\Delta\varphi$ at condition performance $\mu_{eA} = \mu_{eB}$.

The problem becomes simpler in that case when boundary atoms of bodies A and B do not incorporate among themselves valence communications as it takes place in the heterojunctions made by a method of landing to optical contact on the basis of layered compounds of A^3B^6 type. Thus electrochemical potentials both μ_{aA} и μ_{aB} remain invariable and do not bring the contribution to distribution of a contact potential difference. It is natural that at absence or small concentration of borderlines the energy band diagram of such systems will correspond to ideal model of the Anderson.

In work other features and advantages manufacturing HJ by a method of landing to optical contact are discussed also.

SECTION TWO

Characterization techniques, including large scale facilities

I2-1

Electronic structure of ternary chain Tl chalcogenides studied by photoemission spectroscopy

Kojiro Mimura

Department of Mathematical Sciences, Graduate School of Engineering, Osaka Prefecture University, Gakuen-cho 1-1, Naka-ku, Sakai 599-8531, Japan

mimura@ms.osakafu-u.ac.jp, +81-72-254-9367/+81-72-254-9367

The ternary Tl chalcogenides $TlInSe_2$ and $TlGaTe_2$ with quasi one-dimensional chain structure have attracted much attention because of the phase transitions with incommensurate (IC) phase formation that is believed to be behind the record-breaking thermoelectric power (~10^6 μV/K below 413 K) of $TlInSe_2$ [1]. On the other hand, above heavy-elemental Tl chalcogenides may exhibit unique dispersive structures like Dirac cone, observed earlier in the surface bands of Bi_2Se_3 [2]. In this work, the electronic structure of $TlInSe_2$ and $TlGaTe_2$ has been studied by angle-resolved photoemission and hard X-ray photoelectron spectroscopies (ARPES and HX-PES) in order to get a better insight into electronic structure of these materials. The ARPES and HX-PES experiments have been performed at the beamlines BL-9A of HiSOR and BL47XU of SPring-8, respectively.

1. ARPES study of $TlInSe_2$

We have succeeded in high-resolution ARPES measurements of $TlInSe_2$ at 280K and 50K, and in getting data that vividly exposes the transformation of the uppermost valence bands of this material upon passing from IC- to commensurate phase. We have shown that the manifestation of the IC-phase at 280K is the kink-structure positioned at 0.67 $Å^{-1}$ wave-vector in the *A*-direction of the Brillouin zone. Gap-like structures have been shown to emerge at the same wave-vector when temperature is lowered to 50 K. At the last temperature $TlInSe_2$ is believed to be already a commensurate material.

2. HX-PES study of $TlInSe_2$ and $TlGaTe_2$

The temperature dependence of the relative peak position and peak width for each core level (Tl 4f, Ga 2p and Te 3d) in $TlGaTe_2$ suggests that the phonon influence intensively contributes to the physical properties of this material. Comparison between the values of thermoelectric power evaluated from the temperature shift of the valence band maximum of $TlGaTe_2$ and $TlInSe_2$ shows that the former material would also exhibit large Seebeck coefficient. Comparison of Tl 4f spectrum of $TlGaTe_2$ with that of $TlInSe_2$ implicitly suggests that the physical properties of $TlGaTe_2$ closely resemble those of $TlInSe_2$.

3. Peculiar dispersive structure in energy band of $TlGaTe_2$

Two linear dispersive structures that are not reproduced by the band calculations for the bulk material [3] were observed only in the energy band along Γ-N direction perpendicular to the chains. These dispersions form a cross-type structure that is centred at the Γ point and extends along Γ-H-T direction parallel to the chains. The cross-type structure exhibited photon energy dependence, and was obviously observed only on the samples with high-grade quality of the surface. Therefore we believe that, in fact, the disclosed dispersive structures in ARPES of $TlGaTe_2$ are bound to the conduction bands and the ARPES detects the joint density of states.

Acknowledgments: I would like to sincerely thank my collaborators Mr. T. Ishizu, Mr. S. Motonami, and Prof. Y. Taguchi from Osaka Prefecture University, Prof. K. Wakita from Chiba Institute of Technology, Prof. N. Mamedov, Prof. G. Orudzhev, and Mr. S. Hamidov from Institute of Physics, Azerbaijan National Academy of Science, Dr. E. Ikenaga and Dr. K. Yan from JASRI/SPring-8, Prof. K. Kobayashi from NIMS, and Mr. M. Arita, Prof. H. Namatame and Prof. M. Taniguchi from Hiroshima University for their cordial support of this work. This work was also supported by the Grant-in-Aid for Scientific Research (C) from the Japan Society for the Promotion of Science and by the Nippon Sheet Glass Foundation for Materials Science and Engineering.

[1]. N. Mamedov, K. Wakita, A. Ashida, T. Matsui and K. Morii, *Thin Solid Films* **499** (2006) 275.

[2]. See for example, Y. Xia, D. Qian, D. Hsieh, L. Wray, A. Pal, H. Lin, A. Bansil, D. Grauer, Y. S. Hor, R. J. Cava and M. Z. Hasan, *Nature Physics* **5** (2009) 398.

[3]. É. M. Godzhaev, G. S. Orudzhev and D. M. Kafarova, *Physics of the Solid State* **46** (2004) 833.

I2-2

Raman and X-ray diffraction studies of ternary chalcogenides at ambient and high pressure

Hans D. Hochheimer

Department of Physics, Colorado State University, Fort Collins, CO 80523, USA

Ternary chalcogenides as well as rare earth chalcogenides are studied at ambient and high pressure using various techniques to check claims of high pressure phase transitions in these materials.

Most interesting is the result of a study of the nature of the phase transition of $TlGaSe_2$ measuring the real part of the dielectric constant, ε', the heat capacity, c_p, infrared and X-ray diffraction.

The results prove unambiguously that we have found the first example of lone pair ferroelectricity predicted earlier to exist by Orgel (L.E. Orgel, J. Chem. Soc. 4 (1958) 3815).

In the case of rare earth chalcogenides our high pressure optical and X-ray diffraction studies show that the application of high pressure leads to the formation of Se-Se bonds in the case of $KTbP_2Se_6$ whereas

It does not occur in $KPrP_2Se_6$. We suggest a model for the formation of such bonds and show why it can happen in $KTbP_2Se_6$ but not in $KPrP_2Se_6$ based on structural arguments.

O2-1

Confocal laser spectroscopy of $TlInS_2$, $TlGaSe_2$ and $TlGaS_2$ semiconductors-ferroelectrics

Kazuki Wakita[1], Akinori Suzuki[1], Umihito Miyamoto[1], Durdana Huseynova[2], YongGu Shim[3], Nazim Mamedov[2], Oktay Alekperov[2], Arzu Najafov[2], and Tofig Mammadov[2]

[1] Chiba Institute of Technology, 2-17-1, Tsudanuma, Narashino, Chiba 275-0016, Japan
[2] Institute of Physics, H. Javid 33, Baku AZ-1143, Azerbaijan
[3] Osaka Prefecture University, 1-1 Gakuen-cho, Nakaku, Sakai, Osaka 599-8531, Japan

E-mail: kazuki.wakita@it-chiba.ac.jp; Phone/Fax: +81-47-478-0374

Ternary layered thallium chalcogenides, $TlInS_2$, $TlGaSe_2$ and $TlGaS_2$ with quasi-two-dimensional crystal structure continue to attract wide attention for their unique properties which promise novel applications. However, the origin of these properties, which are certainly bound to successive phase transitions with incommensurate phase formation, is not completely clear, because of the absence of the reliable information on the influence of these transitions on electron and phonon spectra of the above materials. In particular, exciton emission, which might have definitely been useful for obtaining such information, has not been observed so far in $TlInS_2$ at temperature higher than 77K which is quite distant from the ferroelectric phase transition point (200K). In the other two materials exciton emission has not been observed at all.

This work reports the first observation of the exciton emission lines in $TlInS_2$ and $TlGaSe_2$ at room temperature by using confocal optical system and second harmonic generation of Ti:supphier laser. The transformation of the exciton spectra with decreasing temperature has then been tracked down and analyzed with due regard to phase transitions. Complimentary, temperature-dependent confocal Raman spectroscopy and photoconductivity data are given and discussed for all three compounds. It is believed that present findings on exciton emission will stimulate further studies on ternary thallium chalcogenides with the use of confocal laser spectroscopy.

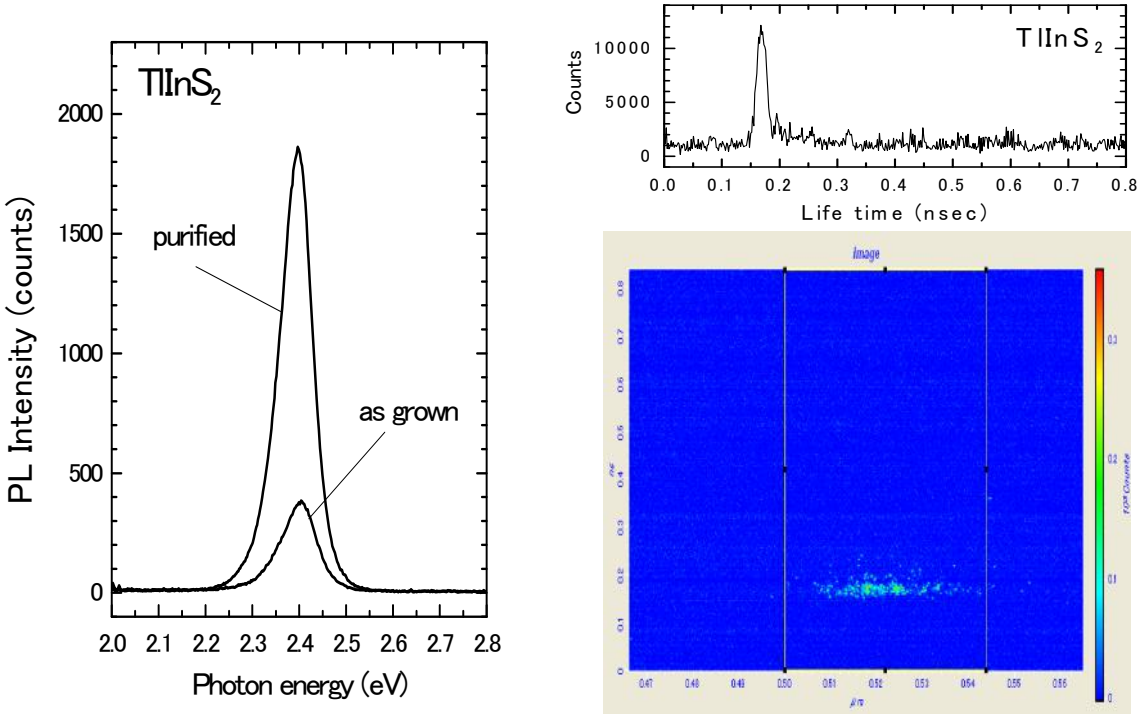

Figure Photoluminescence (PL) of $TlInS_2$ at room temperature: left part-steady state PL; right part – time resolved PL.

O2-2

Microscopic investigations of compositional gradients in CIGS by highly spatially and spectrally resolved cathodoluminescense spectroscopy

Mathias Müller[1], Frank Bertram[1], Jürgen Christen[1], Daniel Abou-Ras[2], Thorsten Rissom[2], Thomas Unold[2], Hans-Werner Schock[2]

[1] Otto-von-Guericke University Magdeburg, Uni-Platz 2, 39106 - Magdeburg, Germany
[2] Helmholtz-Center Berlin for Materials and Energy, Hahn-Meitner-Platz 1, 14109 – Berlin, Germany

mathias.mueller@ovgu.de, phone +49 (0) 391 6711664, fax +49 (0) 391 6711130

$CuInGaSe_2$ (CIGS) thin films for solar cell application have been investigated using highly spatially and spectrally resolved cathodoluminescence (CL) microscopy.
The CIGS films have a thickness of 2 µm and were grown on a Mo-coated glass substrate. The stack was completed by chemical bath deposition of a CdS buffer layer (50 nm) and sputtering of a transparent i-ZnO/ZnO:Al bilayer (130 nm/250 nm). A set of CIGS films with various [In]/[Ga] ratios were grown for comparison. In addition, a cross-section sample was prepared by means of mechanical and ion polishing in order to investigate the lateral distribution of luminescence in CIGS growth direction. The cross-section sample was carbon-coated in order to reduce charge effects during the CL data acquisition.
The T = 4.2 K cathodoluminescence (CL) was performed in a home-built setup based on a modified scanning electron microscope. In the CL imaging mode the focused electron beam is scanned over the area of interest and a complete CL spectrum is recorded at each pixel. The overall spatial resolution is significantly better than 0.1 µm reaching δx =35 nm for optimum conditions.
The integral CL spectra of the [In]/[Ga] series are dominated by donor-acceptor pair (DAP) luminescence. The peak energies of these spectra are ranging from 0.98 eV / 1265 nm ($CuInSe_2$) to 1.67 eV / 742 nm ($CuGaSe_2$). The DAP band shifts to higher energies with higher excitation densities (Figure 1).
Figure 2 shows the wavelength with maximum intensity for each pixel coded in greyscale (CL wavelength image - CLWI) of the cross section sample, which directly visualizes differences between neighboring CIGS grains of the thin film. The luminescence of individual grains differs considerably. These micro-fluctuations can also be seen in monochromatic CL intensity images. The spectral evolution of the CL along the growth direction will be presented.

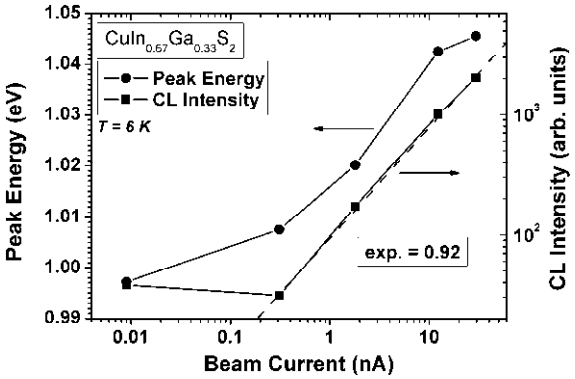

Figure 1: Shift to higher energies of the emission peak with higher excitation density

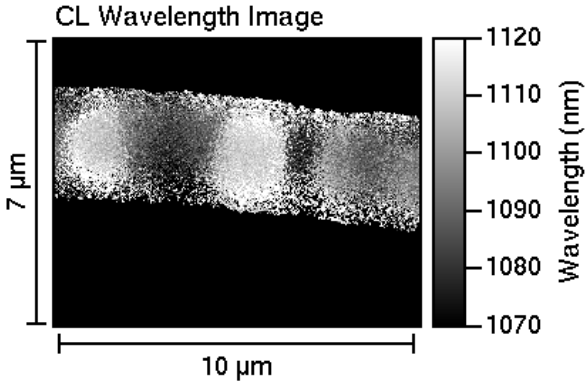

Figure 2: CLWI of the cross section of a CIGS thin film

O2-3

Correlation of the optical properties with ε(T)-dependence at ferroelectric phase transition in $TlInS_2$ doped with different impurities

O.Z Alekperov., A.I. Nadjafov, N. A. Safarov

Institute of Physics, National Academy of Sciences, H. Javid av. 33.
Baku 1143, Azerbaijan,
ozalekperov@physicsab.az (99412)4391105

Impurity doping of semiconductors with ferroelectric phase transition (FPT) leads to the temperature broadening of this transition and shifting of dielectric anomaly (DA) maximum in $\varepsilon(T)-$ dependence to lower temperatures. Usually broadening and shifting are correlated. The more broadening the higher is shifting. The reason of DA shifting is a result of contribution of the energy of carriers to the crystal free energy, which according to Ginzburg-Landau theory of FPT shifts T_c only to lower temperatures for both electrons and holes. This phenomenon is investigated in this report by comparing of the forms of the room temperature photoconductivity (PC) and absorption (α) spectra around the forbidden gap region ($\hbar\omega \le E_g$) with FPT $\varepsilon(T)-$ dependence for samples doped with different impurities. As a result of these investigations it was established that deep level impurities which have no peculiarities in $TlInS_2$ band edge PC and α-spectrums do not lead to any broadening or shifting in FPT $\varepsilon(T)-$ dependence. Rare earth elements Yb, Sm, Ln and other lanthanides form deep levels and do not change FPT. In contrary, when doping creates shallow impurity (SI) states, which broad band edge α-spectrums and create PC lines at $\hbar\omega < E_g$, then FPT broadening and shifting in $\varepsilon(T)$-dependence of samples takes place. At high doping levels in $TlInS_2$ some impurities Fe, Mn, B, Cr and C besides of SI states create deep level states as well. This is seen from comparing of absorption and PC at different doping concentrations. DA of $\varepsilon(T)$ dependence at FPT accompanies by simultaneous conductivity $\sigma(T)$-anomaly as for doped as well as for samples with residual SI. This fact proves that at DA temperatures carriers frozen on charged SI are thrown out utterly into free bands due to SI ionization energy $E_{iDA} = E_i / \varepsilon^2(T)$ decrease as a result of SI Coulomb potential screening at DA. Consequently $\varepsilon(T)$-broadening at FPT in samples doped with SI arises as a result of increase of damping factor $\gamma \sim \tau^{-1}$ due to ionized SI scattering ($\tau \sim N_i^{-1}$) and changing of polarization of crystal cells at FPT by randomly distributed SI. Ionized SI potential fluctuations besides of known effects (broadening of absorption and PC edges, hopping conductivity etc) lead to fluctuations of refractive index n. The visibility of interference spectra (IS) decreases dramatically in samples doped with SI. Model calculation of IS with fluctuations of n testifies this. So doping only with SI in $TlInS_2$ crystals leads to FPT broadening and shifting of DA to lower temperatures.

O2-4

Optical and structural properties of Zn-Cd-Mn-Se double quantum well systems

T. Matsumoto*, K. Ohmori, K. Kodama, M. Hishikawa, S. Fukasawa,
F. Iwasaki, T. Muranaka, and Y. Nabetani

Department of Electrical Engineering, University of Yamanashi, Takeda 4, Kofu 400-8511 Japan
*Corresponding author: e-mail:matumoto@es.yamanashi.ac.jp, phone:+81-55-220-8459, fax:+81-55-220-8777

Excitons localized in and transfering between low-dimensional structures such as quantum dots and quantum wells have been interested from the stand point both of physics and of device application. We reported tunnelling transfer of spin-polarized excitons in coupled diluted-magnetic-semiconductor (DMS) and non-DMS (NMS) double quantum well (DQW) [1, 2]. In this paper, we describe optical and structural properties of the DQW systems.

Asymmetric DQWs were grown on GaAs (001) substrates with molecular beam epitaxy. The DQWs had the following structures: ZnSe lowere barrier layer, $Zn_{1-x}Cd_xSe$ NMS well, ZnSe middle barrier layer, $Zn_{1-x-y}Cd_xMn_ySe$ DMS well, and ZnSe upper barrier layer. The Cd- and Mn-composition were x=0.25 and y=0.03, respectively. The well widths of the DMS well L_m and the NMS well L_n were so designed that the lowest energy level of the DMS well was close to the second excited level of the NMS well. The width of the middle barrier layer L_s was designed to adjust the degree of tunnelling probability. The DQW structure was characterized with X-ray diffraction (XRD), photoluminescence (PL), and PL excitation (PLE) measurements. Polarization selective magneto-PL was also measured under magnetic field up to 8 T.

Figure 1 shows XWD spectra of a DQW sample. The peak at 65.8° comes from the ZnSe barrier layers. The structures appearing 62.2° through 65.4° reflect the DQW structure. Reciprocal lattice map around (224) is shown in Figure 2. Signal from the ZnSe barriers is seen beside that from the GaAs substrate. The lattice of the ZnSe barriers is fully relaxed because the lower ZnSe layer is as thick as 300nm. Figure 3 shows PL (dashed line) and PLE (solid line) spectra of a DQW sample. The vertical bars indicate calculated energies of exciton in the ground (E_1) and excited (E_2, E_3, E_4) states of the DQW system. The PL is due to the recombination of exciton in the ground state localizing in the NMS well. The 2.81-eVpeak in the PLE spectrum is due to free-exciton absorption in the ZnSe barrier layers. The excitation band below the free exciton peak is due to energy levels in the DQW. The E_1 and E_2 are quantum levels derived from the NMS well. The E3 and E4 levels, which are derived from the NMS well or the DMS well, are very close. External magnetic field can bring them in quasi-resonant condition. A broad peak around 2.7 eV in the PLE spectrum is due to absorption creating excitons in these excited states. The exciton in the excited state transfers from the DMS well to the NMS well and relaxes to the ground state, and finally contributes the PL.

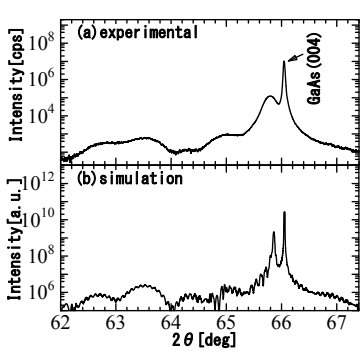

Figure 1. (a) Measured and (b)simulated XRD spectra of a DQW sample.

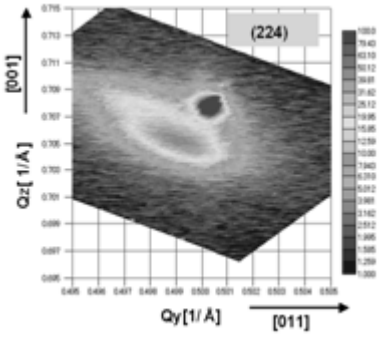

Figure 2. Reciprocal lattice map of the DQW same as in Fig.1. Colour code is in log scale.

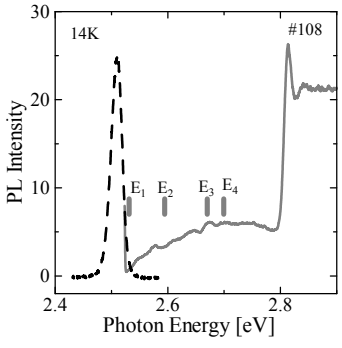

Figure 3. PL (dashed line) and PLE (solid line) spectra of a DQW sample.

[1]. M. Ito, M. Tajima, K. Ohmori, T. Muranaka, Y. Nabetani, T. Kato, and T. Matsumoto, *J. Korean Phys. Soc*. **53**(2008), p.2972.
[2]. K. Ohmori, K. Kodama, T. Muranaka, Y. Nabetani, and T. Matsumoto, *Phys. Status Solidi. (c)* **7**(2010), p.1642.

O2-5

Local structural order in amorphous ternary chalcogenide systems: Magnetic resonance approach

E. Mammadov[1], D. Bobela[2], D. Baker[3] , S. Mehdiyeva, and P. C. Taylor[3]

[1] *Institute of Physics, Azerbaijan National Academy of Sciences, Baku, AZ-1143, Azerbaijan*
[2] *National Renewable Energy Laboratory, Golden, CO 80401, USA*
[3] *Physics Department, Colorado School of Mines, Golden, CO 80401, USA*

E-mail: emammadov@physics.ab.az; Phone: +994 439 3528

The local structural order in ternary glasses such as $Ge_2Sb_2Te_5$ is of interest due to their ability to exhibit reversible crystalline-to-amorphous phase switches used in non-volatile memory devices. In spite of numerous studies there is no a complete understanding of the nearest-neighbor bonding structure in these materials. Namely it is not clear whether chalcogen atoms preserve their two-fold coordination over the different glass compositions.

We report on ^{75}As, ^{51}Sb, and ^{121}Te nuclear magnetic resonance (NMR) experiments on $Ge_xSb_yTe_{1-x-y}$ glasses compared with $Ge_xAs_ySe_{1-x-y}$. The local structural order in $Ge_xAs_ySe_{1-x-y}$ glasses is dominated by "8-N" rule when Ge, As, and Se atoms exhibit 4, 3, and 2-fold coordination, respectively. Se atoms preserve their coordination in $Ge_2As_2Se_5$. This leads to appearance of homopolar or wrong bonds such as Ge-Ge, As-As, and Ge-As in Se-deficient glasses. In particular, ^{75}As NQR results suggest that the majority of As atoms possess two As-As bonds per atom [1]. ^{75}As NMR measurements reveal a broad spectrum with no resolved structure indicating to the contribution from highly distorted arsenic sites. Arsenic atoms in this composition most likely form complex structural units rather than regular pyramidal units characteristic to three-fold coordinated As and Sb atoms.

In $Ge_2Sb_2Te_5$ we have found no evidence of Sb-Sb bonds from ^{51}Sb NMR experiments. No evidence of them has also been reported from EXAFS experiments [2]. ^{51}Sb NMR line in $Ge_2Sb_2Te_5$ exhibits a well-resolved structure with spectral features which have been used to fit the data. These results suggest the presence of three-fold coordinated Sb atoms forming pyramidal units in $Ge_2Sb_2Te_5$. However, a contribution from distorted Sb sites has been revealed by fitting the experimental data. In the absence of Sb-Sb bonds this distortion might be associated with weak interaction of Sb with Te atoms at the non-bonded site of the Sb apex.

The absence of Sb-Sb bonds implies the presence of overcoordinated Te_3^+ sites. The presence of Te_3^+ has been suggested as a possible crucial condition for the phase-change behavior in $Ge_2Sb_2Te_5$. The overcoordination of Te atoms in $Ge_2Sb_2Te_5$ has also been supported by results of ^{121}Te NMR.

[1]. E. Mammadov and P.C. Taylor, J. Non-Crystal. Solids 354 (2008) 2732-2735
[2]. M. A. Paesler, D. A. Baker, G Lucovsky, J. Non-Crystal. Solids 354 (2008) 2706

P2-1

Local structure around Mn atoms in IV-VI ferromagnetic semiconductor $Ge_{0.6}Mn_{0.4}Te$ by X-ray fluorescence holography

N. Happo,[1] S. Senba,[2] S. Hosokawa,[3] K. Hayashi,[4] W. Hu,[5] M. Fujiwara,[1] K. Tanaka,[1] H. Asada,[6] and M. Suzuki[7]

[1] Graduate School of Information Sciences, Hiroshima City University, Hiroshima 731-3194, Japan
[2] Department of Electirical Engineering, Ube National College of Technology, Ube 755-8555, Japan
[3] Center for Materials Sciences Using Third-Generation Synchrotron Radiation Facilities, Hiroshima Institute of Technology, Hiroshima 731-5193, Japan
[4] Institute of Materials Research, Tohoku University, Sendai 980-8577, Japan
[5] SPring-8/JAEA, Hyogo 679-5148, Japan
[6] Graduate School of Science and Engineering, Yamaguchi University, Ube 755-8611, Japan
[7] SPring-8/JASRI, Hyogo 679-5198, Japan
happo@hiroshima-cu.ac.jp, +81-82-830-1553/ +81-82-830-1553

The IV-VI diluted magnetic semiconductor $Ge_{1-x}Mn_xTe$ is expected as a spintronics material, because it shows a ferromagnetic order below 140 K at about $x = 0.51$ [1]. It is believed that the ferromagnetism largely relates to the arrangements of the Mn ions and the vacancies, the latter of which may be induced at the cation positions. Due to such vacancies, the crystal would distort, which may also influence the ferromagnetism of this material. X-ray fluorescence holography (XFH) is a powerful tool to investigate such atomic distortions by obtaining three-dimensional (3D) atomic images. Note that the distortions in crystals cannot be directly obtained from a usual x-ray diffraction technique. We recently performed the XFH experiments on $Cd_{0.6}Mn_{0.4}Te$ [2] and $Zn_{0.4}Mn_{0.6}Te$ [3] in order to investigate the local structure around the Mn and Zn atoms, and the distortions in these mixed crystals were discussed in detail. In this study, Ge *K*α and Mn *K*α XFH measurements were carried out on $Ge_{0.6}Mn_{0.4}Te$ thin film.

A $Ge_{0.6}Mn_{0.4}Te$ thin film single crystal sample was grown on a BaF_2 (111) substrate by a molecular beam epitaxy technique. The Ge *K*α and Mn *K*α XFH experiments were performed at BL6C of the PF/KEK and BL39XU of the SPring-8. Incident X-rays were irradiated onto the (111) sample surface. The hologram data were collected in inverse mode at room temperature at different incident X-ray energies of 11.2–14.2 keV for Ge *K*α and 7.0–10.5 keV for Mn *K*α in 0.5 keV steps. The Ge *K*α (9.885 keV) and Mn *K*α (5.898 keV) fluorescent X-rays were detected by an avalanche photodiode via a cylindrical or toroidal graphite energy-analyzer. From the hologram patterns obtained with the different incident X-ray energies, 3D atomic configuration images were reconstructed using Barton's algorithm [4].

The obtained 3D atomic image from the Mn *K*α XFH was depicted in Fig. 1. The central Mn atom locates at the center of the figure, and the grid lines indicate the unit cell of the host GeTe crystal. A NaCl-like sublattice of Te anions was clearly seen around the central Mn atom. The image obtained from the Ge *K*α XFH also shows a clear fcc anion sublattice. Therefore, it was confirmed that the Mn atoms replace with the Ge atoms in the host GeTe. On the contrary, the images of cations are hardly visible in the figure. This result suggests that the positions of cations largely fluctuate in $Ge_{0.6}Mn_{0.4}Te$.

Acknowledgments: The XFH experiments were performed at PF/KEK (Proposal No. 2009G584) and SPring-8 (Proposal No. 2009B1168).

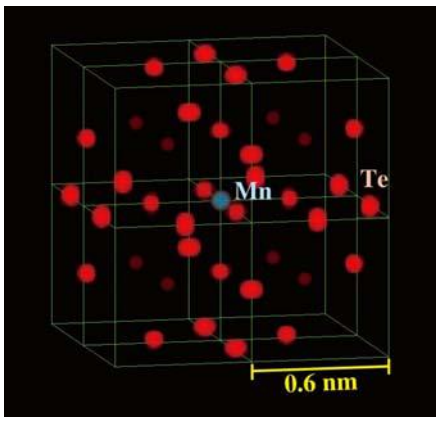

Figure 1. 3D atomic image of Mn *K*α XFH.

[1]. Y. Fukuma, et al., Physica E (Amsterdam) **10** (2001), p.273 .
[2]. N. Happo et al., J. Cryst. Growth **311(3)** (2009), p.990.
[3]. S. Hosokawa et al., Phys. Rev. B **88** (2009), p.134123.
[4]. J. J. Barton, Phys. Rev. Lett. **67** (1991), p.3106.

P2-2

Three-dimensional atomic images of $TlInSe_2$ thermoelectric material obtained by x-ray fluorescence holography

S. Hosokawa,[1] N. Happo,[2] K. Hayashi,[3] K. Mimura,[4] K. Wakita,[5] W. Hu,[6] H. Ishii,[7] J. Jayakanthan,[7] and N. Mamedov[8]

[1] Center for Materials Sciences Using Third-Generation Synchrotron Radiation Facilities, Hiroshima Institute of Technology, Hiroshima 731-5193, Japan
[2] Graduate School of Information Sciences, Hiroshima City University, Hiroshima 731-3194, Japan
[3] Institute of Materials research, Tohoku University, Sendai 980-8577, Japan
[4] Graduate School of Engineering, Osaka Prefecture University, Sakai 599-8531, Japan
[5] Faculty of Engineering, Chiba Institute of Technology, Narashino 275-0016, Japan
[6] SPring-8/JAEA, Hyogo 679-5148, Japan
[7] NSRRC SPring-8 Office, Hyogo 679-5198, Japan
[8] Institute of physics, Azerbaijan National Academy of Sciences, 1143 Baku, Azerbaijan

happo@hiroshima-cu.ac.jp, +81-82-830-1553/ +81-82-830-1553

Tl-based chalcogenides, such as $TlInSe_2$, are promising materials for thermoelectric power plant, because they have semiconducting natures of large thermopower and small thermal conductivity but a relatively large electronic conductivity [1]. Such strange properties originate from low-dimensional atomic structure. In particular, it is believed that Tl atom chains, locating between the $InSe_4$ frameworks, highly affects the thermoelectric nature in $TlInSe_2$.

In this study, x-ray fluorescence holography technique [2,3] was applied to construct three-dimensional (3D) atomic images around the Tl atoms in $TlInSe_2$ single crystal. The experiments were performed at room temperature, where the sample is in the incommensurate phase, at BL6C of PF/KEK and BL12B2 of SPring-8. Incident x-rays with thirteen energies beyond the Tl L_{III} absorption edge (12.66 keV) were irradiated onto the flat sample, and the emitted Tl $L_{\square}$ fluorescent x-rays were energy-analyzed with a cylindrical graphite crystal and detected with an APD detector by changing the tilt and azimuth angles. Using Barton's algorithm [4], a 3D atomic image was obtained around the central Tl atoms.

In the obtained 3D image, the In atoms are clearly visible at the proper positions expected by x-ray diffraction data. However, the Tl images are also observed at the proper positions but very weakly. A theoretical calculation performed without including the spatial fluctuations of Tl atoms shows that the image of the Tl is very strong since the x-ray scattering by Tl atoms (Z = 81) is much stronger than that by the In atoms (Z = 49). Thus, this experimental result should be closely related to the spatial randomness of the Tl atoms in the incommensurate phase of this material. A detailed theoretical interpretation is now in progress for estimating the positional randomness of each element at each neighbouring site from the obtained images.

Acknowledgments: The XFH experiments were performed at PF/KEK (Proposal No. 2007G573) and SPring-8/Taiwan beamline (Proposal No. 2009B4139).

[1]. N. Mamedov et al., Thin Solid Films **499** (2006), p. 275.
[2]. M. Tegze and G. Faigel, Nature **380** (1996), p. 49.
[3]. K. Hayashi, Adv. Imaging Electron Phys. **140** (2006), p. 120.
[4]. J. J. Barton, Phys. Rev. Lett. **67** (1991), p. 3106.

P2-3

Synchrotron-radiation diffraction study of $YbInCu_4$

Hitoshi Sato[1], Yuki Utsumi[2], Chikako Moriyoshi[2], Takashi Hashimoto[2], Yoshihiro Kuroiwa[2], Hirofumi Namatame[1], Masaki Taniguchi[1,2], Koichi Hiraoka[3], Kenichi Kojima[4] and Kunihisa Sugimoto[5]

[1] Hiroshima Synchrotron Radiation Center, Hiroshima University, Higashi-Hiroshima 739-0046, Japan
[2] Graduate School of Science, Hiroshima University, Higashi-Hiroshima 739-8526, Japan
[3] Graduate School of Science and Engineering, Ehime University, Matsuyama 790-8577, Japan
[4] Graduate School of Integrated Arts and Sciences, Hiroshima University, Higashi-Hiroshima 739-8521, Japan
[5] JASRI/SPring-8, Kouto, Sayo-cho, Sayo-gun, Hyogo 679-5198, Japan

jinjin@hiroshima-u.ac.jp, +81-82-424-6293/+81-82-424-6294

$YbInCu_4$ with the C15b-type crystal structure (Fig.1) exhibits the first-order valence transition at T_V=42 K. The ionic valence of Yb changes from z=3 in the high-temperature phase to z=2.9 in the low-temperature phase and the lattice volume expands by 0.5 %, although no cardinal changes in the space group and the atomic coordinations have been detected. Recently, we have carried out the Cu 2p soft x-ray absorption and Cu 2p photoemission spectroscopies to investigate the Cu-derived electronic structure of $YbInCu_4$[1]. The experimental results suggest that the Cu conduction electrons transfer to the Yb 4f states below T_V, which would cause the valence transition. In the present study, in order to investigate behaviour of the Cu ions at the valence transition from the structural viewpoint, we have performed x-ray single crystal structure analysis of $YbInCu_4$ using synchrotron radiation. The experiments were carried out at BL02B1 in SPring-8 with the incidence x-ray energy of 25 keV. The diffracted x-ray from the sample is detected using a large cylindrical camera with an image plate. The diffraction data were collected at 300-10 K.

Fig. 1 shows the crystal structure of $YbInCu_4$. The Yb, In and Cu ions occupy the 4c, 4a and 16e sites in the Wyckoff notation in the space group of F-43m, respectively. The atomic distances $d_{Yb\text{-}In}$ and $d_{Cu\text{-}In}$ derived from analyses of the diffraction data, abruptly increase below T_V. The proportion of the increase relative to the lattice expansion is almost unity. Regarding the Cu ions, on the other hand, the positional parameters slightly deviate from the ideal position of x=0.625. We find two kinds of the Cu-Cu distances $d_{Cu\text{-}Cu}$(I) and $d_{Cu\text{-}Cu}$(II), exhibiting different behaviours at the valence transition as shown in Fig. 2. It is noted that $d_{Cu\text{-}Cu}$(I) increases below T_V, as $d_{Yb\text{-}In}$ and $d_{Cu\text{-}In}$, while $d_{Cu\text{-}Cu}$(II) is almost constant down to 10 K. These two Cu-Cu distances are indicated in Fig. 1 by arrows, in which $d_{Cu\text{-}Cu}$(II) corresponds to the Cu-Cu distance in one Cu_4 tetrahedron and $d_{Cu\text{-}Cu}$(I) to the distance between Cu in one Cu_4 tetrahedron and Cu in other neighbouring Cu_4 tetrahedron. These results indicate that the Cu ions in the crystal form the Cu_4 cluster exhibiting almost no change in the size at the valence transition, and suggest that the conduction electrons distributing the outermost shell of the cluster contribute the valence transition. From the derived temperature factors, we have found that thermal motion of the Cu_4 cluster is significant around the trigonal axes.

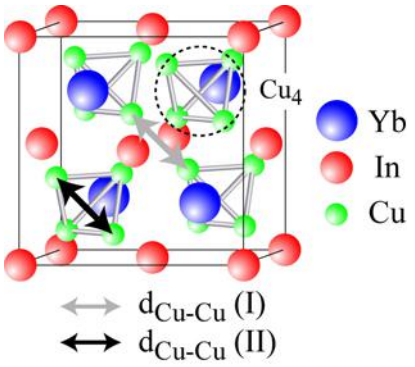

Figure 1. Crystal structure of $YbInCu_4$.

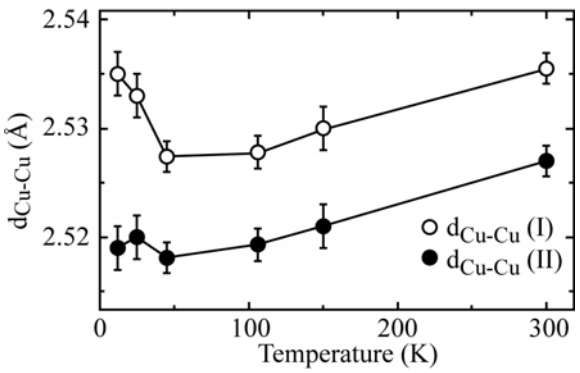

Figure 2. Temperature dependences of $d_{Cu\text{-}Cu}$(I) and $d_{Cu\text{-}Cu}$(II).

[1]. Y. Utsumi *et al*., in preparation.

P2-4

Temperature dependence of the absorption edge in $CuInSe_2$

A.Kh. Matiyev[1], R.M.Yevteyeva[1], A.V. Yevloyev[2]
[1]Grozny State Oil Institute named after M. D. Millionshikov ,Grozny, 364052, Russia
[2]The Ingush State University,Magas, 386001, Russia
email: matiyev-akhmet@yandex.ru

In the paper we report about the temperature dependence of the fundamental energy gap in $CuInSe_2$ in the temperature range from 10 to 300 K determined by absorptions measurements. The samples used in the experiments were grown in analogy to the method described in [1]. A stoichiometric mixture of the pare elements (Cu: 99.999%; In; 99. 9999%; Se: p.A.) was sealed in the quarts ampoule evacuated to about 10^{-4} Torr. To minimize the risk of explosion and to guarantee complete reaction of the elements to the ternary compound stepwise heating procedure was employed. In the first stage the ampoule was heated to 250^0C and maintained at the temperature foe about 6 h. Then beating was continued at the rate of about 20 K/h up to 700^0C. After 3 h at this temperature the ampoule was heated up to 1100^0C and held at the temperature for 15 h. Afterwards the ampoule was cooled at a rate of about 100 K/h up to 600^0C and removed from the furnace. The samples prepared by this technique were polycrystalline aingls crystals with a typical sise of 7x7x0,8 mm^3 could be selectivety cut from the polycrystalline ingots. X-ray analysis was used to confirm the structure of the compound.Hall effect and resistivity measurements showed that the samples are invariably of n-type electron concentrations and electron mobilities ~ 10^{18} cm^{-3} and 40 to 70 cm^2/Vs, respectively. Experimental details of the optical measurements are published [2] and will not be repeated here. The absorptions coefficient α was calculated from the incident light intensivity I_0, the crystal thicknesis d, and reflectivity R by means of the well-known relation

$$\alpha = \frac{1}{d}\ln\left\{\frac{I_0(1-R)^2}{2I_T} + \left(\left[\frac{I_0(1-R)^2}{2I_T}\right]^2\right)^{1/2}\right\}, \qquad (1)$$

using the reflectivity value of R = 0.257 given in [3]. The absorptions coefficient were found to fit a relation of the form $\alpha h\nu = A\left(h\nu - E_g\right)^{1/2}$ indicating a direct energy gap [4] for $CuInSe_2$, in agreement with previous measurements [6]. Extrapolation to $\alpha = 0$ yields the gap energy E_g. The results for the temperature dependence of E_g are shown in Fig.1. At room temperature we obtained E_g = (0.942 ± 0.003)eV in good agreement with the values of 0.96 and 0.95 eV determined by electroreflectance and Schottky barrier photovoltage measurements [6]. Contrary to the results for $AgInSe_2$ and $AgGaS_2$ [6] the temperature dependence of E_g is qualitatively the same as found in III-V and II-VI compounds and can be described by the empirical relation

$$E_g(T) = E_g(0) - \alpha T^2/(T + b) \qquad (2)$$

with $E_g(0)$= 0.966 eV, α = 1.088x10^{-4} eV/K and b = 96 K. The deviations of curve (2) from the experimental points to within experimental uncertainty of ± 0.003 eV. For the linear part of $E_g(T)$ above about 140 K (see Fig. 1) we obtain $dE_g/dT \approx -3\cdot10^{-4}\ eV/K$.

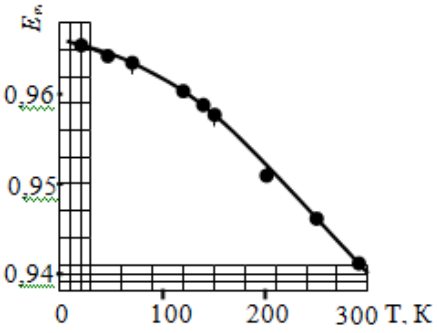

Fig.1

[1]. J. Parkes, R.D. Tomlinson and M.J. Hampshire. J. Crystal Growwth **20**, (1973), p.315.
[2]. W.Hörig and Frieser.Exper. Tech. Phys. **19**, (1971), p.337.
[3]. J.N. Gan, J. Tauc,V.G. Lambrcht, M. Robbins. Phys. Rev., b**12** , (1975), p.5797
[4]. E.J.Johnson. Semiconductors and Semimetals **3**, (1967), p.153,
[5]. J. Parkes, R.D. Tomlinson and M.J. Hampshire. Solid State Electronics, **16**,(1973), p.773.
[6]. J.L. Shay, B. Tell, h.m. Kasper. Phys. Rev., b**7**, (1973), p.4485.

P2-5
Photoluminescence study of $AgInS_2$ by using confocal microscopy system

Umihito Miyamoto[1], Akinori Sizuki[1], Kazuhiro Honjo[2], YongGu Shim[3], Tokuda Takahiro[4], Kenji Yoshino[4], Nazim Mamedov[5] and Kazuki Wakita*, [1]

[1] Chiba Institute of Technology, 2-17-1, Tsudanuma, Narashino, Chiba 275-0016, Japan
[2] Center Office, Nyquist Inc, 144-30 Minami-amabe, Miharaku, Sakai, Osaka 587-0052, Japan
[3] Osaka Prefecture University, 1-1 Gakuenho, Nakaku, Sakai, Osaka 599-8531, Japan
[4] Miyazaki University, 1-1 Gakuen, Kibanadai-nishi, Miyasaki 889-2192, Japan
[5] Institute of Physics, H. Javid 33, Baku AZ-1143, Azerbaijan

*e-mail: kazuki.wakita@it-chiba.ac.jp, phone/ fax number: +81-47-478-0374

Photoluminescence (PL) method is a very sensitive and useful tool to examine an electronic structure and defect-related properties of materials. Practically, we can observe in the microscopic region of the materials by using its confocal microscope system.

On the other hand, the ternary semiconductor $AgInS_2$ of chalcopyrite family has much attention as a promising material for thin-film solar cell. However, the fundamental physical properties of the compound have not been well understood because it is difficult to grow large-size single crystals for the measurements.

In this work, we have investigated PL of $AgInS_2$ crystals at band-edge and deep level region by using a confocal microscope system. Samples for the measurements were bulk crystals of $AgInS_2$ grown by a hot-press method.

X-ray diffraction pattern of the samples indicates that they contain $AgInS_2$ crystals with chalcopyrite and orthorhombic structures and $AgIn_5S_8$ crystals with cubic structure. On the samples, we observed at 77K two dimensional image of PL intensity at 1.88 eV which corresponds to free-exciton energy of $AgInS_2$ with chalcopyrite structure,[1)] as shown in Fig. 1. The detailed positional distribution of PL intensity was obtained because the measurement system has a resolution of micro-meter order in the two dimensional region.

On white and black parts of the image, PL spectra clearly show free-exciton peaks with chalcopyrite and orthorhombic structures (Fig. 2(a) and (b)), respectively.[1)] We focus on the spectra with A-peak located at 1.88 eV and B-peak at 1.62 eV on chalcopyrite structure. The A-peak consists of free exciton and bi-exciton emission, while the B-peak is attributed to donor-acceptor pair transition.

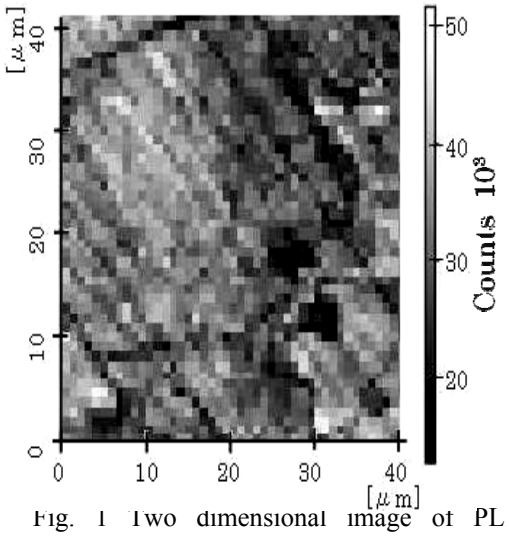

Fig. 1 Two dimensional image of PL intensity at 1.88 eV which corresponds to free-exciton energy of $AgInS_2$ with chalcopyrite structure.

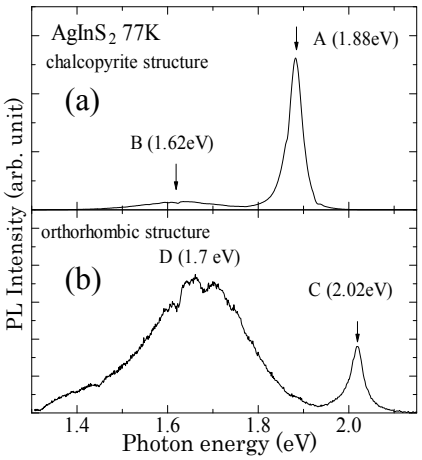

Fig. 2 Photoluminescence spectra with chalcopyrite and orthorhombic structure.

[1]. J. L. Shay, B. Tell, L. M. Schiavone, H. M. Kasper, and F. Thiel, Phys. Rev. B **9** (1974) 1719.

P2-6

Spectroscopic ellipsometry studies of CdS:O layers for solar cells

Yong Gu Shim[1], Junichi Sakamoto[1], Akinori Suzuki[2], Khuraman Khalilova[3], Kazuki Wakita[2], Nazim Mamedov[3], Ayaz Bayramov[3], Emil Huseynov[3], Ilham Hasanov[3]

[1] Osaka Prefecture University, 1-1 Gakuen-cho, Nakaku, Sakai, Osaka 599-8531, Japan
[2] Chiba Institute of Technology, 2-17-1, Tsudanuma, Narashino, Chiba 275-0016, Japan
[3] Institute of Physics, Baku AZ-1143, Azerbaijan

E-mail: shim@pe.osakafu-u.ac.jp; Phone: +81-72-254-9271; Fax: +81-72-254-9908

CdS is used as a window layer for thin film solar cells based on different materials (CdTe, CIS, CIGS) [1,2]. According to the recent report [3], deposition of CdS in oxygen atmosphere on CdTe leads to increased conversion efficiency of the resultant solar cell structures. This increase has been ascribed to the increased energy gap due to reduced grain sizes as compared to those obtained under standard (oxygen free) deposition [3].

This work reports spectroscopic ellipsometry data and their analysis for CdS thin films deposited on glass substrates at room temperature in the presence of oxygen. The final results are given in the Figure with real and imaginary parts of dielectric function. We can see a broadened spectrum of the CdS layer grown in oxygen atmosphere, while CdS film obtained by oxygen-free deposition and bulk CdS have practically the same dielectric function. Since broadening is inversely proportional to the average grain size and oxygen is known to suppress growth of the large grains, the obtained result might have been ascribed to the reduced grain sizes in CdS:O (5%) thin films. However, the observed broadening is accompanied by a very large blue shift of the main structure. It is therefore likely that the observed changes in the Density-Of-States (imaginary part) are due to a growing fraction of the amorphous CdS that emerges under increased oxygen pressure during deposition. The films become more transparent at increased values of O/Ar ratio and this probably leads to the improved parameters reported earlier [3] for CdS:O/CdTe solar cells.

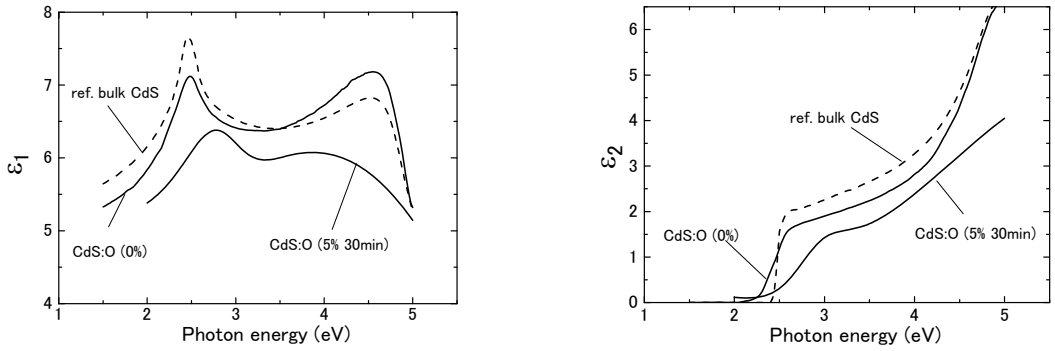

Figure Dielectric function of CdS:O thin films at different values of O/Ar ratio during deposition.

[1]. J. Britt, C. Ferekidis, Appl. Phys. Lett. **62**, (1993), p.2851.
[2]. M. Contreras, K. Ramanathan, J. AbuShama, F. Hasoon, D. L. Young, B. Egaas, R. Noufi, Progress in Photovoltaics:
[3]. Research and Applications **13 (**2005), p.209.
[4]. X. Wu, Solar Energy, **77,** (2004), p.803.

P2-7

Confocal Raman and PL, AFM, and X-ray diffraction studies of CdS:O thin films

Akinori Suzuki[1], Kazuki Wakita[1], YongGu Shim[2], Nazim Mamedov[3], Ayaz Bayramov[3], Emil Huseynov[3]

[1] Chiba Institute of Technology, 2-17-1, Tsudanuma, Narashino, Chiba 275-0016, Japan
[2] Osaka Prefecture University, 1-1 Gakuen-cho, Nakaku, Sakai, Osaka 599-8531, Japan
[3] Institute of Physics, Baku AZ-1143, Azerbaijan

E-mail: kazuki.wakita@it-chiba.ac.jp; Phone & Fax: +81-47-478-0374

CdS has much attention as a window material of thin-film solar cells, for example a CdTe solar cell [1,2]. In this case, increasing band gap of CdS films leads to rise of conversion efficiency of a solar cell. Recently, it was reported that CdS:O films deposited by rf magnetron sputtering consist of nano-crystals of CdS resulting in increasing the band gap [3].

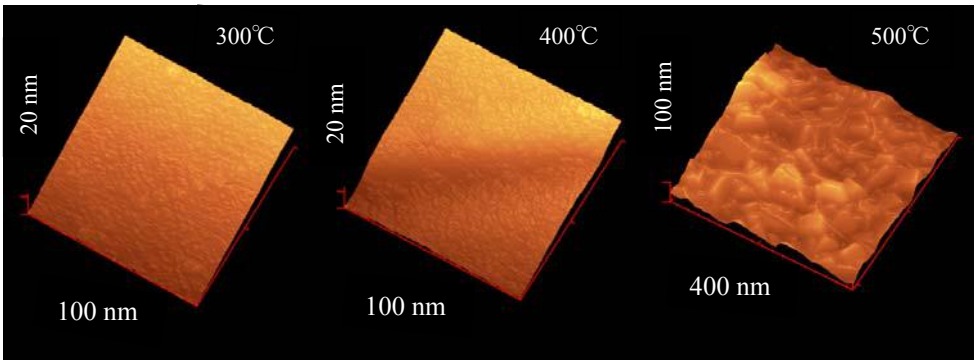

Fig.1 AFM image of CdS:O films annealed at 300, 400 and 500°C.

This work reports confocal Raman and photoluminescence (PL), atomic force microscopy (AFM), and X-ray diffraction studies of CdS:O films deposited by cathode sputtering for formation of nano-crystal of CdS. Figure 1 shows AFM image of CdS:O films annealed at 300, 400 and 500°C. The height of peak and dip on the surface is in the range of 5 and 20 nm in the samples annealed at less than 400°C, while the clear crystalline shape appears in the sample annealed at 500°C.

Figure 2 shows X-ray diffraction pattern of CdS:O films. As grown film shows amorphous structure of CdS. On the other hand, the samples annealed at 400 and 500°C display obvious crystalline pattern. The crystal radius of the samples annealed at 300, 400, and 500°C were estimated to be 20, 27, and 37 nm, respectively, according to Scherrer's formula. Other results related with the confocal spectroscopy will be also presented.

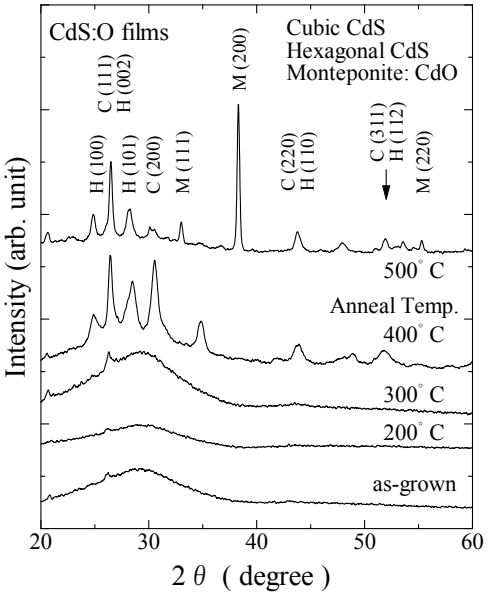

Fig. 2 X-ray diffraction pattern of CdS:O films.

[1]. J. Britt, C. Ferekidis, Appl. Phys. Lett. **62**, (1993), p.2851.
[2]. M. Contreras, K. Ramanathan, J. AbuShama, F. Hasoon, D. L. Young, B. Egaas, R. Noufi, Progress in Photovoltaics:
[3]. Research and Applications **13** (2005), p.209.
[4]. X. Wu, Y. Yan, R. G. Dhere, Y. Zhang, J. Zhou, C. Perkins, B. To, Phys. Stat. Sol. (c), **1** (2004) p.1062.

P2-8

Comparison of optical parameters of Ge-As(Sb)-Se(Te) glassy films.

E. Mammadov[1,4], Y. Shim[2], J. Sakamoto[2], K. Wakita[3]
N. Mamedov[1] and H. Uchiki[4]

[1] *Institute of Physics, Azerbaijan National Academy of Sciences, Baku, AZ-1143, Azerbaijan*
[2], *Osaka Prefecture University, Osaka 599-8531, Japan*
[3] *Chiba Institute of Technology, 2-17-1, Tsudanuma, Narashino, Chiba 275-0016, Japan*
[4]*Nagaoka University of Technology, Nagaoka, Niigata 940-2188, Japan*

E-mail: emammadov@physics.ab.az; Phone: +994 439 3528

Electronic properties of ternary chalcogenide systems strongly correlate with their local atomic arrangement. Depending on constituent elements these materials exhibit a unique property to undergo optically or electrically-induced reversible crystalline-to-amorphous (or glassy) phase transitions. Large difference in reflectivity and resistivity of the crystalline and amorphous phases makes the materials important for optical information storage applications and the next generation non-volatile memory devices. Understanding of correlations between the local structural order and properties of the amorphous phase, however, is not complete.

We present results of optical measurements on thermally evaporated glassy-$Ge_2As(Sb)_2Se(Te)_x$ (x - 5, 7) films. These ternary systems in bulk, exhibit significant decrease in glass-forming ability when As and Se are replaced with heavier Sb and Te atoms. Since the glass-forming ability is directly related to the local structural order one may expect gradual change in the electronic properties of these materials as well.

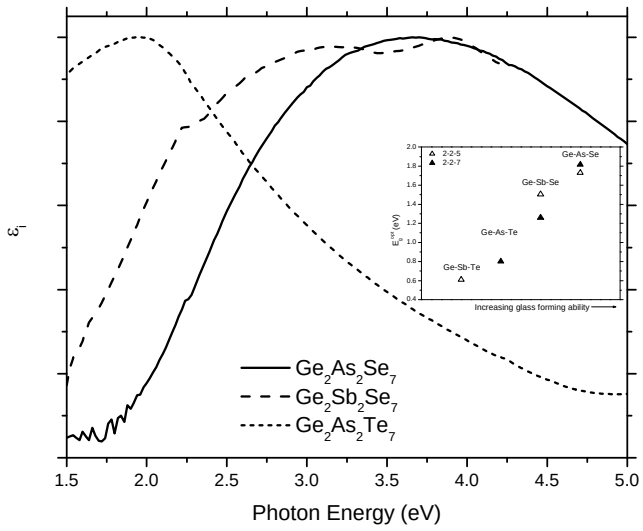

Figure 1. Normalized imaginary part of the dielectric function for 2-2-7 compositions as calculated from ellipsometric data. The inset shows optical gaps obtained from transmittance measurements.

We have obtained optical parameters of the filmed samples by transmittance and reflectance measurements and ellipsometric spectroscopy.

Transmittance and reflectance are measured in the 200-2500 nm spectral range. Optical gaps, obtained through extrapolation of Tauc plots, decrease gradually when going from Ge-As-Se to Ge-Sb-Te films (inset in Fig.1).

Ellipsometric measurements have been performed in the 1.5-5 eV range of the photon energy at 65º of the incidence. The Lorents-Tauc model was utilized to fit the experimental data for samples where interference fringes were observed. For samples where interference was not observed in the energy range studied, thicknesses of the films determined by profilometry and SEM were used to calculate the optical constants. The results show gradual shift of the dielectric functions of the good glass-formers to higher energies (Fig.1). Thus, two independent experiments yield similar results. This supports the initial expectation of gradual variation of electronic properties of the materials.

We will also discuss changes of optical parameters upon crystallization of glassy films.

P2-9

Determination of space charge region width and diffusion length in $Cu(In,Ga)(S,Se)_2$ absorber from solar cell spectral characteristic

M.Tivanov[1], E.Zaretskaya[2], V.Gremenok[2], A.Mazanik[1], N.Drozdov[1]

[1] Belarusian State University, Nezavisimosti av. 4, 220030, Minsk, Belarus
[2] Scientific-Practical Materials Research Centre NAS of Belarus, P. Brovka str. 19, 220072, Minsk, Belarus

E-mail address gremenok@ifttp.bas-net.by, phone +375172841249, fax number +375172840888

The space-charge region width and diffusion length of minority charge carriers in the base region ($Cu(In,Ga)(S,Se)_2$ absorber) are the most important parameters of the solar cell. These parameters determine the efficiency of a solar cell therefore the problem of their control is essential.
In this work we present simple non-destructive method of extracting the parameters of $Cu(In,Ga)(S,Se)_2$-based solar cell (space-charge region width and diffusion length of minority charge carriers in $Cu(In,Ga)(S,Se)_2$ absorber) from the analysis of solar cell spectral photoresponse.
The method is based on one-dimensional model of a solar cell and on the change of in-depth distribution of ~~the~~ photogenerated carriers in the solar cell and, hence, on the change of its photoresponse with the wave-length variation. The following assumptions are accepted: the reflection of charge carriers from a back contact and the «drawing» field in the quasi-neutral area of the absorber layers are absent, window and buffer layers are transparent in the analyzed part of photoresponse spectrum, the injection level of minority charge carriers is low, the recombination losses at the metallurgical *p*-*n*-junction interface of the studied photosensitive structure linearly depend on the photocurrent density.
For the calculation it is necessary to obtain the following set of ~~the~~ experimental data: the spectral density of incident radiation, the spectral dependence of photocurrent or photovoltage of the studied photosensitive structure, the spectral dependences of optical absorption coefficient and reflectance.

Acknowledgments: This work has been supported by Belarusian SCPSR «Space researches».

P2-10

Photo - induced current transient spectroscopy of $TlInS_2$ layered crystals doped by Er, B and Tb impurity

MirHasan Yu. Seyidov[1,2], Rauf A. Suleymanov[1,2], A.P. Odrinsky[3], A.I. Nadjafov[2] and E.G. Samadli[2]

[1] Department of Physics, Gebze Institute of Technology, 41400, Gebze, Kocaeli, Turkey
[2] Institute of Physics Azerbaijan National Academy of Sciences, AZ-1143 Baku, Azerbaijan
[3] Institute Technical Acoustics, NAS of Belarus, 210017 Vitebsk, Repablic of Belarus

e-mail smirhasan@gyte.edu.tr, phone +90 262 605 1308 / fax +90 262 653 84 90

Single crystals of $TlInS_2$ were grown by the Bridgman – Stockbarger method from a stoichiometric melt of the starting materials sealed in evacuated (10^{-5} Torr) silica tubes with a tip at the bottom. The doping was performed by adding the corresponding weighted portion of Er, B or Tb to a cell with the preliminarily synthesized $TlInS_2$ compound. The ohmic contacts were formed on lateral sides of as - grown doped $TlInS_2$ crystals. The traps investigation were performed by photo-induced current transient spectroscopy (PICTS) [1] with using a light excitation with corresponding photons energies hv = 2.12 – 2.28 eV. The PICTS method allow to obtaining the information about traps parameters in ferroelectric - semiconductor by employing the conventionally used technique of DLTS treatment of photocurrent relaxation transient.

In temperature region 100 - 300 K the recharging of eight traps was observed. The temperature region of registrations of trap recharging- ΔT, E_t - activation energy and σ_t - apparently capture cross - section is presented in table 1. The most prominent spectrum feature of rare earth doping samples was the signal from BTE43 traps that was clearly observed in spectrums of boron doping crystal also. From this fact we can conclude about a native origin of this trap. According to work [2 - 3] in high - resistivity undoped $TlInS_2$ semiconductors the traps of majority carrier are acceptor - type. We assume that its indium vacancy in some analogue with situation of the gallium vacancy registration in more investigated crystal of GaSe [4].

The traps registration that labeling B5, B6, B7 only in boron doped sample can point out that it's connected with doping impurities. The observation of its recharging in the temperature region of phase transitions is in a good agreement with reported influence of impurity centers on a peculiarity of phase transitions [5].

Table I. Parameters of traps (B – boron; T - Terbium; E - Erbium).

trap	ΔT (K)	E_t (eV)	σ_t (cm^2)
TE2	100-120	0,21	$4{,}2\cdot10^{-13}$
BT23	114-130	0,23	$1{,}3\cdot10^{-13}$
B3	133-157	0,33	$2{,}3\cdot10^{-11}$
BTE43	147-178	0,27	$1{,}2\cdot10^{-14}$
B5	175-197	0,24	$3{,}5\cdot10^{-17}$
B6	218-239	0,55	$1{,}2\cdot10^{-11}$
B7	244-285	0,48	$2{,}0\cdot10^{-14}$
TE54	272-299	0,32	$1{,}4\cdot10^{-18}$

Acknowledgments: This work was supported by Belarusian Republican Foundation for Fundamental Research under contract no.Ф09А3-006 and Azerbaijan National Academy of Sciences.

[1]. Ch. Hurter, M. Boilou, A. Mitonneau, D. Bois**,** *Appl. Phys. Lett*. **32** (1978), p**.** 821.
[2]. M.Isik, K.Goksen, N.M.Gasanly, H.Ozkan, J. Korean Phys. Soc. **52** (2008), p.367.
[3]. M.Isik, N.M.Gasanly, H.Ozkan, Acta Phys. Polonica, **115** (2009), p.732.
[4]. G. Micocci, P. Siciliano, A. Tepore, *J. Appl. Phys*. **67** (1990)**,** p. 6581.
[5]. S.S.Babayev, E.Basaran, T.G.Mammadov, F.A.Mikailov, F.M.Salehli, M-H.Yu.Seyidov, R.A.Suleymanov, J.Phys.: Condens. Matter **17**, (2005), p. 1985.

P2-11

New electron diffraction rotation methods

M.G. Kyazumov.

Institute of Physics of the National Academy of Sciences of Azerbaijan, H.Javid av.33, Baku, Az-143.

e-mail: elmira@ physics.ab.az

Last years the object of electron diffraction investigations become not only nano thicness samples, and also the samples having the nano- and mikro dimensional areas. Therefore the working out various new electron diffraction methods of the specific advantages is very actual.
Earlier we had been developed two methods:
- During registering of the diffraction process, tilted on a corner φ from perpendicular position of a falling electronic beam, the monocrystal film is rotated around an axis that is located perpendicularly to its plane [1]. As a result from the monocrystal it is artificial it turns out the electron diffraction patterns kind of oblique texture;
- The same, but it is tilted *hk0* plane and the rotation is being around a co-ordinate axis of the reciprocal lattice [2]. In difference from the first method, in the second method on the electron diffraction patterns from crystals with low symmetry, there are layer lines.

The following new electron diffraction methods has been developed:
- During registering of the diffraction process, monocrystal film rotates around one of the axes on the co-ordinate plane of reciprocal lattice which is located perpendicularly to the falling electron beam. This method concerns to the crystals with the hexagonal and higher symmetry (fig. 1);
- During registering, monocrystal film rotates around one of the co-ordinate axes of atomic or reciprocal lattice which is located perpendicularly to the falling electron beam. The rotation around each of these axes differs each other not only under the scheme of obtain of electron diffraction patterns and also by the formulas of their decoding. Therefore each of them is represented as the separate method (fiq.2). Last methods concern to the crystals with low symmetry.

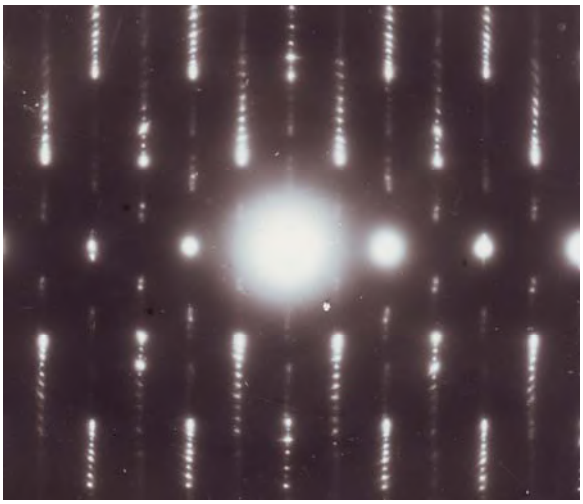

Fiqure 1. Electron diffraction pattern from 2H polytype of $CdInGaS_4$ obtained during rotation of monocrystal film around h00 axis.

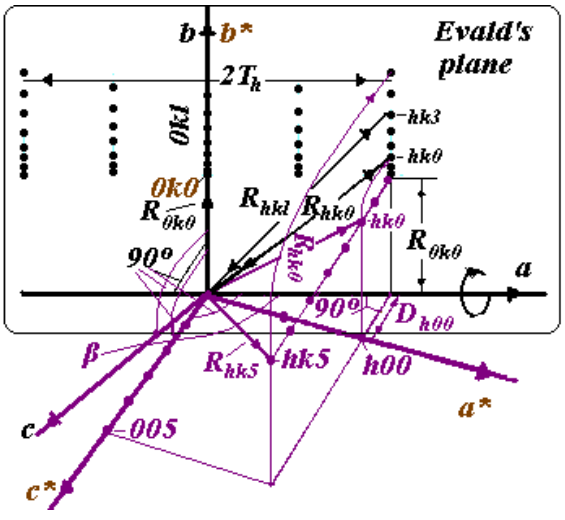

Fiqure 2. The scheme of obtaining of electron diffraction pattern from monoclinic crystal rotating around an axis *a* of atomic lattice.

[1]. B.B. Zvyagin, A.P. Zhuklistov, M.G. Kyazumov, A.M.Fominenkov Kristallografia (Sov.) v. 35, №3, 1990, p.602.
[2]. M.G.Kyazumov Acta Cryst.(2000), A56 (supplement), s.34.

P2-12

Influence of electron irradiation on current-voltage characteristics of $TlGaS_2$ single crystals

A.A. Ismailov, N.D. Ahmedzade, M.M. Shirinov

G.M Abdullayev Institute of Physics NAS of Azerbaijan, AZ-1143 Baku, H.Javid ave,.33

alekper-size@rambler.ru , +99412-432-48-60

Single crystals of the $TlGaS_2$ compound belong to the class of wide-band-gap semiconductors with a layered structure and a high sensitivity to electromagnetic radiation in the visible spectral range. These crystals are perspective for practical application as radians and detectors of optical radiation, detectors of powerful laser radiation, non-linear optical transformers, etc.

$TlGaS_2$ samples for measurements were obtained from massive single crystal by splitting along C-axis of the natural cleavage and were 200 μm thick. The $TlGaS_2$ samples form flat capacitors with plane perpendicular to the crystal C-axis. The capacitor plate area was $3\cdot10^{-2}$ cm^2. The ohmic contacts of samples were made using Ag paste.

First of all current-voltage characteristics of initial crystal at room temperature were studied and then sample is radiated by electron stream. The electron radiation of samples were made by accelerator ELA (electron line accelerator) with minimal energy of electrons 4 MeV at current 2 mkA. Dose of radiation was $D_e=2\cdot10^{12}$e/cm^2, $D_e=8\cdot10^{13}$e/cm^2 and $D_e=4\cdot10^{17}$e/cm^2.

Differences between elektrophysical parameters of inital and radiated samples are not at dose radiation of $D_e=8\cdot10^{13}$e/cm^2 initial.

In figure, current-voltage characteristics (CVC) are presented for Ag-$TlGaS_2$-Ag at room temperature before and after electron irradiation. The curves could be subdivided into three areas. The first area is an ohmic one, the second one is " arrester" quadratic area, and the third one is the area of sharp growth.

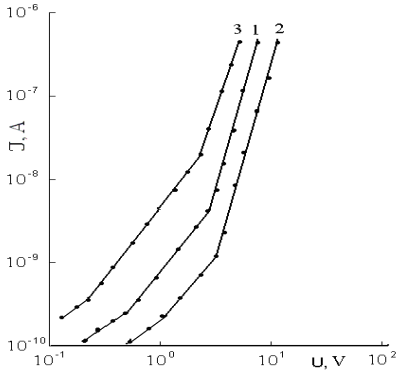

Fig. Current-voltage characteristics at room temperature for Ag-$TlGaS_2$-Ag system.

Curve 1 before irradiation, curve 2-irradiation at dose $D_e=2\cdot10^{12}$e/cm^2 and curve 3- irradiated at $D_e=4\cdot10^{17}$e/cm^2

The experimental results obtained in this study were interpreted within the Lampert theory for an electric current limited by the space charge (SCLC) [1]. Determined have been the following electrical parameters for the samples:

- before irradiation: concentration of traps $N_t= 1.32\cdot10^{11}$cm^{-3}, equilibrium concentration of charge carriers in the allowed band $P_0= 5.6\cdot10^{9}$cm^{-3}, capture factor $\theta=5.6\cdot10^{-1}$, the depth of trap level responsible for the injection current $E_t=0.46$eV.
- after irradiation at $D_e=2\cdot10^{12}$e/cm^2; $N_t=1.0\cdot10^{11}$ cm^{-3}, $P_0= 5.4\cdot10^{8}$cm^{-3}, $\theta=8.1\cdot10^{-2}$, $E_t= 0.52$ eV.
- after irradiation at $D_e=4\cdot10^{17}$e/cm^2; $N_t=1.4\cdot10^{11}$ cm^{-3}, $P_0= 5.6\cdot10^{10}$cm^{-3}, $\theta=4.2$, $E_t=0.41$eV. It has been established that regulayted by radiation doze in single crystals $TlGaS_2$ are possibility.

[1]. M.Lampert, P. Mark. Current Injection in Solids. Academic Press, New York-London, 1970,p.146

P2-13

Magnetic properties of $Fe_{0.76}In_{2.17}S_4$ and $Fe_{1.31}In_{3.13}Se_6$

A. Krimmel, [1] Z.Seidov,[1, 3] H.-A. Krug von Nidda,[1] D.Vieweg, [1] M.Reissner,[2] W.Steiner,[2] A. Loidl,[1] G.Huseynov [3] and A. Najafov[3]

[1]Experimentalphysik V, Elektronische Korrelationen und Magnetismus, Institut für Physik, Univeristät Augsburg, D 86135 Augsburg, Germany
[2]Institute of Solid State Physics, Vienna University of Technology, Vienna, Austria
[3]Institute of Physics, Azerbaijan National Academy of Sciences, AZ-1143 Baku Azerbaijan

Institute of Physics, Azerbaijan National Academy of Sciences, H.Javid ave. 33, AZ-1143 Baku Azerbaijan
e-mail: zsyu@mail.ru, phone: (+99412) 4392043, fax:(+99412) 4395961

In search of new magnetic materials exhibiting ferromagnetic and semiconducting properties $Fe_{0.76}In_{2.17}S_4$ and $Fe_{1.31}In_{3.13}Se_6$ have been synthesized. Standard powder x-ray diffraction at room temperature revealed the cubic spinel structure of $Fe_{0.76}In_{2.17}S_4$. Further structural investigations by high-resolution neutron powder diffraction in the temperature range $1.6 \leq T \leq 280$K confirmed the spinel structure with an almost complete cation inversion corresponding to an inversion parameter of 0.94. ^{57}Fe Mössbauer investigations for $Fe_{0.76}In_{2.17}S_4$ were performed between 4.3 and 295 K. An occupation ratio of 0.05:1 was determined for Fe in the tetrahedral A and octahedral B positions. Magnetic measurements show properties of a canonical spin-glass state below a freezing temperature of T_F = 5 K. A mutually consistent description of the neutron-diffraction data, EDX analysis, magnetic and Mössbauer measurements shows that the present compound $Fe_{0.76}In_{2.17}S_4$ may be written as $(Fe_{0.04}In_{0.89}\square_{0.07})^A (Fe_{0.72}In_{1.28})^B S_4$, with denoting vacancies.
X-ray diffraction analysis of the diluted magnetic compound $Fe_{1.31}In_{3.13}Se_6$ suggests that the compound crystallizes in the hexagonal structure with lattice parameters a = 4.01Å and c = 39.08Å. The magnetic high-temperature susceptibility data follow a typical Curie-Weiss law with θ = -195 K indicating the presence of predominant antiferromagnetic interactions with a high degree of frustration. Low-field susceptibility measurements show irreversibility in the dc susceptibility, as evidenced by field cooled and zero-field cooled measurements below 16 K, suggesting a spin-glass like behaviour.

P2-14

Super-ionic conductivity in (1D) nanofibrous $TlGaTe_2$

R.M. Sardarly[1], O.A. Samedov[1], A.P. Abdullaev[1], F.T. Salmanov[1]
A. Urbanovic[2], F. Garet[2], J.-L. Coutaz[2]

[1]Institute of Radiation Problems, National Academy of Sciences of Azerbaijan, F.Agaev 9, 1143 Baku.
[2] IMEP-LAHC, UMR CNRS 5130, University of Savoie, 73376 Le Bourget du Lac, France.

e-mail: sardarli@yahoo.com, phone: + 994124323631, fax: + 994124398318.

Nanodimension topologic-disorder materials constitute an important feature in the development of modern electronics. Among such materials, $TlGaTe_2$ is a *p*-type semiconductor with a nanofibrous structure $Ga^{3+}Te^{2-}_2$ groups form chains extending along the *c*-axis of the material. These negatively charged chains are bonded together by Tl^+ ions. The resulting tetragonal lattice is characterized by a D^{18}_{4h} group symmetry. Recently, much attention has been paid to systems that behave as if they had less than 3 spatial dimensions. Such materials are often called quasi-one-dimensional (1D) nanorods, nanofibrous or nanochains [1]. We already studied [2] the temperature dependence of conductivity $\sigma(T)$ and current-voltage (I-V) characteristics of $TlGaTe_2$. In the ohmic region of the I-V curve, $\sigma(T)$ exhibits a behavior typical of hopping conductivity, which can be modeled in the framework of the Mott approximation. Moreover, we determined the values of the density of localized states, the activation energy, the hop lengths, and the difference between the energies of states and the concentration of deep traps. The abrupt variation of the I-V curve is ascribed to the Pool-Frenkel thermal-field effect, which allows us to obtain the concentration of ionized centers, the free-path lengths, the Frenkel coefficients and the shape of the potential well of $TlGaTe_2$. For T>300 K, $TlGaTe_2$ crystals present interesting nonlinear electrical behaviors, such as switching effects and a negative-differential-resistance (NDR) region in their *S*-type I-V characteristics. In the NDR region, self-excited oscillations of the voltage were also observed.

Here, we investigate the temperature dependence of $TlGaTe_2$ crystals conductivity $\sigma(T)$ in two experimental geometries, i.e. parallel and perpendicularly to the tetragonal *c*-axis of the crystal. For both geometries, $T \sim 310$ K and a sharp increase of $\sigma(T)$ with T is observed. Experimentally, $\ln(\sigma \times T)$ varies linearly with $1/T$, which is typical of a ionic-type conductivity:

$$\sigma \times T = \sigma_o \exp\left(-\Delta H^a / kT\right)$$

The observed sharp increase of $TlGaTe_2$ conductivity results from a strong change of the number of the high-mobility ions. The increase of $\sigma(T)$ with T is mainly caused by the diffusion of ions T^+ to vacancies in the Tl^+-sublattice. This change happens due to the phase transition accompanying the disordering (fusion) of Tl^+ sublattice in $TlGaTe_2$. Simultaneously, the degree of disorder may change under the influence of external fields. We study the temperature dependence of $\sigma(T)$ in both directions parallel and perpendicular to the *c*-axis under an electric field E=181 V/cm. A strong sharp increase (×1500) of $\sigma(T)$ is observed at T=242 K (along the *c*-axis) and T=267 K (perpendicular to it). This increase is attributed to a transition towards a superionic condition. Over the transition threshold of the superionic condition, disordering of the Tl^+ sublattice in $TlGaTe_2$ occurs, and nanosize topological-disordering arises owing to aperiodicity in placing $Ga^{3+}Te^{2-}_2$ nano-chains, whose size does not exceed the size of area of a nearest order (~1nm). Investigation in the THz region reveals absorption line nearby f~0.2 THz. This frequency is less than the lowest optic active phonon mode (A_{2u} and E_u) [1]. So, f ~0.2 THz is probably the frequency of libration oscillation of nanofibrous (nanochain) $Ga^{3+}Te^{2-}_2$ in $TlGaTe_2$ superionic phase.

[1]. A.M. Panich and R.M. Sardarly, "Physical properties of the low dimensional A^3B^3 and $A^3B^3C^6_2$ compounds," Nova Science Publishers, New York (2010), p. 310.
[2]. R.M. Sardarly, O.A. Samedov, A.P. Abdullayev, E.K. Huseynov, F.T. Salmanov *Semiconductors* **44**, 485 (2010).

P2-15

Properties of PbS thin films grown on GaSe and glass substrates by CBD

G.M. Mamedov[a,*], H. Ertap[a], M. Karabulut[a], G. Uğurlu[a], M.K. Öztürk[b], H. Çelikkan[b]

[a] Kafkas University, Faculty of Arts and Sciences, Department of Physics, 36100 Kars, Turkey
[b] Gazi University, Faculty of Science, Department of Physics, Ankara, Turkey
hasancopuroglu@yahoo.com, 904742251155-3079

PbS thin films were grown on GaSe and glass substrates by Chemical Bath Deposition and their structural, morphologic, optic and electrical properties were investigated. XRD analysis of the films grown on both on hexagonal GaSe crystal and glass substrates showed that the films had cubic structure with lattice constant a= 5,9362 Å. The surface morphology of the films were studied by Atomic Force Microscopy (AFM) and Scanning Electron Microscopy. The films were found to grow as cylindrical stripes. The I-V characteristics of PbS films grown on GaSe crystal was found to be symmetric for the parallel geometry while it was asymmetric for the sandwich geometry (Ag-GaSe-PbS-Ag). The charge carrier concentrations and mobilities of the PbS films grown on both substrates were investigated by the van der Pau method in the 50-300 K temperature interval. From the analyses of the experimental results, at temperatures between T=200-300 K the n-type conductivity of PbS films grown on GaSe substrate was found to be determined by the ionization of the donor centers with energies of 0,354 eV. The carrier density and mobility at this temperature interval was found as 6 x 10^9 cm^{-3} and 5 x 10^2 $cm^2/V.s$, respectively. For temperatures T< 50 K, the conductivity was due to the excitation of the holes from the acceptor centers 0,036 eV above the valence band. From the optic absorption spectra of PbS films grown on glass and GaSe substrates, the energy dependence of absorption was found to be $(\alpha h\vartheta)^2 \sim h\upsilon$ and optic band gaps were determined to be 1,78 eV ve 1,54 eV, respectively. The difference observed in the band gaps of PbS films grown on glass and GaSe substrates is thought to be due to the Quantum Confinement Effect (QCE) resulting from the nano regions of different sizes formed on the substrates.

P2-16

Natural photopleochroism of In/p-Ag_3AsS_3 surface-barrier structures

N.M. Mehtiyev [1], V.Yu. Rud'[2], Yu.V. Rud'[3], E.I. Terukov [3]

[1]Azerbaidzhan State Oil Academy, Azadlig Av. 20, Baku, Az1010, Azerbaijan Republic,
e-mail: nizami-mehdiyev@rambler.ru
[2] Saint-Petersburg State Polytechnic University, 195251 Saint-Petersburg, Russia, e-mail: rudvas@rambler.ru
[3]Ioffe Physico-Technical Institute RAS, 194021 Saint-Petersburg, Russia

The single crystals Ag_3AsS_3 up to now were investigated as materials for nonlinear optics and is widely used in developing exclusively as high efficiency optical convertors of infrared radiation. In this paper we report the first study of the photosensitivity of the metal/Ag_3AsS_3 surface-barrier structures, which may find application for the development of devices for the polarization-sensitive photoelectronics of last generation [1-3].

Homogeneous bulk single crystals p-Ag_3AsS_3 with rhombic structure were grown by direct crystallization from melts with atomic composition corresponding to this ternary compounds. The electrical conductivity of these crystals were determined by activation of acceptor centers $E_A \approx 0.4$ eV.

The photosensitivity structure In/p-Ag_3AsS_3 for the first time were created by thermal sputtering of indium onto the p-Ag_3AsS_3 surface with the (100) crystallographic orientation. When the these structures were illuminated with natural light on the barrier contact surface the voltage photosensitivity reached a maximum $S_U^m \approx 2000$ V/W at T=300 K.

Photosensitivity spectra of In/p-Ag_3AsS_3 structures for the first time were obtained and used to determine the nature and the energy of interband transitions for p-Ag_3AsS_3 crystals. Also for the surface-barrier structures obtained on the oriented crystals p-Ag_3AsS_3 were discovered and investigated of the natural photopleochroism phenomena[4,5]. It was concluded, that the oriented single crystals p-Ag_3AsS_3 can be used in the photoconvertors native and linearly-polarized radiations.

[1]. D.V. Tseng. Appl. Phys. Lett., **21**, 382 (1972).
[2]. M.C. Ohmer, R. Panday. MRS Bull., **23**, 16 (1998).
[3]. B.H. Bairamov, V.Yu. Rud', Yu. V. Rud'. MRS Bull., **23**, 41 (1998).
[4]. V.Yu. Rud'. Thesis Doct. of Sci (Ulyanovsk, UlSU, 2005).
[5]. F.P. Kesamanly, V.Yu. Rud', Yu.V. Rud'. Semiconductors, **30**, 1921 (1996).

P2-17

^{57}Fe Mössbauer Spectroscopy of Sm-Y-Fe-Sb-O Ceramics

S. Lebedev[1], T.Tarasevich[1], O. Ignatenko[1], O. Zheleznyakova[2], V. Dobryanskii[2], J.A. Kasyk[3] and J.A. Fedotova[3]

[1] SSPA "Scientific-Practical Materials Research Centre of NAS of Belarus",220072, Minsk, Belarus
[2] Belarusian State Pedagogical University named after Maxim Tank, Minsk, Belarus
[3] The National Scientific and Educational Centre of Particle and High Energy Physics of the BSU, Minsk, Belarus

lebedev@physics.by

The recent discovery of novel superconductivity in rare-earth iron-based layered superconductors has received great attention in the scientific community. The purpose of the present work was explaining behavior of phase formation and physical properties of Sm-Y-Fe-Sb-O oxypnictides, prepared using both usual ceramic technology and high pressure cold pressing (HP).

Table 1. - The hyperfine interaction parameters for Sm-Y-Fe-Sb-O system derived from the analysis of the Mössbauer spectra

Sample	Sub-spectrum	δ, mm/s	ΔE, mm/s	H_{eff}, T	Fraction , %
SmFeSbO	doublet D_1	0,23	0,75	-	75
	sextet S	0,33	-0,04	49,2	25
SmFeSbO (HP)	doublet D_1	0,34	0,96	-	13
	doublet D_2	0,25	0,31	-	7
	sextet S_1	0,74	0,02	46,2	43
	sextet S_2	0,24	-0,03	48,2	37
$Sm_{0,8}Ca_{0,2}OFeSb$ (HP)	doublet D_1	0,26	1,15		15
	doublet D_2	0,19	0,17	-	11
	sextet S_1	0,75	0,01	46,1	47
	sextet S_2	0,22	-0,05	48,0	27
YFeSbO	doublet D_1	0,37	0,87	-	100
YFeSbOF (HP)	doublet D_1	0,27	0,83	-	46
	sextet S_1	0,69	0,05	45,7	35
	sextet S_2	0,27	0,02	48,8	19

The main peaks in XRD pattern can be well indexed to the cubic structure Fd3m (227) (a =10,3 Å.). The XRD patterns show that the samples prepared without HP are single phase. Large amount of impurity phases are observed in the samples prepared with HP. The Mössbauer spectroscopy of ^{57}Fe (Table 1) in these materials, even at room temperature, can easily discover the presence and amounts of Fe containing foreign phases.
No superconducting transition is observed down to5 K for the samples of Sm-Y-Fe-Sb-O system.

SECTION THREE

Temperature and pressure induced phase transitions, superconductivity

I3-1

High-pressure studies for iron-based superconductors

H.Takahashi[1,2], T. Tomita[1,2], Y. Kamihara[2,3], S. Matsuishi[4], M. Hirano[4,5]and H. Hosono[4,5]

[1] College of Humanities and Sciences, Nihon University, Setagaya-ku, 156-8550, Tokyo, Japan
[2] TRIP, Japan Science and Technology Agency (JST), Chiyoda-ku, 102-0075, Tokyo, Japan
[2] Faculty of Science & Technology, Keio University, Kohoku-ku, 223-8522, Yokohama, Japan
[4] Materials and Structures Labolatory, Tokyo Institute of Technology, Midori-ku, 226-8503Yokohama, Japan
[5] Frontier Research Center, Tokyo Institute of Technology, Midori-ku, 226-8503,Yokohama , Japan

e-mail: hiroki@chs.nihon-u.ac.jp, phone+81-3-3329-1151, fax+81-3-5317-9432

The discovery of an iron-based superconductor $LaFeAsO_{1-x}F_x$[1] with T_c of 26 K had a significant impact in the field of condensed matter physics and had triggered the rapid development of extensive investigation of superconductivity. The crystal structure of $LaFeAsO_{1-x}F_x$ is tetragonal and comprises a stack of alternation LaO and FeAs layers, which is similar to cuprate superconductors having layered structure. Right after the discovery of $LaFeAsO_{1-x}F_x$, applying pressure on optimally doped one increased T_c to 43 K[2], which is the significantly large enhancement of T_c, compared with the cuprate superconductors. In this way, we have been performed high-pressure measurements for several iron-based superconductors.

In this paper, we present the pressure effect on the electrical, magnetic and structural properties for 1111-type $LaFeAsO_{1-x}F_x$[2,3] and $Ca(Fe_{1-x}Co_x)AsF$[3,4] compounds. Undoped LaFeAsO exhibits the magnetic and structural transitions. Electron doping with F-substitution suppressed these phase transitions and raised superconductivity. For x= 0.11 and 0.14 of $LaFeAsO_{1-x}F_x$, the maximum T_c was 43 K under high pressure, as shown in Fig.1. However, pressure effect on T_c of lightly doped one with x = 0.05 was not so large. Pressure-induced superconductivity was observed for x = 0.0. For $Ca(Fe_{1-x}Co_x)AsF$, Co-substitution to Fe, which is also considered to be the electron doping, suppressed the magnetic and structural transitions and raised superconductivity. Pressure-induced superconductivity was also observed for x = 0.0 and 0.05. However, the highest T_c was obtained in parent compound (x = 0.0) under high pressure, in contrast to $LaFeAsO_{1-x}F_x$. These results suggest that the substitution of Co induces disorder in the FeAs superconducting layer, while it increases carrier concentration. X-ray diffraction measurements under high pressure were performed for $LaFeAsO_{1-x}F_x$. Larger compression along c-axis was observed, as often observed in the layered compounds. In iron-based superconductors, the correlation between T_c and structural parameters are considered to be important. Therefore, precise structural refinement under high pressure is in progress for 1111-type superconductors.

We also present the recent results about related compounds.

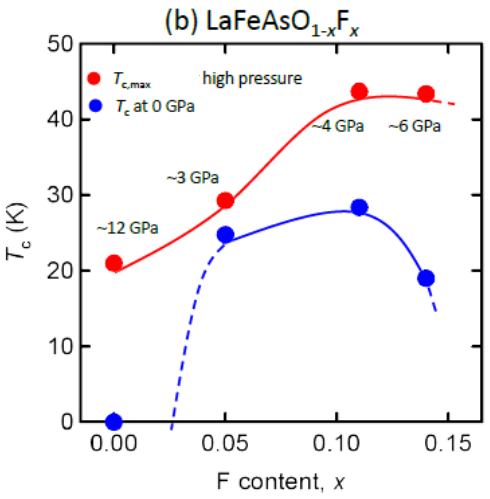

Figure 1.
Maximum T_c ($T_{c,max}$) under high pressure and T_c at atmospheric pressure as a function of F content for $LaFeAsO_{1-x}F_x$[2,3]. The solid and dashed lines are guides to the eye.

[1]. Y. Kamihara, T. Watanabe, M. Hirano and H. Hosono, *J. Am. Chem. Soc.* **130** (2008), p.3296.
[2]. H.Takahashi, K.Igawa, K.Arii, Y.Kamihara, M.Hirano and H.Hosono, *Nature*, **453** (2008), p.376.
[3]. H.Okada, K.Igawa, H.Takahashi, Y.Kamihara, M.Hirano, H.Hosono, .Matsubayashi Y.Uwatoko, *J. Phys. Soc. Jpn.* **77** (2008), p.113712.
[4]. Hironari.Okada, Hiroyuki.Takahashi, Satoru Matsuishi, Masahiro Hirano, Hideo Hosono, Kazuyuki Matsubayashi, Yoshiya Uwatoko and Hiroki Takahashi, *Phys. Rev.* **B81** (2010), p.054507.

I3-2

Microwave surface impedance and complex conductivity of organic and multizone superconductors

M.R. Trunin[1,2] and A.F. Shevchun[1]

[1] Institute of Solid State Physics, Russian Academy of Sciences, Chernogolovka, Moscow region, Russia
[2] Moscow Institute of Physics and Technolodgy, Dolgoprudny, Moscow region, Russia
trunin@issp.ac.ru, tel: +7(496)522-29-42, fax:: +7(496)524-97-01

Results of recent investigations of the temperature dependences of the surface impedance $Z(T)=R(T)+iX(T)$ and microwave conductivity $\sigma(T)=\sigma'(T)-i\sigma''(T)$ in two-band V_3Si_{1-x} and organic κ-$(BEDT\text{-}TTF)_2Cu[N(CN)_2]Br$ single crystals are discussed.

We have performed accurate measurements of the in-plane surface impedance $Z_{ac}(T)=R_{ac}(T)+iX_{ac}(T)$ on several single crystals of organic superconductor κ-$(BEDT\text{-}TTF)_2Cu[N(CN)_2]Br$ in the temperature range $0.5\ K \le T \le 100\ K$ using a "hot-finger" cavity perturbation technique at a frequency of 28.2 GHz.

In the normal state we find the temperature dependence of resistivity $\rho_{ac}(T)$. Just above T_c=12 K, we obtain $\rho_{ac}(13\ K)=2R_{ac}^2(T)/\omega\mu_0=170\ \mu\Omega\cdot cm$ and $\Delta\rho_{ac}(T) \propto AT^2$ for $T_c \le T \le T^* \approx 45$ K. At $T>T^*$ the normal skin-effect condition, $R_{ac}(T)=X_{ac}(T)$, is disturbed (Fig.1), and we observe $X_{ac}(T)>R_{ac}(T)$ due to appearance of the imaginary part of conductivity $\sigma''(T)$ within a smooth crossover from coherent Fermi liquid excitations at $T<T^*$ to the charge density wave conditions at higher temperatures. Moreover, at temperatures about 45 K the normal state skin-depth $\delta(T)$ is comparable with the thin sample thickness (0.03 mm), and the shape of the $\rho_{ac}(T)$ curve in this crystal is influenced by the size effect.

In the superconducting state the in-plane penetration depth $\lambda_{ac}(0)$ = 0.7 μm is determined. The observed linear temperature dependence $\Delta\lambda_{ac}(T) \sim T$ at $T<T_c/3$ in Fig.1 indicates d-wave order parameter symmetry in this compound.

The temperature dependences of the microwave complex conductivity of V_3Si_{1-x} single crystals with different stoichiometry allowed us to observe a number of peculiarities of two-band superconductors, namely, a nonlinear metallic behavior of resistivity at $T>T_c$, a positive curvature of $\sigma''(T)$ curves cloe to T_c (Fig.2), and a coherence peak in $\sigma'(T)$ centered at $T\approx T_c/2$.

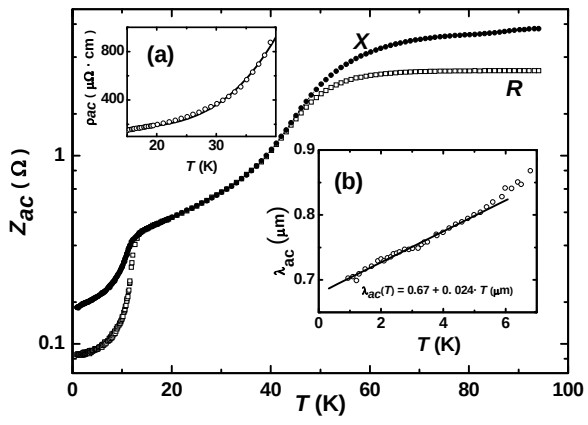

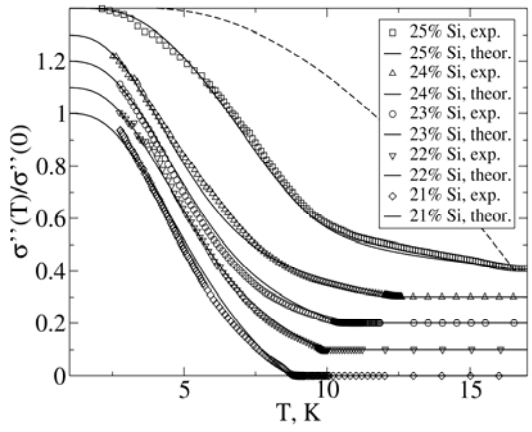

Fig. 1: Temperature dependence of the surface impedance components $R_{ac}(T)$ and $X_{ac}(T)$ in the thick κ-$(BEDT\text{-}TTF)_2Cu[N(CN)_2]Br$ crystal. Inset: (a) In-plane resistivity $\rho_{ac}(T)$. (b) Penetration depth $\lambda_{ac}(T)$ at low temperatures.

Fig. 2: Experimental temperature dependences of the imaginary part of the conductivity (symbols) in V_3Si_{1-x} single crystals with different stoichiometry. Each curve after the lower one is shifted on 0.1 along the axis of ordinates. Solid lines stand for the case of weak-coupling two-band theory. Dashed line show single-band BCS calculations for T_c=16.5 K (stochiometric sample).

I3-3

Pressure dependence of the bandgap, lattice parameters, and pressure-induced phase transitions in $A^{II}B^{III}{}_2C^{VI}{}_4$ compounds

F. J. Manjón[1], I. M. Tiginyanu[2], and V. V. Ursaki[3]

[1] Departament de Física Aplicada, Universitat Politècnica de València, EPSA, 03801 Alcoi, SPAIN
[2] Institute of Electronic Engineering and Nanotechnologies, Academy of Sciences of Moldova, 2028 Chisinau, MOLDOVA
[3]Institute of Applied Physics, Academy of Sciences of Moldova, 2028 Chisinau, MOLDOVA
Presenting author's e-mail address: tiginyanu@asm.md, phone/fax: (373-22) 274047

A review on the behaviour of tetragonal and cubic spinel $A^{II}B^{III}{}_2C^{VI}{}_4$ compounds under hydrostatic pressure is presented. The materials are investigated at room temperature in a diamond anvil cell by means of Raman scattering, X-ray diffraction analysis and optical measurements. It is shown that in all tetragonal $Zn(Cd)Ga_2[S(Se)]_4$ compounds a phase transition to a cubic NaCl-type structure occurs under hydrostatic pressure. The as-grown Zn containing compounds adopt a defect-stannite ($I\bar{4}2m$, Z = 2) structure, while Cd containing materials have a defect-chalcopyrite structure ($I\bar{4}$). The transition to the NaCl-type structure is preceded by order-disorder transitions in the cation sublattice which is determined by the tetragonal distortion of the initial structure. The pressure of transition to the NaCl-type structure is a function of the compound ionicity in accordance with the Chelikowsky theory [1] based on a combination of pseudopotential total-energy method with an empirical ionicity scale. The pressure of this phase transition is discussed in connection with the size criterion. The validity of the empirical rule (size criterion) proposed by Jayaraman *et al.* [2] is confirmed for $A^{II}B^{III}{}_2C^{VI}{}_4$ compounds. According to this rule, the transition pressure from tetrahedral to octahedral coordination in ABX_2 compounds increases with decreasing the ratio between the averaged cation radius and the anion radius.

The reversibility of the phase transition is analysed. The initial defect-stannite or the defect-chalcopyrite structure is never recovered. The high-pressure cubic NaCl-type structure is found upon decompression in most of selenium containing materials. However, a zinc-blende-type structure is sometimes found in $CdGa_2Se_4$ upon decompression, which is rationalized by the complexity of the pressure-induced processes that depend on the rate of pressure increase or decrease. During a fast decompression, the metastable rock-salt structure is recovered to ambient conditions. However, when the sample is decompressed slowly, a disordered zinc-blende structure is obtained. In sulfur containing materials, amorphyzation occurs upon decompression. This process is explained by the pressure dependence of the potential barriers between different low- and high-pressure phases with different degrees of disorder.

In $M^{II}In_2S_4$ (M = Cd, Mg, Mn) with as grown cubic spinel structure a phase transition to a disordered NaCl-type structure, or to a ordered double-NaCl structure of the $LiTiO_2$ or $LiVO_2$-type occurs under hydrostatic pressure. The dependence of the value of phase transition pressure upon the ionicity and the size criterion is found in materials with spinel structure, similarly to those with tetragonal structure. The analysis of the band-gap energies and their pressure coefficients for the three compounds suggests either the presence of two phase transitions, or that the phase transition taking place in the three compounds is rather slow and there is a coexistence of two phases in a certain pressure interval. This phase transition is reversible, however, a strong hysteresis is observed. The peculiarities of pressure induced phase transitions in $ZnAl_2S_4$ spinel and the systematic of phase transitions in $ZnGa_2O_4$ and other oxide spinels are analyzed.

The strong non-linear pressure dependence of the optical absorption edge measured in defect chalcopyrites is discussed in connection with *ab initio* calculations of the non-linear pressure dependence of the direct bandgap energy. The effects of pressure on the lattice parameters and atomic positions are also discussed. The equation of state (EOS) is determined.

[1]. J. K. Chelikowsky, *Phys. Rev. B* **35** (1987), p. 1174.
[2]. A.Jayaraman, P. D. Dernier, H. M. Kasper and R. G. Maines, *High Temp. High Press* **9** (1977), p. 97.

O3-1

Thermodynamics and the quantitative description of polymorphic and superconducting transitions in disordered media

I.K. Kamilov , M.I. Daunov, R.R. Bashirov

Institute of Physics, Daghestan Scientific Center, Russian Academy of Sciences, 367003, M.Yaragskii str., 94, Makhachkala, Russia

rusbash@inbox.ru, tel+7872262-66-50/fax+7872262-89-0

The analysis of the polymorphous phase transitions under uniform external conditions (pressure, temperature etc.) based on thermodynamics of composites, X-ray data and data on kinetic effects in semiconductors [1], testifies the presence of an extended interval in which initial and final states coexist. This interval increases in the presence of disorder; moreover, the second order phase transitions in disordered systems, for example in high-temperature superconductors (HTSC), also occur in some extended interval around a 'pure' critical point. Typical T-P diagram of a reversible polymorphic transformation is presented in the figure 1.

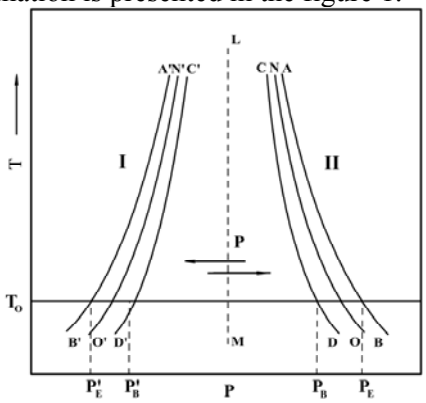

Figure 1. L M - line of balance, NO - line of metastable balance, AB - boundary of the area where extended transition from state 1 to state 2 takes a place when pressure increases. The similar area of extended transition from state 2 to state 1 for the case of decreasing of pressure is presented to the left of LM, specifying the presence of a pressure hysteresis.

To investigate the issue of phase transitions in real imperfect solids, the modified effective media approximation with inclusions of percolation theory has been developed [2]. Proposed model describes phase transitions covering as the vicinity of the percolation threshold as well the area far from critical point. The expressions for effective values of resistivity ρ, thermo-emf Q and thermal conductivity λ have been obtained, allowing calculation of the phase composition, threshold values of external parameters and critical indexes. Data on some porous ceramized glass materials saturated by fluids at T=300K and P=0.1 MPa have been used for verification of λ. Experimental results for bulk n-InAs, n-GaAs and n-ZnO single crystals, n-GaAs nanocrystals, and HTSC $YBa_2Cu_3O_x$ ceramics in the area of polymorphic and superconducting phase transitions under hydrostatic pressure have been analyzed on the basis of the proposed approach. It is found, that prior to phase transitions into metal or superconducting states, the ratio is held: $\rho/\rho_1 \cong Q/Q_1$.

[1]. J. Z. Jiang, Olsen J. Staun, L. Gervard, S. Steensnrup, High Press. Res., **22 (**2002), p. 395.
[2]. M. I. Daunov, I. K. Kamilov, R. K. Arslanov, D. M. Daunova and S. F. Gabibov, J. Phys.:Condens. Matter., **15** (2003), p. 2335.

O3-2

Anomalies in transport and superconducting properties of $Ba_{(1-x)}K_xFe_2As_2$ single crystals.

V.N.Zverev[1], A.V.Korobenko[1], G.L.Sun[2], D.L.Sun[2], C.T.Lin[2], and A.V.Boris[2]

[1] Institute of Solid State Physics, Russian Academy of Sciences, Chernogolovka, Moscow region, Russia
[2] Max-Planck-Institut für Festkörperforschung, 70569, Stuttgart, Germany

zverev@issp.ac.ru, tel: +7(496)522-10-04, fax:: +7(496)524-97-01

The transport properties and the anisotropy of hole-doped $Ba_{(1-x)}K_xFe_2As_2$ single crystals in normal and superconducting states are studied. The samples had the potassium content $x \approx 0.6$ and the superconducting transition temperature T_c about 38 K. The experiments were carried out in the temperature range 4.2 K < T < 300 K and in magnetic fields up to 17 T. Preliminary results were published recently in [1].

Both in-plane ρ_{ab} and out-of-plane ρ_c resistivities were measured by a modified Montgomery method and the influence of the crystal quality on the resistivity anisotropy was found. The in-plane resistivity component ρ_{ab} is characterized by anomalous T-dependence: $\rho_{ab}(T)$ curve is convex with the tendency to saturate at high temperature (Fig.1). The temperature dependences of both hole concentration n_h and momentum relaxation time τ_p were determined from the resistivity and Hall measurements. The hole concentration was found to decrease with the temperature, tending at low T to the value correspondent to potassium content. Interestingly, the $1/\tau_p(T)$ obeys the T^2 low (fig.2), which probably indicates that the momentum relaxation process is determined mainly by electron-electron interactions.

The influence of magnetic field on the superconducting transition was studied and the temperature dependence of the upper critical field H_{c2} was measured when the field was directed either along or perpendicular to Fe-As planes. $H_{c2}(T)$ dependence was found to be linear in the vicinity of T_c. From dH_{c2}/dT values for H||(ab) and H||c one gets $H_{c2}(0)$ equal 266 T and 124 T respectively in frame of BCS-model. The anisotropy of the dH_{c2}/dT value gives the effective mass anisotropy about 4.6 which is in good agreement with the results of the spectral investigations but is much smaller than that evaluated from our resistivity measurements. These results indicate on the extrinsic nature of the out-of-plane resistivity: the presence of flat defects parallel to Fe-As planes leads to the increase of the ρ_c value and, as the consequence, to resistivity anisotropy ρ_c / ρ_{ab}. This statement is also supported by our observation of the so-called "Friedel transition" – the difference in T_c values obtained from the in-plane and out-of-plane resistance measurements, which is due to the existence of some disorder in the c-direction.

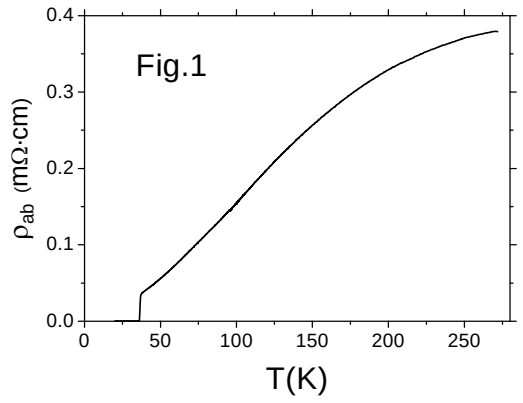

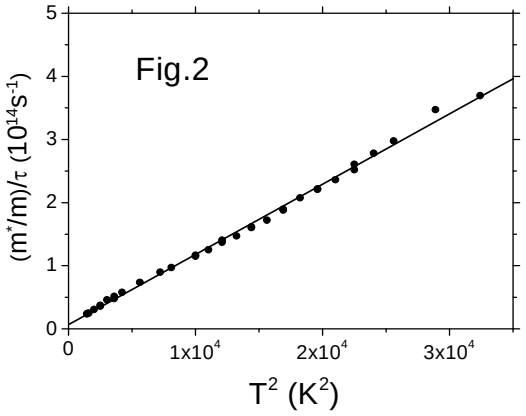

[1]. V.N.Zverev, A.V.Korobenko, G.L.Sun, D.L.Sun, C.T.Lin, and A.V.Boris, JETP Letters, 90(2), 130–133 (2009).

O3-3

Structural and magnetic phase transitions in the single crystals p-$Cd_{1-x}Mn_xGeAs_2$

A. Yu. Mollaev[1], I. K. Kamilov[1], R. K. Arslanov[1], S. F. Marenkin[2], V.M. Novotortsev[2]
U. Z. Zalibekov[1], T. R. Arslanov[1]

[1]Institute of Physics, Daghestan Scientific Center of the Russian Academy of Sciences, 367003, Makhachkala, Russian
[2]Institute of common and inorganic chemistry of the Russian Academy of Sciences, Moscow, Russian

e-mail: a.mollaev@mail.ru

The electrical resistivity ρ and Hall coefficient R_H of the p-$Cd_{1-x}Mn_xGeAs_2$ magnetic semiconductors were measured simultaneously using oriented samples cut from single crystals in the [001] and [100] directions, like in a previous study of $CdAs_2$ [1]. The measurements were performed near room temperature at increasing and decreasing pressure (P < 7 GPa) in «Toroid» anvil cells. In the Hall effect measurements, the cell was mounted in a solenoid which generated magnetic fields H<400 kA/m. The uncertainties in our resistivity, Hall effect, and pressure measurements were within 3, 3.5, and 3%, respectively. The ρ and R_H data for the p-$Cd_{1-x}Mn_xGeAs_2$ samples studied are presented in Table 1.

Table 1. Main parameters of the p-$Cd_{1-x}Mn_xGeAs_2$ (x= 0.053) samples

Crystallographic orientation	ρ, Ω cm	RH, cm^3/C
[100]	1.68	142
[001]	1.1	174

All of the samples were found to undergo structural phase transformations under both increasing and decreasing pressure. Comparison of the data for the two p-$Cd_{1-x}Mn_xGeAs_2$ samples (cut from single crystals in the [100] and [001] directions) leads us to conclude that the phase transition pressures during the loading and unloading processes are independent of the crystallographic orientation of the orientation of the sample.
In given work are measured the relative magnetic susceptibility χ/χ_0 and cross magneto resistance $\Delta\rho_{xx}/\rho_0$ in p-$Cd_{0.947}Mn_{0.053}GeAs_2$ samples oriented towards crystallographic [001] and [100] directions. The magnetic susceptibility increases at P_c=1.7 GPa and reaches a maximum. A maxima position of the magnetic susceptibility in high pressure scale P_c is similar for the samples cut along the axis C [001] and across the axis C [100] and distinguishes itself by a maximum height. The observed maximum in $(\chi/\chi_0)/(P)$ dependences can be interpreted as metamagnetic phase transition. The substantial hysteresis of $(\chi/\chi_0)/(P)$ is observed at pressure release. In studied samples there is observed the negative magnetic resistance in a phase transition region, which distinguishes for different crystallographic directions by a character of $(\Delta\rho_{xx}/\rho_o)(P)$ dependence. The hysteresis is revealed in $\Delta\rho_{xx}/\rho_o\,(P)$ dependence at pressure release.

Acknowledgments: This work was supported by Program of Presidium of RAS “Thermophysics and mechanics of external energetic influences and physics of high compressed material” and Section of High Compressed Material.

[1]. A.Yu. Mollaev, L.A. Saipulaeva, R.K. Arslanov and S.F. Marenkin, *Neorg. Mater.*, **37** (2001), p.405. [*Inorg. Mater.* (Engl. Transl.), **37** (2001), p. 327].

O3-4

Temperature Induced Structural Phase Transitions in Chalcopyrite Type Compound Semiconductors

Christiane Stephan[1], Susan Schorr[2], Diana Thomas[1], Marco Di Michiel[3], Hans-Werner Schock[1]

[1] Helmholtz-Zentrum Berlin fuer Materialien und Energie, Solar Energy Research, Institute of Technology, Hahn-Meitner Platz 1, 14109 Berlin, Germany
[2] Free University Berlin, Department of Earth Science, Malteserstraße 74-100, 12249 Berlin, Germany
[3] European Synchrotron Radiation Facility ESRF, 6 Rue Jules de Horowitz, BP 220, 38043 Grenoble, France

Presenting author's e-mail address: christiane.stephan@helmholtz-berlin.de phone number: 0049/ (0)30 8062 2713

Multinary chalcogenides like $Cu(In,Ga)(S,Se)_2$ are compound semiconductors suitable for applications in thin film photovoltaics. These compounds crystallize in a tetragonal chalcopyrite type structure, which can be described as a *ccp* array of chalcogen atoms, with metal atoms occupying one half of the tetrahedral voids.
The chalcopyrites $Cu(In,Ga)(Se,S)_2$ undergo a temperature dependent structural phase transition from the chalcopyrite to the sphalerite type structure. For $CuInS_2$ and $CuInSe_2$ it is a sharp order-disorder phase transition, which occurs within a small temperature range of about 10 K [1, 2]. The character of this phase transition is dominated by an increasing Cu-In anti-site occupancy. On the other hand, in $CuGaS_2$ no temperature dependent structural phase transition occurs. The phase transition in $CuGaSe_2$ is characterized by the co-existence of a tetragonal and a cubic phase. Recently this study was extended to the $Cu(In,Ga)S_2$ and $Cu(In,Ga)Se_2$ mixed crystals. This presentation will give a comparative discussion of the structural phase transition in ternary and quaternary chalcopyrites.
The basis for our investigations were *in-situ* high temperature powder diffraction experiments using synchrotron X-rays and were performed at the European Synchrotron Radiation Facility (ESRF), Grenoble, at the high energy beamline ID15B in the temperature range from room temperature to 1100 °C. The data were analyzed in detail by the Rietveld refinement method to determine lattice parameters, the anion position and cation site occupancies.
The presentation will give an overview of the structural phase transitions observed in these compound semiconductors. The differences between samples with various In/(In+Ga) ratios (from 1 to 0) will be pointed out, concerning not only the transition temperature, but primarily the character of the phase transition, the order parameter, its critical behaviour and universality.

[1]. Schorr, S., Geandier, G., Korzun, B. V., *Phys. Stat. Sol.(c)* 3 (2006), p. 2610.
[2]. Schorr, S.; Geandier, G., *J. Cryst. Res. Technol*. 41 (2006), p. 450.

P3-1

About high pressure induced negative magneto resistance in $Cd_{1-x}Mn_xGeAs_2$

A. Yu. Mollaev[1], I. K. Kamilov[1], R. K. Arslanov[1], T. R. Arslanov[1], U. Z Zalibekov.[1], V. M. Novotortsev[2], S. F. Marenkin[2]

[1]Institute of Physics, Daghestan Scientific Center of the Russian Academy of Sciences, 367003, Makhachkala, *Russian*
[2]Institute of common and inorganic chemistry of the Russian Academy of Sciences, Moscow, Russian

E-mail: arslanovr@gmail.com

A negative cross $\Delta\rho_{xx}/\rho$ and longitudinal $\Delta\rho_{zz}/\rho$ magnetic resistance was found and studied in ferromagnetic high temperature semiconductor (x=0.06, x=0.18, x=0.3). Measurement were carried out in high pressure devises of «Toroid» type, that was placed in multicoil solenoid H<5kOe. Figures show dependences $(\Delta\rho_{xx}/\rho)(P)$ and $(\Delta\rho_{zz}/\rho)(P)$.

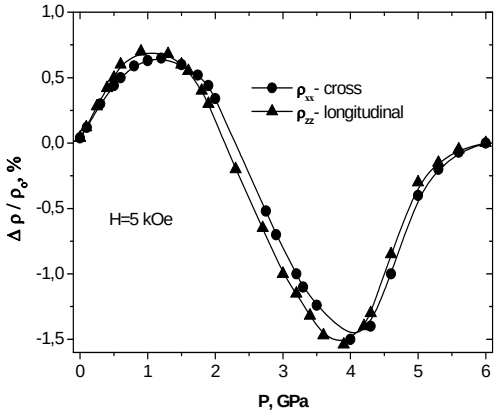

Figure 1. Dependence of cross (circles) and longitudinal (triangles) magnetic resistance from pressure

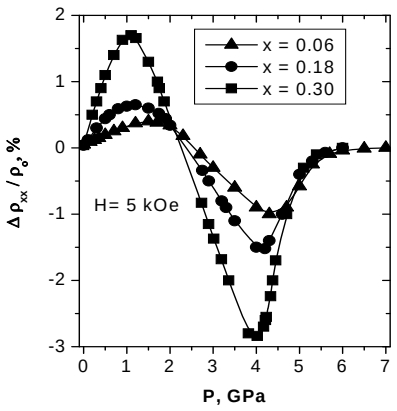

Figures 2. Dependence of cross magnetic resistance from pressure for samples $Cd_{1-x}Mn_xGeAs_2$ (x=0.06, 0.18, 0.3)

It is seen from figure, that magnetic resistance for sample $Cd_{0.7}Mn_{0.3}GeAs_2$ up to pressures P=2.5 GPa is positive and reaches maximum at P≈1 GPa (H=5 kOe). Further increase of pressure leads to suppression of positive magnetic resistance. Magnetic resistance at P>2.5 GPa becomes negative (NMR). Negative magnetic resistance (NMR) at P≈4.5 GPa and H= 5 kOe is about ~3%. Magnetic resistance at P>6 GPa is positive again. A scattering of circuit carriers on fluctuations of may give a considerable contribution in magnetic resistance up to pressure P<1 GPa – magnetic resistance is positive. There takes place a regulation of ions of spin of manganese with rise of pressure and magnetic field; and it lowers the scattering and leads to NMR; this is confirmed by observed at p=1.6 GPa magnetic phase transition ferromagnetic – antiferromagnetic, (FM–AFM) that takes place in the region of magnetic resistive transition from positive to negative. NMR falls from 3% for x=0.3 up to 1% x=0.06 with the decrease of percent content of manganese (right figure).NMR value depend very much on tension of magnetic field maximum at H= 5 kOe and decrease with fall of magnetic field tension, the position of NMR maximum moves to lower pressures with increase of magnetic resistance tension, also grows the NMR region. A hysteresis is observed at falloff pressure.

Acknowledgments: This work was supported by Program of Presidium of RAS “Thermophysics and mechanics of external energetic influences and physics of high compressed material” and Section of High Compressed Material.

P3-2

Crystal structure behaviour of mixed $R_{1-x}Eu_xAlO_3$ (R = La, Pr) perovskites

Tetyana Basyuk[1], Vasyl Berezovets[2], Dmytro Trots[3], Stefan Hoffmann[4], Leonid Vasylechko[1]

[1]Semiconductor Electronics Department Lviv Polytechnic National University, 12 Bandera St., 79013 Lviv, Ukraine
[2]Karpenko Physico-Mechanical Institute of NAS of Ukraine, 5 Naukova St., 79601 Lviv, Ukraine
[3]Bayerisches Geoinstitut, Universität Bayreuth, Universitätsstraße 30, 95447 Bayreuth, Germany
[4]Max-Planck-Institut für Chemische Physik fester Stoffe, Nöthitren St. 40, 01187 Dresden, Germany

e-mail address: tanya.basyuk@gmail.com, phone/ fax number: +380322582696/+ +380322582153

Rare earth aluminates $RAlO_3$ show rhombohedral $R\bar{3}c$ (R = La, Pr) and orthorhombic $Pbmn$ (R = Eu) structures at room temperature. Continuous phase transition $Pm\bar{3}m$– $R\bar{3}c$ is typical for $RAlO_3$ compounds containing "light" rare-earth (R=La, Ce, Pr, Nd), whereas first-order phase transformation $R\bar{3}c$–$Pbnm$ is inherent for $SmAlO_3$, $GdAlO_3$ and $EuAlO_3$. Besides a high-temperature (HT) phase transition, $PrAlO_3$ undergoes a sequence of low-temperature (LT) phase transformations, which is a solely exception among all AMO_3 compounds with perovskite structures [1].

The samples with nominal compositions $R_{1-x}Eu_xAlO_3$ (x=0.1–0.9) were prepared from the initial oxides Pr_6O_{11}, La_2O_3, Eu_2O_3 and Al_2O_3 by solid state reactions with subsequent arc melting. Crystal structure and thermal behaviour of the samples have been studied in a wide temperature range of 12–1173 K by means of high-resolution powder diffraction technique applying synchrotron radiation, thermal analysis and magnetic susceptibility measurements.

At room temperature two kinds of solid solutions $R_{1-x}Eu_xAlO_3$ with rhombohedral and orthorhombic structures are found in the corresponding systems. An immiscibility gaps between two perovskite-type phases in the $PrAlO_3$–$EuAlO_3$ and $LaAlO_3$–$EuAlO_3$ systems occur at x=0.3 and x=0.5, respectively. Lattice parameters and cell volumes decrease monotonically with increasing Eu content. Phase transition from a rhombohedral to the cubic structures and a first-order transformation from an orthorhombic to the rhombohedral structure are observed in $Pr_{1-x}Eu_xAlO_3$ and $La_{1-x}Eu_xAlO_3$ solid solutions depending on compositions. The temperatures of both these HT transitions increase linearly with increasing Eu content. A sequence of LT phase transformations $R\bar{3}c$↔$Imma$ and $Imma$↔$I2/m$ was observed only in the $Pr_{1-x}Eu_xAlO_3$ samples with x<0.3. The temperatures of these transitions display an opposite behaviour: decreasing Pr content leads to an increasing $R\bar{3}c$↔$Imma$ transition temperature and to a decreasing $Imma$↔$I2/m$ transformation temperature. In this respect the studied system is similar to the related $PrAlO_3$–$SmAlO_3$ and $PrAlO_3$–$GdAlO_3$ systems, recently reported [2, 3].

Based on the results of *in situ* synchrotron powder diffraction examinations, DTA/DSC measurement and available literature data, the phase diagrams of the $PrAlO_3$–$EuAlO_3$ and $LaAlO_3$–$EuAlO_3$ pseudo-binary systems have been constructed.

Acknowledgments: The work was supported in parts by the Ukrainian Ministry of Education and Sciences (Project "Tern") and ICDD Grant-in-Aid program.

[1]. L. Vasylechko, A. Senyshyn, U. Bismayer. Perovskite-Type Aluminates and Gallates, in: K.A. Gschneidner, Jr., J.-C.G. Bünzli and V.K. Pecharsky (Eds.), Handbook on the Physics and Chemistry of Rare Earths, Vol. 39. Netherlands: Elsevier–North-Holland, 2009, p.113-295.

[2]. T.V. Basyuk, L.O. Vasylechko, I.I. Syvorotka, V. Berezovets, S.V. Fadeev, *Bull. of Lviv Polytechn. Nat. Univ.* **646** (2009), p.3-10.

[3]. T. Basyuk, L. Vasylechko, S. Fadeev, V. Berezovets, D. Trots and R. Niewa, *Acta Physica Polonica A* **177(1)** (2010), p.98-103.

P3-3

Impurity energy spectrum of indium arsenide at atmospheric and hydrostatic pressures

M.I.Daunov, I.K.Kamilov, A.Yu.Mollaev, S.F.Gabibov

Institute of Physics, Daghestan Scientific Center, Russian Academy of Sciences, 367003, M.Yaragskogo str.94, Makhachkala, Russia

E-mail: i.daunov@mail.ru, phone/ fax +7(8722)628900

It has been found that according to experimental data on hydrostatic pressure up to 7 GPa dependences of Hall coefficient R_H and resistivity ρ at 77 K÷300 K bulk crystals in p-InAs [1], n-InAs [2] и p-InAs<Mn> [3] with density of excess acceptors and donors ~10^{16} cm^{-3}:

- it has been found the pressure coefficients of energy gaps between the conduction band bottom and deep acceptor and resonance donor levels, located at a distance of ε_a=0.13 eV below and at a distance of ε_d=0.35 eV above the bottom of conduction band, respectively, are defined by a "motion" of conduction band with the pressure;
- the energy of deep levels relative to absolute vacuum does not depend on pressure: pressure coefficients $d\varepsilon/dP = |d\varepsilon_d/dP| = d\varepsilon_g/dP \approx 95$ meV/GPa (ε_g – energy gap);
- in p-InAs a deep acceptor band is situated in the tail of the density of states of the conduction band, and a state of the heavily doped, fully compensated semiconductor type is established at low temperatures;
- the acceptor impurity center of Mn is shallow with $d\varepsilon/dP = 39$ meV/GPa relatively top of valens band;
- growth energy ionization impure centre Mn with increasing pressure is conditioned by decreasing of the static (low-frequency) dielectric permeability $\Delta\chi/\chi \cong -0.08$ (an analogue to the magnetic quenching (freezing out) effect [4,5]).

Acknowledgments: The work was supported by the project of Presidium of the Russian Academy of Science "Physics and mechanics of highly condensed matte and of the problem of inner structure of the Earth and Planets".

[1]. A.Yu. Mollaev, R.K. Arslanov, L.A. Saypulaeva, S.F. Gabibov and S.F. Marenkin, Fiz. Tekh. Vis. Davl. **11**, 4 (2001), p. 61.
[2]. M.I. Daunov, I.K. Kamilov, A.B. Magomedov and A.Sh. Kirakosyan, Fiz. Tekh. Poluprovodn. **33** (1999), p. 59.
[3]. A.Yu. Mollaev, I.K. Kamilov, R.K. Arslanov and S.F. Gabibov, Fiz. Tekh. Vis. Davl. **12**, 4 (2002), p. 25.
[4]. M.I. Daunov, R.K. Arslanov, M.M. Gadjialiev, E.V. Kortunova, P.P. Khokhlachev and P.P. Shvansky, Semiconductors **40** (2006), p. 1255.
[5]. M.M. Gadjialiev, I.K. Kamilov, R.G. Dzhamamedov, M.I. Daunov and A.B. Magomedov, Book of Abstract Joint 21st AIRAPT and 45th EHPRG International Conference on High Pressure Science and Technology (Catania, Italy, 2007), p. 283.

P3-4

Influence of polytypism on ferroelectric phase transition in $TlGaSe_2$ crystals

Yu.P.Gololobov[1], N.A.Borovoi[2], G.L.Isayenko[1] and O.V.Prystai[2]

[1] National Transport University, Suvorova st.1, 01010 Kyiv, Ukraine
[2] Physics department, Kyiv National University, building, 2, Glushkova av. 1, 03680 Kyiv, Ukraine

e-mail address: gololo@ukr.net, phone: +38 044 284 6709, fax: +38 044 280 8203

In spite of numerous researches of physical properties of the $TlGaSe_2$ ternary compound not only temperature positions but also physical mechanisms of phase transitions (PT), which take place at the change of temperature in the range T= 100-300 K, are still a subject of debate. In particular, it concerns the transition from incommensurate modulated phase to the commensurate phase, which is ferroelectric PT. It exactly determines that such transition is accompanied by appearance of the polar state with the vector of polarization in the crystal layer plane. The temperatures of ferroelectric PT in $TlGaSe_2$, reported by different authors, are usually found between T_c = 107–110 K [1]. There are very contradictory data in literature regarding the order parameter of this transition. On the one hand, properties, which are characteristic for proper ferroelectrics with an intermediate on a temperature incommensurate phase were found out for the $TlGaSe_2$ crystals. On the other hand, results of neutron diffraction and X-rays researches testify that in the $TlGaSe_2$ crystals at the temperature $T_c \approx$ 107 K ferroelectric PT is accompanied by quadrupling of the unit cell along direction, perpendicular to the layers. It is a cogent argument, that ferroelectric PT is improper. For the polytypes C-$TlGaSe_2$ and 2C-$TlGaSe_2$ (differ by *c* parameter unit cell, i.e. by the number of layers along the C axis) considerable temperature differences of structure are found out recently [2]. In this connection, it is interesting to reveal the features of appearance of the polar state in such polytypes. Therefore in the temperature range T= 100-300 K dielectric researches of the polytypes C-$TlGaSe_2$ and 2C-$TlGaSe_2$ samples used in the X-rays diffraction experiments earlier were realized. The permittivity in the direction perpendicular or parallel to $TlGaSe_2$ crystal layers was measured at a frequency of 1 MHz using E7-12 ac bridge. The temperature was measured with an accuracy of 0.1 K using a copper–constantan thermocouple and was maintained accurate to within 0.5 K using the VRT-2 heat controller. The samples were the same plates used in the X-ray diffraction measurements [2]. As contacts we used indium–gallium paste. It was revealed that polytypism substantially influences on the temperature position and mechanism of polar state occurrence in $TlGaSe_2$ crystals. The character of the obtained temperature dependences of dielectric constant $\varepsilon(T)$ for the two $TlGaSe_2$ polytypes suggests that there are substantial differences in the polar state formation processes with temperature. It was found out that, for the $TlGaSe_2$ crystal, just like for its structural analog, namely, the $TlInS_2$ crystal, the ferroelectric phase transitions in the C and 2C polytypes not only occur at different temperatures but also are characterized by different order parameters. In particular, it is shown that in the C-$TlGaSe_2$ polytype the ferroelectric phase transition is improper and takes place at the temperature $T_c \approx$108 K, at the same time in the 2C-$TlGaSe_2$ polytype such transition is proper and takes place at higher temperature $T_c \approx$111 K. Thus, the results obtained demonstrate that the polytypism of $TlGaSe_2$ crystals should be taken into account in future researches of ferroelectric PT in this ternary compound.

[1]. A.M. Panich, D.C. Ailion, S. Kashida and N. Gasanly, Phys. Rev. B. **69** (2004), p. 24531.
[2]. N. A. Borovoi, Yu. P. Gololobov, G. L. Isaenko and N. B. Stepanishchev, Physics of the Solid State, **51** (2009), p. 2367.

P3-5

$Cd_{1-x}Mn_xGeAs_2$ as a prospective pressure transducer

A. Yu. Mollaev[1], I. K. Kamilov[1], R. K. Arslanov[1], T. R. Arslanov[1], U. Z Zalibekov.[1], V. M. Novotortsev[2], S. F. Marenkin[2], E.S. Ibaev[1]

[1]Institute of Physics, Daghestan Scientific Center of the Russian Academy of Sciences, 367003, Makhachkala, Russian
[2]Institute of common and inorganic chemistry of the Russian Academy of Sciences, Moscow, Russian

e-mail: mix-toor@list.ru

The searching researches of semiconducting materials – pressure transducers were carried out. A search was carried out in two directions: the first is to reveal the semiconducting materials, which can supplement a set of pressure transducers and calibrators for high pressure devices, synthesis of ultra-hard materials, and scientific researches; and the second is to discover new grade materials, which can be offered as command elements in technological processes of obtaining the ultra-hard materials and precious stone materials.

The earlier investigations on high-temperature ferromagnetic materials [1, 2] revealed a number of materials, which can be use as pressure transducers – command elements for synthesis of ultra-hard materials. The p-$Cd_{1-x}Mn_xGeAs_2$ was offered as a material for pressure transducer. We researched the base sample p-$CdGeAs_2$ and samples p-$CdGeAs_2$ doped by Mn x= 0÷0.36 The specific resistivity and Hall coefficient were chosen as indicator of characteristics. The specific resistivity and Hall coefficient were measured at pressure rising and fall in a region of room temperatures in high-pressure device of "Toroid" type. In all studied samples (x = 0, 0.003, 0.053, 0.06, 0.18, 0.3 and 0.36) were found structural phase transitions at pressure rising P = 5.9; 5.7; 5.5; 5.4; 5.2; 4.9; 4.8 GPa and P= 2.9; 2.8; 2.6; 2.5; 2.4; 2.3 GPa at pressure fall. The pressure dependence of location of phase transition point for x=0÷0.36 is presented in Figure 1 (filled circles mean a pressure rise, unfilled circles are pressure fall).

The offered material p-$CdGeAs_2$ Mn-doped can be a pressure transducer as command elements in pressures range P=4.8÷5.9 GPa at pressure rising and P=2.3÷2.9 GPa at pressure fall.

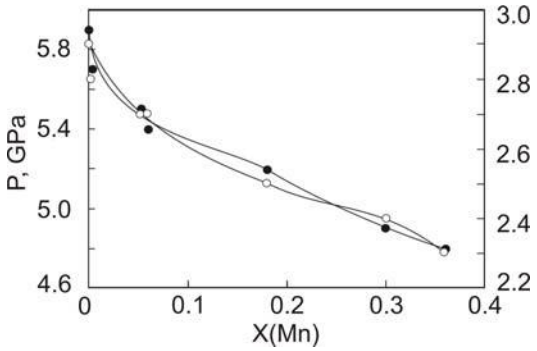

Figure 1. Pressure dependence of location of phase transition point

Acknowledgments: This work was supported by Program of Presidium of RAS "Thermophysics and mechanics of external energetic influences and physics of high compressed material" and Section of High Compressed Material.

[1]. A.Yu. Mollaev, I.K. Kamilov, R.K. Arslanov, U.Z. Zalibekov, S.F. Marenkin, Fizika, **8**, 1-2, (Baku 2007), p. 320.
[2]. A. Yu. Mollaev, I.K. Kamilov, R.K. Arslanov, U.Z. Zalibekov, S.F. Marenkin, V.M. Novotortsev, S.A. Varnavskiy, *High Pressure Research*, **26**, 2, (2006), p. 387.

P3-6

Effects of pressure and temperature on properties of electronic-ionic conductors $(GeS)_{1-x}(CuAsS_2)_x$

Nina Melnikova[1] , Ahmedbek Mollaev[2], Olga Kheifets[1], Luiza Saypulaeva[2], Peter Hohlachev[2], Abdulabek Alibekov[2], Alexey Filippov[1] and Alexey Babushkin[1]

[1]Low Temperature Physics Dept ,Ural State University, Lenina Avenue, 51, 620083, Ekaterinburg, Russia
[2] Institute of Physics of Dagestan Scientific Centre of RAS, M.Yaragsky str., 94, 367003, Makhachkala, Russia

nvm.melnikova@gmail.com , +79221105853 / +7(343)2616885

The study of ionic and mixed electronic-ionic conductors in a broad temperature range and at high pressure are of practical and theoretical interest. The present work deals with polycrystalline copper chalcogenides $(GeS)_{1-x}$ $(CuAsS_2)_x$, x = 0.1; 0.2; 0.3; 0.4; 0.5; 0.6. The researched materials at normal pressure are mixed electronic-ionic conductors. The temperature range of a onset of the ionic transport is 130 K-200 K [1-2]. The aim was to study the electrical properties of the compounds $(GeS)_{1-x}$ $(CuAsS_2)_x$ at pressure 15-45 GPa on a.c. by means of impedance spectroscopy (in the frequency interval 1-200 kHz) and at normal pressure in the temperature range 290-483 K on d.c.
A maximum on baric dependences of resistance at the pressure increase had been observed in studied frequency range in all compounds. The pressure dependences of a real part of impedance of $(GeS)_{1-x}$ $(CuAsS_2)_x$, x = 0.2, on different frequencies at the pressure increase are shown on Fig.1.

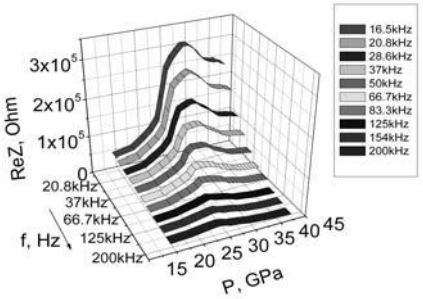

Figure 1. The pressure dependences of a real part of impedance of $(GeS)_{1-x}$ $(CuAsS_2)_x$, x = 0.2, on different frequencies at the pressure increase

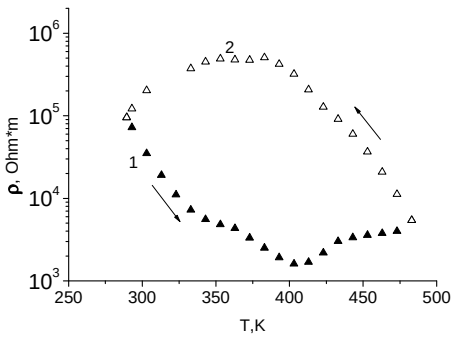

Figure 2. The temperature dependences of the resistivity of $(GeS)_{1-x}$ $(CuAsS_2)_x$, x = 0.2 , in the cell with the ion-blocking electrodes;
1- heating; 2 - cooling

The compression of a lattice can result in the decrease of copper ions mobility and accordingly in the rise of the resistance. At achievement of some pressure there is, probably, a change of a lattice, the resistance starts to decrease. The ranges of pressure, in which there are essential changes in behavior of electrical properties, have been found: for x = 0.1 at 25-27 GPa, for x = 0.2 at 29-31 GPa, for x = 0.3 at 27-29 GPa, for x = 0.4 at 25-27 GPa. In the compounds with x = 0.5 and 0.6 changes in the behavior of the electrical properties were observed only at low frequencies at 26-27 GPa and at 22-26 GPa accordingly. The temperature behaviour of the resistivity at measurement on a direct current in a cell with ion-blocking electrodes can be explained by effects of polarization due to a presence of the ionic conductivity (Fig.2).
The researches were supported by Federal program “Scientific and research and educational personnel of the innovation Russia” to 2009–2013 and by RFBR grant No. 09-02-01316.

[1]. E.R. Baranova, V.L. Kobelev , O.L. Kobeleva , N.V. Melnikova et al, SSI,**124** (1999), p.255.
[2]. N.V. Melnikova, O.L. Kheifets, A.N. Babushkin. , ISJAEE, **49** (2007), p.56.

P3-7
n-InAs and *n*-$CdAs_2$ as repers and calibrators for pressure monitoring

A.Yu.Mollaev, S.L.Saypulaeva, R.K.Arslanov, A.G. Alibekov, N.S.Abakarova

Institute of Physics, Dagestan Scientific Canter, Russian Academy of Sciences, 367003, Makhachkala, Russia,

e-mail: a.mollaev@mail.ru

The present work is the continuation of researches of perspective semiconductor materials, that were began in the Institute of Physical, Daghestan Scientific Centre Russian Academy of Sciences with the aim of forming data bank that can be used either at making pressure transmitters for calibration of high pressure apparatus or as command elements for autoimmunization of processes of synthesis of supersolids and precious stone raw materials [1]. Mono- and polycrystalline n- and *p*-InAs samples (with the concentration of carriers 10^{15} – 10^{17} cm^{-3}) and *n*-$CdAs_2$ monocrystals (n=10^{14}–10^{15} cm^{-3}) have been investigated that were oriented in different crystallographic directions. The measurements were carried out at rise (compression) and fall (decompression) of pressure that was measured by manganine manometer graduated towards reper point [2] in all process of investigations. The error of pressure measurements was about 3 %. Hydrostatic pressure up to $P \leq 9$ GPa was created in teflon capsule whose effective volume was ≈80 mm^3 by the methodic described in work [3] that was partially improved. Monocrystal samples had the form of rectangular parallelepiped with the dimensions of 2.5×0.6×0.5 mm. Polycrystall samples were a kind of circles of cardboard or paper with the hole of 0.5-1 mm in the central part into which 2-3 mg of semiconductor material is pressed. The change of electroresistance from pressure which is easily measured with perfect exactness was chosen as indicator of properties. Typical results of measurements of specific electroresistance *n*-InAs in the region of phase transition at hydrostatic pressure up to 9 GPa at compression and decompression. Phase transitions that can be used as reper points are observed on curves of baric dependences ρ/ρ_0 from pressure at compression (P=6.9 GPa) and decompression (P=2.2 GPa). The carried out analysis of $lg(\rho/\rho_0)$ dependence from pressure shouts that dependence is linear in the range of pressures P=3-9 GPa. Thus the presence of considerable (from several orders) Jumps of electroresistance in the region of phase transition and linear dependence $lg(\rho/\rho_0)$ in the range of pressures 3-6 GPa allows to use indium arsenical as reper and command element i.e. one semiconductor combines two types of pressure transmitters. The position of phase transition on the scale of high pressures at quasihydrostatic pressure in InAs satisfactory coincides with the data obtained at hydrostatic compression.

Diarsenicum cadmium ($CdAs_2$) is one of the least studied semiconductor junctions A^2B^5 that crystallized in tetragonal singonia. The peculiarity of its structure is the presence of As-As contacts alongside with Cd-As contacts that form zigzag chain structures stretched along [001] direction what determines considerable anisotropy of electric properties [4]. The samples were made of parallelepiped form and oriented in such way that their edges coincided with [100] and [001] crystallographic directions. Baric dependences of specific electroresistance $\rho(P)$ for samples of $CdAs_2$ at compression and decompression are shown in fig.3. According to the figure 3 one can see that there are three maxima at P=1.8; 3; 5.5 GPa observed on curve 1and two maxima at P=3 and 5.5 GPa on curve 2. Probably, the maxima at P=1.8 and 3 GPa are connected with peculiarities of band structure of $CdAs_2$, maxima at P=3.2 GPa is stipulated by structural phase transition but at P=3.2 GPa is observed at decompression. Thus the presence of maxima at P=1.8; 3and 5.5 GPa at compression, and presence of maximum at P=3.6 GPa at decompression allows to recommend *n*-$CdAs_2$ as a perspective material for making of reference point of pressure.

[1]. M.I.Daunov, V.I.Danilov, A.B.Magomedov, A.Yu.Mollaev, S.M.Salikhov. *Sverkhtverdye Materialy*, **4**, (1990), p. 7, M.I.Daunov, A.B.Magomedov, A.Yu.Mollaev, S.M.Salikhov, L.A.Saypulaeva. *Phys. Tekh. Vis. Davl.*, **2**, (1992), 3, 2.p. 71.
[2]. N.A.Bendeliani, L.F.Vereschagin. *Phys. Tekh. Exper.*, **4**, (1979), p.218.
[3]. L.G.Khvostantsev, V.A.Sidorov. *Phys. Stat. Sol.* (a), **64**, (1991), p.379.
[4]. S.F.Marenkin, V.A.Morozova. *Neorganicheskie Materialy*, **35**, (1999), p. 1190.

P3-8

Magnetovolume effect and magnetic transitions in the $Cd_{1-x}Mn_xGeAs_2$ at the high pressure

A. Yu. Mollaev[1], I. K. Kamilov[1], R. K. Arslanov[1], T. R. Arslanov[1], U. Z Zalibekov.[1], R. R. Bashirov[1]
V. M. Novotortsev[2], S. F. Marenkin[2]

[1]Institute of Physics, Daghestan Scientific Center of the Russian Academy of Sciences, 367003, Makhachkala, *Russian*
[2]Institute of common and inorganic chemistry of the Russian Academy of Sciences, 119991, Moscow, Russian

E-mail: a.mollaev@mail.ru

The relative volume changes has been measured for $Cd_{1-x}Mn_xGeAs_2$ (x=0.06, 0.18, 0.24 and 0.30) under hydrostatic pressure up to 7 GPa at room temperature. High hydrostatic pressure was generated in the 80mm^3 teflon container filled with liquid and placed in compressible gasket of «Toroid» device [1]. The relative volume change was measured by a strain gauges glued onto the sample [2]. The results of the measurements are shown in figure 1, and the bulk modulus dependences, calculated from figure 1 $\Delta V(P)/V_0$, are shown in figure 2. As it is seen from figure 1, the volume decreases almost linearly up to 4 GPa, and ruptures in the curves are observed as P>1.5 GPa presumably due to metamagnetic transition.

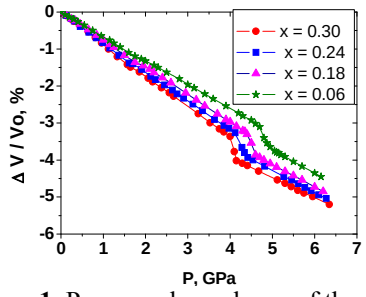

Figure 1. Pressure dependence of the relative volume change of $Cd_{1-x}Mn_xGeAs_2$.

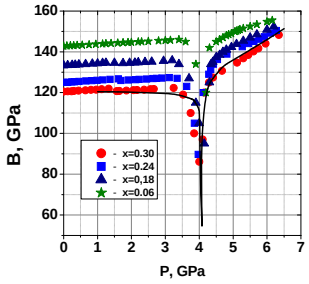

Figure 2. Pressure dependence of the bulk modulus $Cd_{1-x}Mn_xGeAs_2$.

The bulk modulus of $Cd_{1-x}Mn_xGeAs_2$ begins to rise after P>4.1 GPa indicating the continuous disappearance of ferromagnetic state at higher pressure. This transition from ferromagnetic to paramagnetic in $Cd_{1-x}Mn_xGeAs_2$ at P>4.1 GPa is rather abrupt and the giant (order of magnitude) softening of the bulk modulus is observed prior the transition. Futher increase of the pressure a results in a drastic increase of the bulk modulus to a value in excess of initial one. Generally, the pressure dependence of the bulk modulus (and the compressibility) appears as a typical λ-anomaly, that is apparently due to the magnetic transition (disappearance of ferromagnetism) in $Cd_{1-x}Mn_xGeAs_2$ at a pressure near 4 GPa. The solid lines in figure 2 put upon the for $Cd_{1-x}Mn_xGeAs_2$ are fitting the scaling formula: $B = k\left|1 - \frac{P}{P_C}\right|^{-b} + c$, applied usually for analysis of critical phenomena. The critical index b, found from figure 2, is about of 0.8, and Pc = 4.1 GPa.

Acknowledgments: This work was supported by Program of Presidium of RAS "Thermophysics and mechanics of external energetic influences and physics of high compressed material" and Section of High Compressed Material.

[1]. L.G. Khvostantsev, L.P. Vereshagin, A.P. Novikov. High Temp.- High Pressure, **9** (1977), p.637.
[2]. O.B. Tsiok, V.V. Bredikhin, V.A. Sidorov and L.G. Khvostantsev, High Press. Res, **10** (1992), p.523.

P3-9
Comprehensive study of high temperature ferromagnetic semiconductor $Cd_{0.94}Mn_{0.06}GeAs_2$

A. Yu. Mollaev[1], I. K. Kamilov[1], R. K. Arslanov[1], T. R. Arslanov[1], U. Z Zalibekov.[1], V. M. Novotortsev[2], S. F. Marenkin[2]

[1]Institute of Physics, Daghestan Scientific Center of the Russian Academy of Sciences, 367003, Makhachkala, Russian
[2]Institute of common and inorganic chemistry of the Russian Academy of Sciences, Moscow, Russian

E-mail: a.mollaev@mail.ru

Baric dependencies P≤7 GPa, magnetic field H≤5kOe and dependencies of specific resistivity ρ, Hall coefficient R_H dependencies, dependencies of cross magnetic resistance $\Delta\rho_{xx}/\rho$ and dependencies of relative susceptibility χ/χ_0 in high temperature ferromagnetic semiconductor $Cd_{0.94}Mn_{0.06}GeAs_2$ have been studied. There were taken several methods for measuring: baric dependencies were measured at rise and fall of hydrostatic pressure using method [1], magnetic susceptibility using frequency method, magnetic field dependence using standard method. Structural reversible phase transitions semiconductor–metal at P =5.2 GPa were found on baric dependence ρ(P) and R_H(P). One may outline four regions on curve R_H(P): P≤0.6 GPa – region of impurity conductivity, P= 0.6 – 1.9 GPa – region of exhaustion, P=1.9 – 4.5 GPa – region of fall of R_H (reasons are still in discuss) and P=4.5 – 6.5 – region of phase transition. In the region of phase transition P > 5 GPa, curve comes out for saturation, where electric conductivity $\sigma = 3000\ \Omega^{-1}\ cm^{-1}$, and concentration of charge carriers $5\times10^{20} cm^{-3}$ testifies that there takes place semiconductor–metal transition. Metamagnetic phase transition was found for the first time on baric dependence of relative magnetic susceptibility both at rise and fall of pressure. Temperature dependence of metamagnetic phase transition is measured from temperature, phase transition with increase of temperature T=310–334 K moves to low pressures, amplitude of phase transition falls. Cross magnetic resistance was measured in magnetic field up to H≤5 kOe. Magnetic resistance is observed in magnetic field under pressure in $Cd_{0.94}Mn_{0.06}GeAs_2$. The increase of pressure and magnetic field leads to growth of positive magnetic resistance, and the amplitude of positive magnetic resistance reaches maximum in field H = 5 kOe and P≤1 GPa. Further increase of pressure leads to suppression of positive magnetic resistance. In the region of metamagnetic phase transition at P ≅2 GPa, magnetic resistance changes positive sign for negative. Negative magnetic resistance is ≅ 3% at pressure P >4.5 GPa and field H = 5 kOe. To our opinion, at pressures P < 1GPa a considerable contribution in magnetic resistance gives the scattering of carriers on fluctuations of magnetizing–magnetic resistance is positive. With growth of pressure in magnetic field occur regulating of spins of manganese ions, scattering decreases, and it leads to negative magnetic resistance. Hysteresis of magnetic resistance is found on dependencies $\Delta\rho_{xx}/\rho$(P) at pressure fall. Hysteresis of magnetic resistance, apparently, is a characteristic of anomalous scattering of charge carriers, occurring at transition in magnetic regulated state at forming of ferromagnetic clusters of nano-measuring (ferrons).

Acknowledgments: This work was supported by Program of Presidium of RAS “Thermophysics and mechanics of external energetic influences and physics of high compressed material” and Section of High Compressed Material.

[1]. L.G. Khvostantsev, L.P. Vereshagin, A.P. Novikov. High Temp. - High Pressure, **9** (1977), p. 637.

P3-10

Magnetic phase transitions in the $CdGeAs_2$, $CdGeP_2$, and $ZnGeAs_2$ doped by manganese

A. Yu. Mollaev[1], I. K. Kamilov[1], R. K. Arslanov[1], T. R. Arslanov[1], U. Z Zalibekov[1], V. M. Novotortsev[2], S. F. Marenkin[2], I.V. Fedorchenko[2]

[1]Institute of Physics, Daghestan Scientific Center of the Russian Academy of Sciences, 367003, Makhachkala, Russian
[2]Institute of common and inorganic chemistry of the Russian Academy of Sciences, Moscow, Russian

e-mail: a.mollaev@mail.ru

Generally the resistivity is used for pressure transducers as an indicator of characteristics. We offer to use the magnetotransport at high pressures, in particular the magnetic phase transition, as an indicator of characteristics. High-temperature ferromagnetic semiconductors $CdGeAs_2$<Mn>, $CdGeP_2$<Mn>, and $ZnGeAs_2$<Mn>of different doping degree were researched. The relative magnetic susceptibility χ/χ_0 (χ_0 is a value of magnetic susceptibility at the atmospheric pressure) was measured by a frequency method [1].

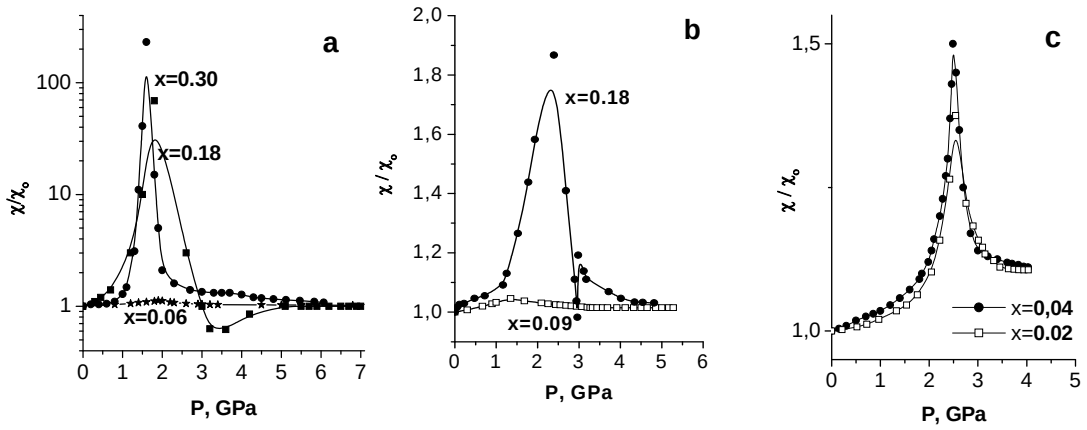

Figure 1. Baric dependences of the magnetic susceptibility for p-$Cd_{1-x}Mn_xGeAs_2$ (a), p-$Cd_{1-x}Mn_xGeP_2$ (b), and p-$Zn_{1-x}Mn_xGeAs_2$ (c)

In figure 1 are presented the baric dependences of the magnetic susceptibility for p-$Cd_{1-x}Mn_xGeAs_2$ (a), p-$Cd_{1-x}Mn_xGeP_2$ (b), and p-$Zn_{1-x}Mn_xGeAs_2$ (c). Figure (a) shows that maximum $(\chi/\chi_0)(P)$ shifts towards the low temperatures from P=2 GPa for x=0.06 to P=1.6 GPa for x=0.3 with increasing of manganese percentage in p-$Cd_{1-x}Mn_xGeAs_2$. The maximum amplitude vice versa increases with increasing of manganese percentage. The same behavior is observed for two samples with x=0.9 and x=0.18 in p-$Cd_{1-x}Mn_xGeP_2$. The studied dependence of relative magnetic susceptibility $(\chi/\chi_0)(P)$ for samples p-$Zn_{1-x}Mn_xGeAs_2$ (x=0.02 and 0.04) is presented in Fig.(c), and as is clear the observed scenario is similar to previous materials.
When pressure decreases, in all studied samples in $(\chi/\chi_0)(P)$ dependences is observed a hysteresis, which maximums can be used grades.

Acknowledgments: This work was supported by Program of Presidium of RAS "Thermophysics and mechanics of external energetic influences and physics of high compressed material" and Section of High Compressed Material.

[1]. A.Yu. Mollaev, I.K. Kamilov, R.K. Arslanov, U.Z. Zalibekov, S.F. Marenkin: *Actual problems of solid state physics* (vol. abstr. of int. conf., Minsk 2009).

P3-11
γ- Radiation stimulated structural transition in $TlInS_2$ from monoclinic to hexagonal phase

O. Z. Alekperov., V.A. Gasymov, A.I. Nadjafov, N. A. Safarov,

Institute of Physics, National Academy of Sciences, H. Javid av. 33, Baku 1143, Azerbaijan

ozalekperov@physicsab.az (99412)4391105

The results of the influence of γ- radiation doze with quantum energy 1.23MeV on photoconductivity (PC), ferroelectric phase transition (FPT) and X-ray diffraction (XRD) in monoclinic (M)-$TlInS_2$ crystal are investigated in this work. For the first time simultaneous XRD measurement also was used after every stage of γ-radiation to detect the possible structural changes of crystal. Irradiation dozes conventionally can be divided into the three stages, differing of the radiation effect on crystal properties. The first stage (FS) of irradiation (≤ 100Mrad) is characterized with PC rise, increase in dielectric function $\varepsilon(T)$, dielectric losses $tg\delta = f(T)$ - and conductivity $\sigma(T)$ -temperature dependencies at FPT accompanying of dielectric anomaly (DA), anomalies of $tg\delta = f(T)$ and $\sigma(T)$. Duration of the FS differs for different samples having dependence on samples perfection, so the pure sample the shorter the FS. At dozes of FS narrowing of DA, $f(T)$ and $\sigma(T)$ anomalies at FPT take place. All reflexes ((002), (004), (008) and (0010)) of room temperature XRD registered by X-ray scanning of [001] surface of M-$TlInS_2$ (c=15A politype) also become narrow and increase in intensity. These facts clearly testify that FS of γ-radiation improves samples parameters as a result of compensation of residual charged impurities with radiation defects; lattice vacancies or interstitials (V-I). The second stage (SS) of irradiation (200-400Mrad) is characterized with gradual broadening of $\varepsilon(T)$, $f(T)$ and $\sigma(T)$ -dependencies at FPT, decrease of these quantities at DA temperatures and some decrease of PC of samples. At the beginning of the SS dozes some decrease of intensity and broadening of (002) reflex in XRD, which corresponds mainly to the reflection from S atomic planes takes place with simultaneous increase and narrowing of the most intensive reflex (004) corresponding to reflection from Tl and In atomic plane of M-$TlInS_2$. At doze about 400Mrad 5-fold broadening of DA in $\varepsilon(T)$ - dependence is observed. These facts show that radiation induced defects arise mainly from sulfur vacancies. As follows from XRD the only structural changes at FS and SS is some politype transformation in M-$TlInS_2$ with even-fold increase of lattice parameter c=15A. The broadening of DA in $\varepsilon(T)$ - dependence takes place without any decrease of the temperature of DA at FPT, indicating that sulfur V-I defects form no shallow impurity states. The third stage (TS) (~1500Mrad) is characterized with structural change of M-$TlInS_2$ to hexagonal H-$TlInS_2$. XRD of crystal [001] surface is identical to powder pattern of H-$TlInS_2$. PC spectra of the crystal after TS is the same as for H-$TlInS_2$ with E_g≈1.1eV. M→H transition takes play only on M-crystal surface within a few μm.

P3-12

Unoccupied electronic structure of iron-based superconductors $NdFeAsO_{0.7}$ and $Ba(Fe_{1-x}Co_x)_2As_2$ (x = 0, 0.11)

Hitoshi Sato[1,4], Yuki Utsumi[2], Osamu Morimoto[1], Yosuke Nakashima[2], Akihiro Ino[2,4], Yoshihiro Aiura[3,4], Akira Iyo[3,4], Hijiri Kito[3,4], Kiichi Miyazawa[3], Parasharam M. Shirage[3], Hiroshi Eisaki[3,4], Chul-Ho Lee[3,4], Kunihiro Kihou[3], Hirofumi Namatame[1] and Masaki Taniguchi[1,2]

[1] Hiroshima Synchrotron Radiation Center, Hiroshima University, Higashi-Hiroshima 739-0046, Japan
[2] Graduate School of Science, Hiroshima University, Higashi-Hiroshima 739-8526, Japan
[3] National Institute of Advanced Industrial Science and Technology, Ibaraki 305-8568, Japan
[4] Japan Science and Technology Agency, Transformative Research-Project on Iron Pnictide (JST-TRIP)

jinjin@hiroshima-u.ac.jp, +81-82-424-6293/+81-82-424-6294

The iron-based new superconductor, $LaFeAsO_{1-x}F_x$, was found in 2008 [1]. NdFeAsO and $BaFe_2As_2$ are one of the parent compounds of the iron-based superconductors and superconductivity appears with electron or hole doping. Both compounds exhibit structural transition at 140-150 K from tetragonal structure (high-T side) to orthorhombic structure with an antiferromagnetic ordering (low-T side). A great number of high-resolution angle-resolved photoemission experiments have been carried out for the iron-based superconductors, so far. In this study, we have observed unoccupied electronic structure of $NdFeAsO_{0.7}$ (Nd1111), and $Ba(Fe_{1-x}Co_x)_2As_2$ with x=0 (Ba122) and 0.11 (Co-Ba122) by means of inverse-photoemission spectroscopy (IPES).

Fig.1 shows IPES spectra of Ba122 taken at the incidence electron energy of E_k=40-60 eV. The spectra of Co-Ba122 show similar behaviour to those of Ba122. We notice three structures around 1, 5 and 12 eV above the Fermi level (E_F). The structure around 1 eV exhibit resonance enhancement between E_k=50 and 60 eV, corresponding to the Fe 3p-3d absorption region. This indicates that the peak around 1 eV is attributed to the unoccupied Fe 3d states. The resonance seems to slightly become remarkable with the Co doping. The structure around 5 eV is attributed to the Ba 5d states and the prominent peak around 12 eV to the Ba 4f states, in comparison with the band-structure calculations [2].

The IPES spectra of Nd1111, Ba122 and Co-Ba122 at E_k=60 eV are compared in Fig. 2. In contrast to (Co-)Ba122, the Fe 3d states of Nd1111 are observed as a weak shoulder around 1 eV and exhibits almost no resonance. The Fe 3d peak width of Co-Ba122 is slightly narrower than that of Ba122. From these experimental results, it is considered that the unoccupied Fe 3d states of Nd1111 are comparatively itinerant, while those of (Co-)Ba122 have nearly localized character. The Co doping seems to marginally increase the localized character of the Fe 3d states.

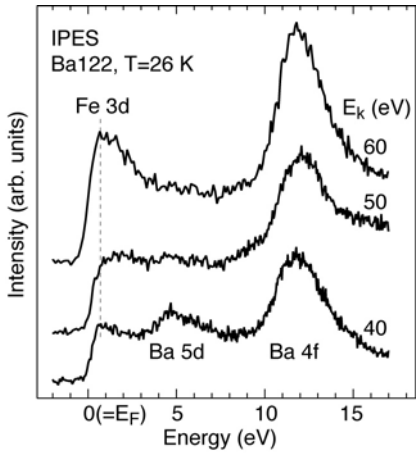

Figure 1. IPES spectra of Ba122.

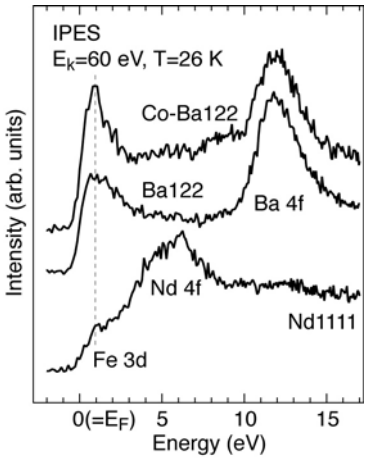

Figure 2. Comparison of IPES spectra of Nd1111, Ba122 and Co-Ba122.

[1]. Y. Kamihara *et al*., J. Am. Chem. Soc. **130**, 3296 (2008).
[2]. T. Oguchi, private communication.

P3-13

Change in Eu 3d hard X-ray photoelectron spectra through the temperature-induced valence transition of $EuPd_2Si_2$

Kojiro Mimura[1] Takayuki Uozumi[1], Takahiko Ishizu[1], Satoru Motonami[1], Hitoshi Sato[2], Yuki Utsumi[3], Shigenori Ueda[4], Akihiro Mitsuda[5], Kenya Shimada[2], Yukihiro Taguchi[1], Yoshiyuki Yamashita[4], Hideki Yoshikawa[4], Hirofumi Namatame[2], Masaki Taniguchi[2,3], Keisuke Kobayashi[4]

[1] Department of Mathematical Sciences, Graduate School of Engineering, Osaka Prefecture University, Gakuen-cho 1-1, Naka-ku, Sakai 599-8531, Japan
[2] Hiroshima Synchrotron Radiation Center, Hiroshima University, Kagamiyama 2-313, Higashi-Hiroshima 739-0046, Japan
[3] Department of Physical Sciences, Graduate School of Science, Hiroshima University, Kagamiyama 1-3-1, Higashi-Hiroshima 739-8526, Japan
[4] NIMS Beamline Station at SPring-8, National Institute for Materials Science, 1-1-1 Koto, Sayo-cho, Sayo-gun, Hyogo 679-5148, Japan
[5] Department of Physics, Graduate School of Science, Kyushu University, 6-10-1 Hakozaki, Higashi-ku, Fukuoka 812-8581, Japan

mimura@ms.osakafu-u.ac.jp, +81-72-254-9367/+81-72-254-9367

$EuPd_2Si_2$ undergoes an abrupt valence transition at around 160 K: The Eu mean valence changes from 2.8 below 130 K to 2.3 above 180 K [1-3]. In order to understand the mechanism of valence transition, we have investigated the electronic structure of $EuPd_2Si_2$ by means of temperature-dependent hard X-ray photoelectron spectroscopy (HX-PES). The HX-PES experiments were performed at the undulator beamline BL15XU of SPring-8.

The temperature-dependent HX-PES spectra clearly show the valence transition, namely, the intensities of the divalent and trivalent Eu 3d components are abruptly changed, as shown in Fig. 1. The Eu 3d spectral shape, especially the drastic change in trivalent Eu 3d feature with temperature, cannot be reproduced by the atomic calculation that had been utilized for the spectral analysis of Eu compounds so far. Therefore, we have done calculations based on the Anderson model in which the hybridization of the trivalent Eu 4f electrons with the conduction electrons and the f-f hybridization between the divalent and trivalent Eu with anisotropic symmetry are taken into account, and we could reproduce the temperature dependence of Eu 3d spectral features reasonably well. According to the model calculation, the change in the trivalent Eu 3d spectral shape through the valence transition is closely related to the degree of admixture of the excitation state (J = 1, 2) and the ground states (J = 0) of trivalent Eu.

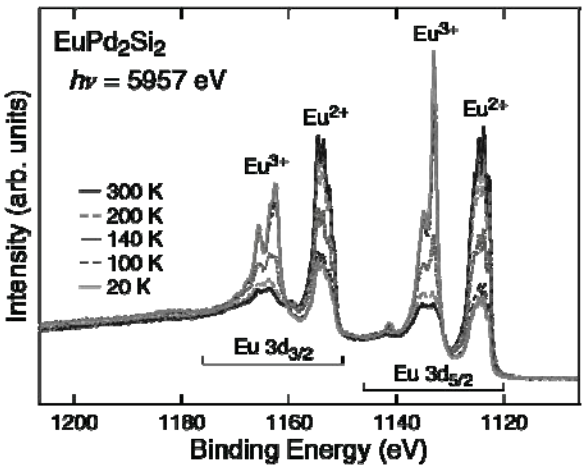

Figure 1. Temperature dependence of Eu 3d core-level HX-PES spectra of $EuPd_2Si_2$

Acknowledgments: This work was partly supported by the Faculty Innovation Research Project of the Graduate School of Engineering, Osaka Prefecture University.

[1]. E.V. Sampathkumaran, L.C. Gupta, R. Vijayaraghavan, K.V. Gopalakrishnan, R.G. Pillay and H.G. Devare, *Journal of Physics C* **14** (1981) L237.
[2]. E. Kemly, M. Croft, V. Murgai, L.C. Gupta, C. Godart, R.D. Parks and C.U. Segre, *Journal of Magnetism and Magnetic Materials* **47&48** (1985) 403.
[3]. G. Wortmann, K.H. Frank, E.V. Sampathkumaran, B. Perscheid, G. Schmiester and G. Kaindl, *Journal of Magnetism and Magnetic Materials* **49** (1985) 325.

P3-14

Influence of hydrostatic pressure on parameters of localized states in $TlGaTe_2$

S.N.Mustafaeva, Sh.G.Gasymov, E.M.Kerimova

Institute of Physics, National Academy of Sciences of Azerbaijan, Baku
G. Javid pr., 33, AZ 1143, Baku, Azerbaijan
E-mail: solmust@gmail.com

$TlGaTe_2$ single crystals are typical representatives of chain-layred semiconductors and attract a lot of attention due to their interesting physical properties. These properties include strong anisotropy of the electric parameters related to special features in the crystalline structure. Chain and layered crystals usually contain structural defects, such as vacancies and dislocations. The presence of these defects results in a high density of localized states near the Fermi level. The states localized in the band gap are responsible for most electronic processes occurring in semiconductors. Both dc and ac charge transport in thallium-gallium chalcogenides proceeds via these localized states. Measurements of temperature-dependent conduction of a crystal can give valuable information on the localized states. The physical properties of $TlGaTe_2$ single crystals are very sensitive to external actions, such as temperature, dc and ac electric fields, laser light, ionizing irradiations, pressure.
The aim of this work is to study the influence of hydrostatic pressure on the dc-electrical properties of $TlGaTe_2$ single crystals over the temperature range from 77 to 296 K.
The crystals used for our study were grown by the Bridgman method and have tetragonal structure of the TlSe type with space group I4/*mcm* and lattice parameters: a = (8.430±0.002) Å, b = (6.858±0.004) Å at room temperature. The samples for electrical measurements had the shape of rectangular plates. Indium was used as a contact material to the $TlGaTe_2$ samples. Dc-electric field from Ohmic region of current-voltage characteristic was applied crosswise to the natural chains of a $TlGaTe_2$ single crystal.
The measurements under pressure (up to 0.82 GPa) were performed in a conventional copper-beryllium vessel with a mixture of dehydrated transformer oil and kerosene (1 : 4) as a pressure transmitting media. This fluid did not cause any irreversible changes in the samples. Pressure was measured with a calibrated manganine gauge with an accuracy not less than 1%.
The effect of hydrostatic pressure (up to 0.82 GPa) on the electric properties of chain $TlGaTe_2$ single crystals has been investigated in the temperature range 77-296 K. It has been shown that pressure leads to a considerably increase of conductivity ($\sigma_\perp$) across the chains of $TlGaTe_2$ single crystals. The increase of conductivity with pressure is described by the formula $\sigma_\perp(P) = \sigma_\perp(0)\exp(-\gamma P/2kT)$, and the pressure coefficient of the indirect band gap $\gamma = dE^i_g/dP$ was found to be -0.207 eV/GPa.
Parameters of localized states in the band gap of $TlGaTe_2$ single crystal according to the low-temperature electrical measurements were obtained at various pressures. It has been established that, as the pressure increases, the density of localized states near the Fermi level N_F decreases exponentially, but average jump distance (R_{av}), energy spread of localized states (ΔE) and activation energy of hopping conduction ΔW in $TlGaTe_2$ single crystal increase linearly (**Table**).

Table
Parameters of localized states in the band gap of the $TlGaTe_2$

P, 10^8 Pa	N_F, $eV^{-1}\cdot cm^{-3}$	R_{av}, Å	ΔE, eV	ΔW, eV
0	$8.6\cdot10^{19}$	50	0.04	0.03
3.1	$8.0\cdot10^{18}$	90	0.08	0.05
5.1	$2.6\cdot10^{18}$	119	0.11	0.07
7.1	$1.3\cdot10^{18}$	140	0.13	0.09

P3-15

The metal dielectric transition induced by temperature in layered compound $Bi_2Te_{3-x}Cl_x$.

N.A. Abdullayev[1], N.M. Abdullayev[1], X.V. Aliguliyeva[1], K.M. Mustafayeva[1], T.G. Kerimova[1], S.A. Nemov[2] , V.N. Zverev[3]

[1]*Institute of Physics, National Academy of Sciences, 33 H. Javid av., AZ 1143, Baku, Azerbaijan*
[2]*St. Petersburg State Polytechnical University, ul. Politekhnicheskaya, 29, St. Petersburg , 195251, Russia*
[3]*Institute of Solid State Physics, Academy of Sciences, 2 Institutskaya ul., 142432, Chernogolovka,, Russia*

e-mail: anadir@azintex.com, phone: (994 12) 4322749

The layered single crystals Bi_2Te_3 are narrow band semiconductors well studied in the connection with their wide use as one of components of high-performance thermoelectric materials. Nowadays the interest to the investigations of doped Bi_2Te_3 strongly increases in the connection with perspectives of working temperature range expansion and enhancement of material thermoelectric figure of merit on the basis of Bi_2Te_3 at doping.

It is well known the undoped single crystals Bi_2Te_3 being the semiconductors are characterized by typical "metallic" type of resistance temperature dependence. This is caused by presence of big number of character defects caused by the transition in crystal lattice of *Bi* atom in positions of *Te* atoms. As such anti-structural defects behave themselves as acceptors, the single crystals Bi_2Te_3 have initially the essential hole concentrations $p \sim 10^{18} - 10^{19} cm^{-3}$. The conduction anisotropy doesn't practically change with temperature change and is usually in limits ~4-6.

The single crystals Bi_2Te_3 doped by chlorine form the replacement solid solutions $Bi_2Te_{3-x}Cl_x$ in which tellurium atoms are substituted by the chlorine atoms in crystal lattice. Moreover, the chlorine atoms give the superfluous electron to the conduction band and initial hole concentration decreases.

It is clear that the doping by chlorine atoms leads to essential increase of conduction anisotropy (more than one order of value) increasing with temperature decrease. The increase of conduction anisotropy takes place because of resistance increase in the direction perpendicular to layers. This takes place of the fact that part of impurity atoms at doping locate in the intervals between layers as a result of atom dense parking inside layers – quintets. Moreover, in temperature interval T=5-18K the conduction has the "metallic" type and at temperature interval T>18K the conduction has the activation character in the direction perpendicular to layers. Thus, the specific transition of metal-dielectric is observed.

To explain the simultaneous existence of two mechanisms of charge transfer as well as in graphite [1] one can suppose that conduction in $Bi_2Te_{3-x}Cl_x$ perpendicular to layers has two channels: "metallic" and "activation". In the framework of this model the charge transfer realizes parallel on narrow metallic paths and wide regions of disorder crystalline structure being as a result of hopping conductivity, conquering between each other with temperature variation.

One can suppose that the presence of weak bond between layers in layered crystals causes to the unequal spread of impurity: the essential part of impurity atoms is in interlayer intervals. This leads not only to essential increase of electric conduction anisotropy, but it causes the change of mechanism of charge transfer.

[1]. N.A. Abdullayev and T. G. Kerimova, Phys. B: Condens Matter, **404**, (2009), p.5215.

P3-16

The role of electronic subsystem in the negative thermal expansion of ferroelectric-semiconductor *$TlGaSe_2$*.

R. A. Suleymanov[1,2]., N.A. Abdullayev[1], T.G. Mammadov[1] , M.-H. Seyidov[1,2], E. Yakar[2]

[1]*Institute of Physics, National Academy of Sciences, 33 H. Javid av., AZ 1143, Baku, Azerbaijan*
[2]*Department of Physics, Gebze Institute of Technology, Gebze, 41400, Kocaeli, Turkey*

e-mail: rauf_suleymanov@gyte.edu.tr, phone: (994 12) 4395163

It is well known, that layered crystals *$TlGaSe_2$* undergo a phase transitions (PT) from para electric phase to incommensurate phase (T_i ~ 120 K) and then to commensurate ferroelectric phase (T_c ~ 110 K). Phase transitions reveal itself in a number of physical phenomena in *$TlGaSe_2$* crystals including thermal expansion.

It was shown [1], that in contrast to the other crystal from the same family, $TlInS_2$, both linear expansion coefficients (LEC), $\alpha_{\perp}(T)$ and $\alpha_{II}(T)$ (perpendicular and parallel to the layers plane, respectively) in $TlGaSe_2$ demonstrate anomalies near the PT temperatures. Predominantly, $\alpha_{II}(T)$ in *$TlGaSe_2$* demonstrates outstanding "negative" anomaly at T_i and negative thermal expansion in *5-135K* temperature range. $\alpha_{II}(T)$ in *$TlInS_2$* is positive and varies monotonically in the all investigated temperature range.

$\alpha_{II}(T)$ in the layered crystals may be negative due to the two main reasons [2]: when Gruneisen parameter γ_{II} is negative due to peculiar phonon spectra and "membrane effect ", and 2) when " Poisson contraction" in the layers plane is extremely large due to large values of elastic constant C_{13} and $\alpha_{\perp}(T)$.

It has been shown, that in *$TlGaSe_2$* elastic constant C_{13} increases considerably decreasing the temperature, whereas it remains almost constant in *$TlInS_2$*. To understand the nature of such unusual behavior of elastic constant C_{13} in *$TlGaSe_2$* the effects of illumination and external electric field on LEC have been investigated.

It turns out, that the absolute value of $\alpha_{II}(T)$ at *~90K* increases more than 3 times after the illumination of the samples with the light of $h\nu > E_g$. On the other hand, electric field leads to increase of α_{II} at $T < T_c$ and as a result shifts the temperature where α_{II} changes its sign to lower temperature region (T<100K). Both of these facts, together with the strong correlation of $\alpha_{II}(T)$ curve and thermally stimulated current curve allow concluding that electron subsystem plays an important role in thermal expansion processes in *$TlGaSe_2$* crystals.

It is supposed, that some deep impurity states which can activate by illumination and external electric field are responsible for negative LEC in *$TlGaSe_2$*. Internal electric fields created by these impurities influence inter atomic distances via inverse piezoelectric effect and electrostriction.

[1]. G.L. Belenkii, E. Yu. Salaev, R.A. Suleymanov, N.A. Abdullaev and V. Ya. Shteinshraiber , *Solid State Comm*., **53** (1985), p. 967.

[2]. N.A. Abdullaev , T.G. Mammadov and R.A. Suleymanov, *Phys. Stat. Sol.(b)*, **242** (2005), p. 983.

P3-17

Charged Defects and Memory Effect in Ferroelectric – Semiconductor $TlInS_2$

MirHasan Yu. Seyidov[1,2], Rauf A. Suleymanov[1,2], A.K. Fedotov[3], T.G. Mammadov[2], S.S. Babayev[2], G.M.Sharifov[2], M.I.Tarasik[3]

[1] Department of Physics, Gebze Institute of Technology, 41400, Gebze, Kocaeli, Turkey
[2] Institute of Physics Azerbaijan National Academy of Sciences, AZ-1143 Baku, Azerbaijan
[3] Belarusian State University, 220050, Independence av.4, Minsk, Belorus
smirhasan@gute.edu.tr, phone +90 262 605 13 29 / fax. +90 262 653 84 90

Semiconductor with layered crystalline structure $TlInS_2$ is a ferroelectric with intermediate incommensurate (INC) phase. Materials with INC – phase demonstrate irreversible effects (global hysteresis and memory effect) due to the pinning of modulation wave by point defects. The memory effect is in the centre of such phenomena. Annealing of the crystals within the INC phase for a long time (hours) leads to anomalies in dielectric constant around the annealing temperature, T_{ann}, thus demonstrating the memory to the annealing temperature. Memory effect is explained on the basis of defect density wave (DDW) formation. When the crystal is kept (annealed) at a finite temperature during some hours within the INC phase, ordered pattern of defects is formed (DDW) as a result of the spatial redistribution of impurities and structural defects in the periodic field of the INC - phase. If T_{ann} is again approached in a time shorter than the relaxation time of the induced state, the DDW interacts with the modulation wave, "captures" it, thus realizing the memory effect. Thus, the interaction between the defects and INC structure plays a central role in the realization of the memory effect. It is commonly assumed today that the formation of DDW is the only result of annealing within the INC phase. The main result of the present investigations is: besides the formation of DDW the parameters of local states responsible for the memory effect are transformed during the annealing process. The impurity states are activated during the annealing procedure acting as electrically active impurities. Following investigations were carried out to come to this conclusion. First of all, the effects of illumination and external electric field on manifestation of memory effect were investigated because both of these external perturbations greatly influence the impurity system. Second, La doped $TlInS_2$ crystals were investigated under the same conditions. The correlation between the memory effects in undoped $TlInS_2$ single crystals and the peculiarities of the temperature dependence of the dielectric constant ε of the $TlInS_2$ compound doped with the lanthanum impurity have been investigated. It is shown that light illumination and dc - electric field substantially change the anomaly related to the memory effect in undoped $TlInS_2$. The dielectric constant of La - doped $TlInS_2$ single crystal has been measured after preliminary cooling of the crystal in dc - electric field and under the illumination. It is concluded that the experimentally observed peculiarities in ε (T) dependences under external fields in the range of the INC phase for the La - doped $TlInS_2$ look like memory effect in undoped but annealed $TlInS_2$ samples. The inference is made for the first time that the annealing within the INC phase leads to the activation of native defects in undoped $TlInS_2$ crystals making them electrically active as photo - and electro - active La impurity. The investigation of the memory effect in undoped $TlInS_2$ single crystals by optical second harmonic generation (SHG) method confirms the process of polarization of impurity centers during the annealing.

Acknowledgments:Work is executed with support of the joint grant of Azerbaijan National Academy of Sciences and Belarusian Republican Fondation for Fundamental Research.

P3-18

Dielectric properties of solid solutions with structure of tetragonal tungsten bronze (TTB) in morphotropic phase transition region

R. Z. Mehdiyeva, A. I. Mammadov, F. A. Kadimova*

Institute of Physics Azerbaijan National Academy of Sciences, AZ-1143,Baku, Azerbaijan
*Baku state university, AZ-1048, Baku, Azerbaijan

e-mail: rafiga_03@rambler.ru

The present work is continuation of researches of ferroelectric properties of solid solutions of system $K_2Pb_4Nb_{10}O_{30}$ – $Na_2Pb_4Nb_{10}O_{30}$ – $K_6W_4Nb_6O_{30}$ [1]. The purpose of the present work - studying of features of ferroelectric phase transition of compositions from various areas of the phase diagram of system $K_2Pb_4Nb_{10}O_{30}$ – $Na_2Pb_4Nb_{10}O_{30}$ – $K_6W_4Nb_6O_{30}$ with TTB structure and the reception of structures perspective for electromechanical converters.

Compositions of solid solutions of triple system $K_2Pb_4Nb_{10}O_{30}$ - $Na_2Pb_4Nb_{10}O_{30}$ – $K_6W_4Nb_6O_{30}$ (KPN - NPN - KWN) have been obtained by solid-phase synthesis from stereometrical mixes of oxides and carbonates of respective elements in two - three stages at temperatures of roasting 1100-1550K and an endurance from 2 up to 8 h. Samples of high density ceramics for dielectric measurements has been obtained using the hot pressing method. For all samples X-ray diffraction method determines symmetry and parameters of elementary cells [1]. For finding out of features ferroelectric phase transition of compositions from various areas of the phase diagram of system KPN-NPN-KWN temperature dependences of dielectric permeability ε(T) have been investigated. Compositions of solid solutions with the tetragonal and rhombic symmetry, located near to MFT area, and also the compositions included in this region and representing a mix of phases has been investigated most in details. Measurements of temperature dependences of a dielectric permeability ε(T) and a tangents of dielectric dissipation factor tgδ(T) were carried out on frequency 103Hz with a rate in 1K/min. and in a temperature range from 300K up to 900K. Frequency measurements ε (T) and tgδ (T) have been carried out on frequencies from $5 \cdot 10^4$Hz up to $1{,}1 \cdot 10^4$ Hz to within 1pF. Temperature dependence ε(T) for compositions with tetragonal symmetry represents the dim maximum covering region up to ~ 300 K. Curves at heating and cooling of a sample practically coincide. Values of dielectric permeability in a maximum reach 1940-2090, that only 1, 5-3 times as much as values of dielectric permeability at room temperature. It is possible, that FT degradation is connected to the structural disorder (structure fluctuations) in solid solutions, caused by occurrence and development of volumetric crystal-chemical defects of mezoscopic scale (clusters). Research of dielectric hysteresis loops has been carried out under the scheme of the Sawyer-Tower on frequency 50Hz, in the temperature range from room up to 605K and intensities of variable field up to 40κV/sm. As a result of the carried out dielectric measurements: - Curie temperatures and character of ferroelectric phase transition are determined; - At rhombic compositions with small contents of KWN the precise phase transitions with performance of the law of Curie-Veiss with a temperature hysteresis, characteristic for phase transitions of I sort, and broadening peak ε are observed at increase in maintenance KWN at the tetragonal compositions, typical for various phase transitions;

- For solid solutions of tetragonal phase are found out relaxation processes and on displacement of curves ε″(T) the energy of activation U=0,3eV testifying to ionic character of polarization has been calculated. - Solid solutions with a tetragonal cell compressed on an axis the double dielectric hysteresis loop has been found out; «bottleneck " is not connected to deficiency of structure and is not eliminated by temperature roasting and electric field effect.

[1]. R. Z. Mehdiyeva, A. I. Mammadov, M. Y. Seyidov, I. B. Baykulov, F. A. Kadimova. X-Ray study of phase transitions in the system of solid solutions $K_2Pb_4Nb_{10}O_{30}$-$Na_2Pb_4Nb_{10}O_{30}$-$K_6W_4Nb_{10}O_{30}$. J Phys. and Chem. Solids 67(2006), p.2623.

P3-19

Structure and magnetic properties of $(FeSe)_{0.96}(GeTe)_{0.04}$

[1]Asadov M.M., [2]Demidenko O.F., [2]Galyas A.I., [1]Mamedov F.M, [2]Yanushkevich K. I.[1] M.F.Nagiyev

Institute of Chemical Problems , 29, H.Javid ave., Baku - AZ1143, Azerbaijan
[2] SSPA «Scientific-Practical Materials Research Centre», NASB, P.Brovki str., Minsk, 220072 Belarus
e-mail: kazimir@ifttp.bas-net.by; mirasadov@gmail.com

To the most interesting results of iron selenides experimental studies of the last years should be carried the detection of superconductivity in α-phase of FeSe, which has the scarcity of anions [1,2]. The disturbance on the anions stoichiometry in α-$FeSe_{1-X}$ can reach values to $x \sim 0.12$. The deformed tetragonal structure in this case remains.

The results of studying the special features of $(FeSe)_{0.96}(GeTe)_{0.04}$ crystal structure and magnetic properties are given in the present report. The X-ray analysis showed that the $(FeSe)_{0.96}(GeTe)_{0.04}$ composition possesses the tetragonal structure of the *P4/nmm* space group. In the *X*-ray photographs, obtained at room temperature in *Cu* K_α - radiation in the $10^0 \le 2\theta \le 90^0$ angles range, besides the reflexes of the basic tetragonal phase of FeSe, the reflexes of the weak intensity of the hexagonal phase of the $P6_3/mmc$ space group are observed. The presence of hexagonal phase in the basic matrix of the $(FeSe)_{0.96}(GeTe)_{0.04}$ composition leads to the reflexes intensity redistribution of tetragonal phase on front 2θ angles of X-ray photographs. In [3] the "crystalline two-phase" reasons of FeSe are explained by the consequence of the cations displacement into the octa- and tetra- pores of the tight anions packing. In Fig.1 the specific magnetization temperature dependences of $(FeSe)_{0.96}(GeTe)_{0.04}$ are represented. The $\sigma = f(T)$ dependences of samples demonstrate the redistribution of the specific magnetization value in two temperature ranges of $77 \le T \le 450$ K and $450 \le T \le 850$ K. The manifestation of anomalies at 450 K and 850 K, most probably, connected with the fact that in the nonequilibrium state of the FeSe magnetic matrix be present two types of exchange interaction. First interaction between the cations in octapores through the selenium anion. Temperature of its destruction is ~ 450 K. In this case the distance between the nearest cations in octapores of the hexagonal close-packed nickel-arsenide structure is equal to half of translation along the *c* axis ($r_0 = c/2$). In the second place the exchange interaction between the *Fe* cations in tetrapores. The distance between the cations in tetrapores is determined by the relationship $r_{0\text{-}t} = 1/4[16/3 \times (a^2) + c^2]^{1/2}$, where *a* and *c* – the unit cell parameters. For such magnetic sublattice the exchange between the cations is direct (passing intermediate *Se* anions). Therefore the magnetic moments ferromagnetic ordering in the correspondence with Geisenberg interaction occurs. As a result we have the high temperature of the magnetic disordering $T_C \sim 850$ K. It should be noted that T_C value in $(FeSe)_{0.96}(GeTe)_{0.04}$ is less than in manganese monoselenide ($T_C = 920$ K) [3]. The magnetic hysteresis loops $\sigma = f(H)$ of the $(FeSe)_{0.96}(GeTe)_{0.04}$ composition are studied at 5 K, 70 K and 300 K. Fragments $\sigma = f(H)$ of dependence at 70 K are represented in Fig.2.

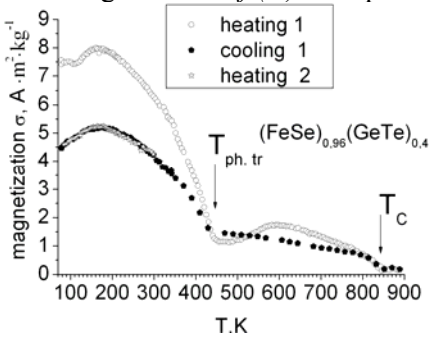

Figure 1

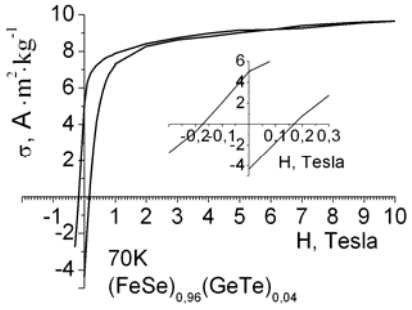

Figure 2

From the Fig.2. dependences it follows: at 70 K the substance does not achieve ideal magnetic saturation in the fields by the intensity of above 2.0 Tesla; residual specific magnetization has a value of $\sigma_0 \sim 4.5$ A·m^2·kg^{-1}; the coercive force is $F_C \approx 0.17$ Tesla.

[1]. Y. Mizuguchi, F.Tomioka, S.Tsuda, et al. Restore Desktop View Appl.Phys.Lett. 2008, V.93, Issue 15, p.4315
[2]. S.Margadonna, Y.Takabayoshi, M.T.McDonald, et al. Chem. Commun., 2008, Issue 43, p.5607
[3]. G. Makovetskii, A.Galias, O.Demidenko, K.Yanushkevich. Abstracts MMA-2002."BGU", Minsk. 2002, p.101

SECTION FOUR

Electron and phonon spectra : ab-initio calculations and experiment

I4-1

Ab initio design of new generation superalloys

Eyvaz Isaev

Department of Physics, Chemistry and Biology (IFM), Linkoping University, Sweden
Theoretical Physics Department, Moscow State Institute of Steel and Alloys, Moscow, Russia

As Ni-Al based superalloys reached their limit (1100C) for the operation temperature there is a challenge to design new generation superalloys with the operating temperature about 1500C. This will allow to increase the efficiency of jet engines with lower environment pollution. In fact, alloys' strength at high temperatures are related to their elastic properties. In our studies we considered Ru-Al-Ni, Pt-Sc and Ni-Al-X alloys. Based on contemporary theory of disordered substitutional alloys we have studied electronic structure, Fermi Surface and elastic properties of the alloys. We have shown that there is alloying limit of B2 RuAl with Ni, up to which mechanical properties of alloys are almost constant, but alloys' specific density is reduced. Pt-Sc alloys have shown to behave as well-known Ni-Al alloys with γ(FCC)/$\gamma'(L1_2)$ type strengthening mechanism. Ni-Al-Co alloys were found to be mechanically unstable upon alloying. Analysis of the electronic structure, Density of States and Fermi Surface for the alloys revealed that peculiarities observed in elastic constants as a function of alloying metal concentration is connected with the electron topological transitions.

Financial support from the Swedish Research Council (VR), the Swedish Foundation for Strategic Research SSF, the MS2E Strategic Research Center and the Göran Gustafsson Foundation for Research in Natural Sciences and Medicine, as well as the Russian Foundation for Basic Researches (10-02-01410-a, 10-02-00194-a) is acknowledged.

[1]. I.D. Bleskov, E.A. Smirnova, P.A. Korzhavyi, L. Vitos, Yu.Kh. Vekilov, M.I. Katsnelson, B. Johansson, I.A. Abrikosov, E.I. Isaev, Applied Physics Letters, 94, 161901 (2009).
[2]. V.I. Razumovskii, E.I. Isaev, A.V. Ruban, P.A. Korzhavyi, Intermetallics, 16, 982 (2008).

I4-2

The phonon percolation scheme for alloys: Pressure-dependence and extension to the whole lattice dynamics

G. K. Pradhan[1], C. Narayana[1], Mala N. Rao[2], M. d'Astuto[3], S.L. Chaplot[2], O. Pagès[4], A.V. Postnikov[4], A. Breidi[4], J. Souhabi[4], S. K. Deb[5], F. Firszt[6] and W. Paszkowicz[6]

[1] Light Scattering Laboratory – JNCASR, Bangalore 560064, India
[2] Solid State Physics Division, Bhabha Atomic Research Centre, Mumbai 400085, India
[3] Institut de Minéralogie et de Physique des Milieux Condensés – CNRS UMR 7590, 75015 Paris, France
[4] Laboratoire de Physique des Milieux Denses – IJB, Université de Metz, 75078 Metz, France
[5] Indus Synchrotron Utilization Division – RRCAT, Indore 452013, India
[6] Institute of Physics, N. Copernicus University, 87-100 Toruń, Poland
[7] Institute of Physics, Polish Academy of Sciences, 02-668 Warsaw, Poland
Presenting author. email: pages@univ-metz.fr, Tel.: 00 33 3 87 31 58 73, Fax: 00 33 3 87 31 58 01

The long-standing classification of the Raman and infrared (IR) spectra of $A_{1-x}B_xC$ zincblende (ZB) semiconductor (SC) alloys (in terms of 2-mode, mixed-mode, modified 2-mode, multi-mode) is based on a generic 1-bond→1-phonon scheme [1], supported by a description of an alloy at a macroscopic scale in terms of a uniform continuum according to the virtual crystal approximation (VCA). Recently, the classification has been unified within a novel 1-bond→2-phonon percolation scheme [2] – apparently a universal one thus – where a random alloy is viewed at the *mesoscopic* scale in terms of a composite of the AC- and BC-like sub-alloys.

In this work, we re-examine two basic alloy-related issues within the novel percolation scheme. In doing so we focus on the model ZnBeSe alloy with small Be content (20-30 at%) that exhibits a uniquely well-resolved Be-Se percolation doublet in its Raman/IR spectra, as due to the large contrast in the physical properties (bond length, bond stiffness) of the constituent species.

First, we explore what can be learned from the VCA→percolation shift of paradigm regarding the phonon behaviour of alloys when approaching a pressure-induced structural phase transition. ZnBeSe is well-suited for such purpose because it exhibits a strong contrast in the transitions of ZnSe (ZB→NaCl, ~13 GPa) and BeSe (ZB→NiAs, ~56 GPa). The key question then is what happens to the minor Be-Se bonds with ZB structure when they are forced to enter the ZnSe-like NaCl phase at ~10 GPa, an unnatural one for these bonds. This is studied by high-pressure Raman scattering (HP-RS), using a diamond anvil cell [3]. We find that at the approach of the transition, the Be-Se percolation doublet condenses into a pure singlet. This is explained by introducing a concept of pressure-induced phonon freezing for the highly self-connected Be-Se bonds from the minor BeSe-like sub-alloy, that 'stop vibrating'. The oscillator strength is transferred to the less self-connected Be-Se bonds from the surrounding ZnSe-like sub-alloy.

Second, we perform an exhaustive study of the whole lattice dynamics of the model ZnBeSe alloy by inelastic neutron scattering (INS) – a world first regarding ZB SC alloys. We find that the 1-bond→2-mode percolation scheme detected by Raman/IR spectra at the Brillouin zone centre further survives throughout the whole Brillouin zone, up to the zone-edge. This reveals that the whole lattice dynamics of an alloy – referring here to optical modes – falls into the scope of the percolation scheme, in principle. This deviates from the admitted picture so far of a basic 1-bond→1-mode scheme, as emerged from the pioneer *ab initio* calculations done by Baroni *et al.* with the ultimate (non-contrasted) AlGaAs alloy [4].

The whole discussion (of both the pressure-induced phonon-freezing and the phonon dispersion curves) is supported by lattice dynamics calculations within a supercell approach, using either an *ab initio* method (INS + HP-RS) or a shell model (INS).

[1]. I.F. Chang and S.S. Mitra, *Phys. Rev.* **172** (1968), p. 927.
[2]. O. Pagès, J. Souhabi, A.V. Postnikov and A. Chafi, *Phys. Rev. B* **80** (2009), p. 035204.
[3]. G. Pradhan, C. Narayana, O. Pagès, A. Breidi, J. Souhabi, A. Postnikov, S.K. Deb, F. Firszt, W. Paszkowicz, A. Shukla and F. El Haj Hassan, *Phys. Rev.* **81** (2010), p. 115207.
[4]. S. Baroni, S. De Gironcoli and P. Giannozzi, Phys. Rev. Lett. **65** (1990), p. 84.

I4-3
Interplay of spin-orbital interactions in a quasi-two-dimensional electron gas with finite thickness under in-plane magnetic field

E. Nakhmedov[1,2], O. Alekperov[2] , and R. Oppermann[1]

[1] Institut für Theoretische Physik, Universität Würzburg, Am Hubland, D-97074 Würzburg, Germany
[2] Institute of Physics, Azerbaijan National Academy of Sciences, H. Cavid str.33, AZ1143 Baku, Azerbaijan
enver.nakhmedov@physik.uni-wuerzburg.de, +49-931-3180288

Although the electron gas, formed on the semiconductor/insulator interface in quantum wells and MOSFET structures, has a finite thickness, it was taken as a strictly two-dimensional (2D) object in the most previous activities concerning the spin-orbital (SO) interactions. Finite thickness is essential in the time-dependent gate-voltage manipulation of electron spins [1] and in understanding orbital effects of an in-plane magnetic field. In this work, we report on our investigation of both orbital and spin effects of an in-plane magnetic field in a quasi-two-dimensional (quasi-2D) electron gas with a finite thickness on the spin precession and splitting in the presence of Rashba and Dresselhaus SO interactions. A quantum mechanical problem of one particle in a quasi-2D system, restricted by a parabolic confining potential in the transverse direction, is solved under in-plane magnetic field in the presence of Rashba and Dresselhaus SO interactions. The problem is solved numerical exactly. We give the detailed studies of the energy spectrum and the Fermi surface under variations of SO coupling constants, the magnetic field and Landé g-factor. The energy spectrum and the Fermi surface at the intersection points of different energy branches are splitted in the presence of both non-equal Rashba and Dresselhaus SO constants, whereas the degeneracies at the intersection point persist if the Rashba and Dresselhaus SO constants are equal each other. The dependence of the energy spectrum on the magnetic field shows strongly non-linear behavior. The magnetic field opens a gap at the intersection points, whereas the Zeeman splitting alone does not remove a degeneracy at the intersection point, shifting the energies of spin-up and spin-down electrons in the opposite directions. Competitions of the SO constants, the orbital and spin-splitting effects of the in-plane magnetic field and anticrossing effect create multi-extrema in the energy spectrum (Fig.1a), which change considerably the periodic plateau structure of the ballistic conductance. The equilibrium charge- and spin-currents are studied.

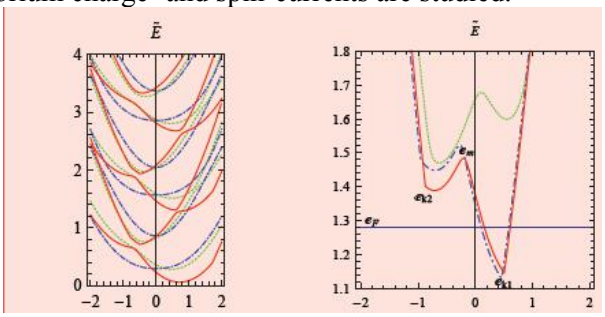

a) b)

Figure 1: a) E vs k_y for the first three quantized transverse levels at non-zero magnetic field. Dashed (green) and dot-dashed (blue) curves correspond to non-zero Rashba and Dresselhaus SO interactions respectively, whereas both SO interactions are non-zero for solid (red) curve. (b) Typical two-valley Gunn spectrum for different SO couplings and magnetic field.

The multi-valley band structure, typical for the Gunn effect in GaAs and InP semiconductors, is formed for particular values of the SO constants, magnetic field and g-factor (Fig.1b), which allows us to suggest a spin-Gunn effect in the quasi-2D electron gas with finite thickness. The energy separation between the valley minima can be controlled by the gate potential and the in-plane magnetic field. We calculate the spin polarization in the upper-lying Gunn subband under external electric field at different temperatures.

[1]. E. I. Rashba and Al. L. Efros, Phys. Rev. Lett. **91**, (2003), p. 126405.
[2]. E. P. Nakhmedov, R. Oppermann, and O. Alekperov, submitted to Phys. Rev. B (2010).

O4-1

Electronic band structure and surface reconstruction of $CuInSe_2$ and its copper-deficient defect phase

Andreas Hofmann, Carsten Lehmann and Christian Pettenkofer [1]

[1] Helmholtz-Zentrum Berlin, Institute for Charge Carrier Dynamics E-I4
Albert-Einstein-Str. 15, 12489 Berlin, Germany

andreas.hofmann@helmholtz-berlin.de

Chalcopyrites are excellently suited as absorber materials for thin film solar cells. Their ternary or multinary composition brings about low defect formation energies, which lead to intrinsic defects and complex electronic properties of photovoltaic devices. Near the interface with the buffer layer, a copper depletion of the $Cu(In,Ga)Se_2$ absorber seems to be crucial for the efficiency of the solar cell [1]. This copper-poor phase is described theoretically as an ordered defect compound of the chalcopyrite [2].

Up to now, although a great effort has been made to improve the performance of solar devices, experimental data on the electronic band structure and surface reconstructions of chalcopyrites and their defect phases are rare. Our approach therefore is to study epitaxial $CuInSe_2$ films as model systems with different orientation and stoichiometry.

We prepared $CuInSe_2$ samples with varying stoichiometry and orientation by molecular beam epitaxy on Si and GaAs substrates. All analysis is performed *in situ* under UHV conditions. The surface morphology for different orientations was investigated by STM (Fig. 1). LEED measurements of the $CuInSe_2$ (112) surface confirmed a c(4x2) reconstruction, which is also predicted by a first-principles calculation [3]. In contrast, a (1x1) reconstruction is found for the copper-deficient surface. ARPES data was recorded for the stoichiometric (001) and (112) surface (Fig. 2) as well as for (112) surface of the defect compound and showed in general a good agreement with the band structure from DFT [4].

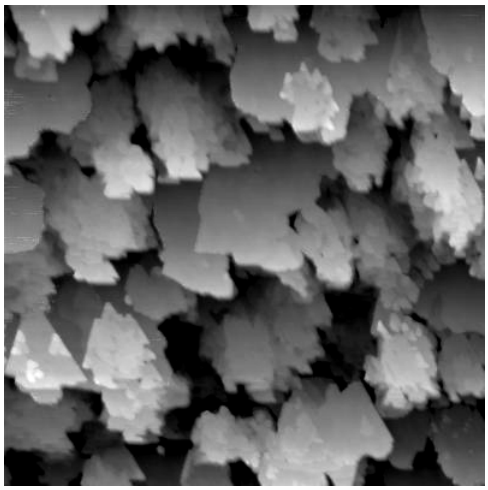

Figure 1 5 x 5 μm^2 STM image of the $CuInSe_2$(112) surface.

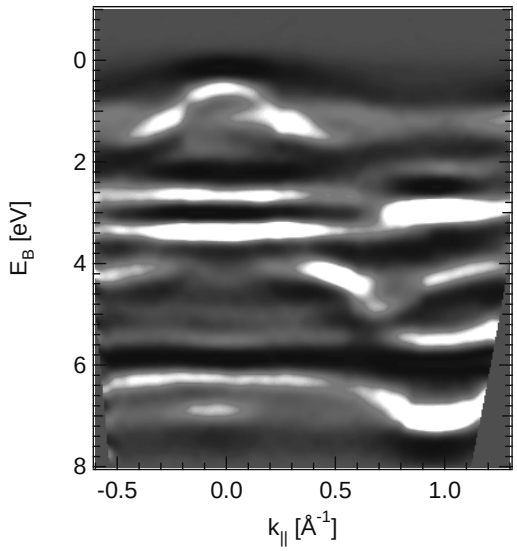

Figure 2 ARPES data for $CuInSe_2$(112) recorded at hν = 25 eV.

[1]. S. Siebentritt, U. Rau, "Wide Gap Chalcopyrites" (Springer, Berlin Heidelberg, 2006)
[2]. S.B. Zhang, S.-H. Wei and A. Zunger, Phys. Rev. Lett. **78**, 4059 (1997)
[3]. S.B. Zhang and S.-H. Wei, Phys. Rev. B **65**, 081402 (2002)
[4]. S.B. Zhang, S.-H. Wie, A. Zunger and H. Katayama-Yoshida, Phys. Rev. B **57**, 9642 (1998).

O4-2

Ab initio band structure and phonons in kesterite $Cu_2ZnSnSe_4$

N. B. Mortazavi Amiri and A. Postnikov

LPMD, Institute Jean Barriol and Paul Verlaine University - Metz, 1 Bd Arago, F-57078 Metz, France
e-mail: postnikov@univ-metz.fr, phone: +33-387315873, fax: +33-387315801

Electronic structure of a promising indium-free photovoltaic compound, $Cu_2ZnSnSe_4$ (CZTSe), in its kesterite-type crystal modification, is studied from first principles, using local density approximation (LDA) and, specifically, the SIESTA method. The calculation finds a small direct gap in Γ, obviously underestimated in the LDA, and a slightly negative indirect gap. The overall band structure resembles very much those reported earlier for similar compounds (sulphite, or stannite-type CZTSe) – see Ref. 1,2. Zone-center phonons have been obtained using small finite displacements of atoms to calculate the force constants. We analyze the vibration spectrum of CZTSe (Fig. 1, bottom panel) in comparison with that of structurally close chalcopyrite-type $CuInSe_2$ (top panel). For this latter compound, the calculation yields three main groups of lines: the mostly Cu+In ones at about 70 cm^{-1}, an isolated Cu+In at 170 cm^{-1}, and a bunch of modes at 200-250 cm^{-1}, showing an interplay of Cu, In and Se. One notes a satisfactory agreement in positioning these peaks with the earlier calculations, e.g., [3]. Coming to CZTSe (the bottom panel) shows that the three main group of lines rest in place, the role of In is taken over by Sn and Zn, without much shift in frequency, whereas the contribution of Se is hardly affected at all. There are, however, noticeable differences: the low frequency band (between 50 and 100 cm^{-1}) becomes broader and more structured; the Cu contribution is cut at the high-frequency side and "replaced" by a large Zn-related peak. Our theoretical prediction gets support from the only experimental measurement (Raman spectrum) of lattice vibrations we could find on the CZTSe system [4]. It shows a peak at about 80 cm^{-1} (in perfect agreement with calculated Cu-Zn-Sn modes of 75 and 81 cm^{-1}), intense peaks at 173 and 196 cm^{-1}, and the peak at 231 cm^{-1}, whose frequency strongly shifts on Zn/Cd substitution. Hence this latter peak must have a large Zn composition, that agrees with what has been found for our calculated upper vibration frequency (239 cm^{-1}). Other differences in vibration spectra of chalcopyrite and kesterite are due to symmetry lowering in the latter, which makes visible some Raman-silent modes of the former.

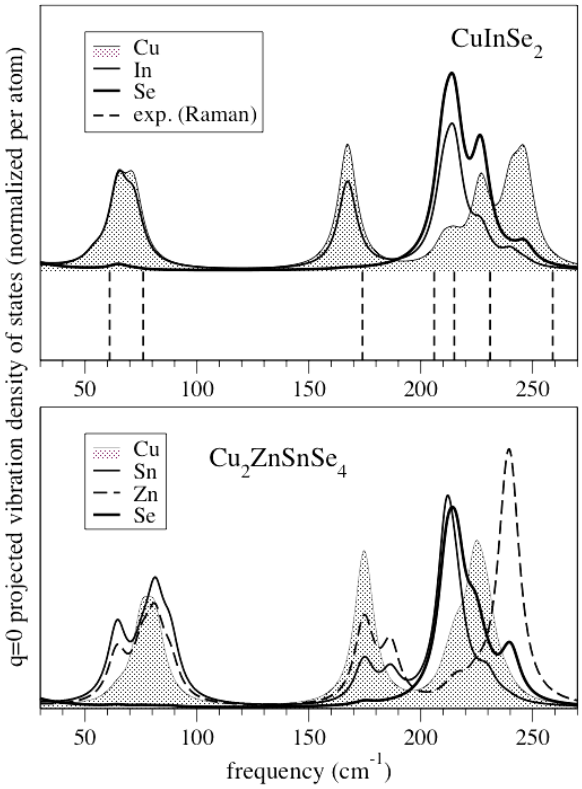

Figure 1. Zone-center vibration modes in $CuInSe_2$ (top panel, compared with experiment) and in CZTSe (bottom panel).

[1]. S. Nakamura, T. Maeda, T. Wada, *Phys.stat.solidi C* **6** (2009), p.1261.
[2]. J. Paier, R. Asahi, A. Nagoya and G. Kresse, *Phys.Rev.B* **79** (2009), p.115126.
[3]. J. Łażewski, K. Parlinski, B. Hennion and R. Foure, *J. Phys.: Cond. Matter* **11** (1999), p. 9665.
[4]. M. Altosaar, J. Raudoja, K. Timmo, M. Danilson, M. Grossberg, J. Krustok, E. Mellikov, *Phys. stat. solidi A* **205** (2008), p. 167.

O4-3

First principles spectroscopy of $CuInSe_2$, $CuGaSe_2$, and $CuInS_2$ chalcopyrite compounds

Tomoyuki Hamada[1,3] and Takahisa Ohnor[2,3]

[1] Advanced Research Laboratory, Hitachi Ltd., Hatoyama, Saitama, 350-0395, Japan
[2] Institute of Materials Research, 1-2-1 Sengen, Tsukuba, Ibaraki, 305-0047, Japan
[3] Institute of Industrial Science, University of Tokyo, 4-6-1, Meguro-ku, Tokyo 153-8505, Japan
tomoyuki.hamada.tk@hitachi.com, phone:+81-49-296-6111/ +81-49-295-6005

Chalcopyrite compounds as represented by $CuInSe_2$ are known to be a strong light absorber, and their optical properties have attracted much attention both from academic and industrial viewpoints. In this study, we theoretically calculated optical spectra of $CuInSe_2$ $CuGaSe_2$, and $CuInS_2$ by using our first principles spectroscopy system PHASE/UVSOR.[1] The system is the first principles software working as a virtual spectrometer on computer, based on the density functional pseudopotential (DFT-PP) method. Electronic structures of $CuInSe_2$, $CuGaSe_2$, and $CuInS_2$, were calculated in the GGA approximation, by using ultra-soft PPs of the Vanderbilt type, and optical absorption spectra of these compounds were calculated from the electronic structures by considering the direct transition between valence to conduction bands at each k-point in the Brillouin zone. The band gap underestimation by DFT calculations, which is due to the self-interaction of Kohn-Sham electrons, is corrected by using the scissors operator approach that introduces the rigid shift of conduction bands in energy to reproduce experimental band gaps. Figures 1 (a) and (b), respectively, show GGA calculated optical absorption spectra of $CuInSe_2$ and $CuGaSe_2$, along with experimental spectra[2,3] for these compounds. The first principles calculation well reproduced experimental spectra of these compounds; the spectra of both the compounds have a plateau region in absorption strength in a lower energy region (2.6 to 3.6 eV for $CuInSe_2$ and 3.5 to 4.5eV for $CuGaSe_2$), and the spectra of $CuGaSe_2$ has a blue-shifted structure of those of $CuInSe_2$. Electronic structure analyses revealed the plateau region in the spectra is due to Se *4p*-Cu*3d* valence bands near the band gap, which are less dispersive because of localized Cu *3d* bands. Calculations showed that $CuInS_2$ have similar optical absorption spectra having a plateau region in 3 to 4 eV. The chalcopyrite compounds investigated here have similar optical spectra though the position of plateau region depends on the compounds. The optical spectra of CuInSe2 has the plateau region in visible wavelengths so that the material is confirmed to be an effective photovoltaic material compared with the other compounds, absorbing solar light more strongly.

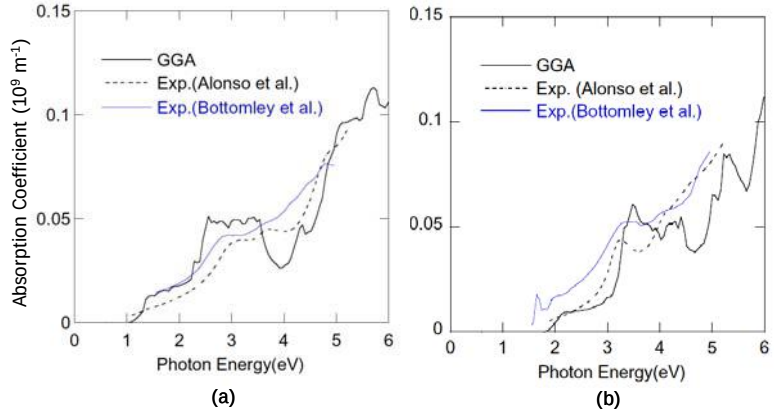

Figure 1. Optical absorption spectra of chalcopyrite compounds: (a) $CuInSe_2$; (b) $CuGaSe_2$. Experimental spectra by Bottomley *et al*.(ref.2) and Alonso *et al*. (ref.3) are shown for comparison

Acknowledgments: This work is partially supported by the RISS project of Japanese Government.

[1]. "PHASE 8.01 and UVSOR 3.21" (University of Tokyo, 2010), http://www.ciss.iis.u-tokyo.ac.jp/english/dl/index.php.
[2]. M. I. Alonso *et al*., *Phys. Rev .B* **63** (2001), p. 075203.
[3]. D. J. Bottomley *et al*, *J. Appl. Phys*. **82** (1997), p. 817 (1997).

O4-4

Ab initio lattice dynamics of $TlGaSe_2$ and $TlGaS_2$

D.A. Huseinova[1], K.R. Allakhverdiev[1,3*], F.M. Hashimzade[1], M.A. Nizametdinova[2], G.S. Orudzhev[1,4]

[1] Institute of Physics, Azerbaijan National Academy of Sciences, Baku, Azerbaijan
[2] Azerbaijan University of Architecture and Construction, Baku, Azerbaijan
[3] TUBITAK, Marmara Research Center, Materials Institute, Gebze/Kocaeli, Turkey
[4]Azerbaijan Technical University, H. Javid ave. 25, Baku Az-1073, Azerbaijan
* e-mail: kerim.allahverdi@mam.gov.tr

We present first-principles calculation of lattice dynamics of the $TlGaSe_2$ and $TlGaS_2$ ternary semiconductor compounds. Ternary $TlGaSe_2$ and $TlGaS_2$ compounds crystallizes in a monoclinic system with base-centered lattice and space group symmetry C_{2h}^6 at room temperature [1]. The primitive cell contains 8 formula units. The crystal structure consists of layers composed of tetrahedral complexes Ga_4S_{10} linked together by the common atoms of selenium. Univalent thallium ions are in trigonal-prismatic voids between these complexes. Two layers within the unit cell are rotated relative to each other at 90^0.Each layer consists of two atoms of Tl1, Tl2, Ga1, Ga2, S3, S4, S5 and one atom of S1 and S2. A rotation about the second-fold axis accompanied by a shift along *c*-direction transforms each layer into itself.

Calculation of the phonon spectrum of $TlGaS_2$ has been performed in the framework of the density perturbation functional theory using the local-density approximation. We used the software package ABINIT [2] and the norm preserving pseudopotentials [3]. The basis of plane waves was truncated at electron kinetic energy of 40 Hartrees. Integration over the Brillouin zone was carried out using a 2×2×2 grid according to the scheme proposed by Monkhorst and Pack [4]. The equilibrium structure was determined by minimizing the total energy with respect to the lattice constants and the internal structural parameters. Dynamic matrix describing the phonon spectrum throughout the Brillouin zone was obtained by Fourier interpolation using the ANADDB program of the ABINIT software package. The calculated phonon spectrum is shown in figure 1and 2.

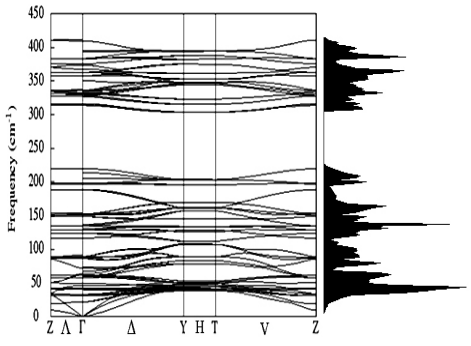

Figure1. Phonon spectrum of $TlGaS_2$

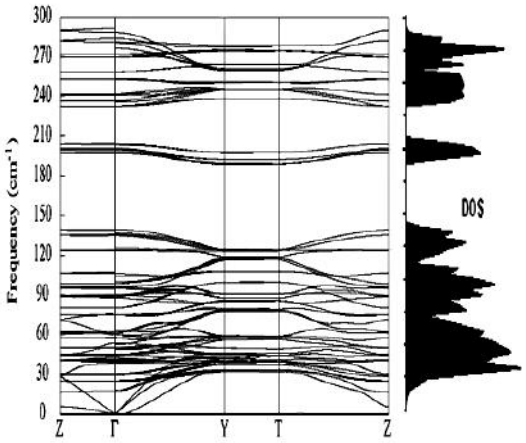

Figure2. Phonon spectrum of $TlGaSe_2$

As one can see from figures, the dispersion of optical phonon branches along Λ line perpendicular to the layers is weak. In the direction parallel to the layers, all optical modes are split into pairs with nearly identical dispersion, which is, naturally, a consequence of stratification of the crystal structure and of the fact that the crystal unit cell contains two layers. In the direction of V, on the border of the Brillouin zone, these pairs are degenerate due to the symmetry with respect to time reversal. Figures show also the calculated phonon density of states. The phonon frequencies in the centre of Brillouin zone are in a good agreement with available experimental data.

[1]. Henkel W, Hochheimer H D, Carlone C, Werner A, Ves S and von Shnering H G *Phys. Rev.* B **26** 1982 3211
[2]. Gonze X, Beuken J-M, Caracas R, Detraux F, Fuchs M, Rignanese G-M, Sindic L, Verstraete M,
[3]. Zerah G, Jollet F, Torrent M, Roy A, Mikami M, Ghozes Ph, Raty J-Y and Allan D C
[4]. *Comput. Mater. Sci.* **25** 2002 478
[5]. Troullier N and Martins J L *Phys. Rev.* B **43** 1991 1993
[6]. Monkhorst H J and Pack J D *Phys. Rev.* B **13** 1976 5188

O4-5
II-IV-V_2 and Zn-III-IV-As_3 compounds for photovoltaic applications

A. V. Krivosheeva[1], V. L. Shaposhnikov[1], V. E. Borisenko[1], F. Arnaud D'Avitaya[2] and J.-L. Lazzari[2]

[1]Belarusian State University of Informatics and Radioelectronics, P. Browka 6, 220013 Minsk, Belarus
[2]Centre Interdisciplinaire de Nanoscience de Marseille, CINAM, UPR CNRS 3118, Aix-Marseille Université, Case 913, Campus de Luminy, 13288 Marseille cedex 9, France
anna@nano.bsuir.edu.by, +375 17 202 10 33

Main aspects of interest for a semiconductor to be used in optoelectronics are emission of light and photoelectric or photovoltaic effect [1]. New materials for photovoltaic applications are proposed on the base of II-IV-V_2 ternary and Zn-III-IV-As_3 quaternary compounds, where II=Mg, Zn, Cd; IV=Si, Ge, Sn; V=P, As; III=Al, Ga. Their structural, electronic and optical properties are determined using VASP and WIEN2k *ab initio* simulation packages [2, 3] within the generalized gradient approximation (GGA) [4]. Stability of these compounds is evaluated on the base of calculations of enthalpies, which are found to be negative for all of them. It was revealed that ternary compounds have a body-centred tetragonal chalcopyrite structure while Zn-III-IV-As_3 quaternary alloys are considered to be monoclinic. Lattice parameters of Zn(Si,Ge)P_2 and Zn(Si,Ge)As_2 compounds are found to be close to silicon or to GaAs ones, respectively. Band structure calculations show all studied compounds to be semiconductors. The most of them have direct-band gap located at the Γ-point with the values ranging from about 0.1 to 1.5 eV (Fig. 1, Fig. 2). It is found that band gaps for P-based II-IV-V_2 are higher in comparison with corresponding As-based ones. For Al-containing Zn-III-IV-As_3 quaternary alloys, band gaps are higher when compared with Ga-containing ones. Similarly, quaternary compounds with Si as IV group element have higher gaps than those with Sn. Calculated absorption coefficients for some II-IV-V_2 and Zn-III-IV-As_3 compounds are comparable with those for widely used GaAs, GaP and $CuInSe_2$. In order to increase the quantum efficiency of solar cell one need to use multilayered heterostructure consisting of semiconducting materials with different band gaps. Thus, the combination of different II-IV-V_2 ternary or Zn-III-IV-As_3 alloys looks promising for fabrication of multicolor heterostructural solar cell device with specified properties due to their lattice constants matched to GaAs or Si, appropriate band gaps and absorption coefficients. Moreover, compounds considered here do not contain rare or toxic elements like indium or selenium.

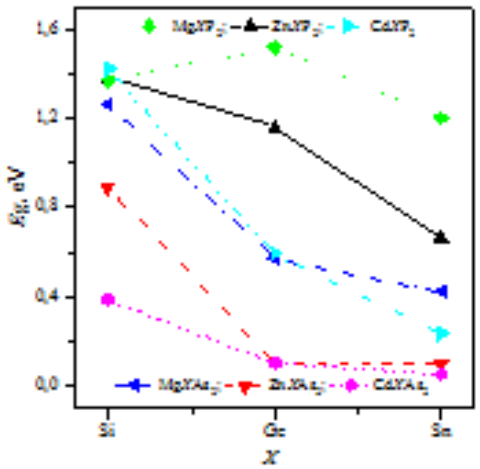

Figure 1. Band gaps of II-IV-V_2 compounds

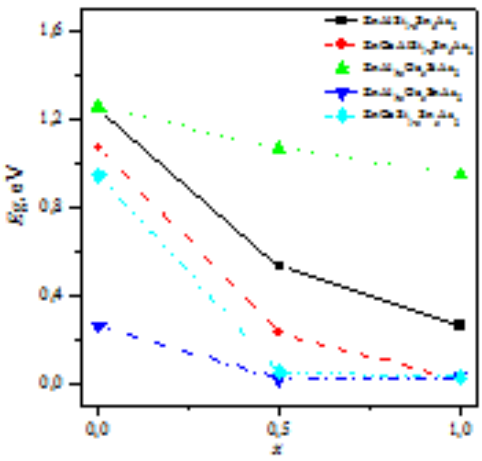

Figure 2. Band gaps of Zn-III-IV-As_3 compounds

[1]. E. Rosencher, B. Vinter, *Optoelectronics* (Cambridge University Press, 2002) 725 p.
[2]. G. Kresse, J. Furthmüller, *Phys. Rev. B* **54** (1996) p. 11169.
[3]. P. Blaha, K. Schwarz, G. K. H. Madsen, D. Kvasnicka, J. Luitz, "*WIEN2k, An Augmented Plane Wave + Local Orbitals Program for Calculating Crystal Properties"* (Karlheinz Schwarz, Techn. Universitat Wien, Austria, 2001).
[4]. J. Perdew, Y. Wang, *Phys. Rev. B* **45** (1992) p. 13244.

O4-6

Structural, optical and electrical properties of semiconductor compounds studied by means of inelastic light scattering from phonon, electron and coupled electron-phonon excitations: From bulk to nanoscale structures

B.H. Bairamov, V.V. Toporov

Ioffe Physico-Technical Institute RAS, 194021, 26 Polytekhnicheskaya ul., St. Petersburg, Russia

Presenting author's e-mail address, phone: Bairamov@mail.ioffe.ru (812) 292 7140

We present results of our systematic investigation by means of quasi-elastic and inelastic laser light scattering (QEILS) from the acoustical (AP) and optical (OP) phonons and electronic excitations of the structural, optical and electronic properties of the bulk ternary ABC_2 compounds, including I-III-VI_2 (*n,p*-$CuAlS_2$, and *n*-$HgGa_2S_4$) and II-IV-V_2 (*n*-$ZnGeP_2$, *n,p*-$CdGeAs_2$) type compounds as compared to their relative binary analogs – II-VI (*n*-CdTe, *n*-ZnSe, *n*-ZnO), III-V (*n,p*-GaP, *n,p*-GaAs, *n,p*-InP, *n*-InGaP, InGaAsP for the concentration range from 10^8 to 10^{18} cm^{-3}. Electronic excitations include electon-*(e)* and hole-*(h)* gas of free carriers, coupled LO(Γ)-plasmon excitations, and [$1s(\Gamma_2) \rightarrow 2p_{\pm}$]-, and [$1s_{3/2}(\Gamma_8) \rightarrow 2s_{3/2}(\Gamma_8)$]-type electronic transitions, [LO(Γ), $1s_{3/2}(\Gamma_8) \rightarrow 2p_{3/2}(\Gamma_8)$]-type dielectric local modes, etc. Results for InAs quantum dots (QDs) embedded into GaAs matrix as well as colloidal TiO_2 and shelled CdSe/ZnSe QDs will be also considered. The QD structures are attractive for fabrication of the low-cost solar cells allowing increasing the interfacial area and enhancement of the conversion efficiency. First direct experimental observation of the resonant Brillouin scattering by the APs in ZnSe and InGaP has allowed to develop the multi-zone theory (MZT) by taking into account the deformation-potential interaction for the electron-phonon coupling by the intra- and inter-band transitions with discrete and continuous exciton states involving the conduction band and different valence bands of heavy and light holes and split-off bands. From the scattering tensor the expressions for the photoelastic coefficients $p_{ij}(\omega)$ and those of deformation-potential constants *a, b* and *d* have been derived, allowing direct experimental determination of a full set of these parameters. The MZT demonstrated the decisive role of the multi-zone excitons (MZE) have recently become widely and used by numerous researchers to recalculate the absolute value of the RRS efficiency for comparison with the corresponding experimental data performed early with the *e-h* uncorrelated theory for a number bulk compounds as well as are 2D, 1D and 0D low dimensional structures. For the QDs with multi-band confined excitonic bands on the example of the InAs/GaAs QD nanostructures the fist experimental detection of the polarization sensitive resonant QEILS due to different type of *e, h* and *e-h* fluctuations have been observed. The spectra are obtained under the condition of the near IR self-selective resonance excitation due to the tunneling of photogenerated charge carriers out of the InAs quantum dots into GaAs layers, when many excitons confined to single QDs are created. The excitation energy 1.17 eV is centred within the energy distribution δE of the confined ground state excitons when δE is of the order of $\Gamma \leq \Delta$. Here Γ is the FWHM of the photoluminescence line consisted from many elemental lines of the single confined exciton levels and Δ is the spin-orbit splitting for the valence bands. We show that many body effects contribute significantly to the energy states of *e–h* pairs confined in QDs giving rise to pronounced optical response. Observed giant enhancement ($>10^5$) can be explained by the sum of the partial resonant contributions of the each individual transition of the many confined exciton bands, and at the same time highlighting again the decisive role of the MZE. In consequence the spectra of ZnO/CdS/$CuInGaSe_2$ cells have allowed to differentiate the complex structure of the layers. Characterizations of strain, compositional fluctuation, defects, chemical type and concentrations of impurities, sensitivity to radiation damage, mobility and concentration of free carriers, net acceptors (donor) and etc, are performed. The results provide key insights for the design and optomization of the high efficiency solar cells and other devices.

[1]. B.H. Bairamov, et al., Physics-Uspekhi, **36**, 1993, p. 392-437, Phys. Reports, **229**, 1993 p. 221-293.

[2]. B.H. Bairamov, et al., Phys. Stat. Sol. (c) **1,** 2004, p. 2773-2778; ibid **3**, 2006, p. 2635-2638; Thin Solid Films, **515,** 2007, p. 5763-5766; Proc. Int. Conf. Combinational Scattering, Moscow, 2009, p. 386-401.

P4-1

Ab initio phonons in metals, compounds, and alloys

Eyvaz Isaev

Department of Physics, Chemistry and Biology (IFM), Linkoping University, Sweden
Theoretical Physics Department, Moscow State Institute od Steel and Alloys, Moscow, Russia

Phonons play an important role in solid state physics. Ab initio calculation of phonons in condensed matter made it possible to study a wide variety of physical properties, that are dynamical stability of phases, thermodynamical stability of crystalline phases, construction of P-T phase diagram, electron-phonon interaction and, thus, superconductivity. In the talk the background for ab initio phonon calculations is given and their applications for the abovementioned problems are illustrated.

Financial support from the Swedish Research Council (VR), the Swedish Foundation for Strategic Research SSF, the MS2E Strategic Research Center and the Göran Gustafsson Foundation for Research in Natural Sciences and Medicine, as well as the Russian Foundation for Basic Researches (10-02-01410-a, 10-02-00194-a) is acknowledged.

[1]. S. Baroni, S. de Gironcoli, A. Dal Corso, P. Giannozzi, Rev Mod Phys 73, 515 (2001)
[2]. Stefano Baroni, Paolo Giannozzi, and Eyvaz Isaev, Reviews in Mineralogy and Geochemistry 71, 39 (2010)

P4-2

Ab initio phonons in shape memory magnetic alloys

L.Isaeva[1], D.Bazhanov[2], E.Isaev[3,4], S.Kulkova[5], I.Abrikosov[3], O.Eriksson[1]

[1] Uppsala University, Department of Physics and Astronomy, Materials Theory Group, SE-751 20 Uppsala, Sweden
[2] M.V.Lomonosov Moscow State University, Department of Physics, Leninskie Gory 1, bld. 2, Moscow 119991, Russia
[3] Depatrment of Physics, Chemistry and Biology (IFM), Linkoping University, SE-581 83 Linkoping, Sweden
[4] Theoretical Physics Department, Moscow State Institute of Steel and Alloys (Technological University), Leninskii prospect 4, Moscow 119049, Russia
[5] Institute of Strength Physics and Materials Science, Siberian Branch of the Russian Academy of Sciences, Akademicheskii prospect 2/1, Tomsk 634055, Russia

leyla_isaeva@yahoo.com

Heusler alloys is a unique class of materials which possesses shape memory effect [1-4], magnetostrain effect [5], large magneto-optical Kerr effect [6] and others, making them good candidates for practical applications. It was shown [5] that magnetostrain effect in Ni_2MnGa in magnetic field about 1 T can achieve a huge value, up to 9.5%, making it useful for sensor applications. Magnetic shape memory effect was observed in metallic compounds such as Ni-Mn-Ga [1], Co-Ni-Al [2], Co-Ni-Ga [3], Ni-Fe-Ga [4], etc. Multilayers based on Heusler alloys can also yield giant magnetoresistance effect [7].

It is well known that martensitic phase transition which is the underlying process of the shape memory effect is strognly connected with softenings in the phonon spectrum. Thus, in this work we performed ab-initio calculations of dynamic and electronic properties of full Heusler alloys Ni_2MnMe (Me=Al, Ga, In, Sb, Sn) by means of density functional theory [8] and the linear response method [9]. Peculiarities of the calculated phonon spectra, in particular, softenings connected to the nesting of Fermi surface sheets have been studied. We found soft modes for all alloys along the Γ-X [110] direction, except Ni_2MnAl, which does not show imaginary frequencies, thus, no martensitic transformation takes place in accordance with recent experimental measurements [10].

[1]. K.Ullakko, J.K.Huang, C.Kanter, V.V.Kokorin, and R.C. O'Handley, *Appl. Phys. Lett.* **69** (1996), p.1966.
[2]. K.Oikawa, L.Wulff, T.Iijima, F.Gejima, T.Ohmori, A.Fujita, K.Fukamichi, R.Kainuma, and K.Ishida, *Appl. Phys. Lett.* **79** (2001), p.3290.
[3]. M.Wutting, J.Li, and C.Craciunescu, *Scr. Mater.* **44** (2001), p.2393
[4]. K.Oikawa, T.Ota, T.Ohmori, Y.Tanaka, H.Morito, A.Fujita, R.Kainuma, K.Fukamichi, and K.Ishida, *Appl. Phys. Lett.* **81**(2002), p.5201.
[5]. A.Sozinov, A.A.Likhachev, N.Lanska, and K.Ullakko, *Appl. Phys. Lett.* **80** (2002), p.1746.
[6]. P.G.Van Engen, K.H.J.Buschow, R.Jongebreur and M.Erman, *Appl. Phys. Lett.* **42** (1983), p.202.
[7]. A.Bergmann, J.Grabis, A.Nefedov, K.Westerholt and H.Zabel, *J.Phys.D:Appl.Phys.* **39** (2006) p.842
[8]. W.Kohn, L.J.Sham, *Phys.Rev.* **40** (1964), p.A1133
[9]. S.Baroni, S. de Gironcoli, A. Dal Corso and P.Giannozzi, *Rev. Mod. Phys.* **73** (2001), p.515
[10]. X.Moya, L.Mañosa, A.Planes, T.Krenke, M.Acet, V.O.Garlea, T.A.Lograsso, D.L.Schlagel and
[11]. J.L.Zarestky, *Phys. Rev. B* **73** (2006), p.064303

P4-3
Diamagnetic shift of the A free exciton in $CuGaSe_2$ in magnetic fields

F .Luckert[1] and M.V. Yakushev[1] and R.W. Martin[1] and C. Faugeras[2] and A.V. Mudryi[3] and A.V. Karotki[3]

[1]Department of Physics, SUPA, Strathclyde University, G4 0NG Glasgow, UK
[2]Grenoble HMFL, 25 Avenue des Martyrs, BP 166, 38042 Grenoble Cedex 9, France
[3]Scientific-Practical Material Research Centre of the National Academy of Science of Belarus, P.Brovki 19, 220072 Minsk, Belarus
franziska.luckert@strath.ac.uk, 0044(0)1415483458

$CuGaSe_2$ is a promising chalcopyrite compound for the absorber layer of thin-film solar cells. In order to optimise the efficiency of $CuInSe_2$-based cells, $CuInSe_2$ is alloyed with $CuGaSe_2$, forming $Cu(In,Ga)Se_2$ (CIGS), to match the band-gap of the CIGS absorber layer to the solar spectrum. Current achieved efficiencies for CIGS-based solar cells saturate towards 20% [1] which is significantly lower than the theoretical limit for one-junction solar cells of 30%. To improve the device performance, it is essential to understand the fundamental physical properties of this material. The application of high magnetic fields can provide important information on the electronic properties of semiconductors. High magnetic fields have two effects on the excitonic energy levels. The first effect is the Zeeman spin-splitting and the second effect is a non-linear diamagnetic shift. The diamagnetic shift of an exciton can be used to estimate its binding energy, Bohr radius and reduced mass as well as the effective masses of the charge carriers. Single crystals of $CuGaSe_2$ were grown by the vertical Bridgman technique. Magneto-optical photoluminescence (MPL) measurements were carried out at the Grenoble High Magnetic Field Laboratory using a 20 T resistive magnet at 4.2 K. Fibre optics were used to transport the 514 nm line of an Ar^+ laser to the sample and the MPL to the entrance slit of a 0.5 m Princeton Instruments spectrometer and detected by a 1340 Silicon CCD.

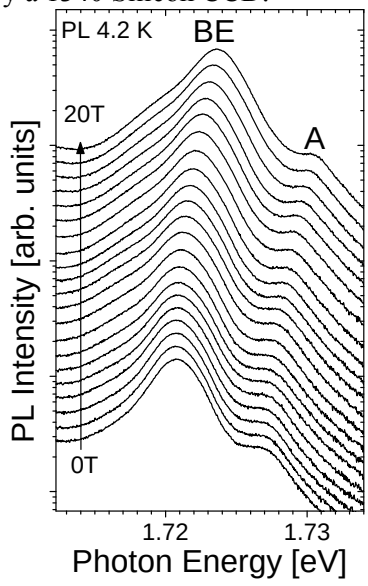

Fig. 1 Near band-gap PL spectra of $CuGaSe_2$ under magnetic fields from 0 to 20 T taken at 4.2K**.**

At zero magnetic field, the near band-gap PL of $CuGaSe_2$ taken at 4.2 K (Fig. 1) reveals two peaks A at 1.727 eV and BE at 1.721 eV which correspond to the A free exciton and to an exciton bound to a neutral acceptor [2], respectively. An increase in the magnetic field strength from 0 to 20 T results in a gradually increasing blue shift of both the bound exciton and the A free exciton, as shown in Fig. 1. Within the weak field approximation the magnetic field can be treated as a perturbation and the diamagnetic energy shift ΔE_d is given by [3]:

$$\Delta E_d = (e^2 a_B^2 / 4\mu) B^2 = (4\pi^2 \hbar^4 \varepsilon^2 \varepsilon_0^2 / e^2 \mu^3) \qquad (1)$$

From the evolution of the A free exciton PL peak position a diamagnetic shift rate c_d = 9.82 x 10^{-6} eV/T^2 has been determined. From equation 1 and with ε = 11 [2], a reduced mass μ = 0.115 m_0 of the A free exciton has been calculated which is less than the literature value μ = 0.125 [4, 5]. Assuming an effective electron mass of $m_e = 0.14\ m_0$ [4] results in an effective hole mass of $m_h = 0.64\ m_0$. An exciton binding energy of 12.9 meV and an exciton Bohr radius a_B = 5.07 nm have been calculated using the hydrogenic model.

Acknowledgement: This work has been supported by the EPSRC (EP/E026451/1), the Royal Society (RD5529) and Belarus Council for Fundamental Research (F09MC-003).

[1]. Contreras, M.A., et al.,. Progress in Photovoltaics, 2005. **13**(3): p. 209-216.
[2]. Bauknecht, A., et al., Jpn. J. Appl. Phys., 2000. **39**(Suppl. 39-1): p. 322.
[3]. Taguchi, S., et al.,. J. Phys. Soc. Jpn., 1988. **57**: p. 3256.
[4]. Wasim, S.M. and G. Sanchez-Porras,. Phys. Stat. Sol. (a), 1983. **79**: p. K65.
[5]. Quintero, M., C. Rincon, and P. Grima,. Journal of Applied Physics, 1989. **65**(7): p. 2739-2743.

P1-4

Influence of exchange interaction on properties of optical polaron in ternary semimagnetic compounds

S.M. Seyid-Rzayeva

National Academy of Sciences of Azerbaijan, Institute of Physics, AZ – 1143, AZERBAIJAN-BAKU
S-Nisa@rambler.ru

In most of semimagnetic compounds (SMC) on the basis of A^2B^6 semiconductors, that have wide technical significance, is realized polaron of large radius and they are more clearly show theirs properties in a magnetic field. The study of polaron effects give unique possibilities to determine the band parameters and to investigate of the electronic spectrum of these materials in a magnetic field.

The band structure of SMC compared with ordinary semiconductors are more sensitive to external magnetic field due to the presence of the exchange interaction between conduction electrons and localized electrons of magnetic ions. In particular, the exchange interaction influence on the parameters of band structure and the energy spectrum of charge carriers in the SMC becomes anisotropic, which leads to the appearance of new physical effects in these materials.

The principal objective of this work is theoretical study of the effect of the exchange interaction, due to the presence of magnetic impurities, on the basic characteristics of the polaron (such as the polaron mass of the electron, ground state energy of polaron) in the narrow gap SMC on the basis A^2B^6 semiconductors.

SMC on the basis A^2B^6 semiconductors possess in mostly one-walley cubic crystal structure. Therefore it was solved in general form problem for the anisotropic optical polaron in one-walley cubic structure. The energy spectrum of band electrons is in form an ellipsoid of rotation in this structure.

The anisotropy of the phonon spectrum was not considered taking into account that phonons with any wave vector $\vec{q}$ is divided into longitudinal and transverse. Introducing a positive $\gamma = m_\perp / m_z$ anisotropy parameter, given problem also was solved for negative values m_z, here $m_\perp$, m_z - transverse and longitudinal effective mass of band electrons in the xy plane and the direction of z axis, respectively.

In accordance above-stated assumptions problem for the anisotropic optical polaron was solved using standard perturbation theory. For that in the framework of the perturbation theory contribution to the energy of a conduction electron is calculated in the second order due to the weak interaction with phonons at low temperatures. At that conduction electrons was considered in the one-electron approximation. Also it is assumed that the weakly bound conduction electrons are moving quite slowly.

Then, on the basis of this solution the expressions for the polaron binding energy, transverse and longitudinal polaron masses of the electron are given for the SMSC which possess an anisotropic energy spectrum in the magnetic field. The expression for anisotropic electron energy spectrum of the SMSC is taken into account the influence of weak magnetic field through the exchange interaction between spins of conduction electrons and paramagnetic ions.

From an analysis of calculating results it is established that the polaron binding energy decreases in comparison with standard case due to the exchange interaction in weak magnetic field.

Based on numerical calculations of the transverse and longitudinal polaron masses of the electron carried out for the $Hg_{1-x}Mn_xSe$ SMC with $x = 0.066$(which has the structure of zinc blend-sphalerite up to $x = 0.37$) it is found that the transverse and longitudinal polaron mass, renormalized due to electron-phonon interaction, increases compared with corresponding band values. However, polaron mass of electrons decreases owing to exchange interaction with increasing magnetic field. Also it has been established that ground-state energy of polaron decreases as to standard case owing to exchange interaction with increasing magnetic field.

P4-5

Band structure and optical properties of ternary compounds - $A^5B^6C^7$: *Ab initio* calculation

Husnu Koc[1,*], Harun Akkus[2] and Amirullah M. Mamedov[1]

[1]Physics Department, Cukurova University, Adana, Turkey
[2]Physics Department, Yuzuncu Yil University, 65080 Van, Turkey

E-mail: hkoc@student.cu.edu.tr, harunakkus@yyu.edu.tr and mamedov@cu.edu.tr

The electronic band structures, density of states (DOS) and optical properties of prototypical family of quasi-molecular layered solid of the type $A^5B^6C^7$ where A= Sb, Bi and As; B=S and Se; C=I, Cl and Br are investigated using the density functional theory under the local density approximation (LDA). The obtained electronic band structure show that all investigated materials have indirect forbidden band gaps. The structural optimization for $A^5B^6C^7$ have been performed using the LDA. The result of the structure optimization of $A^5B^6C^7$ have been compared with the experimental and theoretical values and have been found to be in good agreement with these results. The linear photon-energy dependent dielectric functions and some optical properties such as the imaginary part of dielectric function versus real part of dielectric function, the effective number of valance electrons and the effective optical dielectric constant are calculated and are found excellent agreement with the available experimental data.
Also refractive-index dispersion data near the interband absorption edge in $A^5B^6C^7$ compounds are analized using effective-oscillator fit of the form $n^2 - 1 = E_d E_0 / (E_0^2 - \hbar\omega)$ where E_0-single oscillator energy, and E_d is the dispersion energy.

The theoretical results are related to the fundamental $\varepsilon_2(\hbar\omega)$ spectrum via appropriately defined moment integrals. It is found, using relationships between moment integrals, that for a particularly simple choice of a model ε_2 spectrum, viz., constant optical-frequency conductivity with high- and low- frequency cutoffs, the band gap parameter E_a in the high– frequency sum rule introduced by Hopfield provides the connection between oscillator parameters and Phillips static– dielectric-constant parameters.

P4-6
Studies of Electrons Trapping Centers Surrounded by a Repulsive Barrier in $CdIn_2S_4$

Z.Kadiroğlu, T.G.Kerimova, I.G.Nasibov

National Academy of Science, Institute of Physics, Az-143, H.Cavid av.33, Baku, Azerbaijan

E-mail:zafark@mail.ru

Cadmium indium sulfide ($CdIn_2S_4$) is a semiconducting ternary chalcogenide of $A^{II}B_2^{III}C_4^{VI}$ type. It has an indirect band gap energy E_g^i =2.28 eV at 300K. The $CdIn_2S_4$ is an attractive material with a potential capability for applications in photoconductors, solar sell, and light emitting diodes.

$CdIn_2S_4$ has two kinds of atoms in cationic sublattice. It is possible formation of antistructural defects, due to substitution of cations (Cd_{In} and In_{Cd}), cadmium vacancies (V_{Cd}), sulfur vacancies (V_s), cadmium interstitials (Cd_{int}), sulfur interstitials (S_{int}), and complexes of these point defects. As a result, in the forbidden band of $CdIn_2S_4$ presence a lot of local levels [1]. However, the energy spectra of the local levels and nature of local centers in $CdIn_2S_4$ are investigated insufficiently.

Investigation of carrier recombination in $CdIn_2S_4$ shows that in these crystals there have been photosensitivity centers of two types (m and r). Centers of r-type are arranged near v-zone in energy range E_{vr}^o =0.73 eV from it and their exchange with v-zone occurs at about 140 K. Centers of m-type are arranged near the middle of energy band (E_{vm}^o =0.96 eV) and their exchange with v-zone occurs at higher temperatures (usually above 250K). Besides in crystals $CdIn_2S_4$ there have been centers with big electron capture cross-section called s-centers of quick recombination, also t-centers of trapping.

It has been earlier shown that in $CdIn_2S_4$ there have been existed centers surrounded by repulsive Coulomb-barrier for majority carriers as analogous observed in CdS by Bube et al. [2-4]. Long-term relaxation of non equilibrium negative (σ-$_n$) residual conductivity, effects of thermally stimulated conductivity (TSC) spectrum change under the effect of light due to illumination temperature and an abrupt transition from the state of increased comparatively dark conduction into the state of conduction below dark one in $CdIn_2S_4$ is explained by existence of repulsive potential barriers for electrons [5].

By presence a repulsive centers for main carriers in crystal, carrier capture on these centers has been determined by electron energy and their ability to overcome repulsive barriers. Capture rate of repulsive barrier depends on temperature as follows: $B_o = \beta_0 \exp(-\varphi / kT)$, where φ - is the height of the barrier center, β_0 - the rate of electron capture, overcome the barrier, B_o -the effective rate of trapping [6]. Therefore the study of temperature influence on the photoelectron processes in $CdIn_2S_4$ seems interesting. The aim of the work was to study the influences of centers surrounded by repulsive potential barrier for electrons on the photoelectron processes in $CdIn_2S_4$ single crystals. There have been studied TSC, temperature dependence of optical quenching of photocurrent, temperature quenching of photoconductivity and photoluminescence. Experiments were carried out in the temperature region of 100÷300 K, by stationary method in the spectral range of 400÷2000 nm, under various conditions of the optical excitation. Some assumptions about the nature of deep centers in $CdIn_2S_4$ are made.

[1]. Z. Kadiroğlu, T.G. Kerimova. Defects in Semiconductors ISDS-25, Book of abstracts, St Peterburg, Russia,2009, p.310
[2]. G.L.Belenkiy, L,S,Larionkina, N.V.Markevich,R.X.Nani. Izvestiya AN Az.SSR ser.fiz.-mat.nauk, №4, 1975, p.62
[3]. T.Takuzava, K.Kanbara. J.Phys. Soc.of Japan, v.55, 1986, p.3503
[4]. R.H. Bube, G.A. Dussel, C.T. Ho, L.D.Miller. J.Appl. Phys., v. 37, 1966, p.21
[5]. C.T Guseynov, T.G. Kerimova, Z. Kadiroğlu. Fiz-tex.polup., v.30, 1996 , p.974
[6]. B.K.Ridley, T.B. Wotkins. Proc. Phys. Soc., v.78, 1961, p.710

P4-7
Multi-scale simulation of nano-structured materials and systems

V. Nelayev[1], V. Barkaline[2], T. Brechko[3], A. Chashynski[2], V. Lyskovski[1], N. Mamedov[4]

[1] Belarusian State University of Informatics and Radioelectronics, 6 P. Brovki str., 220013, Minsk, Belarus, *nvv@bsuir.by*, phone +375 17 293 84 09, fax +375 17 292 96 28.
[2] Belarusian National Technical University, 65 Nezavisimosti ave., 220013, Minsk, Belarus
[3] University of Bialystok, 64 Sosnowa str.,15-887, Bialystok, Poland
[4] Institute of Physics, National Academy of Sciences of Azerbaijan, 33 G. Javid ave, AZ1141, Baku, Azerbaijan

Multiscale and hierarchically organized calculations are valuable and effective for modern theoretical studies of complex atomic and molecular systems such as nanostructured materials and systems [1]. Next *ab initio* simulations was performed in the frame of that approach.
Biomolecular structure "membrane protein rhodopsin+retinal chain" were considered from the position as potential element of quantum computer [2]. The absence of spin polarization, as the possible quantum effect in chromophore-rhodopsin structure, was detected. Nevertheless, there is the possibility of it use as a photon detector due to the high light sensitivity of chromophor system.
The structural arrangements and magnetic properties of carbon nanotube including systems "iron encapsulated in carbon nanotubes" and "graphene with vacancy cluster" are investigated. Geometry and magnetic structure of freestanding and encapsulated Fe and cementite Fe_3C clusters were calculated in the single and multiwall wall carbon nanotubes [3]. When the ratio of the cluster to nanotube diameter is small the system is stable and the spin polarization at the Fermi energy is large. Therefore such system has potential application in spintronics.
Systematic investigation of magnetic properties of graphene with vacancy cluster was carried out [4]. Influence of vacancy number and configuration of the vacancy cluster were investigated in order to reveal the regularities of spin polarization in the system "graphene+vacancy cluster". Spin polarization in the system was confirmed. Monotonic increasing of the magnetic moment of the investigated systems was stated with the exclusion of some configurations.
Electronic and magnetic properties of $TlMeX_2$ compounds (Me=Ga, In. Tl; X=S, Se, Te) in conditions of the of strain deformation were studied [5]. Magnetic domain structure and physical properties of Ni_2MnGa alloy were simulated.
Analysis of DOS, band structure and charge densities in Heusler alloys reveals presence of high polarization [6]. Character of differences in density of states in Fermi level area for electrons with spin up and electrons with spin down allows conclude that contribution of first type of carriers predominates above the contribution of second type carriers. Then, cluster approach was used for calculation of electronic properties of the simplest structure cell of the $NiMn_4Ga_4$.
Multi-scale simulation is demonstrated on the example of ordered carbon nanotube array based chemical sensors with acoustic pickup [7] including quantum mechanical simulation of physical and chemical adsorption of hydrogen on such arrays resulting in change of the array geometry and mechanical properties leading to the change of array density and acoustic wave velocities as macroscopic parameters of arrays.

[1]. Barkaline V., Medvedev S., Nelayev V., Slutchak P., Jurkevich S. Hierarchical system of physical processes and material properties simulation with use supercomputer SKIF K-1000 // Proc. of all-Russia Scientific Conf. on Scientific Services in Internet: Large Scale Problems Solutions, 2008, Novorossiysk, Russia, P.101-105 (in Russian).
[2]. Nelayev V., Dovzhik K., Lyskouski V. Quantum effects in biomolecular structures // Review of Advanced Material Sciences, Vol. 14, 2007. - P. 13-34.
[3]. Nelayev V., Dovzhik K. *Ab-initio* simulation of magnetically functionalized carbon nanotubes // Proc. of SPIE. 2009, Vol. 7377-04, 8 pp.
[4]. Nelayev V., Mironchik A. Magnetism of graphene with vacancy cluster // Proc. of the 12th Int. Conf. on New Approaches to High-Tech: Nano-Design, Technology Computer Simulations, 2009, Vilnius, Lietuva, P. 32-42.
[5]. Nelayev V., Lyskouski V., Mamedov N.Ternary $TlMeX_2$ compounds for MEMS application // Proc. of the 6th Int. Conf. on Perspective Technologies and Methods in MEMS Design, 2010, Lviv, Ukraine, P.250-253.
[6]. Nelayev V., Breczko T., Dovzhik K. Experimental investigations and computer simulations of selected physical properties of the Ni_2MnGa alloys / Proc. of SPIE. 2009, Vol. 7377-19, 10 pp.
[7]. V.Barkaline, Y. Douhaya, A. Chashynski, A. Pletezhov, T. Szepieniec. Hierarchical Approach to Nanodesign// Proc. of the 6th Int. Conf. on Perspective Technologies and Methods in MEMS Design, 2010, Lviv, Ukraine, 2010, P.3-12.

P4-8
Bulk and surface electron states in quasi-one-dimensional $Tl^{1+}Tl^{3+}Se_2$

Zakir Jahangirli[1] , Kojiro Mimura[2], Kazuki Wakita[3], Sadig Hamidov[1], Satoru Motonami[2], Kei Imai[3], YongGu Shim[2], Huseyn Orudzhev[4], Nazim Mamedov[1], and Firudin Hashimzade[1]

[1]Institute of Physics, H. Javid ave. 33, Baku Az-1143, Azerbaijan
[2]Osaka Prefecture University, Sakai, Osaka 599-8531, Japan
[3]Chiba Institute of Technology, Narashino, Chiba 275-0016, Japan
[4]Azerbaijan Technical University, H. Javid ave. 25, Baku Az-1073, Azerbaijan

cahanzakir@yahoo.com, +99 412-439-32-61

Very recent angle-resolved photoemission spectroscopy (ARPES) studies have disclosed peculiar dispersion of some electron states in quasi-one-dimensional TlSe ($Tl^{1+}Tl^{3+}Se_2$) and its ternary counterparts[1]. The observed dispersion looks similar to that observed in quasi-two-dimensional Bi_2Se_3 in which, owing to the strong spin-orbital interaction, surface states form a single Dirac cone[2]. However, the results obtained for TlSe, $TlInSe_2$, and $TlGaTe_2$ appear to be excitation energy dependent while those for Bi_2Se_3 do not depend upon excitation energy.
In this work we report the results of our surface electronic structure calculations for TlSe. The (110) surface was modelled by a structure consisting of 8 slabs separated from each other by a distance of 5 Å. The calculations were performed using WIEN2k program package. Exchange-correlation potentials were introduced within well-known generalized gradient approximation (GGA).
Figure 1 shows the band structure of bulk TlSe (Fig.1a), energy spectrum with account of spin-orbital interaction in TlSe with a surface that includes both Tl^{1+} and Se atoms (Fig.2a), and projected band structure of the bulk TlSe (Fig.1c). The obtained data clearly demonstrate that there exist flat surface states positioned at 7eV inside the energy pocket in the conduction band. These flat surface states are extending along Γ-N direction of the Brillouin zone and may cause the linear-like dispersion observed in TlSe by ARPES.

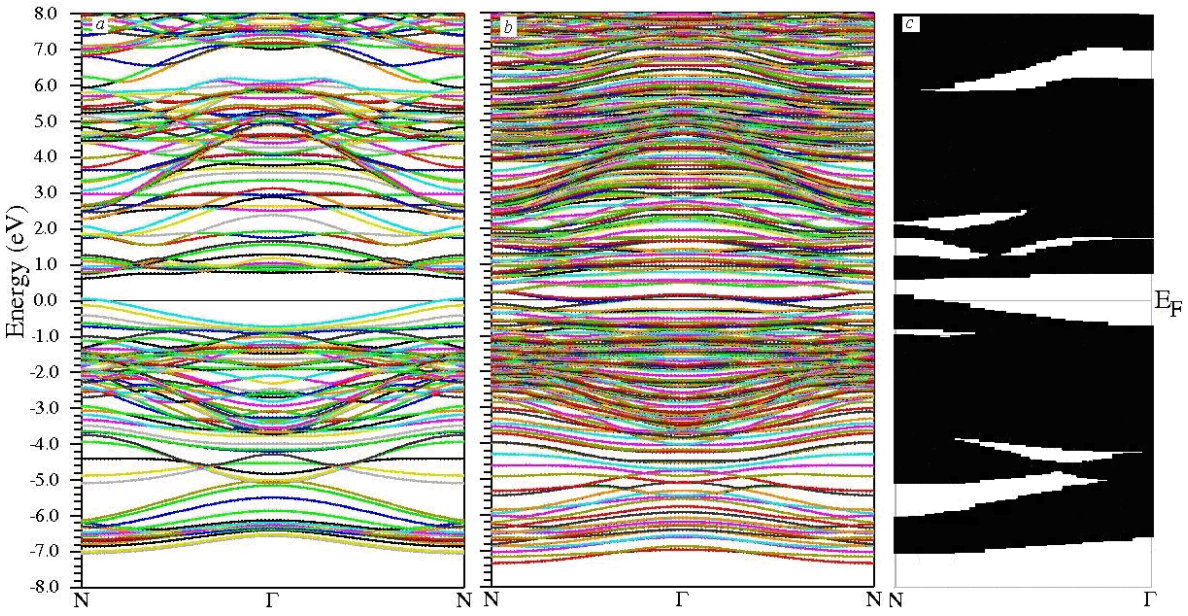

Figure 1

[1]. K. Mimura et al, will be submitted
[2]. Y. Xia et al., Nature Physics **5** (2009), p. 398.

P4-9

Optical properties and deformation potentials of $A^2B^3{}_2C^6{}_4$ group compounds

T.G. Kerimova, R.A. Guliev, I.A. Mamedova
Institute of Physics of Academy of Sciences of Azerbaijan
Baki, 370143, H.Javid pr.33
Phone(99412)695-163,Fax:(99412) 395-961,E-mail:ktaira@physics.ab.az

Compounds of $A^2B^3{}_2C^6{}_4$ (sp.gr.$S_4{}^2$) group owing to their optical activity, birefringence, dazzling luminescence, high photosensibility with the large band gap and stability to external influence are perspective materials for semiconductor devices.

Earlier investigations of the optical spectra of $A^2B_2{}^3C_4{}^6$ compounds in polarized light showed that nonlinear dependence of the absorption edge exists in these compounds in the temperature region of 5÷300 K. In low temperature region in $CdGa_2Se_4$, $CdGa_2S_4$ and $ZnGa_2Se_4$ the sign of the temperature coefficient of the absorption edge is positive. Isotropic point ($k_\parallel=k_\perp$) is observed in $CdGa_2Se_4$ at 70 K. The polarized dependence of the photoluminescence intensity is equivalent to the dependence of the absorption coefficient at high and low temperatures. The jump in the E_g~f(x) dependence in x~0,5 of $CdGa_2S_{4x}Se_{4(1-x)}$ is observed. The influence of the pressure on the absorption edge in CdGa2S4 has been investigated.

It is known that behavior of electron spectra under the influence of the external factors (temperature, pressure) are described by the deformation potentials of bands extrema. Lately, deformation potentials of bands extrema of semiconductors are determined by Manoodian-Leclerc [1] method, using the temperature dependence of absorption edge shift.

According to [2] the temperature coefficient of absorption edge shift in semiconductors is described by following equation:

$$E(0) - E(T) = UT^x + V\varphi[\coth\varphi/2T - 1] \quad (1)$$

U, V, φ and x – independent parameters of temperature. Parameter U describes lattice deformation, V– electron-phonon interaction, φ – parameter of temperature demention. Electron-phonon interaction and lattice deformation contributions to the temperature coefficient are represented as:

$$(dE/dT)_1 = - (V\varphi^2)/(2T^2)\ \mathrm{cosech}^2(\varphi/2T) \quad (2)$$

$$(dE/dT)_2 = -xUT^{x-1} \quad (3)$$

By means of equation (1) fitting in experimental dependence of band gap by the least squares method, the contributions of electron-phonon interaction and lattice deformation have been determined by the equations (2) and (3), which connected with bands extrema deformation potentials by following equations:

$$(dE/dT)_1 = 8/9\pi(3/4\ \pi)^{1/3}(k_B\cdot\Omega)/(\hbar Mv^2)(m_ec_e{}^2 + m_hc_h{}^2) \quad (4)$$

$$(dE/dT)_2 = 2\alpha_L(c_e + c_h) \quad (5)$$

By using these equations the deformation potentials of conduction band bottom (c_e) and top of valence band (c_h) have been determined for $CdGa_2Se_4$, $CdGa_2S_4$, $ZnGa_2Se_4$: -11,2eV, -12,3ev, -25 eV for c_e and 4,79eV, - 10,9eV, 23,7eV for c_h , respectively.

As the result an analyse of both the experimental results and values of deformation potentials of bands extrema have been established :

- The sign and the value of deformation potentials of the valence band top of *$CdGa_2Se_4$* in Γ(000) are distinguished.
- The jump in the E_g~f(x) dependence in *$CdGa_2S_{4x}Se_{4(1-x)}$* solid solutions is due to the different rates of motion of conduction bands.
- The nonlinear dependence of the absorption edge in $A^2B^3{}_2C^6{}_4$ group compounds is due to that the thermal expansion gives the main contribution to the temperature coefficient at the low temperature, but at the high temperature - the electron-phonon interaction.
- The scheme of bands extrema motion in Γ(000) under the single-axis pressure ($P\perp c$ and $P\parallel c$) was constructed.

[1]. A.Manoogian and A.Leclerc, Phys.Stat.Sol., 92, k23,(1979)

P4-10

Entropy of superlattices in a quantizing magnetic field

B.M.Askerov[1], S.R.Figarova[1], M.M.Mahmudov[1], V.R.Figarov[2]

[1] Baku State University, Z.Khalilov 23, AZ1148, Baku, Azerbaijan
[2] Institute of Physics, ANAS, H.Javid 33, AZ1143, Baku, Azerbaijan
E-mail: figarov@bsu.az

Investigations into statistical properties of the electron gas, in particular entropy S, current carrier distribution in energy bands, the chemical potential ζ dependence on current carrier concentration and temperature are important when considering transport phenomena. In a quantizing magnetic field the current carrier spectrum substantially changes, and consequently all the thermodynamic properties change. Knowledge of the thermodynamic potential dependence on the electron concentration, magnetic field strength and temperature is necessary to determine field and temperature dependences of separate kinetic coefficients in a quantizing magnetic field. Besides, it should be noted that having determined such a statistical characteristic of an electron gas as entropy, one can calculate the thermoelectrical power of a degenerate electron gas in superlattices in a quantizing magnetic field.

In the present paper, proceeding from the general expression of the grand thermodynamic potential, in a quantizing magnetic field we calculate entropy of a degenerate and a nondegenerate low dimensional electron gas. Entropy in the case of a nondegenerate low dimensional electron gas is larger than entropy of a three dimensional electron gas by an additive term. For conduction electrons with the cosinusoidal dispersion law, that holds true for natural layered conductors and superlattices entropy has the appearance:

$$S_{2D} = S_{3D} + \frac{1}{2} kn \ln\left(\frac{m_{\|}}{m_{\perp}}\right), \qquad (1)$$

where $m_{\perp}$ and $m_{\|}$ are transverse and longitudinal effective masses of conduction electrons, respectively, $S_{3D} = kn\left(\frac{3}{2} + \frac{\mu B}{kT} cth \frac{\mu B}{kT} - \frac{\zeta}{kT}\right)$, μ is the Bohr effective magneton, B is the magnetic field induction, T is temperature, k is the Boltzmann constant, n is the concentration of conduction electrons.

In the case of a strongly degenerate electron gas entropy both of the three dimensional electron gas and superlattices is expressed through the density of states at the Fermi boundary $g(\zeta_F)$ [1]:

$$S = \frac{\pi^2}{3} k_0^2 T g(\zeta_F), \qquad (2)$$

where ζ_F is the Fermi level. For the cosinusoidal energy spectrum in a quantizing magnetic field the density of states is appreciably distinct of that for the three dimensional case and the entropy ratio can be written as:

$$\frac{S_{2D}}{S_{3D}} = 2\frac{m_{\|}}{m_{\perp}}, \qquad (3)$$

As it is seen from (1) and (3), inasmuch as $m_{\|} > m_{\perp}$, the decrease of dimensionality of the electron gas leads to an increase in entropy. Moreover, in superlattices of the $GaAs / Al_xGa_{1-x}As$ type we revealed entropy quantum oscillations, the form of which significantly depends on the degree of band filling (the mini-band width), the degree of electron gas degeneracy and temperature. The dependence of entropy on the field and temperature, and also the degree of band filling was studied.

[1]. B.M.Askerov, S.R.Figarova. Thermodynamics, Gibbs Method and Statistical Physics of Electron Gases, Springer-Verlag Berlin Heidelberg, 2010, 374 p.

P4-11

Carrier transport and electron charge distribution in $TlInSe_2$

K. Imai[1], K. Abe[2], K. Wakita*, [1], Y. Shim[2], S. Hamidov[3], N. Mamedov[3]

[1] Chiba Institute of Technology, 2-17-1, Tsudanuma, Narashino, Chiba 275-0016, Japan
[2] Osaka Prefecture University, 1-1 Gakuen-cho, Nakaku, Sakai, Osaka 599-8531, Japan
[3] Institute of Physics, Baku AZ-1143, Azerbaijan

E-mail: kazuki.wakita@it-chiba.ac.jp; Phone & Fax: +81-47-478-0374

Quasi-one-dimensional $TlInSe_2$ has recently been reported to have a giant Seebeck coefficient, 10^6 μV/K, below 150 °C [1]. The discovered super thermopower has been attributed to inhomogeneous charge distribution in incommensurate phase that emerges in $TlInSe_2$ with temperature and has correlation length at the nanoscale. However, even if normal phase, carrier transport of $TlInSe_2$ is not well understood.

In this work we have studied room temperature current-voltage (*I-V*) characteristics on single-crystals of $TlInSe_2$ grown by Brigdman-Stockbarger method and have discussed its carrier transport using calculated electronic charge distributions.

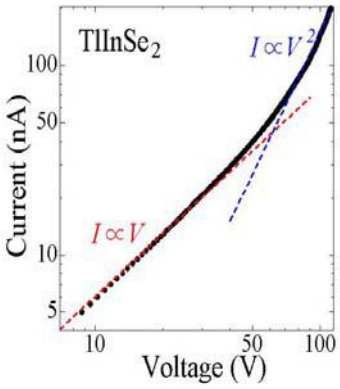

Fig. 1 *I-V* properties of $TlInSe_2$.

Figure 1 display *I-V* characteristics on $TlInSe_2$. *I* is proportional to *V* below 40 V and V^2 above 70 V. Space-charge-limited current (SCLC) model with a sallow trap-level is found to well describe above data [2].

For consideration of carriers transport, the electronic charge distributions of $TlInSe_2$ in the range of the lowest conduction band at T point and the upper level of 0.1 eV from the energy were calculated by using the first principle method [3], as shown in Fig. 2. A strong distribution connection in the one-dimensional chain bond of In-Se atoms was found, while a week distribution connection in the chain bond of Tl atom was observed. Therefore, the connection of the charge distribution in the In-Se chain is considered to be significantly contributed for the electron transport of $TlInSe_2$.

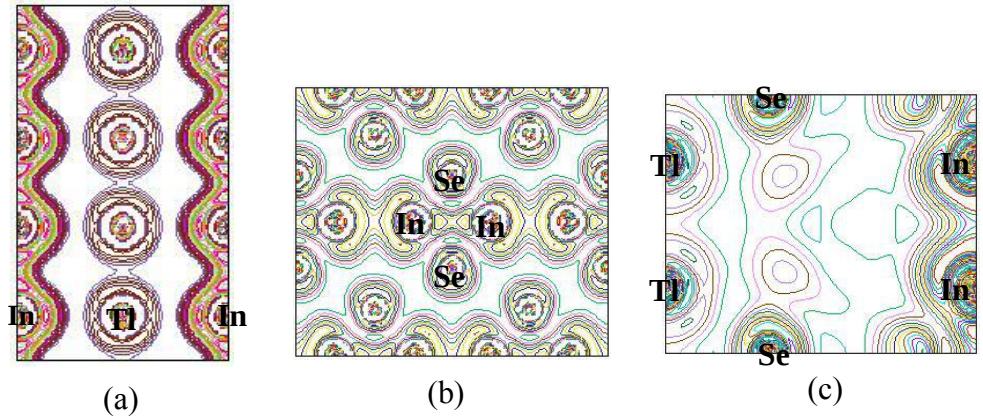

(a) (b) (c)

Fig. 2 Electron charge distribution due to the lowest conduction band on (a) the (0,2,0) plane containing Tl and In atoms, (b) the (0,2,0) plane containing In and Se atoms, and (c) the (2,2,0) plane containing Tl, In, and Se atoms of $TlInSe_2$.

[1]. N. Mamedov, *et al*., Thin Solid films, **499** (2006), p.275.
[2]. K. C. Kao and W. Hwang, *Electrial Trabsport in Solids*, (Pergamon Press, Oxford, 1981) Chap.3, p145.
[3]. P. Blaha, *et al*., Computer code WIEN2k (Vienna University of Technology, Austria, 2001).

P4-12

Experimental realization of the Dirac cone in 3D topological insulator of ternary chalcogenide $TlBiSe_2$

Kenta Kuroda,[1]Mao Ye,[1] Akio Kimura,[1]Yoshifumi Ueda,[2]
Koji Miyamoto,[3]Taichi Okuda,[3] Kenya Shimada,[3] Hirofumi Namatame[3]and Masaki Taniguchi[1, 3]

[1]Graduate School of Science, Hiroshima University,
1-3-1 Kagamiyama, Higashi-Hiroshima 739-8526, Japan
[2]Kure National College of Technology, Agaminami 2-2-11, Kure 737-8506, Japan
[3]Hiroshima Synchrotron Radiation Center, Hiroshima University,
2-313 Kagamiyama, Higashi-Hiroshima 739-0046, Japan

Kuroken224@hiroshima-u.ac.jp, +81-82-424-7140/ +81-82-424-0719

Following the recent theoretical prediction and experimental discovery of the quantum spin Hall effect in the two dimensional system[1, 2], the concept of three-dimensional topological insulators has attracted a lot of attention because they exhibitthe spin-helical Dirac surface state inside the bulk band gap. This exoticquantum phasenewly appeared in condensed matter physics has been predicted to exist in a number ofbinary compounds, such as $Bi_{1-x}Sb_x$, Bi_2Te_3, Bi_2Se_3 and Sb_2Te_3 [3]. The experimental realization of the three-dimensional topological insulators has opened a way for application tothenext generation spintronicsdevices, the quantum topological computing and so on [4].

Recently, thallium-based ternary compounds have been proposed as the new family of 3D topological insulators [5, 6]. In contrast to the layered binary chalcogenides with their inert surface due to the weak bonding between quintuple layers, in the ternary compounds, the broken bonds may give rise to trivial surface states. In fact, the theoretical studies [6, 7] have indeed revealed the presence of such surface state on the surface in addition to the topological ones. So, the experimental realization of topological surface state has been called for.

In this work, we have performed the angle resolved photoemission spectroscopy with synchrotron radiation to prove the existence of Dirac surface state on the $TlBiSe_2$(111) surface and to determine the energy and k-space location of the bulk continuum state with respect to the Dirac point. Finally, we have revealed three important aspects: (i) the surface state Dirac cone is confirmed to be present at the $\bar{\Gamma}$ point in $TlBiSe_2$. (ii) The Dirac cone is partially ideal, especially near the Dirac point, and its velocity is larger than for Bi_2Se_3. (iii) There are no bulk continuum states that energetically overlap with the Dirac point. This means that the scattering channel from the topological surface state to the bulk continuum is suppressed. Our experimental results favour the realization of the topological spin-polarized transport with high mobility and long spin lifetime in $TlBiSe_2$.

Acknowledgments: The experimentwas performed with the approval of the Proposal Assessing Committee ofHSRC (Proposal No.10-A-30).This work was financially supported by the JSPS Grant-in-Aid for Scientific Research (B) 20340092.

[1]. B. A. Bernevig, T. L. Hughes, and S. C. Zhang, Science **314**(2006), 1757.
[2]. M. König, S. Wiedmann, C. Brüne, A. Roth, H. Buhmann, L. W. Molenkamp, X. L. Qi, and S. C. Zhang, Science **318** (2007), 766.
[3]. Zhang, C. X. Liu, X. L. Qi, X. Dai, Z. Fang, and S. C. Zhang, Nature Phys. **5** (2009), 438.
[4]. M. Z. Hasan and C. L. Kane, arXiv:12002.3895v1.
[5]. B. Yan, C.X. Liu, H.J. Zhang, C.Y. Yam, X.L. Qi, T. Frauenheim, and S.C. Zhang, Europhys. Lett.**90**(2010), 37002.
[6]. H. Lin, R.S. Markiewicz, L.A. Wray, L. Fu, M.Z. Hasan, and A. Bansil, Phys. Rev. Lett. **105** (2010), 036404.
[7]. S. V. Eremeev,Yu. M. Koroteev, and E. V. Chulkov, Pis'maZh. Eksp. Teor.Fiz.**91**(2010), 664 [JETP Lett. **91**(2010), 594].

P4-13

Dispersion relation of optical parameters of Bi_2Te_3-Bi_2Se_3 thin films

N.M.Abdullayev[1], N.Z.Djalilov[2], N.R.Memmedov[2], I.T.Mamedova[1]

1-Research and Development Center for Hight Technologies MCIT, 2, Ac.Abbaszadeh k., Baku, AZ-1073, Azerbaijan
2-H.Abdullayev Institute of Physics of Academy of Azerbaijan, 33 H.Cavid pr, Baku, AZ-1043, Azerbaijan

e-mail: nadir_abdulla@physics.ab.az, tel.: (+ 994 12) 439 40 57

Bismuth telluride and solid solutions based on it are used in the manufacture of different energy converters [1]. In this case, mostly used monocrystalline or polycrystalline Bi_2Te_3 and its solid solutions. Single-crystal samples Bi_2Te_3 easy to cleave along the cleavage planes [0001], forming a reflective, resistant to oxidation that requires no special chemical treatment and is very important for optical measurements.

Studying the band structure Bi_2Te_3 not yet reached such a level as Germanium, the united $A^{III}B^{V}$, due to the complexity of its crystal and band structure [2].

Optical parameters of a single crystal, such as the reflection coefficient R, the imaginary and real ε_1 ε_2 part of the permittivity ε and loss of electrons $-Im\varepsilon^{-1}$ and others, are essential for a full explanation of the physical properties of the material, but also for direct practical application - the design of semiconductor devices.

The objective of this study is to determine its optical parameters on the basis of experimental data of the reflection coefficient of polycrystalline films Bi_2Te_3-Bi_2Se_3.

For thin-film samples, used one of the most widely used methods - vacuum thermal deposition. We studied thin films Bi_2Te_3-Bi_2Se_3, doped terbium, in the amount of 0,0075 *atm*. % Chlorine and 0,035 *atm*. %. The substrate was used glass. The deposition was carried out in a vacuum of 10-3 *Pa*. Getting films Bi_2Te_3-Bi_2Se_3 occurred in the temperature range of the substrate 200°*C*. To improve the structure of thin film samples, and reduce the concentration of point defects in them applied annealing, which was conducted at a temperature of 230°*C* for 30 minutes. The films were obtained at a rate of 2 *nm/sec*. The films Bi_2Te_3-Bi_2Se_3 doped with *Tb* and *Cl* has a thickness from 70 to 150 *nm*. The thickness of the films was measured using an atomic force microscope (AFM) NanoScope IIIa firm Digital Instruments [3]. The films were doped with *Se* and *Tb*, were *p*-and *n*-type conductivity.

Way of dual beam spectroscopy were investigated reflection spectra of polycrystalline films Bi_2Te_3-Bi_2Se_3, at T=293 *K* in the 1÷6 *eV*. Measurements were conducted parallel to the axis "*c*" of a polycrystalline structure. The procedure for determining the optical parameters of semiconductors on the basis of experimental data on reflection is described in [4]. The results of the optical parameters of ε_1, ε_2, $-Im\varepsilon^{-1}$ of these films Bi_2Te_3-Bi_2Se_3, calculated on the basis of data on the reflection by the Kramers-Kronig relations.

The studies show that the probability of the lowest inter-band transition in the films Bi_2Te_3-Bi_2Se_3 in the fundamental absorption edge 0÷1 *eV* is 3×104 cm^{-1}, and the high interband transition in the region 1÷1,5 *eV* is 50×104 cm^{-1}.

Peaks or step functions R and ε_2, usually identified with interband or excitonic transitions in certain areas of the Brillouin zone.

Thus, the experimental values of the reflection coefficient R of light in the energy range 1÷6 *eV* of the incident radiation is normal to the surface of the films Bi_2Te_3-Bi_2Se_3 *p*-and *n*-type conductivity doped with *Tb* and *Cl*, defines the functions of the optical parameters of ε_1, ε_2, $-Im\varepsilon^{-1}$ and interband transitions.

[1]. V.L.Gurevich. Kinetics of Phonon Systems. Nauka, Moscow, 1980, 14.
[2]. B.M.Goltsman, V.A.Kudinov, I.A.Smirnov. Semiconductor thermoelectric materials based on Bi_2Te_3. Nauka, Moscow, 1972, 216.
[3]. The influence of annealing on the structure of the films Bi_2Te_3-Bi_2Se_3. N.M.Abdullaev, S.I.Mekhtiyeva, N.R.Memmedov, M.A.Ramazanov, A.M.Kerimov. FTP, 44, 6, (2010), p.856.
[4]. Optical Properties of Semiconductors (Ed. Bira), IL, M, 1970.

SECTION FIVE

Computational material design and modeling at the nanoscale

I5-1

Theoretical study of quaternary compounds as thin-film solar cell absorber

Su-Huai Wei

National Renewable Energy Laboratory, Golden, CO 80401, USA

e-mail address: swei@nrel.gov, phone/ fax number (+01) 303-384-6432 / (+01) 303-384-6432

Design of chalcogenide photovoltaic absorbers is carried out systematically through sequential cation mutation, from binary to ternary to quaternary compounds, using first-principles electronic structure calculations. Several universal trends are found for the ternary and two classes of quaternary chalcogenides [1-2]. For example, the lowest-energy structure always has larger lattice constant *a*, smaller tetragonal distortion parameter $\eta=c/2a$, and larger band gap than the metastable structures for common-row cation mutations. The band gap is reduced during the mutation. The band gap decreases from binary II-VI to ternary I-III-VI_2 are mostly due to the *p-d* repulsion in the valence band, the decreases from ternary I-III-VI_2 to quaternary I_2-II-IV-VI_4 chalcogenides are due to the downshift in the conduction band caused by the wavefunction localization on the group IV cation site. We find that I_2-II-IV-VI_4 compounds are more stable in the kesterite structure, whereas the widely-assumed stannite structure reported in the literature is most likely due to partial disorder in the I-II (001) layer of the kesterite phase.

Among the derived quaternary compounds, Cu_2ZnSnS_4 (CZTS) is one of the ideal candidate absorber materials for thin-film solar cells with an optimal band gap, high absorption coefficient, abundant elemental components, and is adaptable to various growth techniques. We have performed a series of first-principles electronic structure calculations for CZTS [3-4]. We find that in the ground state kesterite structure, (i) the chemical potential region that CZTS can form is very small. Therefore, it will be very difficult to obtain high quality stoichiometric CZTS samples; (ii) The dominant p-type acceptor in CZTS is Cu_{Zn}, however, the associated acceptor level is relatively high, suggesting that p-type doping in CZTS is more difficult than ternary compounds such as $CuInSe_2$; (iii) The formation of the self-compensated defect pair [Cu_{Zn}+Zn_{Cu}] will not lead to a strong carrier separation, and thus will not contribute the same beneficial effect observed in ternary chalcopyrite compounds; (iv) We predict that to avoid the aforementioned issues in (ii) and (iii), it will be optimal to grow the sample under Cu-poor/Zn-rich conditions, so V_{Cu} and Zn_{Cu} become the dominant defects in the system. However, in this case, non-equilibrium growth techniques may be required to avoid the formation of secondary phases. Our predictions will be compared with available experiments.

Acknowledgments: This work was done with Shiyou Chen, Xingao Gong, and Aron Walsh.

[1]. S. Chen, X. G. Gong, A. Walsh, and S.-H. Wei, Appl. Phys. Lett. **94** (2009), 041903.
[2]. S. Chen, X. G. Gong, A. Walsh, and S.-H. Wei, Phys. Rev. B **79** (2009), 165211.
[3]. S. Chen, X. G. Gong, A. Walsh, and S.-H. Wei, Appl. Phys. Lett. **96** (2010), 021902.
[4]. S. Chen, X. G. Gong, A. Walsh, and S.-H. Wei, Phys. Rev. B **81** (2010), in press.

I5-2

Self-consistent GW and Bethe-Salpeter equation: applications to optoelectronic properties of multinary compounds

Julien Vidal[1,2,3] , Silvana Botti[2,3,4] , Jean-François Guillemoles[1] and Lucia Reining[2,3]

[1] Institute for Research and Development of Photovoltaic Energy (IRDEP), UMR 7174 CNRS/EDF/ENSCP, 6 quai Watier, 78401 Chatou, France
[2] Laboratoire des Solides Irradiés, École Polytechnique, CNRS, CEA-DSM, 91128 Palaiseau, France
[3] European Theoretical Spectroscopy Facility (ETSF)
[4] LPMCN, Université Claude Bernard Lyon I and CNRS, 69622 Villeurbanne, France

julien.vidal@polytechnique.edu , Laboratoire des Solides Irradiés, École Polytechnique, CNRS, CEA-DSM, 91128 Palaiseau, France, Phone: +33 (0)1 6933 4486

For many years, Density Functional Theory (DFT)[1] has been regarded as the method of choice in order to calculate the electronic properties of materials. While DFT certainly demonstrates a rare efficiency at predicting ground state properties, it fails in correctly describing excited states properties such as bandgaps for example. In this paper, we will focus on two methods based on the Many Body Perturbation Theory (MBPT) that overcome DFT deficiencies: the GW method and Bethe-Salpeter equation (BSE)[2]. We will present GW and BSE results obtained for two families of ternary compounds: the photovoltaic materials $Cu(In,Ga)(S,Se)_2$ (CIGS) and the transparent conducting oxides $CuXO_2$ (X=Al, Ga, In) (CXO) in order to illustrate the efficiency of such methods.

In the case of CIGS, GW calculations reveal a strong dependence of the bandgap of CIGS on an internal structural parameter: the anion displacement u [4]. This dependence contrasts with the stability of the bandgap of CIGS and the large dispersion of values of u reported in the literature. We solved this apparent paradox considering the coupled effect on the bandgap of copper vacancies V_{Cu} and lattice distortions.

In the case of CXO, the bandgap is found to be indirect with a large direct/indirect bandgap ratio, in good agreement with DFT calculations. However, within GW, the direct/indirect bandgap ratio is significantly decreased, which, in the case of $CuAlO_2$, results in comparable indirect and direct bandgaps. Therefore, the experimentally observed absorption at low energy was incorrectly assigned to a small indirect bandgap rather than to the presence of defects. Moreover, GW severely overestimates both indirect and direct bandgaps compared to optical experiments. However, the inclusion of both polaronic and excitonic effects yields bandgaps in good agreement with experiments and demonstrates the strong dependence of the bandgap on lattice and electronic polarization.

Acknowledgments: We acknowledge funding from ANR (NT05-343900, JC05_46741), the European projects Athlet (FP6n.019670) and EPRI (EP-P23606/C11428), the EC 7th Framework Programme (FP7) under grant agreement n.211956 . Julien Vidal acknowledges support by the EDF/ANR CIFRE.

[1]. W. Kohn and L. J. Sham, *Physical Review*, **140**, (1965), p. A1133
[2]. G. Onida, L. Reining and A. Rubio, *Review of Modern Physics*, **74** (2002), p. 601
[3]. J. Vidal, S. Botti, P. Olsson, J.-F. Guillemoles and L. Reining, *Physical Review Letters,* **104** (2010), p. 056401
[4]. J. Vidal, F. Trani, F. Bruneval, M. A. L. Marques and S. Botti, *Physical Review Letters,* **104** (2010), p. 136401

O5-1
Characteristics of chemical bonds in $CuInSe_2$, and its thin film deposition processes used to fabricate high efficiency CIS solar cells

Takahiro Wada and Tsuyoshi Maeda

Department of Materials Chemistry , Ryukoku University, Seta Otsu 520-2194 Japan
tel: +81-77-543-7468, fax: +81-77-543-7483, e-mail: twada@rins.ryukoku.ac.jp

The use of $CuInSe_2$ (CIS) in thin-film solar cells has recently been gaining attention. CIS is one of I-III-VI_2 compound semiconductors with a chalcopyrite-type crystal structure. Recently, the electronic structure and chemical bonds in CIS were studied. It was found that the characteristics of chemical bonds in CIS differ from those of conventional III-V and II-VI compound semiconductors[1]. The chalcopyrite-type CIS has two kinds of chemical bonds, Cu-Se and In-Se. The Cu-Se bond is a weak covalent bonding because electrons occupy both bonding and antibonding orbitals of Cu 3d and Se 4p and occupy only the bonding orbital (a_1) of Cu 4s and Se 4p and do not occupy the antibonding orbital (a_1*) of Cu 4s and Se 4p. On the other hand, the In-Se bond has a partially covalent and partially ionic character because the In 5s orbital covalently interacts with Se 4p; the In 5p orbital is higher than Se 4p and so the electrons in the In 5p orbital move to the Se 4p orbital. The average bond order of the Cu-Se and In-Se bonds can be calculated to be 1/4 and 1, respectively. The bond order of Cu-Se is smaller than that of In-Se. The crystal structure of CIS is almost entirely made by the chemical bond between In and Se. Figure 1 shows band diagram of CIS and In 5p + Se 4p (t_2) bonding orbital shown in the unit cell.
In this paper, we outline the characteristics of chemical bonds in CIS. Then, we describe that the characteristics of chemical bonds in CIS offer advantages for the fabrication of high-quality CIS thin films used in solar cells. We explain why the fabrication of high-efficiency solar cells uses the "three-stage process" (a type of multi-source vapour deposition) and the "selenization process" (a method that uses a metal multilayer film as a precursor).

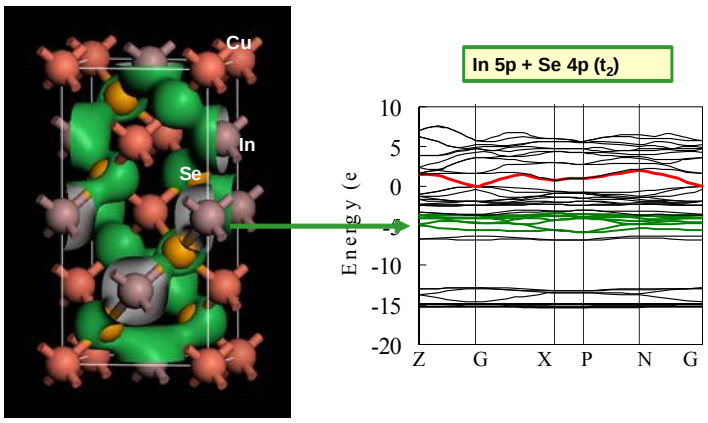

Fig.1 Band diagram of CIS and In 5p + Se 4p (t_2) bonding orbital shown in the unit cell.

Acknowledgments: This work was supported by the Incorporated Administrative Agency New Energy and Industrial Technology Development Organization (NEDO) under the Ministry of Economy, Trade and Industry (METI). It was also partially supported by a grant based on the High-Tech Research Center Program for private universities from the Japan Ministry of Education, Culture, Sports, Science and Technology.

[1]. "Characteristics of chemical bond and vacancy formation in chalcopyrite-type $CuInSe_2$ and the related compounds", T. Maeda and T. Wada, phys. status solidi (c) **6**, No. 5, 1312 (2009).
[2]. "Electronic Structure and Characteristics of Chemical Bonds in $CuInSe_2$, $CuGaSe_2$ and $CuAlSe_2$", T. Maeda and T. Wada, Jpn. J. Appl. Phys., **49** No.4, 04DF07.

O5-2

Ab initio study of 3d transition metal doping of binary semiconductors for magnetic intermediate band photovoltaics

P. Olsson[1,2], C. Domain[1,2] and J.-F. Guillemoles[1]
[1]IRDEP, UMR-7174 CNRS ENSCP EDF R&D, 6 quai Watier, F-78401 Chatou, France
[2]EDF R&D, Département MMC, Les Renardières, F-77250 Moret sur Loing, France

Email: olsson.par@gmail.com / Phone: +33 1 60 73 65 89

The photovoltaic conversion efficiency in usual semiconductors is limited to 30%[1] while thermodynamics sets an upper limit of above 70%[2]. Here we show how efficiencies in the 50% range could be achieved using carefully chosen magnetic doping in wide gap semiconductors due to Pauli blocking of the recombination. To meet the requirement to obtain useful dilute magnetic semiconductor (DMS) compounds we propose rules and a selection method based on *ab initio* calculations coupled with material efficiency predictions. The electronic structure of such a compound is schematically displayed in Figure 1 and the efficiency predictions as a function of the electronic structure are displayed in Figure 2.

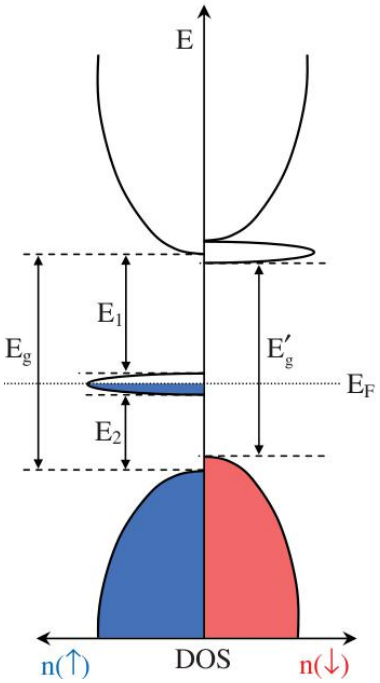

Figure 1. Schematic density of states of a DMS (spin up and down) optimal for photovoltaic conversion.

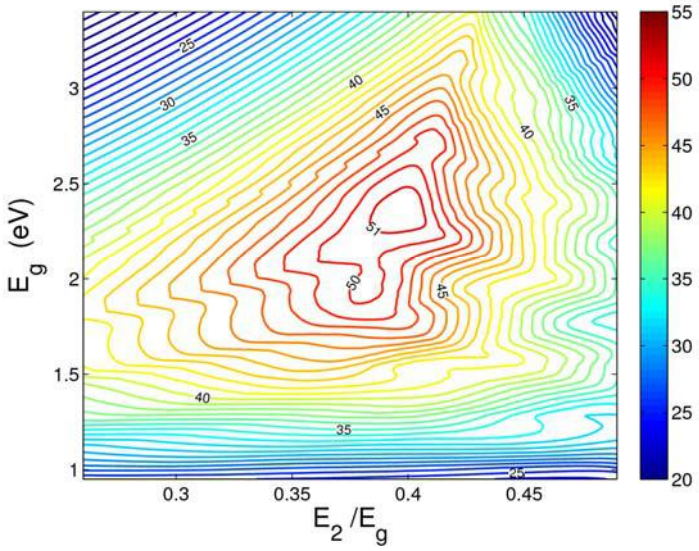

Figure 2. Contour plots of the conversion efficiency of an AM 1.5 illumination spectrum by a DMS solar cell as a function of E_2 and E_g gaps.

Hundreds of compounds have been systematically investigated for opto-electronic and magnetic properties. The trends based on the transition metal dopant, crystal structure and host matrix group (II-VI, III-V, etc) are discussed. The binary zincblende AlP doped with Cr was found to be the most promising semiconductor compound for photovoltaic applications[3].

Acknowledgments: The authors acknowledge the support by the French National Research Agency in Project THRI-PV, contract ANR-PSPV-014-003, and by the Electric Power Research Institute, contract EP-P23606/C11428. The DFT computations were carried out on the EDF Blue-Gene/L parallel calculator.

[1]. W. Shockley and H. J. Queisser, *J. Appl. Phys.* **32** (1961), p. 510.
[2]. M. A. Green, "Third Generation Photovoltaics: Advanced Solar Electricity Generation" (Springer, Berlin, 2003).
[3]. P. Olsson, C. Domain and J.-F. Guillemoles, *Phys. Rev. Lett.* **102** (2009), p. 227204.

O5-3

The conception of e-transformations in wave-function and phonon engineering

R. R. Bashirov

Institute of Physics, Daghestan Scientific Center, Russian Academy of Sciences, 367003, M.Yaragskii str., 94, Makhachkala, Russia

rusbash@inbox.ru, tel+7872262-66-50/fax+7872262-89-00

Topologically, the most of quantum semiconductor heterostructures with nontrivial 2D and 3D geometry fall into three large classes of X-, T-, and L- shaped quantum wells(wires) and superlattices made up of them [1,2]. Within each class, the objects inherit some general features conditioned by their topology. The producing an object with desirable properties is a great challenge for band structure and phonon engineering. In this work we propose a new method for analytical treatment of carrier and phonon spectrum problem for such objects. The approach is based on non-smooth transformations, first applied for pulse exited systems [3]. Our consideration is based on two sorts of piecewise functions, e_s and e_p, presented in fig.1. A class of 2D potentials for single particle Schrödinger equation investigated here can be represented as (see Fig.1):

$$V(x,y) = V_0 + V_1 \cdot e_1 + V_2 \cdot e_2 + V_3 \cdot e_3 , \qquad (1)$$

where V_i are constants and e_1=e(x), e_2=e(y), e_3= $e_1 \cdot e_2$, and e_i are either s- or p- type. Cyclic algebra for e_i products takes place due to attribute e_i^2=1, thus e_1= $e_3 \cdot e_2$ and e_2= $e_3 \cdot e_1$. Then a wave function adopts the same structure (e-transformation): $\psi(x,y) = \varphi_0 + \varphi_1 \cdot e_1 + \varphi_2 \cdot e_2 + \varphi_3 \cdot e_3$ and Schrödinger equation becomes a matrix one of 4x4 dimension. The corresponding matrix potential then does not depend on spatial variables ***x*** and ***y***. It has been shown that Schrödinger equation with potential (1) has analytical solutions. These solutions appear to be interesting themselves, giving eigen-values and eigen-functions for two crossing quantum wires or three-terminal T-shaped quantum knot generated by e_s, for instance. Another example is a quantum well grown on the cleaved edge of a superlattice – a pattern, generated by e_s and e_p and had been investigated numerically earlier [4]. Besides, analytical solutions available now grant us an unprecedented opportunity for wave-function and phonon engineering in a general case of complex heterostructures of 2D and 3D geometry.

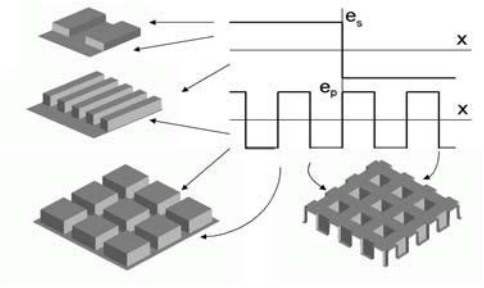

Figure 1. The four patterns for potential V(x,y): T-shaped single quantum knot, 1-D superlattice made from T-shaped quantum wells, 2-D antidot array, and 2-D dot array.

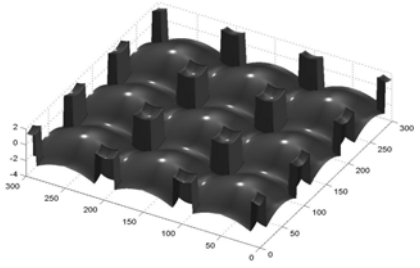

Figure 2. 2D periodic potential (3x3 cells) presented by local sums: $V_i = a_i x^2 + b_i y^2 + c_i$, i=1÷4, with the potential of a heterostructure imposed on them and describing 2D antidot array doped by donors.

[1]. Madhud Menon, Antonis N. Andriotis, and Deepak Srivastava. *Phys. Rev. Lett*. **91** (2003), p.145501
[2]. L. Pfeiffer, K.W. West, H.L. Stormer, J.P. Eisenstein, K.W. Baldwin, D. Gershoni and J. Spector *Appl. Phys. Lett.* **56** (1990), p. 1697
[3]. V.N. Philipchuk. *Jornal of Sound and Vibration* **249** (2) (2002), p. 399
[4]. Z. S. Gribnikov, R. R. Bashirov, H. Eisele, V. V. Mitin, and G. I. Haddad. *J. Appl. Phys.* **93** (2003), p. 330

P5-1

Phase stability and electronic structure of In-free photovoltaic compounds, $Cu_2ZnSnSe_4$, $Cu_2CdSnSe_4$, and $Cu_2HgSnSe_4$

Satoshi Nakamura, Tsuyoshi Maeda and Takahiro Wada

Department of Materials Chemistry, Ryukoku University, Seta, Otsu 520-2194, Japan
E-mail: t10d003@mail.ryukoku.ac.jp, TEL: +81-77-543-7468 / FAX: +81-77-543-7483

$Cu_2ZnSnSe_4$ (CZTSe) and Cu_2ZnSnS_4 (CZTS) are anticipated as indium-free absorber materials. Recently, wide and narrow band gap absorber materials have been studied for thin film full spectrum solar cells. New materials, which have wide band gap (E_g >1.7 eV) and narrow (E_g <1.0 eV) band gap, are required. For the Cu(*I*)$_2$-Zn(*II*)-*IV*-*VI*$_4$ compounds, three kinds of crystal structures, i.e. kesterite- (KS), stannite- (ST), and wurtz-stannite-type (WST), have been reported. These crystal structures resemble each other and the KS and ST phases cannot be easily distinguished from powder x-ray diffraction. We predicted the KS phase is most stable in CZTS and CZTSe by first-principles calculation [1]. Then, we identified the kesterite-type CZTSe by neutron powder diffraction [2]. We also reported the electronic structure of CZTSe and CZTS by first principles calculations [3]. However, phase stability and electronic structure of Cu_2*II*$SnSe_4$ compounds (*II*= Zn, Cd, Hg) are not reported.

In this research, we have theoretically evaluated the phase stability and electronic structure of new photovoltaic compounds, Cu_2*II*$SnSe_4$ compounds (*II*= Zn, Cd, Hg).

Calculations were performed using a plane-wave pseudopotential method within the density functional formalism. Phase stability of these compounds was evaluated from enthalpy of formation.

Figure 1 shows the enthalpy of formation for KS-, ST- and WST-type Cu_2*II*$SnSe_4$. The difference in ΔH between the KS, ST and WST phases is also shown. For $Cu_2ZnSnSe_4$, ΔH of the KS phase (-312.7 kJ/mol) is smaller than those of the ST (-311.3 kJ/mol) and WST (-305.7 kJ/mol) phases. On the other hand, for $Cu_2CdSnSe_4$ and $Cu_2HgSnSe_4$, ΔH of ST phase is smaller than those of WST and KS phases. For $Cu_2CdSnSe_4$ and $Cu_2HgSnSe_4$, the ST phase is more stable than the WST and KS phases. For Cu_2*II*$SnSe_4$, the valence band maximums (VBMs) consist of antibonding orbitals of Cu 3*d* and Se 4*p*. The conduction band minimums (CBMs) consist of antibonding orbitals of Sn 5*s* and Se 4*p*. The *nd* state of group *II* elements localized at about -7 eV in the valence band. The band gap energies of $Cu_2CdSnSe_4$ and $Cu_2HgSnSe_4$ calculated with sX-LDA (screened eXchange LDA) are a little smaller than, but nearly equal to that of $Cu_2ZnSnSe_4$ because the *II* elements do not affect both of the VBMs and the CBMs in these compounds. Therefore, for Cu_2*II*$SnSe_4$, stability of the crystal structure depends on the group *II* elements, but the electronic structure and band gap energy do not much depend on the group *II* elements.

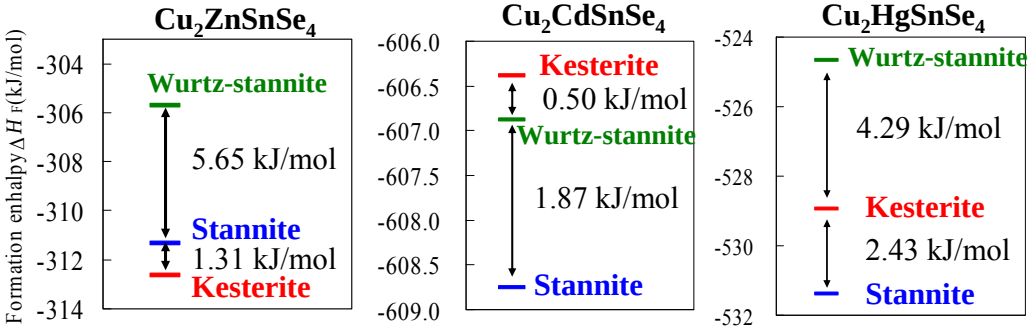

Figure 1. Enthalpy of formation of Cu_2*II*$SnSe_4$ (*II*=Zn, Cd, Hg)

Acknowledgments: This work was supported by the Incorporated Administrative Agency New Energy and Industrial Technology Development Organization (NEDO) under the Ministry of Economy, Trade and Industry (METI).

[1]. T. Maeda, S. Nakamura and T. Wada, *Mat. Res. Symp. Proc.* **1165** (2009), M04-03.
[2]. T. Maeda *et al*, *Technical Digest of PVSEC-19* (2009), No.CIG-4-O-1.
[3]. S. Nakamura, T. Maeda and T. Wada, *Phys Status Solidi* C **6** (2009), 1261.

P5-2

Carrier spectra in complex GaAs/ $Al_xGa_{1-x}As$ / $In_yAl_{1-y}As$ T-shaped superlattices

T.H.Effendieva, R.R.Bashirov

Institute of Physics, Daghestan Scientific Center, Russian Academy of Sciences, 367003, M.Yaragskii str., 94, Makhachkala, Russia, rusbash@inbox.ru, tel+7872262-66-50/fax+7872262-89-00

The inventions of cleaved edge overgrowth (CEO) [1] and glancing-angle deposition (GLAD) [2] in the early 90th of the last century stimulated the occurrence of new classes of nanostructures based on the well known semiconductor materials. In our work one of the such classes - superlattice ***A/B,*** bypassed by channel ***C*** formed by either one or several conducting layers separated by a barrier material, and oriented transversely to superlattice layers, is considered. Delta-doping of external barrier ***D*** by donors, and acceptors of barrier ***B*** effectively keep mobile electrons in the strip of width ***d*** near to the channel (Fig. 1). Electronic spectra for such ***A/B // C*** heterostructures have been calculated earlier [3, 4], in particular for structures GaAs/p-$Al_xGa_{1-x}As$ // $Al_yGa_{1-y}As$ and $In_xGa_{1-x}As$/p-$In_yAl_{1-y}As$ // $In_{0.53}Ga_{0.47}As$ and simple channel ***C*** of width a_o. CEO and GLAD technologies allow to vary flexibly geometrical and physical parameters of a heterostructure and to modify its spectrum over a wide range. In the present paper, the new opportunities of quantum design arising in the case of complex channel structure are considered. Spectra of heterostructures ***A/B // C/D/E …*** containing up to three conducting layers in the channel are investigated numerically.

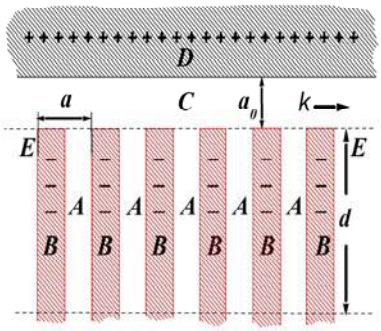

Figure 1. Superlattice ***A/B,*** bypassed by channel ***C*** and capped with n-doped top barrier ***D*** .

Modelling is based on the Schrödinge equation with imaginary time. For carriers of conduction band, parameters of the Schrödinger equation were defined on the basis of one-band effective mass approximation. In particular, the spectra giving N-type dependence of the drift velocity on applied electric field are obtained. In the frame of *(k-p)*-method, the system of differential equations is generalized for the case of several bands. The developed algorithm has allowed to model the mini-bands created by dimensional quantization of holes in ***A/B // C/D/E …*** structures, however its applicability is much wider: from quantum dots separated by 3-D hetero-interface off surrounding wide-band host material, to heterostructures, similar to considered here and based on II-type superlattices.

[1]. Y L. Pfeiffer, K.W. West, H.L. Stormer, J.P. Eisenstein, K.W. Baldwin, D. Gershoni, and J. Spector, *Appl. Phys. Lett.* **56** (1990), p. 1697.
[2]. K. Robbie, M. J. Brett, and A. Lakhtakia, *J. Vac. Sci. Technol*. **A 13** (1995), p. 2991.
[3]. Z. S. Gribnikov, R. R. Bashirov, and V. V. Mitin., IEEE Journal of Selected Topics in Quantum Electronics,**7** (2001), p. 630.
[4]. Z.S.Gribnikov, N. Z. Vagidov, R. R. Bashirov, V. V. Mitin and G.I.Hadad, *J. Appl. Phys*. **93** (2003), p. 330.

P5-3

On the heat capacities of (Ti, Sn) O_2 thin films

E. Eser [1], H. Koç [2], B. A. Mamedov [1], and I. M. Askerov [1]

[1] Department of Physics, Faculty of Arts and Sciences, Gaziosmanpasa University, Tokat, Turkey
[2] Department of Physics, Vocational School, Muş Alparslan University, Muş, Turkey

Corresponding author: erhaneser06@yahoo.com, Phone: +90 356 252 16 16, Fax: +90 356 252 15

In the present study, our aim is to calculate the heat capacities of (Ti, Sn)O_2 thin films in the 0-2000 K temperature range by using analytical relation of the heat capacities calculated in terms of integer and non-integer n-dimensional Debye functions. The proposed approach is novel as it uses the non-integer n-dimensional Debye functions for accurate calculations of the heat capacity. The obtained results have been compared with the corresponding experimental and theoretical results, and the agreement between the calculated and the corresponding values of heat capacity has been found to be in excellent agreement.

P5-4

Estimation of the heat capacities of Ti_2AlC and V_2AlC crystals

I. M. Askerov [1], H. Koç [2], E. Eser [1]

[1] Department of Physics, Faculty of Arts and Sciences, Gaziosmanpasa University, Tokat, Turkey
[2] Department of Physics, Faculty of Arts and Sciences, Alparslan University, Muş, Turkey

Corresponding author: aztovuz@yahoo.com, Phone: +90 356 252 16 16, Fax: +90 356 252 15

In this study, the heat capacities of the ternary carbides of Ti_2AlC and V_2AlC in the 0-300 K temperature range were calculated using the analytical formula for n-dimensional Debye functions. The approach obtained is new as it uses the non-integer n-dimensional Debye functions and enables the straightforward calculation of the heat capacities for arbitrary temperature values. The method is completely general and free of any restrictions on its application to analysis of thermophysical properties of crystals. The obtained results have been compared with the results of other researchers and found to be in agreement.

P5-5

Modeling and Simulation of Ferroelectric Based MEMS for Inertial Measurement Unit

Zafer Özer[1,*] and Amirullah M. Mamedov[2]

[1]Mersin University, Mersin M.Y.O., Adana, Turkey
[2]Physics Department, Cukurova University, Adana, Turkey
E-mail: zaferozer@hotmail.com and mamedov@cu.edu.tr

This paper present the design, modeling and finite element model (FEM) simulation of a micro-electromechanical systems (MEMS) on the based ternary ferroelectric compounds (PZT and $Ba_xSr_{1-x}TiO_3$).
A detailed model of MEMS is generated at the continuous field level, which considers multiple physical domains, such as structural dynamics, fluidics and electrostatics. To reduce the large order of the problem, a compact model is derived by decomposition of the deformation field into basic mode shape functions. The dynamic behavior of the sensor structure is described by super position of its dominant vibration mode shapes. The resulting model still considers all physical domains and is even able to capture nonlinear phenomena, such as stress stiffening of constraint structures or frequency and stiffening caused by squeezed gas in the sensor cell. Algorithms of this model were extended to account for MEMS package transducer interactions. Process induced and thermally induced residual stresses and resulting deformation of the transducer elements are considered.

P5-6

Modeling of optical properties of reflectionless coatings on the basis of nanocomposite materials

Ramiz Karamaliyev [1], Chingiz Qajar [2], Terlan Efendiev [3]

[1] Baku State University , Z. Khalilov str., 23, AZ-1148, Baku, Azerbaijan

[2] Institute of Physics, NAS of Azerbaijan, H. Javid Ave., 33, AZ-1143, Baku, Azerbaijan

[3] B.I. Stepanov Institute of Physics, NAS of Belarus, Nezavisimosti Ave., 68, 220072 Minsk, Belarus

e-mail: karamaliyev@ yahoo.com, phone: (994 12) 561-23-72

Investigations on creation of layered systems, which provide practically reflectionless transmission through them electromagnetic radiations, are very important for many applications in optics [1]. Coatings on the basis of nanocomposite materials can be optimized for specific applications by modifying their particle size, shape, volume fraction, microstructure, etc. Composite materials that contain particles much smaller than the wavelength of incident radiation can be modeled by effective medium theories.Optical properties of composite medium consisting of a transparent dielectric matrix with inclusion of metallic nanoparticles are investigated theoretically. At the assumption of small sizes of filler particles (in comparison with the incident radiation wavelength), the effect of volume fraction of metallic particles δ (copper, gold, etc.), layer thickness l and optical parameters of substances of a coating are investigated on the antireflection conditions. The fundamental quantity describing the dielectric response of nanocomposite material is the effective complex dielectric function ε which can be expressed by following formula [2]:

$$\varepsilon = \varepsilon_1(1 + 3\delta\frac{\varepsilon_2 - \varepsilon_1}{\varepsilon_2 + 2\varepsilon_1})$$

where ε_1 and ε_2 are the complex dielectric constant of surrounding matrix and metal, respectively. The complex refractive index of gold for incident radiation wavelength λ_0=0.5 mkm is 0.84 – i 1.84 [3]. Using complex reflection coefficient expression for multilayer system the selective quantities of coating thickness and volume fraction of metal particles to realize antireflection are calculated.

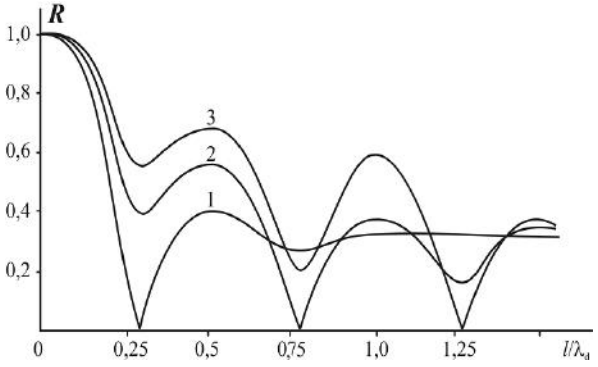

Figure. Reflection coefficient

R of the light radiation (with the wavelength $\lambda_0 = 0.5$ мкм in the vacuum) versus the film thickness *l* for various values of the volume fraction of gold particles $\delta = 15.2$ (curve 1), 6.8(curve 2) and 4.6(curve 3) % at its refractive index $n_1 = 1.5$, when the film is located on the metallic substrate. λ_d is the wavelength in the medium.

[1]. J.D. Rancourt, "Optical Thin Films: User Handbook" (SPIE Press, 1996), 286 pages.
[2]. L.D. Landau, E.M. Lifshitz, "Electrodinamics of Continuous Media" (Oxfotd, 1984), 460 pages.
[3]. P. Yeh, "Optical waves in layered media" (New York, 1988), 406 pages

SECTION SIX

Light emitting materials and devices

I6-1
Effect of REE co-doping on the Mn red emission in Ca and Sr thiogallates - Focusing on its mechanism through ESR study using single crystals

Takeo TAKIZAWA, [1] Toshimitsu OBONAI, [1] Shigetaka NOMURA*, and Chiharu HIDAKA[1]

[1] Department of Physics, College of Humanities and Sciences, Nihon University
Sakura-josui 3-25-40, Setagaya-ku, Tokyo 156-8550, Japan
* Department of Electro Engineering, Tokyo University of Science
1-14-6 Kudan-kita, Chiyoda-ku , Tokyo 102-0073 Japan

E-mail : takiz@phys.chs.nihon-u.ac.jp, Phone/Fax: +81-3-5317-9772

The alkaline earth thiogallates are regarded as potential materials for phosphors because of their blue and green emissions when doped with Ce and Eu elements, respectively. Only the drawback is the lack of red emission. We have succeeded to make red emission by doping Mn element,[1,2] though it was very weak. However, the weak red emission can be enhanced by one order of magnitude by co-doping some proper REE's. [1,2] Here we report the results of its enhancement under Ln's elements through PL, PLE and optical absorption measurements. To clarify the mechanism of the enhancement, we have carried out the relativistic DV-Xα calculation using cluster models co-doped with Mn and Ln's elements,[3] where the dopant sites play an important role for the electron energy transfer. We have also made ESR measurements using a single crystal containing 0.1 mol% Mn to identify the Mn substitutional site in the thiogallate lattice.[4]
Here we will present additional ESR results of a single crystal of $CaGa_2S_4$:Eu(0.1 mol%) where Eu atoms are supposed to exclusively replace the Ca sites, to get useful and correct information for identifying the Mn substitutional site in the compounds.

[1]. Fabien Boitier, Chiharu Hidaka, Takeo Takizawa, Journal of Luminescence, Volume **129**, Issue 5, May 2009, Pages 554-562
[2]. T.Obonai, C.Hidaka, and T.Takizawa, phys. stat. sol. A **206** (5), 1026-1029 (2009)/ DOI: 10.1002/pssa.200881190
[3]. S. Nomura, T. Takizawa, M. Kai, and S. Ando, phys. stat. sol. C **6**(5), 1317-1320 (2009)/ DOI: 10.1002/pssc.200881188
[4]. T. Obonai, C. Hidaka, and T. Takizawa, Opt. Mater. (2010), DOI:10.1016/j.optmat.2010.05.012

I6-2

Radiative properties of halogen intercalated transition metal dichalcogenide layered crystals

L. Kulyuk, A. Colev, C. Gherman

Institute of Applied Physics, Academy of Sciences of Moldova, Academiei Str. 5, Chisinau, MD-2028, Republic of Moldova

E-mail: kulyuk@phys.asm.md, Phone: +373-22-731055, Fax: +373-22-738149.

The transition metal dichalcogenides (TX_2) compounds belong to a large class of the two-dimensional solids. Owing to their layered structure, these indirect band gap semiconductors can be intercalated with foreign atoms and molecules. However in spite of numerous papers on intercalation complexes of transition metal dichalcogenides [1], as well as of a direct analogy with bromine intercalated graphite compounds [2], the intercalation of the halogen molecules in lamellar TX_2 crystals has been not investigated.

In this work the luminescence properties of WS_2, WSe_2, MoS_2 and $Mo_{1-x}W_xS_2$ compounds intercalated with halogen molecules (Br_2, I_2 or Cl_2) are presented.

Single crystals were grown by chemical-vapor method, using iodine, bromine and chlorine as transport agents. The steady-state and time-resolved photoluminescence measurements were made in the temperature range T=2÷150K.

The sharp-lines IR photoluminescence observed at low temperatures at the energy values of about 0.1eV lower than those of the indirect band gaps of the samples, is shown to be produced by bound excitons related to the transport agent, intercalated in 2H-TX_2 crystals during the growth process. The diatomic halogen molecules unambiguously positioned in the adjacent tetrahedral sites of the van der Waals gap (Fig.1), yield neutral centers, providing an efficient radiative recombination.

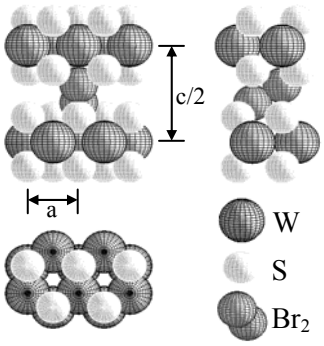

Figure 1 Structural arrangement in a 2H-polytype transition metal dichalcogenide (exemplificative of WS_2) with a diatomic halogen molecule (Br_2) arranged between the X-T-X sheets.

Because of their large electronic affinity, the neutral halogen molecules exhibit properties of electron-attractive centers, creating a short-range potential similar to that of the isoelectronic traps in the indirect band gap semiconductors, such as GaP or Si.

Beside the excitonic emission caused by halogen impurities, a structured IR luminescence broad band associated with an intrinsic defect (deep center) of the 2H-TX_2 host lattice was detected for all samples, including natural molybdenite and synthetic crystals grown without transport agents [3]. The recombination of the excited carriers via these defects is treated as a shunt channel for excitonic emission.

A kinetic model is proposed to describe the recombination processes taking place in the halogen-intercalated 2H-TX_2 crystals. The fast thermal quenching of the sharp-lines emission at T>50K is accounted for by the self-trapping of the bound excitons [4]. The simulation, carried out in the frame of the kinetic model using the experimentally determined lifetime and energy values of the excitonic states, shows a good agreement with the observed characteristics of the luminescence.

Acknowledgments. The authors are grateful to Ying-Sheng HUANG from the National Taiwan University of Science and Technology, Taipei, Taiwan for providing us with $Mo_{1-x}W_xS_2$ samples.

[1]. R. H. Friend and A. D. Yoffe, *Adv. Phys.* **36 (**1987) p. 1.
[2]. M. S. Dresselhaus and G. Dresselhaus, *Adv. Phys.* **30** (1981) p. 139 and **51** (2002) p. 1.
[3]. L. Kulyuk, L. Charron and E. Fortin, *Phys. Rev.* **B 68** (2003) p. 075314.
[4]. A.Colev, C. Gherman, V. Mirovitskii, L. Kulyuk, E. Fortin, *J. Luminescence* **129** (2009) p. 1945.

O6-1
Photoluminescence of $Cu(In,Ga)Se_2$ in the solar cell preparation process

Sho Shirakata, Shinji Yudate, Jyunji Honda and Naoki Iwado

Faculty of Engineering, Ehime University, Matsuyama, Ehime 790-8577, Japan
shirakata.sho@eng.ehimme-u.ac.jp

Sequential step by step photoluminescence (PL) measurements have been carried out on $Cu(In,Ga)Se_2$ (CIGS) films just after each thin-film processes for the fabrication of the CIGS solar cell. These include, (i) the CIGS film deposition on the Mo-coated soda-lime glass substrate by three-stage method (CIGS/Mo/SLG), (ii) the chemical-bath deposition (CBD) of CdS buffer layer, (iii) deposition of undoped ZnO window layer by RF sputtering, (iv) deposition of Al doped ZnO high-conductive window layer by RF sputtering, (v) Al grid electrode deposition for the CIGS solar cell, and (vi) the mechanical scribing for the electrical isolation of small test cells. Room-temperature PL measurements have been done with the excitation of a He-Ne laser (632.8 nm, 1mW) focused on the sample surface to 0.2 mm diameter. PL was dispersed by a polycromator (Horiba: MicroHR) and detected by a cooled InGaAs multichannel detector (1024 pixels). In order to study the uniformity of PL within CIGS films, the two dimensional PL spectrum mapping measurement has been done (0.4-0.6 mm step) using an x-y stage operating in the raster scanning mode [1]. Acquisition time of one PL spectrum was 1s.

Once the fresh CIGS film is exposed to the air, intensity of the near-band-edge PL decreases slowly with time. After few days, PL intensity was one order of magnitude weaker than its initial value. Thus, PL measurement was performed just after the deposition. Figure 1 shows PL spectra of CIGS films taken for each process in the CIGS solar cell preparation. PL of the CIGS film exhibited near-band-edge peak at 1.18 eV. The slight increase of PL intensity was observed after depositions of CdS and ZnO films. After the high conductive ZnO:Al deposition, PL intensity decreases to one third of the initial PL intensity of the fresh CIGS film. No change has been observed with respect to the line shape of PL peaks during the process. In the CIGS solar cell (open circuit condition), PL intensity recovers that in the CIGS film just after the deposition. These changes of PL intensity can be seen as a two dimensional PL intensity images as shown in Figure 2. The best solar cell has been obtained in the center position of the substrate (5 cells are fabricated in one substrate as shown in Figure 2). In such a best cell, conversion efficiency was 10.1%, fill factor was 69%, open circuit voltage was 0.67V, short circuit current was 22mA/cm^2, and the diode quality factor was 1.9. Apart from the center, the cell performance degraded slightly (down to 9.2%) mainly due to the decrease in the fill factor (down to 59%). In view of solar cell parameters and PL intensity images, it can be said that the solar cell performance is correlated to PL intensity. The results are discussed in terms of the effect of photovoltage on PL intensity [2]. The usefulness of PL mapping method for the characterization of the CIGS solar cell process is demonstrated.

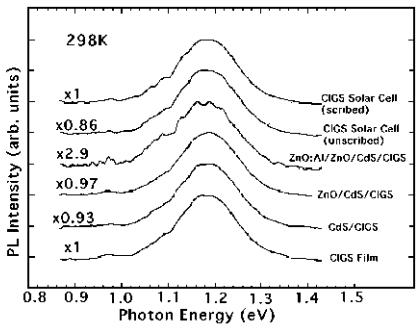

Figure 1 PL spectra of CIGS films for each solar cell process.

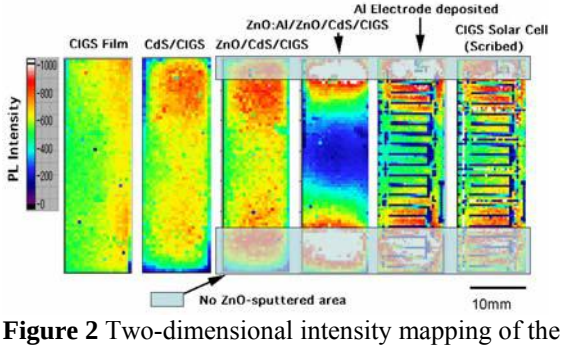

Figure 2 Two-dimensional intensity mapping of the near-band-edge PL of CIGS films for each solar cell process.

[1]. S. Shirakata and T. Nakada, Solar Energy Materials and Solar cells (2010) in press.
[2]. S. Shirakata and T. Nakada, Physica Status Solidi (c) **6** (2009), p1059.

O6-2

Luminescence properties of barium thio- and selenogallates doped with Eu, Ce, Eu+Ce

G. P. Yablonskii[a], V. Z. Zubialevich[a], E. V. Lutsenko[a],
A M. Pashaev [b, c], B. G. Tagiev [b, c], O. B. Tagiev [b, d], S. A. Abushov [b]

[a] Institute of physics of NAS of Belarus, Independence ave. 68, 220072 Minsk, Belarus
[b] Institute of Physics of NAS of Azerbaijan, H. Javid ave. 33, AZ-1143 Baku, Azerbaijan
[c] Academy of Aviation, Bina, 25th km, AZ-1045 Baku, Azerbaijan
[d] Branch of Moscow State University in Baku, F. Agayev str. 14, AZ-1141 Baku, Azerbaijan
e-mail :yablonskii@ifanbel.bas-net.by

Spectra of photoluminescence (PL), PL excitation (PLE), influence of temperature and power density of polycrystalline $BaGa_2S_4$ doped with Eu, Ce ions have been studied in the wavelength region of 300–800 nm over the temperature (T) and excitation intensity (I_{exc}) intervals of 10–320 K and 10^{-3}–10^6 W/cm^2 respectively. Monochromated light of Xe lamp, radiations of cw InGaN-laser (405 nm), HeCd-laser (325 nm) and pulse N_2-laser (337 nm, 8 ns) were used for luminescence excitation. Registration was performed by a monochromator equipped with photomultiplier or by a spectrograph with CCD line. PL integral intensity and excitation power were detected by the same calibrated power meter. Close-cycle helium cryostat was used for the temperature stabilization.

PL band of $BaGa_2S_4$:Eu in the 420–650 nm region with maximum around 500 nm related to the Eu^{2+} ion transition ($4f^65d \rightarrow 4f^7$) does not change significantly its spectral position in the whole intervals of T and I_{exc}. Its efficiency remains constant up to $I_{exc} \sim 10^4$ W/cm^2 (Fig. 1). PL intensity of $BaGa_2S_4$:Eu, Ce is significantly higher (about 2 times) than that of $BaGa_2S_4$:Eu. The PLE spectrum of $BaGa_2S_4$:Eu,Ce at room temperature (RT) constitutes of a broad band with a weakly pronounced structure in the region of 300–500 nm.

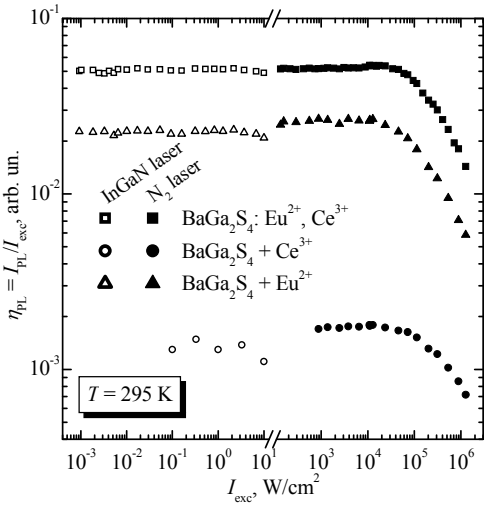

Fig. 1. – PL efficiencies of $BaGa_2S_4$: Eu^{2+}, $BaGa_2S_4$: Ce^{3+}, and $BaGa_2S_4$: Eu^{2+}, Ce^{3+}as functions of excitation level

PL spectrum of $BaGa_2Se_4$:Eu is located in the wavelength region of 400-800 nm and it consists of two bands with maximums around 515 and 680 nm at RT with PLE bands around 360 nm and 430 nm for each PL band. PL spectrum of $BaGa_2Se_4$:Ce at RT has a wide band at 510 nm, corresponding to radiation transition of 5d→ $^2F_{7/2}$, 5d→ $^2F_{5/2}$ of the Ce^{3+} ions as well as the band at 680 nm belonged to the donor-acceptor pair recombination in the $BaGa_2Se_4$ matrix. Intensity of PL band corresponding to the transition of Eu^{2+} ions in $BaGa_2Se_4$:Eu,Ce is significantly higher than that of crystals doped only with Eu.

In conclusion, it has been demonstrated a very high spectral and efficiency stability of the photoluminescence emission from barium thio- and selenium gallates doped with Eu, Ce, Eu+Ce in the broad ranges of temperatures and excitation intensities. Increasing of quantum effectiveness of $BaGa_2S_4$:Eu and $BaGa_2S_4$:Eu,Ce in the radiation band of Eu is related with effective transition of excitation energy from Ce^{3+} to Eu^{2+} ions. Possible reasons and physics mechanisms are discussed. These results show the doped barium thio- and selenogallates as materials perspective in light sources with high temperature- and output power-stable spectra. It is also possible to use the doped thiogallates in addition to 'yellow' phosphors in conventional white light emitting diodes. This allows increasing their color rendering index for the account of filling by luminescence of doped $BaGa_2S_4$ the spectral gap between "blue" InGaN-related and "yellow" phosphor-related bands of LED.

O6-3

Effect of Ho co-doping on the long lasting emission in $CaGa_2S_4$:Eu

Chiharu Hidaka[1] and Takeo Takizawa[1]

[1] Department of Physics, College of Humanities and Sciences, Nihon University
Sakura-josui 3-25-40, Setagaya-ku, Tokyo 156-8550, Japan

E-mail : komaz@phys.chs.nihon-u.ac.jp, Phone/Fax: +81-3-5317-9772

In $CaGa_2S_4$ compounds co-doped with Eu and other rare earth elements, afterglow has been observed and the longest one is reported in the Ho co-doping case [1-3]. However, the mechanism of the afterglow has not been clarified yet. Here we present the results of our study of Eu emission in $CaGa_2S_4$:Eu,Ho as a function of dopant concentration. We discuss the possible mechanism and the effect of Ho co-doping on it.

We have prepared the above compounds with different Eu and Ho concentration. Photoluminescence (PL) spectra of Eu and Ho co-doped $CaGa_2S_4$ are measured. Figure 1 shows a PL spectrum of $CaGa_2S_4$: Eu0.1mol%, Ho0.5mol%. Emission from both Eu and Ho ions is seen. The Eu emission at 2.2eV decreases and Ho one at 1.9eV increases with increasing Ho concentration. This strongly suggests energy transfer from Eu ions to Ho ones occurring in this material.

Figure 2 shows the decay curves of Eu emission in $CaGa_2S_4$: Eu (0.1~5.0 mol%) co-doped with Ho 0.1mol%. The decay time of Eu emission decreases with increasing concentration of both Eu and Ho. It means that shortening the distance between Eu and Ho leads to strengthening the interaction between them, resulting in the reduction in the lifetime of the Eu afterglow.

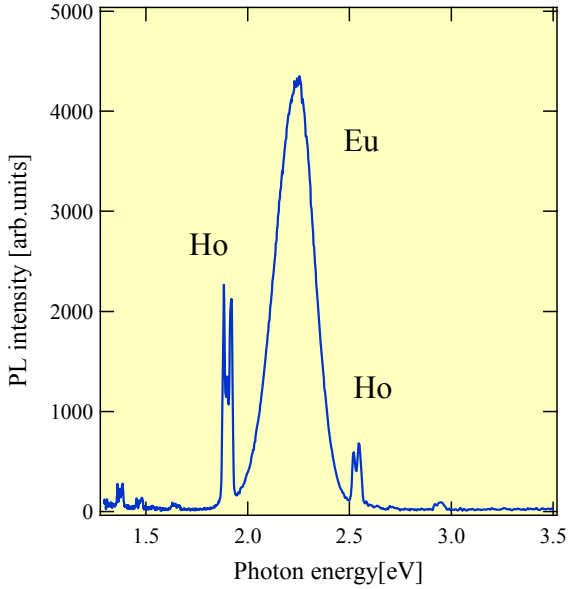

Figure 1. A PL spectrum of $CaGa_2S_4$ doped with Eu0.1mol%, and Ho0.5mol% under irradiation of 325nm He-Cd laser.

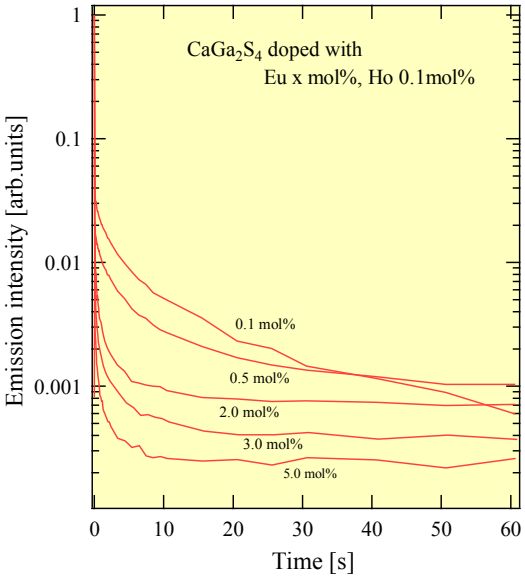

Figure 2. Decay curves of Eu emission in $CaGa_2S_4$:Eu co-doped with Ho 0.1mol%.

These results are discussed in view of the relation of their fast decay properties with the long lasting components.

Acknowledgments: This work is partly supported by Nihon University Research Grant for 2009 and 2010.

[1]. C. Guo, Q. Tang, C.Zhang, D. Huang, Q. Su, *J. Lumin.* **126** (2007) p.333
[2]. C. Guo, Q. Tang, C.Zhang, D. Huang, Q. Su, *J. Phys. Chem. Sol.* **68** (2007) p.217
[3]. C. Guo, Q. Tang, C.Zhang, D. Huang, Q. Su, *Mater. Res. Bull.* **42** (2007) p.2032

O6-4

Excited states of the A and B free excitons in $CuInSe_2$

M.V. Yakushev[1], F.Luckert[1], R.W. Martin[1], C. Faugeras[2], A.V.Karotki[3] and A.V. Mudryi[1,3]

[1]Department of Physics, SUPA, Strathclyde University, G4 0NG Glasgow, UK
[2]Grenoble HMFL, 25 Avenue des Martyrs, BP 166, 38042 Grenoble Cedex 9, France
[3]Scientific-Practical Material Research Centre of the National Academy of Science of Belarus, P.Brovki 19, 220072 Minsk, Belarus

michael.yakushev@strath.ac.uk +44 (0) 141 5483374

Solar cells with $CuInSe_2$-based semiconductor compounds in the absorber layer are amongst the leading thin-film technologies in terms of conversion efficiencies and stability. However, efficiencies for $CuInSe_2$-based solar cells currently saturate near 20% rather than 30%, which is the theoretical limit for a one-junction solar cell, suggesting a lack of fundamental understanding and control of these materials. One of the milestones in the development of every semiconductor material for optoelectronics applications is establishing properties of the free excitons and their excited states. It is difficult to underestimate the importance of such information since the spectral distance between the ground $E_{FE}(n = 1)$ and excited $E_{FE}(n = 2)$ states of the free exciton provides an accurate and independent value for the binding energy E_b of the exciton and thus for the band gap E_g, one of the most important parameters for any semiconductor, which is given by $E_g = E_{FE}(n = 1) + E_b$. Despite a significant amount of research on $CuInSe_2$ no information on the excited states of its free excitons can be found in the literature. Therefore the band gap in this material can not be considered as accurately established.

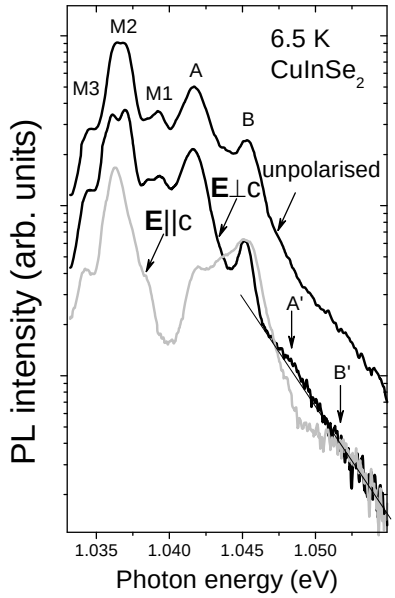

Figure 1. Near bandgap regions of the PL spectra in $CuInSe_2$ single crystals taken for the non-polarised as well as for $\mathbf{E}\perp\boldsymbol{c}$ and $\mathbf{E}\|\boldsymbol{c}$ polarised conditions. The A and B free excitons reveal their first (n = 2) excited states A' and B'.

Single crystals of $CuInSe_2$ were grown by the vertical Bridgman technique. Oriented samples were examined by polarisation resolved photoluminescence (PL) at 6.5 K. **Figure 1** shows the free exciton region of PL spectra with the polariser oriented perpendicular $\mathbf{E}\perp c$ and parallel $\mathbf{E}\|c$ to the c axis along with the unpolarised spectrum. The spectra reveal the A and B free excitons as well as the M1, M2 and M3 bound excitons as established earlier [1]. The A free exciton is polarised perpendicular to the c-axis, consistent with the Γ_{6v} - Γ_{6c} transition selection rule [2]. The B exciton is represented by the Γ_{7v} - Γ_{6c} transition, which is allowed in both the $\mathbf{E}\perp c$ and $\mathbf{E}\|c$ polarisations, and therefore its intensity does not change much as the polarisation changes. With the intensity of the A exciton minimised ($\mathbf{E}\|c$) the n = 2 excited state of B can be seen. With the intensity of the B exciton minimised ($\mathbf{E}\perp c$) the n = 2 excited state of the A exciton is resolved.

The energies of the first (n = 2) excited states for the A and B free excitons are 1.0481eV and 1.0516eV, respectively. Accurate values of the A and B exciton binding energies have been calculated assuming a hydrogenic model, giving $E_b^A = 8.5$ and $E_b^B = 8.4$ meV. The model also gives values for the Bohr radii $a_B^A = 7.5$, $a_B^B = 7.5$ nm as well as the static dielectric constant $\varepsilon = 11.3$. The bandgaps of the A and B excitons are estimated as 1.0502 eV and 1.0537 eV, respectively, at 6 K.

Acknowledgement: This work has been supported by the EPSRC (EP/E026451/1), the Royal Society (RD5529), GHML SE3703 and Belarus Council for Fundamental Research (F09MC-003).

[1]. A.V.Mudryi, M.V.Yakushev, R.D.Tomlinson et al. *Appl. Phys. Lett.* **77** (2000), p. 2542.
[2]. J.L.Shay, H. M. Tell, H. M. Kasper et al. *Phys.Rev. B* **7** (1971), p. 4485.

P6-1

Switching of multiples solitons in arrays of coupled cavities

Keivan M. Aghdami[1], Reza Kheradmand[2] and Roghayyeh Karimi[2]

[1] Physics Department, Payame-Noor University, Mini City, 19569 Tehran, Iran
[2] Research Institute for Applied Physics and Astronomy, University of Tabriz, 51665-163 Tabriz, Iran

K_aghdami@pnu.ac.ir, Cell: (+98) 9141184624/ Fax: (+98) 4812245115

We consider an array of coupled nonlinear cavities with Kerr nonlinearity in de-focusing case which is excited by an external driving field (Fig. 1). Properties of their nonlinearly localized modes frequently termed discrete cavity solitons differ considerably from those of their continuous counterparts [1,2]. The appropriately scaled evolution equations for the slowly varying envelopes read as [1]

$$i\frac{\partial u_n}{\partial T} + C(u_{n+1} + u_{n-1} - 2u_n) + (i+\Delta)u_n + \gamma|n_n|^2 u_n = E_0 e^{iqn} \tag{1}$$

In Eq.(1) all quantities are dimensionless where the evolution time are scaled by the photon lifetime and the field amplitudes by the effective nonlinear coefficient. Now C accounts for the next-neighbor evanescent coupling between cavities, Δ for the detuning from the cavity resonance, E_0 for amplitude of holding beam, T for time and γ for the sign of nonlinearity (+1 for the focusing and −1 for the self-defocusing case, respectively). In this paper we concentrate to self-defocusing state i.e $\gamma = -1$.

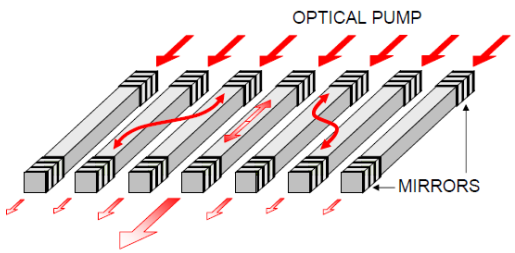

Figure 1. A arrays of coupled cavities

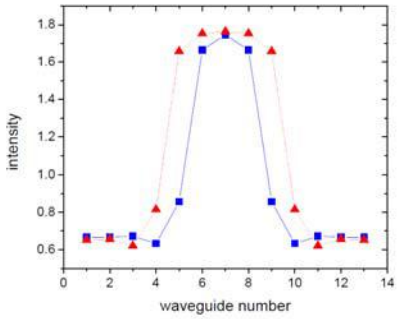

Figure 2. two different orders of stable solitons

Numerical methods are used to integrate coupled equations (1) to simulate dynamics of light propagation in these systems. It was observed that superposition of appropriate Gaussian control beam and plane wave holding beam can be used to write and erase of discrete cavity soliton in given place and switch between different orders of solitons (Figure 2) to each other. This method develops as an important issue of light control and all optical switching.

[1]. U. Peschel, O.A. Egorov, and F. Lederer, Opt. Lett. **29** (2004), p. 1909
[2]. O. A. Egorov, F. Lederer, and Y. S. Kivshar, Opt. Express **15** (2007),p. 4149

P6-2
Control of self-focusing and self-defocusing in the array of waveguides

Keivan M.Aghdami, Fatemeh Mokhtari and Abdorrasul Gharaati

Physics Department, Payame-Noor University, Mini City, 19569 Tehran, Iran.
k_aghdami@pnu.ac.ir, Cell:(+98) 9141184624/ Fax:(+98) 4812245115

Spatial solitons are self-trapped and self-conducted beams which are formed due to a balance between diffraction and nonlinear phenomena like self-focusing. Discrete solitons which constitute special classes of spatial solitons are formed like array of bulk or surface waveguides because both diffraction and nonlinear phenomenon exist simultaneously in the environments with alternative and discrete change of refractive index [1]. In this article, propagation of a Gaussian beam in arrays of coupled waveguides in the absence and in presence of nonlinear phenomenon is studied by numerical solving the equations. Effect of inclined input Gaussian beam which lands on the edge of the waveguides is investigated and will be compared with experimental results.

Behaviour of light is described by one-dimensional discrete nonlinear Schrodinger equation for array of N waveguides [2]

$$i\frac{dE_n}{dz}+\beta E_n+C\left(E_{n-1}+E_{n+1}\right)+\gamma\left|E_n\right|^2E_n=0 \qquad (1)$$

'E_n' is field amplitude in nth waveguide, C is coupling coefficient and β is light propagation constant in the waveguide and the fourth term illustrates nonlinear Kerr phenomenon in which γ is proportional to the Kerr constant, n_2. Self-focusing medium with γ>0 is taken into account in this paper.

Runge-Kutta method is used in order to solve coupled equations (1) and to simulate light propagation. As previous works [2] our results in the absence of nonlinear Kerr phenomenon (γ=0) shows normal dispersion when light is shined to entrance facet perpendicularly (Figure 1-a). But in awry radiation, when the input light takes tilt angle 't' respect to waveguides axis, initial phase become different in adjacent wave guide. Outgoing beam width decreases by increasing tilt angle and reaches its minimum in t=1.1° corresponds to π/2 in adjacent waveguide phase difference (Figure 1-b) which is known as soliton beam propagation [2]. After then beam width increases and experiences anomalous diffraction which is for discrete medium exclusively, maximum at t=2.2° (Figure 1-c).

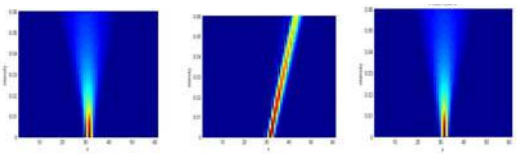

2.2° (c 1.1° (b t=0° (a

Figure 1. Intensity distribution of a Gaussian beam while pass the waveguides.

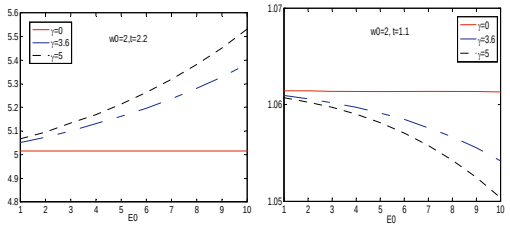

t=2.2° (b t=1.1° (a

Figure 2. Output over input beam width ratio for two tilt angle respect to beam intensity for γ=0 (line), γ=3.6 (dash) and γ=5 (dot).

Moreover, effect of nonlinear Kerr phenomenon is investigated. According to our results, in presence of positive Kerr coefficient in waveguides (self-focus), system shows different convergence/divergence behaviour for the beam depend upon tilt angle. Beam converges more by increasing γ when beam is inclined to t=1.1° (Figure 2-a) while it diverge for t=2.2° (Figure 2-b). The value of convergence/divergence is directly proportional to the input beam intensity.

[1]. Y.S.Kivshar and G.P. Agrawal, "OPTICAL SOLITONS From Fibers to Photonic Crystals", (Academic Press, San Diego,2003) p.386.
[2]. T. Pertsch and *et. al.*, *Phys. Rev. Lett* **88** (2002), p.093901.

P6-3

Incoherent Switching On/Off of Cavity Solitons in Semiconductor Microresonators above Laser Threshold

Reza Kheradmand and Mansour Eslami

Photonics Group, Research Institute for Applied Physics and Astronomy, Tabriz University, Tabriz, Iran

m.eslami87@ms.tabrizu.ac.ir, +989149104588

In this work we studied the Cavity Solitons (CSs) and their switching in a semiconductor Fabry-perot type microresonator where the active medium is multiple quantum well nano-structure. We take benefit of the full set of Maxwell-Bloch equations to describe the dynamical behavior of the system, since the rate equation model for a two-level system fails to explain the system when considering femto-second time scales in consequence of adiabatic elimination of polarization variable. The gain parameter which is included in polarization variable is one of the parameters in study, in that we considered nonlinear gain [1-3].

Stationary state studies of dynamical equations of the system show a bi-stable behaviour and stability analysis of the stationary state solutions results to instability domains which are slightly different from those of linear gain.

Numerical simulations imply formation of stable CSs which is done by local carrier injection as a switching method which has been investigated in this system. Using this method, which is introduced by the name of 'Incoherent Switching', we were able to simulate the solitonic branch. Since of the important applications of CSs is in information technology, it is essential for the CSs to be erased in the appropriate time. To switch off these CSs we used the same method but with negative amplitude of the injection function. It is also realized that the successive switching On/Off of CSs by such a scheme is possible in this system [4-5].

[1]. S. Barland, J. R. Tredicce , M. Brambilla, L. A. Lugiato, S. Balle, M. Giudici, T. Maggipinto, L. Spinelli, G. Tissoni, T. Knodl, M. Miller, And R. Jager, "Cavity solitons as pixels in semiconductor microcavities," *Nature*, vol. 419, pp. 699–702 , London, 2002

[2]. X. Hachair, F. Pedaci, E. Caboche, S. Barland, M. Giudici, R. Tredicce, F. Prati, G. Tissoni, R. Kheradmand, L. A. Lugiato , I. Protsenko and M. Brambilla, *IEEE* J, vol 12, No 3, 2006.

[3]. J. Yao, G. P. Agrawal, P. Gallion and C. M. Bowden, 'Semiconductor laser dynamics beyond the rate equation approximation,' Opt. Comm, 119, 246-225, 1995.

[4]. S. Barbay, Y. Ménesguen, X. Hachair, L. Leroy, I. Sagnes, and R. Kuszelewicz, 'Incoherent and coherent writing and erasure of cavity solitons in an optically pumped semiconductor amplifier *OPTICSLETTERS*, Vol.31, No.10, May15, 2006.

[5]. S. Barbay and R. Kuszelewicz, 'Physical model for the incoherent writing/erasure of cavity solitons in semiconductor optical amplifiers' *OPTICS EXPRESS,* Vol. 15, No. 19, 2007.

P6-4

Controlling and stabilizing of thermally travelling optical structures in semiconductor microresonators

Reza Kheradmand[1] , Najmeh Montazeri[1]

[1] Research Institute for Applied Physics and Astronomy, University of Tabriz, 51665-163 Tabriz, Iran

Montazeri.najmeh@gmail.com, +984113393008 /+984113344050

We consider a broad-area vertical-cavity semiconductor microresonator of the Fabry-Perot type with distributed Bragg reflectors. The Bragg reflectors and the active layer are orthogonal to the direction Z of propagation of the radiation inside the cavity. The dynamics of the system can be described by considering the intracavity electric field, the carrier density in the active material, and the temperature of the device.

We formulate a model that includes the thermal dynamics in time evolution of a semiconductor multiple quantum-well microresonator, driven by a coherent holding beam. The presence of thermal effects introduces a hopf instability which in certain regions of the parameter space, dominates the dynamics of the system. The oscillatory instabilities can develop a modulational character, meaning that travelling patterns can be found. These phenomena develop over the slow timescale (microseconds) characterizing thermal effects in the devices. As it has been studied in our last works both the amplitude and the phase of the injected field can be spatially perturbed with an optical mask [2]. We investigated a method for stabilizing and switching the travelling patterns by using spatial perturbation, which can be used as an all optical switch.

[1]. R.Kheradmand, M.Sahrai, H.Tajalli, G.Tissoni, and L.A.Lugiato, Eur. Phys. J.D 47(2008), P.107
[2]. R.Kheradmand, L.A.Lugiato and Tissoni ,Optics Express Vol.11 (2003),P 3612
[3]. L.Spinelli, G. Tissoni, M.Brambilla, F.Prati and L.A. Lugiato , Phys.Rew.A Vol.58 (1998) ,P. 2542
[4]. R. Martin, A.J. Scroggie, G.l.Oppo, and w.J.Firth, Phys.Rew.lett Vol.77 (1996), P.4007
[5]. A.J.Scroggie, J.M.McSloy, and W.J.Firth, Phys.Rew E66 (2002), P.036607
[6]. H.M. Gibbs, "Optical Bistability: Controlling light with light"(Academic Press, Orlando, FL,1985)
[7]. R.Ramaswami, K.N.Sivarajan, " in optical networks: A practical Perspective" 2end edn.(Morgan kaufman, San Francisco, CA,2002), Chap.12

P6-5

Phosphor materials for solid state white light generation

R.B.Jabbarov, N.N.Musayeva, S.H. Abdullayeva

H.M. Abdullayev Institute of Physics, Azerbaijan National Academy of Sciences
Research and Development Center for High Technologies, MCIT, Baku, Azerbaijan
e-mail: rjabbarov@physics.ab.az

Solid-state lighting (SSL) is emerging as a highly competent field and a possible alternative to existing lighting technologies. Using a blue LED to excite one or more visible light-emitting phosphors, which have been integrated into the phosphor-converted LED (pc-LED) package is a cost-competitive method. The pc-LED is designed to leak some of the blue light beyond the phosphor to generate the blue portion of the spectrum, while phosphor converts the remainder of the blue light into the red and green portions of the spectrum. Such phosphor-converted white LED represented as an innovation in solid-state lighting, because they are small, lightweight, has a long lifetime and they can easily operate.

Major developments in wide-band-gap III-V nitride compound semiconductors and color converted phosphors have led to the commercial production of white phosphor-converted light-emitting diodes. It is important to improve the conversion efficiency of the phosphor layer in order to meet the goal of solid-state lighting in the conventional pc-LED structure. For expanding LED applications toward general white lighting is very important to develop white LEDs as cost-competitive, energy-efficient alternative to conventional electrical lighting.

Phosphor materials play the most important role in light extraction and color control. The requirements of phosphor include: high absorption near corresponding wave lengths, high quantum efficiency, high color rendering index (CRI), high chemical stability to elevated temperature, and maintenance of high quantum efficiency in an encapsulating matrix.

Among the rare earth ions, Eu^{2+} emits intense and broad luminescence due to $4f^{6}5d \rightarrow 4f^{7}$ transition. The wavelength of its luminescence is strongly dependent on the crystal field strength and covalence of the local structure of the divalent rare earth ions, so that various emission wavelengths can be achieved depending on the crystalline host. In the present work, we have prepared InGaN light emitting diode structure by low pressure metalorganic vapor phase epitaxy on a c-plane sapphire substrate and bicolor composite phosphor doped with Eu^{2+} for creation white pc-LED. Intense green and red simultaneous emission were observed under (415-460 nm) excitation, where the red emission was considered to be due to the cascading excitation.

P6-6

Photoconductivity and photoluminescence spectra of $CdIn_2S_4$:Ti and $CdIn_2S_4$:Fe crystals

O. Kulikova, A. Siminel, A. Kuznetsov, V. Tezlevan, L. Kulyuk

Institute of Applied Physics, Academy of Sciences of Moldova, 5 Academiei str., Kishinev, MD-2028, Moldova

e-mail: olga.kulikova@phys.asm.md, *fax:* +373 2 738149

Wide-gap semiconductor compounds with spinel structure doped with 3*d* transition metal ions continue to attract interest owing to their current and promising applications in solid-state lasers. In this work the steady-state photoluminescence (PL) and photoconductivity (PC) spectra of $CdIn_2S_4$ single crystals doped with Ti and Fe are investigated. Bulk stoichiometric $CdIn_2S_4$ crystals with Fe or Ti impurity (0.02-0.9 at.%) were grown using the method of gas transport reactions with halogen as a transport agent. The chemical composition of the host compound and the impurity concentration were measured by a Cameca SX-50 electron microprobe.

The steady-state PL and PC measurements were carried out at temperatures 80-300K in the wavelength range of 400-2000nm using PbS cell or photomultiplier as photo-detectors.

Photoconductivity spectra at 80K consists of two peaks with maxima at E_{PC1}~2.5 eV and E_{PC2} ~2.3 eV. The position of the edge peak at E_{PC1} corresponds to the characteristic region of optical absorption spectra (band-to band transitions) of the undoped samples. The PC spectral peak at E_{PC3}=2.05 eV manifested at T = 300K can be assigned to the Ti impurity.

The PL were excited using two lines – λ_{ex1}=532 nm and λ_{ex2}=633 nm, in accordance with the spectral positions of the PC peaks E_{PC2} and E_{PC3} respectively. The PL spectral maximum of $CdIn_2S_4$:Ti samples with a small concentration of Ti (less than 0.05 at.%) is located at 1.65 eV and corresponds to the radiative recombination of the excited carriers via intrinsic defects of the undoped $CdIn_2S_4$. Starting from the Ti concentration 0.05 at.% and higher the intra-center titanium emission suppresses the characteristic luminescence of $CdIn_2S_4$. The relatively heavy doped samples (0.2 at.%) exhibit a broad-band infrared emission centered at 1.32 eV. Under the "green" excitation ($\hbar\omega_{ex1}$), the steady-state PL spectra of $CdIn_2S_4$:Ti crystals consist of two broad bands centered at E_{PL1}=1.32eV and E_{PL2}=1.65eV. The contribution of the recombination emission caused by the defect states of the matrix is more intensive at shorter wavelength excitation (λ_{ex1} = 532 nm, $\hbar\omega_{ex1}$=2.33eV i.e. closer to E_g^{ind}) as well as at the temperature reduction. The increasing of the impurity concentration leads to the quenching of luminescence. It can be supposed that as in the case with α-$ZnAl_2S_4$:Ti spinel type crystals [1], Ti^{3+} ions in $CdIn_2S_4$:Ti are absent and the observed IR emission bands can be ascribed to the Ti^{4+} charge transfer transitions in the frame of the cluster composed of the central Ti^{4+} ion and six sulfur ligands. The ground state of this cluster is the $^1A_{1g}$.

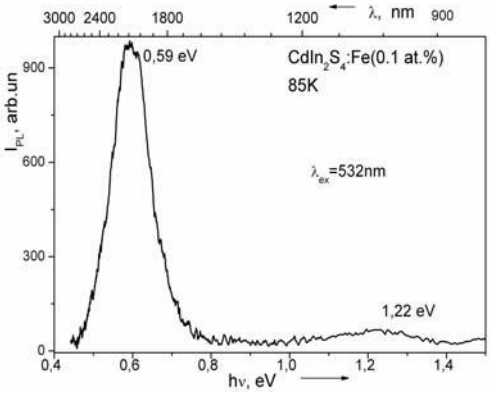

The PL spectra of $CdIn_2S_4$ single crystal doped with Fe measured at T=85 K contain several lines in visible and near infrared range of the spectrum. The high intensity spectral band at 0.59eV of $CdIn_2S_4$:Fe crystals may be related to the $^3T_1 \rightarrow {}^5E$ transition of Fe^{2+} ions. The weak luminescence at 1.22eV is attributed to the transition $^3T_1 \rightarrow {}^5T_2$.

The following mechanism of transitions is proposed: an electron from shallow donor → Fe^{3+} deep donor and subsequent emission identified as $^3T_1 \rightarrow {}^5E$ transitions at ions: $Fe^{3+} \rightarrow e_D \rightarrow Fe^{2+}(^3T_1) \rightarrow Fe^{2+}(^5E)$.

On the basis of the obtained spectroscopic characteristics the single coordinate configuration diagrams for both investigated crystals are constructed.

[1]. Anghel, G. Boulon, A. Brenier, E. Fortin, S. Klokishner, D. Koshchug, L. Kulyuk, K. Sushkevich, *J. Phys.: Condens. Matter* **Vol. 22,** Issue 5, (2010), p. 055903.

P6-7

Photoluminescence of $ZnGa_2Se_4$ and $ZnGa_2Se_4$: Eu

B.G. Tagiyev[1], O.B. Tagiyev[1,2], S.G. Asadullayeva[1]

[1]Institute of Physics of Azerbaijan NAS, H.Javid ave., 33

[2]Baku Branch of Moscow State University named after M.V. Lomonosov

e-mail: oktay@physics.ab.az

$ZnGa_2Se_4$ belongs to the group $A^2B_2^3C_4$ compounds (where A-divalent cations of Zn, Cd; B-trivalent cations of Ga, In, Al, but C- chalcogens of S, Se, Te). Presence of birefringence, optical activity, major values of non-linear susceptibility coefficient, wide band gap, bright luminescence, high sensitivity is characteristic of these compounds. Above-mentioned properties propose these compounds to be prospective materials for semiconductive optoelectronics. $ZnGa_2Se_4$ has been first synthesized by author, X-ray analysis has been carried out. It is shown that $ZnGa_2Se_4$ crystallizes in tetragonal structure (space group S_4^2), lattice parameters a=5.496A^0, c=10.99A^0, c/a=2.

For $ZnGa_2Se_4$ compound synthesis there have been used initial components Zn, Ga and Se which in stoichiometric relationship are charged into the ampoule and evacuated up to 10^{-4}mm Hg. Then the ampoule is placed into preliminary heated furnace up to 900^0 ~1000 ^{0}C. At 800^0-900^0C vigorous reaction has been started. Bu passing the reaction the temperature of the furnace rises slowly up to 1150 ^{0}C and holds 3 hours. At this temperature there has been take place remelting of synthesis product, then temperature decreases up to 500^0C and holds for 24 hours, then the furnace goes off and the ampoule cools within the furnace. Activation of $ZnGa_2Se_4$ compound by europium has been carried out in synthesis process. For $ZnGa_2Se_4$ activation EuF_3 compound has been used.

PL investigation results in $ZnGa_2Se_4$ and $ZnGa_2Se_4$: Eu compounds obtained at 77÷230 K . Samples are excited by Hg lines of wavelengths 365 nm and 375 nm. Excitement of $ZnGa_2Se_4$ and $ZnGa_2Se_4$: Eu mentioned wavelengths do not bring about significant change of PL spectrum form and appearance of new structures. PL intensity with the rise of temperature decreases. PL spectrum in $ZnGa_2Se_4$ is effective into the wavelength 530÷ 670 nm, in $ZnGa_2Se_4$: Eu into the wavelength 530÷ 630 nm. In $ZnGa_2Se_4$ spectrum only one maximum at 591 nm (2.10 eV) is shown in the investigated temperature range. At T 77 K in PL spectrum of $ZnGa_2Se_4$: Eu there have been 3 maxima; at 566 nm (2.19 eV), 591 nm (2.10 eV) and 646 nm (1.92 eV). Maxima at 591 nm and 646 nm at temperature above 100 K have not been observed. Analysis of obtained data shows that maxima at 566 nm in PL spectrum of $ZnGa_2Se_4$: Eu is caused by transition $4f^65d \rightarrow 4f^7(^8S_{7/2})$ of Eu^{2+} ion, but maxima at 591 nm and 646nm are related to donor-acceptor pairs [3]. Conducting experiments at various temperatures shows that maximum values at 566 nm in $ZnGa_2Se_4$: Eu and 591 nm in $ZnGa_2Se_4$ with the decrease of temperature have been increased. Half widths (FWHM) of PL spectra for both crystals with temperature rise have been increased.

There has been synthesized $ZnGa_2Se_4$ compound, lattice parameters (a=5.496 Å, c=10.99 Å, c/a=2) are determined, during the synthesis this compound is activated by Eu^{2+}. In PL spectrum of $ZnGa_2Se_4$ maximum at 591nm has been found out, in PL spectrum of ZnGa2Se4: Eu maxima at 566, 591 and 646 nm have been found out at 77÷230 K in $ZnGa_2Se_4$ and $ZnGa_2Se_4$: Eu compounds.At the temperature (T) of the temperature 77÷230K FWHM spectra varies within 0.4÷0.8 eV and 0.14÷0.18 eV, respectively. From analysis of temperature dependences Γ (T) probability of non-radiative transfers (A=10^8÷10^9sec^{-1}), energy of optical phonons ($\hbar\omega$=25÷30 meV), Huan Rice parameter (S=8÷10), energy of thermal quenching (ΔE=0.02÷0.06 eV) have been determined. PL spectrum maximum of $ZnGa_2Se_4$: Eu at 566 nm is due to the transition $4f^65d \rightarrow 4f^7(^8S_{7/2})$ of Eu^{2+} ions, maxima at 591 and 646 nm are due donor-acceptor pair.

P6-8

Laser heterostructures with ZnCdSe quantum well embedded in ZnMgSSe/ZnSe graded-index superlattice waveguide

G. P. Yablonskii[1], A. G. Vainilovich[1], E. V. Lutsenko[1], I. V. Sedova[2], S. V. Sorokin[2], S. V. Gronin[2], P .S. Kop'ev[2], and S. V. Ivanov[2]

[1] Stepanov Institute of Physics of NASB, Independence ave. 68, Minsk 220072, Belarus
[2] Ioffe Physical Technical Institute of RAS, Polytekhnicheskaya str. 26, St. Petersburg 194021, Russia

e-mail g.yablonskii@ifanbel.bas-net, phone/fax +(375) 17 2840428 / +(375) 17 2840879

Compact green semiconductor lasers are promising for numerous applications, like projection television, biological cell fluorescence studies etc. Optically pumped undoped II-VI heterostructures with ZnCdSe quantum well (QW) or quantum dot (QD) active region can be used as active elements of the green lasers, as demonstrating the high quantum efficiency and good enough degradation stability [1,2].

ZnMgSSe/ZnCdSe laser heterostructures emitting in green (λ~520 нм) were grown by molecular beam epitaxy (MBE) on GaAs(001) epitaxial buffers, using a two-chamber MBE setup. Their active region involves a single 7-nm-thick ZnCdSe QW surrounded by an extended ZnSe QW (Fig.1). An efficient carrier transport into the active region and localization of the fundamental optical mode maximum near the active region were provided by a ZnMgSSe graded-gap waveguide. Since it is difficult to grow the quaternary alloy with accurate simultaneous variation of Mg and S contents, keeping it lattice-matched to the GaAs substrate, the waveguide comprises a set of short-period (<4 nm) ZnMgSSe/ZnSe and ZnSSe/ZnSe superlattices (SL) with varying barrier-to-well thickness ratio, so that they provide both a potential gradient for the carriers, directed to the QW, and stress compensation within the waveguide. Photoluminescence (PL) and lasing were investigated under excitation by the HeCd (325 nm), N_2 (331.7 nm) and InGaN (416 nm) laser lines. The laser cavities were fabricated by cleaving the wafers along the (110) crystallographic planes.

The QW PL band intensity was established to be by 3 orders of magnitude higher than that from the waveguide (λ~450 нм) even at low excitation intensities, which confirms proper alignment of electronic subbands in the neighboring waveguide SLs, providing fast carrier transport to the QW. Lasing was achieved at 300 K under very low excitation intensity of 1.5 kW/cm^2 (Fig.2). The maximum external quantum efficiency was as high as 44.5 % at the output pulse power of 16 W.

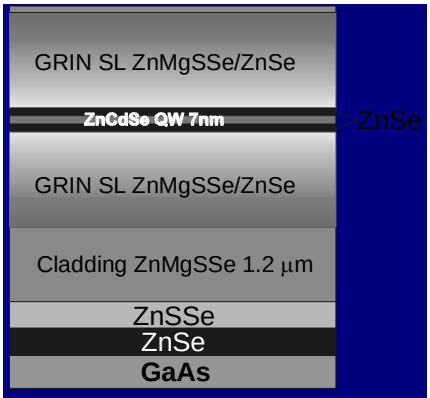

Figure 1. Design of the laser nanoheterostructure.

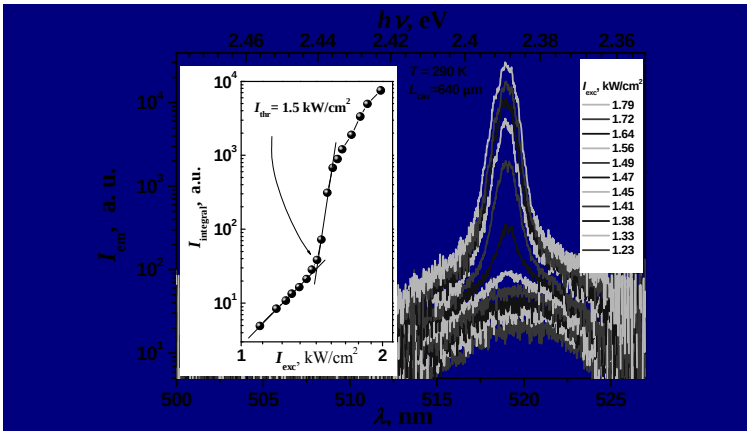

Figure 2. PL spectra below and above laser threshold. Inset shows the output intensity as a function of excitation density.

Thus, employing of the ZnMgSSe/ZnSe graded-index SL waveguide in the laser heterostructures with ZnCdSe QW active region has enabled fabrication of low-threshold high efficiency optically-pumped lasers emitting in the green spectral range (520 nm).

[1]. S. V. Ivanov et al., J. Crystal Growth **311**, 2009, p. 2120.
[2]. E. V. Lutsenko et al., Phys. Stat. Sol. b, 2010, 10.1002/pssb.200983275.

P6-9

Optical, luminescence and photovoltaic properties of layers and ZnO/CdS/$CuInGaSe_2$/Mo/glass heterostructures for solar cells

E. V. Lutsenko[1], A. G. Vainilovich[1], M.V. Rzheutski[1], V. N. Pavlovskii[1], G. P. Yablonskii[1], V.Y. Shiripov[2],S. M. Nastachkin[2], E.A. Hohlov[2]

[1] Stepanov Institute of Physics of NASB, Independence ave. 68, Minsk 220072, Belarus
[2] IZOVAC Ltd, P.O. Box 184, Minsk 220040, Belarus
e-mail e.lutsenko@ifanbel.bas-net, phone/fax +(375) 17 2840419 / +(375) 17 2840879

Semiconductors compound $CuInGaSe_2$ (CIGS) is promising as the sun light absorber for thin-film solar elements which efficiency has exceeded 20% [1]. In this work, thin CIGS films were obtained using method of reactive magnetron sputtering of metal alloyed targets in selenium vapor, being promising for mass production, with multistage growth temperature alteration (from 340°C to 550°C) at Aspira setup produced by IZOVAC Ltd. A CdS buffer layer for heterojunction creation was deposited on the CIGS surface in a chemical bath from solution of thiourea, $CdCl_2$ and ammonia at 70°C.

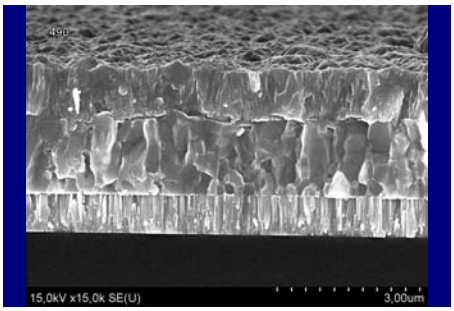

Figure 1. SEM CIGS solar cell

Top layers of ZnO:Al and ZnO were deposited by ion-beam sputtering. A typical SEM image of cleavage of the structure is presented in figure 1.
Photoluminescence and absorption spectra as well as influence of postgrowth annealing on separate CdS, ZnO:Al and CIGS layers were investigated under excitation by emission of HeCd and HeNe lasers. It was shown that annealing in neutral atmosphere of nitrogen of as deposited CdS and CIGS layers leads to an increase of photoluminescence intensity by several times and ZnO absorption edge becomes sharper at annealing on air.

Based on the investigations, a fabrication technology of ZnO/CdS/Cu(In,Ga)Se_2/Mo/glass solar cells and monolithically integrated modules based on them was developed.
The main characteristics (open-circuit voltage, short-circuit current, load characteristics, maximal power, fill factor and spectra of quantum efficiency) of the solar cell were investigated at excitation by Xe lamp and laser diode (λ=808 nm) emission.
It was shown that the external quantum efficiency in the short-circuit current regime at excitation by laser diode emission amounted the value of 93-95% in a wide interval of excitation intensities (from 10 to 600 mW/cm^2). This shows that practically all photoinduced charge carriers are effectively separated by p-n junction field. At that, maximal efficiency of a single cell of SC was reached at the emission power density of about 200 mW/cm^2 and it was equal to 22% (U=0.42 V, I=2.6 mA at I_{exc}=4.25 mW). The fill factor at this excitation intensity was of about 66% and open-circuit voltage was 0.54 V. Comparatively low conversion efficiency value in comparison with external quantum efficiency is obviously due to enough large series resistance of the solar cell and non-ideality of the p-n junction.
Maximal light conversion efficiency at excitation by white light of Xe lamp was reached as well at the emission power density of about 200 mW/cm^2 and it amounted the value of 14.5%. It should be noted that the given value is slightly understated in comparison with CIGS solar cell measurements on solar simulators of AAA type owing to small spectral mismatch between Xe lamp and sun emission. The excitation spectra of short-circuit photocurrent showed that photocurrent quantum efficiency drops drastically for wavelengths shorter than 530 nm. Thus lower solar conversion efficiency value is explained by both an absence of utilization of the emission with wavelength larger than 1000 nm defined by CIGS absorption spectrum with band gap E_g=1.1 eV and nonradiative recombination of photoexcited carriers absorbed in CdS layers as well as in density of states tails in ZnO:Al band gap.

[1]. http://www.renewableenergyfocus.com/view/9182/zsw-thinfilm-solar-cell-reaches-201-efficiency/

P6-10

Light emission of the gas discharge from nanopores of zeolite

N.N.Lebedeva, V.I.Orbukh, Ye.Yu.Bobrova, T.Z.Kuliyeva

Baku State University, Z.Khalilov str., 23, AZ-1148, Baku, Azerbaijan

nnlebedeva@gmail.com

The zeolites are the classic representatives of nanoporous materials.The zeolites are the nonstechiometric compounds whose compositions vary within the wide limits and form a variety of solid solutions. The zeolite value is caused by the scroll alumosilicate carcass forming the system of pores and cavities, the dimension of input window of which is enough big one that the molecules and ions of many organic and inorganic compounds can penetrate in them. The zeolite carcasses are like to bee`s cells and formed by chains of silico and aluminum anionites. The carcass has the negative charge because of its structure and this charge is compensated by water molecules and cations of alkali and alkali-earth metals weakly connected with it. The zeolite pores have the right forms. Connecting between each other through «windows» they form the perforated channel chain. That`s why the zeolites can be considered as the object on which besides well-known phenomena (adsorption, ion-exchange phenomena) investigate the electron porous emission, electron multiplication and gas discharge in pores.

The object of investigation was the zeolite of clinoptilolite type: monoclinic syngony,symmetry space group C2/m; elementary cell parameters: a=1.761nm, b=1.780nm, c=0.741nm, β=115.2°. For experiment the monoblock of the natural zeolite was wafering. The sizes of samples are 20x10x1.2mm. The chemical composition (is supporded by X-raying [1]) involved :Al_2O_3-11.36, SiO_2-67.84, KJ-11.64, Na_2O-1.25. K_2O-3.01,Fe_2O_3-1.19, MgO-0.49, P_2O_5-0.11,CaO-0.29, TiO_2-0.08, MnO-0.078.The zeolite wafer was assembled in a cartridge between two electrodes, one of them (the anode) was a conductive transparent SnO_2 layer deposited onto the glass disk. The cartridge was placed in a chamber eqipped with windows for visual or photographic recording of the gas-discharge`s light emission, with electrical leads-in, and with a tube fore exhausting the gas from the chamber.The current-voltage characteristics of zeolite wafer with push electrodes were measured at different fixed gas pressures in the chamber. The shape of I-V curves varies from linear to exponential with the increasing of V. At the voltages V_{ign} corresponding to transition from linear part of curve to the exponential part the luminous points appear on the wafer`s side pushed to anode.The dependence of $V_{ign}$ on gas pressure follows the Paschen`s law. Spectral composition of emission (0.3-0.4μ) conforms with gas discharge`s light emission in air. Gas discharge, homogeneous over the entire gap`s volume, arises in the discharge cell with the narrow (40-60μ) gap, where the cathode is a zeolite wafer. The gas discharge`s light emission can be observed visually through the transparent anode or can be amplified by electron- excited phosphor coating of anode (fig.1).

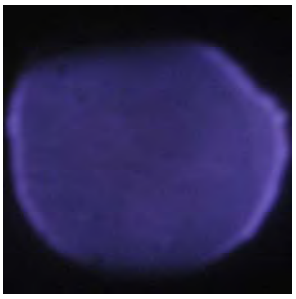

Fiq.1

[1]. T.Z.Kuliyeva, N.N.Lebedeva, V.I.Orbuh, Ch.A.Sultanov, Fizika, 2009, XV, №3, p.43
[2]. Н.Н.Лебедева, В.И.Орбух, Т.З.Кулиева, Ч.А.Султанов,Xəbərlər 2009, v.XXIX, №5, p.162

P6-11

Analysis of the enhancing effect of rare earth ion co-doping on the red emission of $CaGa_2S_4:Mn^{2+}$ in view of its decay time

Akihiro Suzuki[1] , Chiharu Hidaka[1] , Takeo Takizawa[1] , Shigetaka Nomura[2]
[1]Nihon University, 3-25-40 Sakurajosui, Setagaya-ku, Tokyo, Japan
[2] Tokyo University of Science, 1-14-6 Kudankita, Chyoda-ku, Tokyo, Japan
E-mail:akihiro_k_s_z_b@yahoo.co.jp

The ternary $CaGa_2S_4$ has been studied as a candidate for host materials of phosphors, because of its various emissions when doped with rare earth elements (REE) [1]. Especially, the compound doped with Ce^{3+} or Eu^{2+} shows blue or green emission with high intensity [2]. However, in order to obtain three primary colours from the same host material, red emission with sufficient intensity is required. We have found Mn^{2+} ions exhibiting red emission in $CaGa_2S_4$. As shown Fig.1, the emission was enhanced by co-doping with a REE^{3+} [3]. It is expected that there is energy transfer from REE^{3+} to Mn^{2+}. However, the origin of the enhancement is not well understood. The aim of the present paper is to explain the mechanism based on the study of emission decay.

Decay Curves of the Mn^{2+} red emission of $CaGa_2S_4$: Mn^{2+}, REE^{3+} prepared by the solid-state reaction have been measured. From the decay curves, it is found that the lifetime of the emission increases by doping a REE^{3+}. Figure 2 shows a tentative transition model including charge transfer from the trap levels of REE^{3+} ions to the excited d-states of Mn^{2+}, where *a,b,c* and *g* stand for the transition probabilities, and *A* and *B* represent the rates of electron excitation per unit time. From the solution of the rate equation derived from this model, the intensity of the emission from the d-d transition of Mn^{2+} is given as a function of time as

$$I = \left\{ \frac{aA}{P_1} + \frac{abB}{P_2}\left(\frac{1}{P_1} - \frac{1}{P_1 - P_2} \right) \right\} \exp(-P_1 t) + \frac{abB}{(P_1 - P_2)P_2} \exp(-P_2 t), \qquad (1)$$

where $P_1=a+c$ and $P_2=b+g$. This equation indicates two possible processes; one is a rapid decay and the other an afterglow. In the case of Mn^{2+} only doping, decay curves are expressed by a single exponential, while in the co-doping case of Mn^{2+} and REE^{3+}, two exponential components are needed. Moreover, from decay curves of the 5d-4f emission of REE^{3+}, it is found that the luminescence intensity and the decay time significantly decrease with the increasing the doping concentration of Mn^{2+}. These results suggest that there is energy transfer from REE^{3+} to Mn^{2+} arising from the overlapping d-levels of Mn^{2+} and REE^{3+}. The enhancement of the d-d emission of Mn^{2+} is due to the increase in number of electrons in the excited d-levels of Mn^{2+}.

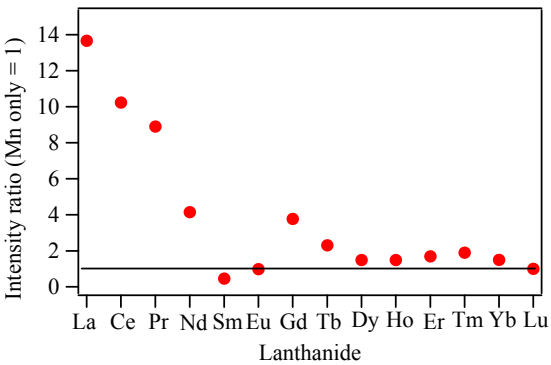

Fig.1 Enhancing effect of a REE^{3+} co-dopant on the Mn^{2+} red emission.

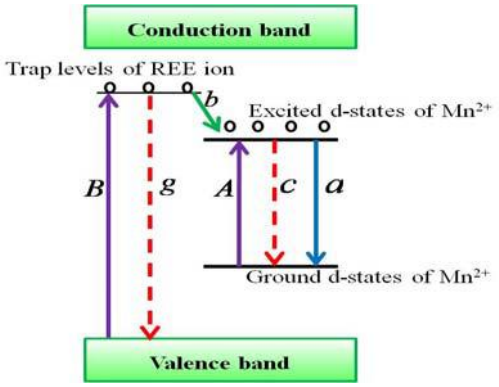

Fig.2 A tentative transition model in $CaGa_2S_4$: (Mn^{2+}, REE^{3+}.) system.

[1]. A.N.Georgobiani, B.G.Tagiev, B.M.Izzatov, Inorganic Materials, **31** (1995) 16-19
[2]. T.E.Peters, J.A.Baglio, J. Electrochem. Soc. **119** (1972) 230-236
[3]. F.Boitier, C.Hidaka, T.Takizawa, J. Lumin **129** (2009) 554-562

SECTION SEVEN

Photovoltaic, thermoelectric and multiferroic materials and applications

I7-1
Chalcopyrite solar cells: Formation of the buffer / absorber interface and related transport mechanisms

M. Rusu

Institut Heterogene Materialsysteme, Helmholtz-Zentrum Berlin für Materialien und Energie GmbH, Lise-Meitner Campus, Hahn-Meitner-Platz 1, 14109 Berlin, Germany

E-mail: rusu@helmholtz-berlin.de, phone / fax: +49 30 8062-2604 / -3199

We investigate the chemistry and electronics as well as the related transport mechanisms of low-gap chalcopyrite $Cu(In_{1-x}Ga_x)Se_2$- (CIGSe; Ga/(In+Ga) = 0.24) and wide-gap $CuGaSe_2$- (CGSe; $0.94 \leq Ga/Cu \leq 1.39$) based solar cells by addressing the following issues: (i) condition of the absorber surface, (ii) condition of the buffer layer preparation, and (iii) thermal annealing of the devices. The chemical structure is investigated by applying heavy-ion elastic recoil detection analysis (ERDA), non-destructive x-ray photoelectron spectroscopy (XPS) and x-ray emission spectroscopy (XES). The electronic structure is investigated by UV photoelectron spectroscopy (UPS) and Kelvin probe force microscopy (KPFM) in UHV ($p \leq 10^{-10}$ mbar). The device transport properties have been investigated by illumination- and temperature-dependent current-voltage [J(V,T)] measurements.

The investigation of the CdS/CIGSe interface formation by KPFM revealed a lower work function above the CIGSe grain boundaries (GBs) than above CIGSe grains [1,2]. This is ascribed to donor-like defects in CdS layers that are associated with S-related vacancies formed due to S diffusion into the CIGSe absorber along GBs. Pronounced S diffusion in CGSe films is also found in the ERDA study on the CdS/CGSe interface [3]. Furthermore, the ERDA and XES measurements reveal an additional Cd diffusion. Based upon those findings, a three-dimensional (3D) model for the buffer/absorber junction in chalcopyrite solar cells is proposed.

For low-gap CIGSe-based solar cells with physical vapor deposited (PVD) CdS buffer layers on fresh (Se-decapped) absorbers we additionally observe a thermally stimulated formation of a region with a higher band gap than that of the absorber bulk at the CdS/CIGSe interface, which determines the height of the potential barrier at the latter interface and, consequently the dominant thermally activated recombination process [1].

For wide-gap CGSe absorbers with bulk Ga/Cu ratios increasing from 0.94 to 1.39 a transition of the Cu:Ga:Se surface composition from 1:1:2 to 1:3:5 and a downward shift of the valence band maximum with respect to the Fermi energy were observed. At the CdS/$CuGaSe_2$ interface a "cliff-like" offset to the conduction band minimum of $CuGaSe_2$ is formed [4]. As a result, for respective solar cells we find that independently from the absorber bulk composition the dominant recombination process takes place at the buffer/absorber interface. However, while in devices from near-stoichiometric absorbers a tunnelling enhanced interface recombination takes place competitively at CdS/$CuGaSe_2$ – CdS/$CuGa_3Se_5$ interfaces, in solar cells from Ga-rich absorbers a dominant thermally activated Shockley-Read-Hall recombination via deep levels in the $CuGa_3Se_5$ layer occur at the buffer/absorber interface. Furthermore, we find that the monotonic increase of the devices open circuit voltages is determined by the monotonic variation of the potential barrier of recombination.

Acknowledgments: Gratefully acknowledged is Prof. M.Ch. Lux-Steiner for continuous support of the topic and all the colleagues who contributed to this work.

[1]. M. Rusu, Th. Glatzel, A. Neisser, C.A. Kaufmann, S. Sadewasser, M.Ch. Lux-Steiner, *Appl. Phys. Lett.* **88** (2006) 143510.

[2]. Th. Glatzel, M. Rusu, S. Sadewasser, and M.Ch. Lux-Steiner, *Nanotechnology* **19** (2008) 145705.

[3]. M. Rusu, M. Bär, S. Lehmann, S. Sadewasser, L. Weinhardt, C.A. Kaufmann, E. Strub, J. Röhrich, W. Bohne, I. Lauermann, Ch. Jung, C. Heske, and M.Ch. Lux-Steiner, *Appl. Phys. Lett.* **95** (2009) 173502.

[4]. M. Bär, M. Rusu, S. Lehmann, Th. Schedel-Niedrig, I. Lauermann, and M.Ch. Lux-Steiner, *Appl. Phys. Lett.* **93** (2008) 232104.

I7-2

Thermoelectric Functions in Multinary Intermetallic Clathrates.

Peter Rogl[1]

[1] Institute of Physical Chemistry, University of Vienna, Waehringerstrasse 42, A-1090 Wien,

peter.franz.rogl@univie.ac.at, phone: +43 1 427752456, fax: +43 1 42779524

The worldwide energy shortage and decreasing supplies of primary energy promote the increased use of thermoelectric devices. Automotive application of thermoelectric generators (TEGs) for the conversion of waste heat of combustion engines into electricity becomes a most timely issue. Following the "Phonon Glass–Electron Crystal" strategy (Slack, 1995), "intermetallic" clathrates - as cage compounds near a metal to insulator transition - have shown interesting thermoelectric properties due to their intrinsically low thermal conductivity and due to the tune-ability of structure-property relations by void filling, doping and selected atom substitution. Among the bulk of clathrate structure types, hitherto two series of clathrate type I compounds have shown TE properties with good thermoelectric efficiencies: $EA_8M_{16}Ge_{30}$ and multinary $EA_8M_{x1}M'_{x2}Ge_{46-x1-x2-y}\mu_y$ (EA=earth alkaline metal, M, M' are main group elements or a transition metal). The presentation will focus on the systematic of (i) type I clathrate formation/stability, (ii) crystallography of void-filling, and (iii) structure-TE property relations/bonding. Experimental routes to optimize TE-properties are backed by DFT–DOS calculations to monitor chemical stability, Seebeck coefficient, electrical and thermal conductivities. The correlations obtained, although not complete for many systems, may be useful in defining compositional regions of interest for further search/optimization of clathrate materials with technologically attractive thermoelectric properties.

Acknowledgments:
The financial support by the Austrian FFG, Project "THECLA" is gratefully acknowledged.

I7-3

Anisotropic Physical Properties in Sulfosalt Structures

H. Dittrich, D. Topa, A. Stadler, J. Stöllinger, A. Pachler, G. Aigner

Dep. Material Research and Physics, University of Salzburg, Hellbrunner Str. 34, A-5020 Salzburg

Complex crystal structures with low symmetry are characteristics of sulfosalt compound semiconductors [1, 2]. From more than 260 known sulfosalts, about 80% crystallize in the orthorhombic and monoclinic system. Therefore, physical properties can be strongly anisotropic and must be described by tensors. Due to possible applications in thermoelectric and photovoltaic energy conversion, anisotropic transport properties are of basic importance.
In this contribution, the anisotropic electrical conductivity of typical sulfosalts will be investigated and correlated to their crystal structures. Single crystals of natural grown bournonite ($CuPbSbS_3$) and jamesonite ($Pb_4FeSb_6S_{14}$) were oriented, cut, and polished. As a corresponding but more simple material, a stibnite crystal (Sb_2S_3) was cleaved to produce atomically smooth (010) crystal planes. The electrical conductivities in different directions of the polished and cleaved planes were measured by a 2point probe and a 4point probe technique. In addition, a newly developed micro-conductivity measurement system was used in SEM to scale down the measured region [3].
Results were correlated to the continuous axis of the different structures and the perpendicular directions.

[1]. Y. Moëlo, E. Makovicky, N.N. Mozgova, J.L. Jambor, N. Cook, A. Pring, W. Paar, E.H. Nickel, S. Graeser, S. Karup-Møller, T. Balić-Žunić, W.G. Mumme, F. Vurro, D. Topa, L. Bindi, K. Bente, M. Shimizu, J. Mineral. **20** (2008), 7-46.
[2]. H. Dittrich, A. Stadler, D. Topa, H.-J. Schimper, A. Basch, Phys. Status Solidi A **206** (2009), No. 5, 1034–1041.
[3]. www.capres.com

O7-1

Electronic structure and magnetism in multiferroic material $LuFe_2O_4$: first-principles calculations and spectroscopic studies

A. V. Postnikov[1], K. Kuepper[2], C. Taubitz[3], C. Derks[3], M. Neumann[3], D. Prabhakaran[4] and S. J. Blundell[4]

[1]LPMD, Institute Jean Barriol and Paul Verlaine University, 1 Bd Arago, F-57078 Metz, France
[2]Institute of Ion Beam Physics and Materials Research, Forschungszentrum Dresden-Rossendorf, P.O. Box 51 01 19, D-01314 Dresden, Germany
[3]Department of Physics, University of Osnabrück, D-49069 Osnabrück, Germany
[4]Department of Physics, Clarendon Laboratory, University of Oxford, Oxford OX1 3PU, United Kingdom

[1]e-mail: postnikov@univ-metz.fr, phone: +33-387315873, fax: +33-38731580

$LuFe_2O_4$, a compound exhibiting unusually large magnetoelectric coupling and an interplay between charge and spin degrees of freedom, was subject to a combined study by spectroscopic techniques: X-ray photoelectron spectroscopy (XPS), X-ray emission and absorption spectroscopy (XES, XAS), X-ray magnetic circular dichroism (XMCD), first-principles density-functional calculations and ligand field multiplet calculations. The study[1] lead to the following results.

1. From core-level XPS, the nominal charge state of iron is $Fe^{2.5+}$, or more specifically a perfect superposition of 2+ and 3+ charge states.
2. The combined use of XPS and XES allowed to reveal the composition of valence band, yielding good agreement with *ab initio* calculations. Those latter have been done using the WIEN2k code,[2] in the framework of the density functional theory (DFT), whereby the GGA+U technique was used to better account for correct energy placement of strongly correlated states of Fe and Lu. Specifically, the *U* parameter values of 0.7 Ry for Lu4*f* and 0.3 Ry for Fe3*d* states were found optimal to reproduce the positions of the corresponding peaks in the experiment. On this basis, the analysis of chemical bonding, charge and spin density distribution etc. could be performed, in order to predict the characteristics not directly probed by the actual experiments. We show that the inclusion of charge ordering in a tripled unit cell, with an appropriate arrangement of spins at the Fe sites, is essential for obtaining a correct electronic structure with a band gap.
3. The XMCD signal recorded at the Fe L_3 edge allowed, in a very neat way, to extract quantitative information about spin and orbital moments at the Fe sites, amounting to 1.1 μ_B and 0.76 μ_B per formula unit, correspondingly. It was found that all Fe^{2+} ions are in the majority-spin state, and among the Fe^{3+} one third is in majority and the rest in minority state. The subtleties related to the extraction of these numbers from the measurement, imposing the sum rules, etc. are analyzed.
4. For the theory description of XAS and XMCD signals, single-atom calculations with the *TT*-multiplets package[3] were used, which allowed to probe different spin orderings and resulted in very satisfactory agreement. As a by-product, the assumption of frustrated spin configuration suggested by Nagano *et al*.[4] was found to be inconsistent with the observed XMCD spectrum.

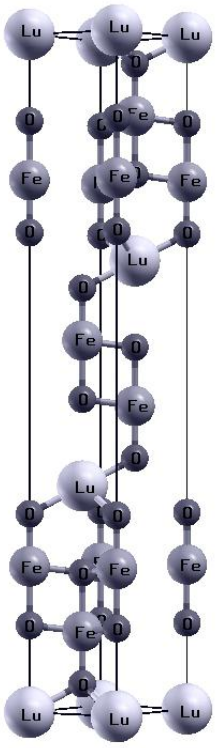

Figure 1. Hexagonal unit cell of $LuFe_2O_4$.

Acknowledgment: calculations have been done at the PMMS facilities at the Paul Verlaine University - Metz.

[1]. K. Kuepper M. Raekers, C. Taubitz, M. Prinz, C. Derks, M. Neumann, A.V. Postnikov, F.M.F. de Groot, C. Piamonteze, D. Prabhakaran and S. J. Blundell, *Phys.Rev.B* **80** (2009), p. R220409.
[2]. http://www.wien2k.at
[3]. F.M.F de Groot, *J.Electron Spectrosc.Relat.Phenom*. **62** (1993), p.111.
[4]. Nagano, M. Naka, J. Nasu, and S. Ishihara, *Phys. Rev. Lett*. **99 (2007)**, p. 217202.

O7-2

Surface and Interface Properties of chalcopyrite / ZnO interfaces

C. Pettenkofer, A. Hofmann
Helmholtz-Zentrum Berlin
Albert-Einstein Str 15
12489 Berlin
Germany
pettenkofer@helmholtz-berlin.de
Tel:-4930 63925696

Chalcopyrites are promising absorber materials for thin film solar cells. A Buffer of CdS is technologically used between Absorber and TCO window layer. To study the junction properties investigations on well defined model systems were performed. $CuInSe_2$ (112) and (001) surfaces were prepared by MBE and investigated by UPS, XPS, LEED and PEEM with respect to their junction properties to ZnO. ZnO as TCO is deposited by MOMBE or ALD in situ without breaking UHV conditions between preparation, transfer and analysis. Instead of an abrupt $CuInSe_2$-ZnO interface an intermediate ultra thin buffer layer of epitaxial ZnSe is formed on the chalcopyrite substrate despite of the admittance of the oxidizing agent (H_2O) in the MOMBE process. On top of a 2 monolayer thin ZnSe film ZnO growth is observed. ZnO grows for $CuInSe_2$ (112) in registry with the ZnSe(111) with its own lattice parameters in the (0001) direction as proven by LEED. Annealing to temperatures above the TCO deposition temperature shows In diffusion into the ZnO layer forming an oxide as derived from the Auger-parameter. Interfaces prepared by ALD and MOMBE will be compared with respect to junction formation and interface morpholgy. Energy filtered PEEM reveals an inhomogenity of the annealed interface with local In enrichment in the ZnO film. For the $CuInSe_2$ (001) substrate the same reaction is observed: an ultrathin ZnSe Bufferlayer growth before ZnO growth takes place. The Band alignments for the two different orientation will be given. Band alignments determined from our data for the in situ formed $CuInSe_2$-ZnSe-ZnO junction are beneficial for an application in solar cells.

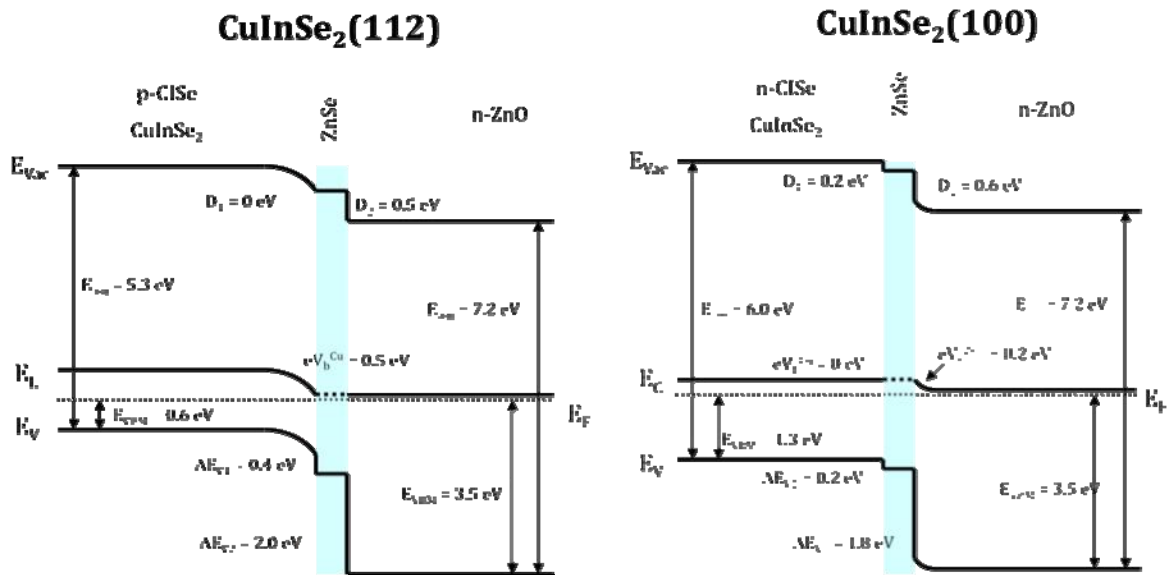

Figure 1, Bandalignment of the $CuInSe_2$-ZnSe-ZnO heterocontact for the (112) and (100) surface as determined by photoemission investigations.

O7-3

Time-resolved micro-photoluminescence studies of $Cu(In,Ga)Se_2$

T. Sakurai,[1] K. Taguchi,[1] M.M. Islam,[1] S. Ishizuka,[2] A. Yamada,[2] K. Matsubara,[2] S. Niki,[2] and K. Akimoto[1]

[1] Institute of Applied Physics, University of Tsukuba, Tennodai 1-1-1, Tsukuba, Ibaraki 305-8573, Japan.
[2] National Institute of Advanced Industrial Science and Technology (AIST), 1-1-1 Umezono, Tsukuba, Ibaraki 305-8568, Japan.

E-mail address: sakurai@bk.tsukuba.ac.jp; tel.: +81-29-853-6150; fax: +81-29-853-5205.

Study of the carrier recombination processes in $Cu(In_{1-x},Ga_x)Se_2$ (CIGS) is necessary for enhancing its device performance. In this study, we applied the time-resolved micro-photoluminescence (μ-PL) for the characterization of the carrier recombination in CIGS thin films.

$Cu(In_{1-x},Ga_x)Se_2$ ($x \sim 0.45$) thin films were grown on Mo-coated soda-lime glass substrates by means of the three-stage process using a molecular beam epitaxy (MBE) system. CdS layers were deposited on the CIGS films by chemical bath deposition to prevent the air oxidation of CIGS [1]. The time-resolved μ-PL was obtained at room temperature through the confocal laser scanning microscopy using a 635 nm diode laser for excitation. The CIGS-based solar cells fabricated with the same specimens gave the device efficiency of approximately 16 %[2].

Figure (a) shows the μ-PL intensity mapping image for the CIGS thin film. The detection wavelength was fixed at 1100 nm, which corresponds to the donor-acceptor pair emission of the CIGS thin film. The spatial distribution of PL intensity (~10 μm) is much larger than the grain size of ~1 μm; thus, we cannot confirm the carrier recombination at the grain boundaries. Figure (b) shows the PL decay curves at points (i) and (ii) in Fig. (a), suggesting the bright- and dark-PL spots, respectively. We observed that the PL decay lifetime at the point (i) was much longer than that at the point (ii), corresponding to the PL intensity. The reduction of the PL decay lifetime suggests the formation of non-radiative recombination center. From these considerations, we conclude the non-uniform distribution of the non-radiative recombination centers in CIGS thin films affects the carrier recombination processes in solar cells.

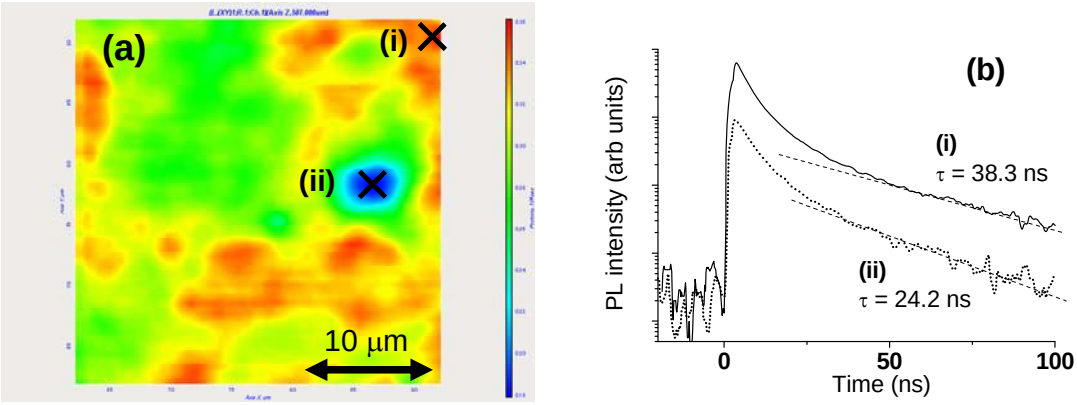

Figure (a) 30 × 30 μm^2-scale micro-PL intensity mapping image for the CIGS thin film; (b) PL decay curves at the points (i) (bright spot) and (ii) (dark spot) shown in Fig. (a).

Acknowledgments: This work was supported in part by the Incorporated Administrative Agency, New Energy and Industrial Technology Development Organization (NEDO).

[1]. W.K. Metzger et al., Thin Solid Films 517, 2360 (2009).
[2]. T. Sakurai et al., Sol. Energy Mater. Sol. Cells, in press.

P7-1

Thermoelectric properties of $Pb_{1-x}Mn_xTe$ single crystals

E.A. Allahverdiyev, G.Z. Bagiyeva, G.M. Murtuzov, D.Sh. Abdinov

Institute of Physics, Azerbaijan National Academy of Sciences, H. Javid 33, AZ 1143 Baku, Azerbaijan
eynullaa@rambler.ru, Phone: (99412) 432 52 34

$Pb_{1-x}Mn_xTe$ single crystals have been grown by the Bridgman method. In the 80 ÷ 300 K temperature region thermo-e.m.f. (α), electrical conductivity (σ), Hall (R_h) and heat conductivity (χ) factors have been investigated.

It have been shown that values and temperature dependences of kinetic factors of the compounds are essentially determined by structural defects, structure of the valence band and manganese atoms content. The analysis of the temperature dependence of electrical conductivity and Hall factor show that in samples at ~ 77 K not completely ionized acceptor centers exists with 0.1 eV activation energy, those with a high probability are caused by deformation defects of crystals arising during their growing. With increasing of the temperature these centers being ionized result in increasing σ and reduction R_h. With increasing of the temperature, as well as with introduction Mn atoms the energy gap between two valence bands decreases that results in growth of relative concentration of heavy holes in conductivity. In result the average effective mass of holes increases that causes growth of the thermo-e.m.f. factor.

The analysis of results of research of heat conductivity for $Pb_{1-x}Mn_xTe$ was made under the assumption of elastic scattering of charge carriers, a parabolic band and arbitrary degeneration. It is appreciated values of electronic and lattice parts of heat conductivity. With increasing of temperature total and lattice heat conductivities decrease. The increase in manganese contents also results in reduction in the total and lattice heat conductivities. At annealing curing of structural defects occurs that results in growth of the total and lattice heat conductivities. Concentration of the specified dot defects in non-annealed single crystals has been determined and it is shown that this concentration is in a good agreement with the data received from the Hall factor. It is established that heat transfer in $Pb_{1-x}Mn_xTe$ single crystals is realized basically by phonons.

Researches also have shown that small substitution (up to 4 at. %) of Pb atoms by Mn atoms possible to improve thermoelectric quality factor Z of PbTe crystals at low temperatures that is caused by change of the energy gap between edges of heavy and light hole bands, resulting in change of width of the forbidden band and average effective mass of holes, optimization of the concentration of the charge carriers, as well as reduction of lattice part of the heat conductivity.

P7-2

Magnetic properties of Co implanted $TlInS_2$ and $TlGaSe_2$ crystals

T.G. Mammadov[1], F. Mikailzade[2], A.G. Şale[2], S. Kazan[2], R. Khaibullin[3], N.I. Khalitov[3], V.F. Valeev[3]

[1] Institute of Physics, Azerbaijan Academy of Sciences, 370143, Baku, Azerbaijan
[2] Department of Physics, Gebze Institute of Technology, Gebze, 41400, Kocaeli, Turkey
[3] Kazan Physical-Technical Institute, 10/7, Sibirsky Trakt, 420029, Kazan, Russia

mamedov_tofik@mail.ru, phone (+99412) 4397479 / fax (+99412) 4470456

In recent years there has been a great interest in magnetoelectric (ME) materials due to their attractive physical properties, multifunctionality, wide applications in the fields of sensors, data storage, transducers for magnetic-electric energy conversion, information technology, radioelectronics, optoelectronics, and microwave electronics [1]. In these materials the coupling interaction between ferroelectric and ferromagnetic substances could produce a magnetoelectric effect in which change in magnetization is induced by an electric field and change in electric polarization is induced by an applied magnetic field [2]. As it is known from the literature, a strong ME effect could be realized in the composite consisting of magnetostrictive and piezoelectric effects. In this frame the production and research of new composite structures, especially on the base of intensive incorporation of magnetic nanoparticles into the crystal matrix of ferroelectric crystals is of great interest.

In this paper the results of investigation of magnetization and magnetic resonance spectra of Co implanted $TlInS_2$ and $TlGaSe_2$ ferroelectric crystals in a wide temperature interval are presented. The samples were prepared by Co ion implantation into (001)- oriented single crystalline plates of $TlInS_2$ and $TlGaSe_2$ substrates at the fluences of between 0.5 and 1.5×10^{17} ion/cm^2 and with a current density of 8 μA/cm^2. Magnetic resonance measurements were carried out using commercial EMX X-Band (9.8 GHz) spectrometer. The static magnetization measurements made by VSM Magnetometer (PPMS, Quantum Design Corp.) for parallel orientations of the applied magnetic film with respect to the implanted surface plane in a wide temperature interval.

It has been revealed that the implantation with Co on different fluencies of metal concentrations produces a granular composite film in the surface layer of $TlInS_2$ and $TlGaSe_2$ substrates, which exhibits remarkable ferromagnetic behavior. Magnetic resonance measurements revealed Ferromagnetic Resonance spectrum from Co-implanted surface layer, exhibiting an out-of-plane uniaxial magnetic anisotropy. The magnetization measurements performed in a wdie temperature range show that the magnetic properties of the obtained ferromagnetic/ferroelectric structures display peculiarities near the temperatures of the structural phase transitions in $TlInS_2$ and $TlGaSe_2$ observed in recent years. It has been also shown that the magnetization and coercivity of ferromagnetic state depends on the fluence of implantation. The observed phenomena are discussed on the base of strong magnetic dipolar interaction between Co nanoparticles inside the granular composite film formed in a result of implantation.

Acknowledgments: The authors from Gebze Institute of Technology are indebted to Research Projects Commission of Gebze Institute of Technology for supporting this work by the Grant No. 2009-A11. The authors from Kazan Physical-Technical Institute, Russia, acknowledge support through the RFFI, Grant No. 07-02-00559, OFN RAN Programme "New materials and structures", and Russian Federal Agency on Education, contract P902.

[1]. G. R. Slemon, Magnetoelectric Devices Transducers, Transformers and Machines, Wiley New York, 1966.
[2]. M. Fiebig, J. Phys. D: Appl. Phys. **38** (2005) R123.
[3]. G. Dearnaley, J.H. Freeman, R.S. Nelson, J. Stephen, Ion Implantation, North-Holland, Amsterdam, 1973

P7-3

Band gap engineering in $Cu(In,Ga)(S,Se)_2$ absorber layer by technological regimes of synthesis

M.Tivanov[1], E.Zaretskaya[2], V.Gremenok[2], V. Zalesski[3]

[1] Belarusian State University, Nezavisimosti av. 4, 220030, Minsk, Belarus
[2] Scientific-Practical Materials Research Centre NAS of Belarus, P. Brovka str. 19, 220072, Minsk, Belarus
[3] B.I.Stepanov Institute of Physics NAS of Belarus, Nezavisimosti av. 68, 220072, Minsk, Belarus

E-mail address gremenok@ifttp.bas-net.by, phone +375172841249, fax number +375172840888

Using of semiconductor solid solution such as $Cu(In,Ga)(S,Se)_2$ allows to produce solar cells with the band gap changing throughout the absorber layer. Introduction of a band gap grading in the absorber can improve cell performance.
Back grading (increase of conduction band energy level towards the back contact) creates an additional drift field for the minority electrons which assists in carrier collection and reduces back contact recombination resulting in an increase of photocurrent. Front grading (the locally increased band gap in the space-charge region) results in the increase of open-circuit voltage.
In our work $Cu(In,Ga)(S,Se)_2$ thin films were prepared using reactive annealing of copper-indium-gallium alloy films in S/Se-containing atmosphere under the N_2 flow. As the band gap grading throughout the absorber layer is determined by the change of In/Ga and S/Se ratios, the AES depth profile was used to study the distribution of elements concentration in the volume of grown $Cu(In,Ga)(S,Se)_2$ films. The measured AES compositions as a function of depth were used to calculate the conduction band energy and valence band energy profiles throughout the absorber layer.
It was determined that using recrystallization temperature and partial pressure of S/Se vapor synthesis regimes the energy-band structure control of the synthesized layers is possible. This discovery is important for the design of band gap graded absorbers for high efficiency device fabrication.

Acknowledgments: This work has been supported by Belarusian Republican Fund for Fundamental Research and Belarusian SCPSR «Space researches».

P7-4

CdTe-based solar cells prepared by physical vapor deposition and close-spaced sublimation methods

R.Hajimammadov[1], N.Fathi[1], M.Sadigov[1], E.Mirzoyev[1], A. Bayramov[1], G. Khrypunov[2], N. Klochko[2], and T. Li[2]

[1] Institute of Physics, Azerbaijan National Academy of Sciences, H. Javid ave. 33, 1143 Baku, Azerbaijan
[2] National Technical University "Kharkiv Polytechnic Institute", 21 Frunze St.,61002 Kharkiv, Ukraine
bayramov@physics.ab.az, Phone: +99412 439 1308, Fax: +99412 447 0456

In the photovoltaic material family, cadmium telluride is regarded as one of the most promising material for fabrication of high efficiency polycrystalline CdTe/CdS thin film solar cells [1,2] because of its near-optimum band gap of about 1.46 eV and high optical absorption coefficient in visible range. The maximum efficiency of about 16.5% of the laboratory samples of polycrystalline CdTe based thin film solar cells was achieved by using nanostructured CdS:O window layer and the modified device structure [2]. In spite of the large lattice mismatch between cubic CdTe and hexagonal CdS (nearly 9.7%) the CdTe/CdS solar cells are characterized by essentially high efficiencies caused by interdiffusion at the junction interface removing the lattice mismatch [3]. "$CdCl_2$ heat treatment" is considered as a key step in CdTe/CdS device processing leading to interdiffusion between CdTe and CdS. It is usually carried out either by means of deposition of $CdCl_2$ layer onto CdTe surface with following air annealing or annealing the structure in $CdCl_2$ vapor. However in the former case the optimal cadmium chloride thickness value varies in the wide range depending on the base layer technology [4]. To identify the structural mechanisms leading to the solar cell efficiency increase we have studied the effect of "$CdCl_2$ treatment" on the output parameters of CdS/CdTe-based solar cells and crystal structure of the base layers deposited on glass substrates by different ways. In the first way both of CdS and CdTe layers were deposited by physical vapor deposition (PVD) method meanwhile in the second way the chemical bath deposition (CBD) and close-spaced sublimation (CSS) methods were used for CdS and CdTe films deposition, respectively.

The obtained heterostructures were then subjected to "$CdCl_2$ treatment". For the PVD structures, $CdCl_2$ films of different thickness were deposited onto unheated CdTe surface by vacuum evaporation and then were air-annealed at 430 ^oC during 25 min. $CdCl_2$ treatment results in the significant recrystallization of CdTe layer. The average grain size of the film increases from 1 μm to 4 μm due to the lattice strain caused by macrodeformations and stacking faults. The maximum efficiency (η=10.3%) of solar cells on the basis of cadmium telluride layers deposited by PVD method corresponds to 0,35 μm $CdCl_2$ thickness at "$CdCl_2$ treatment".

CBD/CSS samples were exposed to $CdCl_2$ vapor at 400 ^oC for 5-7 min in vacuum chamber in the presence of 100 torr oxygen and 400 torr helium [5]. "As-grown" CdTe films were characterized by clearly faceted surface morphology and an average grain size of about 3-4 μm. Unlike the thermally evaporated CdTe films, no considerable changes after $CdCl_2$-treatment in the structural properties and surface morphology were observed for the CdTe films obtained by CSS method. The difference between the results on $CdCl_2$-treatment can be explained by a lower concentration of defects and grain boundary area in CSS deposited CdTe films resulting in lower lattice strain energy which promote recrystallization and grain growth. As a result the CSS deposited CdTe films do not recrystallize at the temperatures and times used in the $CdCl_2$ treatment. The highest efficiency in the CBD/CSS fabricated solar cells was obtained with the parameters: V_{oc}=773 mV, J_{sc}=23.92 mA/cm^2, fill factor (FF)=68.7%, a total area conversion efficiency of 12.71%

Acknowledgments: The work was supported by STCU under Project 4301

[1]. J. Britt and C. Ferekidis, Appl. Phys. Lett. 62, (1993), p 2851.
[2]. X. Wu, Sol. Energy, 77, (2004) , p.803.
[3]. D. G. Jensen, B. E. McCandless, and R. W. Birkmire, 25th Photovoltaic Specialists Conference, (1996), p. 773.
[4]. H. Moutinho, F. Hasoon, F. Abufoltuh, and L. Kazmerski, Journal Vacuum Science Technology, 13, (1995), p.2877
[5]. D. H. Rose, F. S. Hasoon, R. G. Dhere, D. S. Albin, R. M. Rebelin, X. S. Li, Y. Mahathongdy, T. A. Gessert, and
[6]. P.Sheldon, Prog. Photovolt.: Res. Appl. 7, (1999), p.331.

P7-5

Peculiarities of I-V characteristics of tunnel MIS structures Al-p-CdxHg1-xTe

E.K. Huseynov, N.J. Ismaylov

Institute of Physics of National Academy of Sciences of Azerbaijan,
H.Javid avenue, 33, Az10043, Baku, Azerbaijan

emil@azeuro.net; Phone/Fax: (99-412)-432-4336

The narrow bandgap $Cd_xHg_{1-x}Te$ single crystals are still keeping the leading position in IR optoelectronics. Creation of large format matrix with the Schottky-barrier, MIS-structure and p-n junction basic elements is the main direction of the development of IR photodetectors. Among them the MIS-structures with tunnel dielectric thin layer are of special practical interest since they can be used as detectors with interior amplification.

In this work the results of complex studies of *I-V, C-U* characteristics and kinetics of photocurrent relaxation of Al-p-$Cd_xHg_{1-x}Te$ structures with tunnel thin isolating layer measured at liquid nitrogen temperature are given. The structures were manufactured on the basis of p-$Cd_xHg_{1-x}Te$ with x = 0.25-0.3 and concentration of $N_a - N_d = (5\text{-}8)\cdot 10^{15}$ cm^{-3}. Semitransparent *Al* layer were deposited through a mask by thermal evaporation in vacuum.

Significant change of dark thermo-emission current of the structure due to the additional tunnel barrier was observed in the structure. However, the photocurrent equal to a photo-generation current occurs in the presence of illumination at some back bias V_0. Value of potential barrier φ_b as well as a sign of photocurrent shows that the photocurrent is transferred by minority charge carriers. The saturation of the *C-U* characteristics observed at the values $|U| > |U_0|$ indicates the formation of non-equilibrium depletion layer. Magnitudes of the dielectric capacity and differential resistance of the space charge area R_ω are found from the analysis of kinetics of photocurrent relaxation and *C-U* characteristics. It was established that the value of R_ω is limited by the surface leakage current that strongly weakens the dependence of voltage across the dielectric on the quantity of accumulation in the space charge area and as a result the amplification of photocurrent is absent. However, the realization of high amplification coefficient of photocurrent is probable at corresponding passivation of the surface.

P7-6

Reflectance Profile of $BaTiO_3$ on Multilayer Antireflection Coating Systems

Filiz Karaomerlioglu

Department of Electronic and Computer Education, Faculty of Tarsus Technical Education, Mersin University, Mersin Turkey
filizkrm@gmail.com, filizkrm@mersin.edu.tr, +90.532.4779815/ +90.324.6274804

Antireflection (AR) coating systems are very important technology for optoelectronic devices. The optical characteristics of the system can be regulated by external electric or thermal field, and designed broadband ultra low reflection coating systems.
We investigated optical properties of multilayer AR coatings based on different ferroelectric materials to reduce reflectance in other studies [24-28]. In this study, reflectance profile of $BaTiO_3$ on multilayer AR coating systems has been developed in the visible region. It has been used ZnSe and ZrO_2 as multilayer AR coatings, and $BaTiO_3$ as the substrate. Fortran program has been simulated on Fresnell equations base.

Key Words: Multilayer, Antireflection (AR) Coating, $BaTiO_3$

Acknowledgement
I would like to express my gratitude to Prof. Dr. Amirullah M. MAMEDOV for his guidance and suggestions.

[1]. Asghar, M. H., Khan, M. B., Naseem, S., Quantum Electronics & Optoelectronics, v:6, n:4 (2003), p:508.
[2]. Asghar, M. H., Khan, M. B., Naseem, S., Khan, Z. A., Tübitak Turk Jr. Phys, 29 (2005), p:43.
[3]. Azzam, R. M. A., Howlader, M. M. K., Optics Letters, v:26, n:20 (2001), p:1607.
[4]. Braun, D. M., Jungerman, R. L., Optics Letters, v:20, n:10 (1995), p:1154.
[5]. Lee, J., Tanaka, T., Sasaki, S., Uchiyama, S., Tsuchiya, M., Kamiya, T., Journal of Lightwave Technology, v:16, n:5 (1998), p:884.
[6]. Li, L., Dobrowolski, J. A., Sankey, J. D., Wimperis, J. R., Appl. Optics, v:31, n:28 (1992), p:6150.
[7]. Dobrowolski, J. A., Guo, Y., Tiwald, T., Ma, P., Poitras, D., Appl. Optics, v:45, n:7 (2006), p:1555.
[8]. Dobrowolski, J. A., Sullivan, B. T., Appl. Optics, v:35, n:25, p:4993, 1996.
[9]. Dobrowolski, J. A., Tikhonravov, A. V., Trubetskov, M. K., Sullivan, B. T., Verly, P. G., Appl. Optics, v:35, n:4 (1996), p:644.
[10]. Duyar, Ö., Durusoy, H. Z., Tübitak Turk Jr. Phys, 28 (2004), p:139.
[11]. Liou, Y. Y., Jpn. J. Appl. Phys., v:45, n:5A (2006), p:4051.
[12]. Liou, Y. Y., Jpn. J. Appl. Phys., v:41 (2002), p:5578.
[13]. Mclachlan, A. D., Appl. Optics, v:17, n:3 (1978), p:447.
[14]. Mouchart, J., Appl. Optics, v:16, n:10 (1977), p:2722.
[15]. Poitras, D., Dobrowolski, J. A., Appl. Optics, v:43, n:6 (2004), p:1286.
[16]. Rancourt, J., Kamerling, M., Monaco, D., IEEE CH2953-8-91-0000 (1991), p:1518.
[17]. Schallenberg, U. B., Appl. Optics, v:45, n:7 (2006), p:1507.
[18]. Schulz, U., Schallenberg, U. B., Kaiser, N., Appl. Optics, v:41, n:16 (2002), p:3107.
[19]. Vassallo, C., Optical Amplifiers for Communication ,IEE Proceedings, v:137, n:4 (1990), p:193.
[20]. Tikhonravov, A. V., Dobrowolski, J. A., Applied Optics, v:32, n:22 (1993), p:4265.
[21]. Verly, P. G., Dobrowolski, J. A., Willey, R. R., Applied Optics, v:31, n:19 (1992), p:3836.
[22]. Yoldas, B. E., Partlow, D. P., Applied Optics, v:23, n:9 (1984), p:1418.
[23]. Macleod, H. A., (Adam Hilger Ltd, Brisol, 1986), p:519.
[24]. Karaomerlioglu, F., Mamedov, A. M., Optoelectronics and Advanced Materials, , v:1, n:8 (2007), p:408.
[25]. Karaomerlioglu, F., Modern Physics Letters B, v:24, n:11 (2010), p:1145.
[26]. Karaömerlioğlu, F., ÇÜFBE J. of Science & Engineering, 19(4) (2008), p:96.
[27]. Karaömerlioğlu, F., ÇÜFBE, PhD Thesis (2008).
[28]. Karaömerlioğlu, F., Mehmetov, E., ÇÜFBE J. of Science & Engineering, 18 (1) (2008), p:98.

P7-7

Quenching of short circuit current and excitonic decay in $CuGaSe_2$ single crystals

I. Kasumoqlu, I.A.Mamedova, Q.S.Mehdiyev

Institute of Physics of NAS of Azerbaijan
Baku, 370143, ave. H.Javid, 33, E-mail:ktaira@physics.ab.az

$CuGaSe_2$ single crystal is the representative of $A^IB^{III}C^{VI}_2$ ternary compounds group being isoelectronic analogous of $A^{II}B^{VI}_2$ group compounds. With a small exception, all compounds of $A^IB^{III}C^{VI}_2$ were p-type conducting. Some of these compounds have birefringence that is of interest for nonlinear optics [1]. Properties of these compounds vary over a wide range, that is why they represent interest for practical application. Electrical, optical and luminescent properties have been investigated [2-5].

This report deals with of investigation results of influence of γ-radiation on short-circuit current in $CuGaSe_2$ at 77K.

$CuGaSe_2$ single crystal has been grown by method of chemical transport reactions. $CuGaSe_2$ is p-type conductivity and is low-resistant ($\rho=10^3$ Ohm·cm). In was used as ohmic contacts. The measurements carried out in vacuum cryorefrigerator. Values of signals were measured by high-sensitive electrometrical voltmeter B7-30. Registration was carried out by method of comparison of spectra before and after radiation.

In unradiated $CuGaSe_2$ sample, the spectral dependence of short-circuits current in the range of 200÷1000 nm has complex character. Maximum of short-circuit current is observed at λ=710 nm. This spectral position is corresponds to energy of optical transitions from valence band to the conduction band. Quenching of current is observed at short-wave and long-wave range of spectra. The mechanism of impurity quenching is explained, if to use scheme of two-level model of recombination centres [6]. Electrical properties of $CuGaSe_2$ strongly depend on indemnification of donor and acceptor states, at the expense of existence of slow (r) and fast (s) recombination centers in investigated samples. Quenching maximum corresponds to position 2,7 eV in unradiated sample and 2,5 eV in γ-radiated sample.

Spectra of samples γ-radiated by 18 R/s doze during 5, 10, 15 minutes is changed. In spectra of current of sample radiated during 5 minutes, two lines in long-wave range (780nm, 820 nm) are observed, but in the case of radiation during 10 minutes, energy distance between these lines increased (735 nm, 840 nm). In the sample radiated during 15 minutes, these lines merge and are narrowed which is observed in the form of a narrow line at 710 nm. . Sharp decrease of short circuit current is also observed at ~710 nm. Current quenching in short-wave range increases. Sharp decrease of short-circuit current is also observed at ~710 nm, corresponding to excitonic position. We consider this behavior is excitonic decay.

[1]. G.D., Bold, H.Kacper, Mc FEE, HJEEE J. of Quantum electronics N12, 1971
[2]. Mandel,L., Tomilson,R D and Hampshire, M J, H Neuman Solid state communications, V.32, pp.201-204 (1979)
[3]. C.Paorisi, N.Romeo G., Sbervegliers and I.Torricone, J.Luminescence 15 (1977) 101
[4]. A.V.Mudrui, I.V.Bodnar, I.A.Victorov, V.F.Gremenok, A.L.Patuk and I.A.Shakin, Conf. On Ternary and Multinary Compounds, ICTMC-11, Salford, 8-12 September, 1997
[5]. Kasumoglu I., Kerimova T.G., Mamedova I.A., Mehdiyev Q.S., Aliyev *M.A.*/Xeberler, Transactions, HAS Azerbaijan, 2010, №2
[6]. L.G.Paritskiy, S.M.Rivkin, Soviet Semiconductors (fizika i tekhnika poluprovodnikov)ç v.1, N.5, p.718, (1967)

P7-8
The impedance spectra and current voltage behaviour of MSM junction structure

A. Sertap Kavasoglu[*a,b], Nese Kavasoglu[a,b], Ozcan Birgi[a,b], and Sener Oktik[a,b]

[a]*Mugla University, Clean Energy Research & Development Centre, 48170-Kotekli, Mugla, Turkey*
[b]*Mugla University, Faculty of Arts and Sciences, Department of Physics, 48170-Kotekli, Mugla, Turkey*

E-mail address : sertapster@gmail.com, phone : +90 252 2111674

In this work, theoretical impedance spectra and current-voltage relation of Metal-Semiconductor–Metal (MSM) device structures are studied by writing programs Qbasic and FORTRAN routine in the frequency range between 5 Hz and 13 MHz. The current-voltage and impedance characteristics of a MSM (based on two metal-semiconductor contacts connected back to back) have been studied theoretically at different temperature by considering the thermionic field emission theory. MSM based photodetectors from various semiconductors material have been fabricated so far. A proper understanding of the MSM device operating condition is crucial. It is well known that the AC and DC electrical properties of the MSM device strongly influence the device performance. In particular, the accurate evaluation of impedance spectra data can give valuable information about operating frequency band and the AC electronical properties of the device. It has been shown that impedance spectrum of the device is strongly affected by device parameters of the two junctions. Especially, the barrier heights of the two sides play important role in device operating conditions. The Nyquist plot of the device exhibits depressed two semi-circles after critical threshold forward bias point and frequency depended dielectric loss tangent spectra exhibits significant peaks.

P7-9

Experimental investigation of photodetectivity on n-ZnO/p-Si heterojunction structure

Nese Kavasoglu[*1,2], A. Sertap Kavasoglu[1,2], Osman Pakma[1,2], Murat Kabakci[1,2], Ozcan Birgi[1,2], Sener Oktik[1,2]

[1] Mugla University Clean Energy Research & Development Centre, TR-48170, Mugla, TURKEY
[2] Mugla University, Faculty of Arts and Sciences, Physics Department, TR-48170, Mugla, TURKEY

e-mail address: knese@mu.edu.tr
phone/ fax number: +0090 252 211 1673

n-ZnO/p-Si heterojunction photodiode was fabricated by sol-gel spin coating deposition of n-ZnO layers on float zone <111> p-type substrates. Zinc acetate 2-hydrate[$Zn(CH_3COO)_2.2H_2O$] was dissolved in ethanol (C_2H_5OH) for preparing ZnO solution. Current–voltage (I-V) characteristics were investigated in dark and under illuminating conditions. n-ZnO/p-Si heterojunction photodiode shows typical rectifying behaviors in dark conditions. Photoelectric effects have been exhibited under illumination using monochromatic infrared light with a wavelength of 950 nm. Photodetector efficiency decreases as temperature increases. Photocurrent is strongly affected by illumination intensity between the temperature range of 70-160 K. Frequency dependent capacitance-voltage (C-V) measurements have been also performed for calculating space charge region width, interface state density and carrier concentration.

P7-10

Single-phase cadmium telluride thin films deposited by electroless electrodeposition

Khrypunov G.[1], Klochko N.[1], Volkova N.[2], Lyubov V.[1], Li T. [1]

[1]National Technical University "Kharkiv Polytechnic Institute", 61002, Frunze Str 21., Kharkiv, Ukraine
[2] National Aerospace University "Kharkiv Aviation Institute", 17 Chkalov St., 61070 Kharkiv, Ukraine

khrip@ukr.net, 380-572-971928

Today cadmium telluride (CdTe) is a leading base material for the fabrication of thin film solar cells. Equally with the creation of traditional thin film photovoltaic devices on the base of CdTe in recent years several approaches have been investigated to develop solar cells with extremely thin (80-500 nm) CdTe absorber (so-called η(eta)-solar cells) that offer the potential to reduce recombination losses in the base layers and thus use low cost materials. Until today the CdTe depositions for the η-solar cells manufacture were performed by vapour phase epitaxy under dynamical vacuum at working temperature 750^{o}C or by electrodeposition in the special electrochemical cell equipped with the potentiostat. Development research of simple and inexpensive method for obtaining of the single-phase stoichiometric cadmium telluride films has required an improvement of the electroless electrodeposition technique, which theretofore was characterized by some disadvantages, namely, the CdTe films were polluted by free tellurium additions and the composition of the films was Cd:Te=55:45. So, for the showing up the synthesis of doped or stoichiometric cadmium telluride films conditions and in order to decide the problem of the deposition of single-phase CdTe layers we have researched the electrochemical processes going during electroless electrolysis in sulfate solutions with different acidities and $CdSO_4$ concentrations. In addition we investigated influence of illumination on the film growth as such as impact of the illumination and "chloride treatment" on the film crystallinity.

In this research 100 – 300 nm thick CdTe films were deposited on glass substrates coated by indium tin oxide (ITO) layers or by tin oxide (TO) films (Pilkington) with sheet resistances of 20 Ohm/sq and visible transmittance of 80% by electroless electrolysis in sulfate solutions at 95^{o}C. Some film samples during deposition were illuminated by 500 W halogen lamp. Deposition time was 10-15 min. The phase composition and structure of the deposited films were determined by XRD-method, the average sizes of the crystalline grains in the films were estimated using Debye-Scherer formula. The transmittance spectra of the samples were measured by double beam spectrophotometer in the spectral range of 0.6-1.1 μm. Surface morphology of the films was researched by scanning electron microscopy.

By means of analysis of the electrochemical processes taking place during electroless deposition in aqueous cadmium sulfate and tellurium (IV) oxide solution we have elaborate method for obtaining of the stoichiometric cadmium telluride films. X-ray investigations of crystal structure of the film samples acknowledge the receipt of single-phase cadmium telluride films in the optimal conditions of the electroless electrodeposition. As a result of our researches, the stoichiometric single-phase CdTe films with a cubic structure were obtained by electroless electrodeposition in the solution contained 0.0002M TeO_2 and 0.2M $CdSO_4$ (pH 2). X-ray diffraction spectra exhibit the absence of the preferred orientations of the film grains. The illumination of the growing cadmium telluride layers has increased their thickness and improved film crystallinity. The following improvement of the CdTe structure was riched by "chloride treatment" of the electroless electrodeposited films by means vacuum deposition of $CdCl_2$ film onto CdTe surface and by subsequent air annealing at 430 ^{o}C for 20 min. As it has been shown by optical estimations, the CdTe absorption coefficients α for visible light were in order 10^5 cm^{-1}. The optical band gap values of the CdTe films obtained from transmission measurements and by plotting $(\alpha h\nu)^2$ vs. hν indicated that the electroless electrodeposited CdTe films represented direct band gap material. The intercept on the energy axis gave characteristic for CdTe value of the direct band gap.

Acknowledgments : The work was supported by STCU under Project 4301.

P7-11

Low material and energy saving close box $CuInSe_2$ film deposition technology

Khrypunov G., Khachenko M.

National Technical University "Kharkiv Polytechnic Institute", 61002, Frunze Str.21, Kharkiv, Ukraine
khrip@ukr.net, 380-572-971928

Presently the most prominent material for thin film solar cells (SC) is $CuInSe_2$ (CIS). Polycrystalline CIS thin film solar cells have shown long-term stable performance and high efficiency up to 20% under AM 1.5 illumination. Now certain companies in USA and Germany produce such solar cells in industrial mode. Costs of these CIS base SC are on the same level as of SC on the base of polycrystalline silicon, because the production of the last one requires consumptive equipment, high material and energy inputs. Traditionally high-performance thin film SC on the base of CIS is made by thermal vacuum evaporation method on glass substrates at substrate temperatures above 500 ^oC. Such high temperatures ensure intensive interphase interaction of the components in the open vacuum and obtaining of CIS layers characterized by optimal photoelectrical properties. Temperatures of indium and copper evaporators exceed 1000^oC that additionally enhances energy consumption of the technological process. In addition, it is common knowledge that source materials during thermal vacuum deposition are spent inefficiently and as such as film properties are very sensitive to the deviations of the composition, so expensive vapour phase control and direction systems must be used for the film deposition.

It has been shown before [1] that high Se–vapour pressure permits to improve the properties and morphology of CIS film. Such high Se–vapour pressure can be obtained by using close box deposition technique. In own developed close box technique for $CuInSe_2$ film deposition graphite chamber consists of three zones: Se evaporation zone, the vapour preparation zone and the condensation zone. The general idea of this technique is as follows: the film deposition is carried out in small evacuated chamber under conditions similar to thermodynamic equilibrium. This allows obtaining of the polycrystalline semiconductor films with perfect crystal structure. Such deposition conditions are obtained by decreasing of the difference between temperatures of evaporator and of the condensation surface. Therefore close box deposition technique is material- and energy saving technology.

With the aim to apply the close box deposition technique for the preparation of CIS thin films as base layer for the solar cells the investigation of the mechanisms of binary intermediate compounds of Cu-Se and In-Se systems formation and of their transformation into CIS were carried out. The first stage of these investigations had shown that reaction of elemental Cu with Se–vapor in close box deposition chamber begins as formation of Cu_2Se phase and continue up to the total utilization of elemental Cu. The temperature of Se–source is within the range 330-350^oC. Only after Cu_2Se phase creation the formation of more Se enriched phase starts in Se atmosphere. The rate of this reaction is less than rate of Cu_2Se formation. The film saturation by selenium is realized through chemisorption. Reaction kinetics is limited by selenium saturation of the film surface and by selenium diffusion into the film. At substrate temperatures below 320 ^oC the structures with variable compositions across films are formed. For the preparation of In_2Se_3 films in the close box deposition chamber In–source temperature was reduced to 400-580^oC, the Se-source temperature was 400-470^oC and the substrate temperature decreased to 350-400^oC. The process of In_2Se_3 film formation was multi-step one. On the first stage of this process the formation of some In-Se compounds on the In-grain surface took place. The following stage consisted in the evaporation and condensation of these compounds in order to create In_2Se_3. The subsequent annealing of Cu_2Se and In_2Se_3 films in Se–vapor results in formation of compound $CuInSe_2$.

Acknowledgments : The work was supported by STCU under Project 4301.

[1]. F.O. Adurodija, M.J. Carter and R.Hill, A novel method of synthesizing p-CuInSe2 thin film from stacked elemental layers using a closed graphite box, " 1st Word Conferences on Photovoltaic Conversion", Hawaii, December,1994, P.1-4.

P7-12

Electrical and photoelectrical properties of multi-component copper chalcogenides $CuSnAsSe_3$, $CuInAsSe_3$ and $CuInAsS_3$

Nina Melnikova[1], Ahmedbek Mollaev[2], Olga Kheifets[1], Luiza Saypulaeva[2], Fazil Gabibov[2], Abdulabek Alibekov[2], Alexey Babushkin[1] and Kirill Kurochka[1]

[1]Low Temperature Physics Dept ,Ural State University, Lenina Avenue, 51, 620083, Ekaterinburg, Russia
[2] Institute of Physics of Dagestan Scientific Centre of RAS, M.Yaragsky str., 94, 367003, Makhachkala, Russia
nvm.melnikova@gmail.com , +79221105853 / +7(343)2616885

The chalcogenides of copper and silver $ABCD_3$, A=Ag,Cu; B=Ge,Sn,Pb,In; C=As,Sb,Bi; D=S,Se, are novel objects for study. These compounds possess the interesting physical features: ferroelectric, piroelectric, photoelectric, optical [1-4]. The physical characteristics of such materials at high pressure are still not well investigated. We report here some results of the complex studies of physical characteristics of $CuSnAsSe_3$, $CuInAsSe_3$ which show ferroelectric properties and $CuInAsS_3$. The temperature dependences of conductivity and permittivity of the last compound are typical for ion conductor (the specific conductivity at 300 K is 0.01 S/m, at 78 - $7*10^{-5}$ S/m).
Photoelectrical studies were carried out at atmospheric pressure. Experiments were aimed at explanation of the influence of nonequilibrium carriers on ferroelectric characteristics and phase transitions and on determination of the spectral range of photosensitivity. The thermoinduced currents, photoconductivity, optical quenching of photoconductivity have been measured.
The spectral distribution of photoconductivity in $CuInAsS_3$ at 295 K is shown on Figure 1.

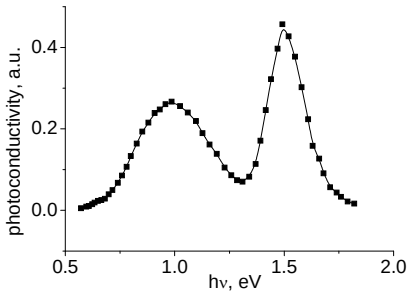

Figure 1. Spectral dependence of photoconductivity in $CuInAsS_3$, T=295 K, u=60 V, f= 12 Hz, Uo=4.6 mV

Electrical properties at high pressure were measured by impedance analyzer in the region of frequencies 0.1-200 kHz at pressure 12-50 GPa. High pressure up to 50 GPa has been generated in the diamond anvil cell (DAC) with anvils of the "rounded cone-plane" type made of synthetic carbonado-type diamonds. These anvils are good conductors and allow to measure the electrical properties of the sample placed in the DAC [5]. From analysis of the baric and frequency dependences of impedance, tangent of dielectric loss angle, resistance and conduction the ranges of the noticeable changes of electric characteristics were determined: 34-37 GPa in $CuInAsSe_3$ and $CuInAsSe_3$, 35-37 GPa and 39-41 GPa in $CuSnAsSe_3$. Changes can be connected to phase transitions at these pressures.

The researches were supported by Federal program “Scientific and research and educational personnel of the innovation Russia” to 2009–2013 and by RFBR grant No. 09-02-01316.

[1]. O.L.Kheifets, L.Ya. Kobelev, N.V. Melnikova, L.L. Nugaeva, Tech. Phys., **52**(1), (2007), p. 86.
[2]. O.L.Kheifets , N.V. Melnikova , A.N. Babushkin, Proc. Int. Conference “Phase Transitions, Criyical and Nonlinear Phenomena in Condenced Metter”, Makhachkala (2007), p.334.
[3]. O.L.Kheifets, N.V. Melnikova , L.A.Saipulaeva et al, Book of Abs. EHPRG 46. Conf.(2008), p.86.
[4]. O.L.Kheifets, N.V. Melnikova , A.N. Babushkin et al, Book of Abs. EHPRG 46. Conf.(2008), p.117.
[5]. L.F.Vereshchagin et al, High Temperatures - High Pressures, **6**, (1974), p. 499.

P7-13

Thermopower in the region of hopping conduction in $(TlInSe_2)_{0.2}(TlGaTe_2)_{0.8}$

S.N. Mustafaeva, A.I. Jabbarov

Institute of Physics, National Academy of Sciences of Azerbaijan, Baku
G. Javid pr., 33, AZ 1143, Baku, Azerbaijan
E-mail: solmust@gmail.com

Samples of the composition $(TlInSe_2)_{0.2}(TlGaTe_2)_{0.8}$ in the tetragonal system with the unit cell parameters a = 8.3455, c = 6.8254 Å are synthesized. The results of the investigation into the electrical and thermoelectrical properties of $(TlInSe_2)_{0.2}(TlGaTe_2)_{0.8}$ samples in the temperature range 77–347 K indicate that $(TlInSe_2)_{0.2}(TlGaTe_2)_{0.8}$ is a p-type semiconductor. It is found that, at temperatures ranging from 100 to 175 K, $(TlInSe_2)_{0.2}(TlGaTe_2)_{0.8}$ samples in a dc electric field possess variable-range-hopping conduction at the states localized in the vicinity of the Fermi level. The density of localized states near the Fermi level is determined to be $N_F = 3.18\times10^{19}$ $eV^{-1}\cdot cm^{-3}$, and the scatter of the states is estimated as J = 0.025 eV. Estimates are made for the average jump distance R = 84 Å.

At low temperatures (**Figure**) the thermopower of $(TlInSe_2)_{0.2}(TlGaTe_2)_{0.8}$ is adequately described by the relationship

$$\alpha(T) = (86 + 1.14T)\ \mu V/K, \tag{1}$$

which is characteristic of the hopping mechanism of charge transfer.

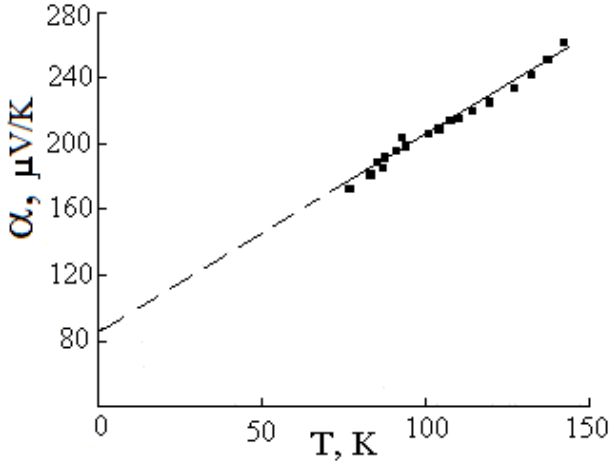

Figure. Low-temperature dependence of thermopower in $(TlInSe_2)_{0.2}(TlGaTe_2)_{0.8}$.

At temperarures from 300 to 347 K the thermopower of $(TlInSe_2)_{0.2}(TlGaTe_2)_{0.8}$ is described by the relationship

$$\alpha(T) = -\frac{k}{e}\left[\frac{\Delta E}{kT} - \frac{\gamma}{k} + 1\right], \tag{2}$$

where k is the Boltzmann constant, e is the elementary charge, ΔE is the activation energy of conduction and γ is the temperature coefficient of activation energy of conduction. It is found that ΔE = 0.24 eV and $\gamma = 1.86\times10^{-4}$ eV/K for $(TlInSe_2)_{0.2}(TlGaTe_2)_{0.8}$ samples.

P7-14

Development of high ZT didymium-skutterudites: thermoelectric and mechanical properties, thermal expansion.

Gerda Rogl[1,2,3], Andriy Grytsiv[1], Peter Rogl[1], Ernst Bauer[2], Michael Zehetbauer[3]

[1] Institue of Physical Chemistry, University of Vienna, Waehringerstrasse 42, A-1090 Wien,
[2] Institute of Solid State Physics, University of Technology, Wiedner Hauptstrasse 8-10, A-1040 Wien, Austria
[3] Group Physics of Nanostructured Materials, University of Vienna, Boltzmanngasse 5, A-1090 Wien, Austria

gerda.rogl@univie.ac.at, phone: +43 1 427752456, fax: +43 1 42779524

With a worldwide energy shortage and decreasing supplies of primary energy, thermoelectric devices are becoming more and more important. For high thermoelectric energy conversion efficiency, materials constraints request high ZT for both legs but also thermal expansion and mechanical properties are important features. The development of such alloys started from undoped antimonides towards doped and multi-filled skutterudites employing nanostructuring. This development can be outlined on various p-type didymium skutterudites showing ZT>1.2. With multifilling we gained n-type skutterudites with ZT>1.4. It is equally important to produce materials that show a good stability and sufficient mechanical strength for device integration. We calculated porosity, measured Vickers hardness, Young's modulus (RUS) and Poisson's ratio showing dependencies on hardness and porosity. A balanced thermal expansion coefficient for p- and n-legs is necessary to build thermoelectric generators, features we have successfully investigated. Although the car industry presently uses Bi_2Te_3-based thermoelectrica, our new materials are more promising due to the fact of being usable at temperatures up to 800 K.

Acknowledgments:
We thank the Treibacher Industrie AG, Austria for a generous supply of didymium and mischmetal.

P7-15

Thermal conductivity of $Sn_{3(1-x)}In_{2x}Te_3$ semiconducting phase

E.I. Rogacheva and O.N. Nashchekina

National Technical University "Kharkov Polytechnic Institute", 21 Frunze Str., 61002 Kharkov, Ukraine
E.I. Rogacheva: e-mail: rogacheva@kpi.kharkov.ua, telephone: +38 057 7076092

Thermal conductivity coefficient λ belongs to the most important parameters that determine the value of thermoelectric figure of merit of a material $Z = S^2\sigma/\lambda$ (S is the Seebeck coefficient, σ is the electrical conductivity), which, in turn, determines to a great extent the efficiency of thermoelectric converters. When developing thermoelectric materials and optimizing their properties, the formation of solid solutions is widely applied with a view to increasing Z.

Earlier we have established [1-3] that semiconducting $Sn_{3(1-x)}In_{2x}Te_3$ alloys based on tin telluride into which In_2Te_3 is introduced, after appropriate heat treatment aimed at reducing thermal conductivity, exhibit sufficiently high values of Z even at room temperature. This stimulates detailed studies of the thermal phenomena in the above mentioned alloys.

The goal of the present study is to investigate the temperature dependences of thermal conductivity of $Sn_{3(1-x)}In_{2x}Te_3$ phase with different indium concentrations and under additional introduction of dopants (Bi_2Te_3, PbTe and others) into the alloy with the minimum value of λ.

The thermal conductivity was measured by the dynamic calorimeter method using the monotonic heating mode in the temperature range 300-800 K with an error not exceeding ± 10 %. The measurements were carried out on cylindrical samples prepared by the hot pressing method at temperature 670 K and pressure 4 t/cm^2. The samples were annealed for 200 hours at 820 K and cooled down in air. Lattice thermal conductivity λ_p was separated from total thermal conductivity $\lambda=\lambda_p+\lambda_e$ by deducting the electronic component λ_e determined using the Wiedemann-Franz law. Electrical conductivity σ and the Hall coefficient R_H were measured by a conventional *dc* method with an accuracy not less than ± 5%. Charge carrier mobility was calculated as $\mu = R_H \cdot \sigma$

Using the above described methods, the temperature dependences of λ, R_H and σ were obtained. It was established that with increasing indium concentration the character of the temperature dependences of thermal conductivity changes. Up to x ~ 0.03, a drop in λ is registered with increasing temperature. Under further increase in In_2Te_3 concentration, λ grows with increasing temperature, i.e. an additional electronic mechanism of the heat transfer whose origin is not established yet and which is not accompanied by a significant increase in electrical conductivity comes into play. The change in the behavior of the temperature dependence of thermal conductivity with changing concentration x results in the fact that the maximum values of Z in the temperature range 600-900 K are observed in the alloy with x ~ 0.03, while the maximum values of thermoelectric power $P = S^2\cdot\sigma$ correspond to the alloy with x ~ 0.06. It was shown that additional doping with Bi_2Te_3, PbTe and other dopants does not lead to a decrease in thermal conductivity, and for all dopants λ grows as temperature increases.

On the basis of the temperature dependences, isotherms of λ and λ_p were plotted. In all the $\lambda(x)$ and $\lambda_p(x)$ dependences, similarly to what was observed at room temperature [1-3], sections of anomalous increase in λ and λ_p in the concentration range x ~ 0.03-0.06 were observed. It was found that the concentration dependences of hole mobility exhibit a similar non-monotonic behavior in the same concentration range. With increasing temperature, Z grows for all concentrations, and in the Z(x) isotherms the maximum in the vicinity of x ~ 0.03 becomes more and more distinct. The observed concentration anomalies of thermal conductivity, having to all appearance a general character, are of interest from the point of view of developing concepts of solid state physics in the field of the heat transport and should be taken into account when developing new high-efficiency thermoelectric materials.

[1]. E.I. Rogacheva, N.I. Dzyubenko, Proc. 18 Intern. Conf. on Thermoelectrics, Baltimore, 1999. p. 226.
[2]. E.I. Rogacheva, O N. Nashchekina, M.S. Dresselhaus, J. Thermoelectricity, **4** (2005), p.82.
[3]. E.I. Rogacheva, O N. Nashchekina, M.S. Dresselhaus, Proc. 22 Intern. Conf. on Thermoelectrics, La Grande Motte, 2003, p.263

P7-16

Structure and transport properties of the Pb<Bi>Te ternary semiconductor phase of variable composition based on PbTe

E.I. Rogacheva, O.S. Vodorez and V.I. Pinegin
National Technical University "Kharkov Polytechnic Institute", 21 Frunze Str., 61002 Kharkov, Ukraine
E.I. Rogacheva: e-mail: rogacheva@kpi.kharkov.ua, telephone: +38 057 7076092

Materials based on lead telluride semiconductor compound are placed among the best medium-temperature thermoelectric materials. Bismuth is one of the most important donor impurities in PbTe. The introduction of bismuth makes it possible to control electron concentration for attaining maximum values of thermoelectric figure of merit in lead telluride crystals and thin films. To control properties, it is necessary to know the mechanism of defect formation and character of the change in properties under the introduction of impurity.

Bismuth can be introduced into lead telluride in a number of ways: by cation substitution Pb→Bi [1], by introduction of elementary Bi into PbTe [2], by introduction of Bi_2Te_3 compound [3], etc. In this connection there arise questions regarding the electrical activity of Bi impurity, the character of the change in properties in each case, and selection of the optimal way of doping.

The goal of the present work is to study the crystal structure, mechanical, galvanomagnetic, and thermoelectric properties of the phase of variable composition based on lead telluride in the ternary system Pb-Bi-Te as functions of composition and temperature under change in composition along the PbTe-Bi_2Te_3 section (0 – 10 mol. % Bi_2Te_3). In [3], it was established that the homogeneity region of the PbTe<Bi> phase in the indicated section has maximum extension, however detailed and complex studies of structure and properties have not been performed.

The PbTe-Bi_2Te_3 alloys were synthesized by direct melting of high-purity components in evacuated quartz ampoules and subsequent homogenizing annealing at 820 K for 300 hours.

The dependences of unit cell parameter, width of X-ray diffraction lines and microhardness on Bi_2Te_3 concentration were plotted. It was found that within the homogeneity region of PbTe (~ 0 – 6 mol.% Bi_2Te_3) these dependences exhibit unusual for solid solutions non-monotonic behavior, which indicates qualitative changes in the defect subsystem of the crystal occurring under increasing Bi concentration.

The measurements of electrical conductivity, the Hall coefficient, and the Seebeck coefficient were carried out in the temperature range of 77-300 K. It was shown that within the homogeneity region, the inversion of the conductivity type from p to n takes place, and the isotherms of electrophysical, galvanomagnetic and thermoelectric properties have also a complex character. The results of the studies of structural and kinetic characteristics are in good agreement.

The experimental results were interpreted taking into consideration complex mechanisms of the defect formation occurring in the PbTe crystal lattice under the introduction of Bi_2Te_3, percolation effects and the possibility of the realization intermediate ordered structural states (for example, the processes of complex formation) in solid solutions.

The results obtained in this work were compared with the earlier obtained data on the character of change in the kinetic properties of PbTe under shift in the Gibbs concentration triangle along the PbTe- Bi [1] and PbTe-BiTe [2] sections.

[1]. E.I. Rogacheva and S.G. Lyubchenko, J. of Thermoelectricity, **3** (2005), p. 24
[2]. T.V. Tavrina, E.I. Rogacheva, V.I. Pinegin, Mold. J. Phys. Sci. **4** (2005), p.430.
[3]. E.I. Rogacheva, S.A. Laptev, V.S. Ploskaya, B.A. Efimova, Izv.AN SSSR. Neorgan. Mater. **20** (1984), p.1350.

P7-17

Impacts of electron irradiation on the optical and electrical properties of CIGS thin films and solar cells

M. Sugiyama[1], Y. Hirose[1], M. Warasawa[1], K. Takakura[2], S. Kimura[1], S. F. Chichibu[3] and H. Ohyama[2]

[1] Department of Electrical Engineering, Tokyo University of Science, 2641 Yamazaki, Noda 278-8510, Japan
[2] Department of Information, Communication and Electronic Engineering, Kumamoto National College of Technology, 2659-2 Suya, Koshi, Kumamoto 861-1102, Japan
[3] CANTech, Institute of Multidisciplinary Research for Advanced Materials, Tohoku University, 2-1-1 Katahira, Aoba, Sendai 980-8577, Japan
Presenting author optoelec@rs.noda.tus.ac.jp, phone/ fax number +81-4-7121-1585 (M. Sugiyama)

A thin film solar cell composed of polycrystalline Cu(In,Ga)Se_2 (CIGS) is essentially light-weight and shows high conversion efficiency and excellent radiation tolerance. These characteristics lead to CIGS solar cells very attractive for space applications. However, only a few irradiation studies have been carried out on CIGS thin films and entire solar cell structure, resulting in limited knowledge on the mechanisms responsible for the irradiation-induced damage [1]. In addition, the cell performance is known to change due to the damp heat and/or light soaking effects. Accordingly, understanding the degradation mechanisms of CIGS, ZnO, a buffer, Mo, and even glass components is necessary for not only space use but also commercial use. In this presentation, electron irradiation effects will be discussed for CIGS solar cells and each layer that composed the CIGS solar cell structure such as CIGS, CdS, undoped ZnO, and Ga- or Al-doped ZnO films.

Electron irradiation experiments were carried out using the DYNAMITRON electron accelerator. The electron energy was fixed at 2MeV and the fluence was varied between 1×10^{13} and 1×10^{18} cm^{-2}.

All the irradiated CIGS films exhibited common PL peaks originating from donor to acceptor transitions. PL peak intensity due to Cu-related point defects, which did not affect solar cell performance significantly, increased in CIGS thin films with increasing electron irradiation. Conversely, transmittance spectra of all the irradiated ZnO and ZnO:Al films did not change by the electron irradiation up to 6×10^{17} cm^{-2}.

The normalized performance parameters of the irradiated CIGS solar cell such as V_{OC}, J_{SC}, and η are shown in Fig. 1 as a function of irradiation fluence. η tended to decrease in comparison with V_{OC} and J_{SC} for large irradiation fluence. Shunt resistance and series resistance of the CIGS solar cells degraded even though the resistivity of each layer did not change after electron irradiation. The result indicates that CdS/CIGS interface or another heterojunction tended to degrade easily in comparison with each bulk of solar cell composed of semiconductors.

Acknowledgments: This work was supported in part by Inter-University Laboratory for the Joint Use of JAEA Facilities and by the Advanced Device Laboratories, Research Institute for Science and Technology, Tokyo University of Science.

[1]. M. Sugiyama *et al.* Jpn J. Appl. Phys 49 (2010) 042302.

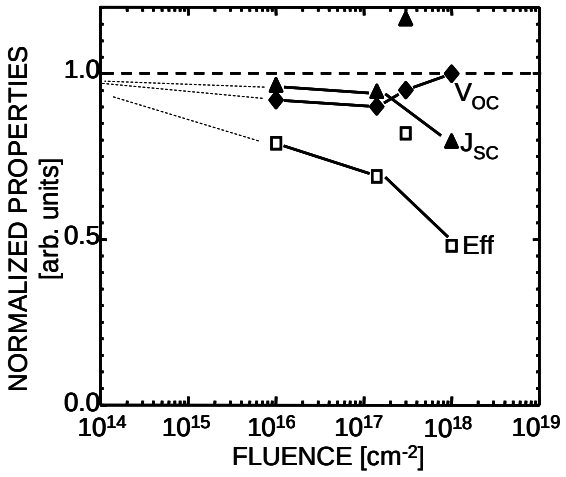

Fig.1. Normalized performance parameters of the irradiated CIGS solar cell.

P7-18

Sulfurization growth of SnS thin films and optimization of pn-junction of SnS-related solar cells

M. Sugiyama[1], Y. Murata[1], T. Shimizu[1], N. Revathi[2] , C. Venkataiah[2] ,
K. Yoshida[1], T. Sato[1], and K. T. R. Reddy[2]

[1] Department of Electrical Engineering, Tokyo University of Science, 2641 Yamazaki, Noda 278-8510, Japan
[2] Department of Physics, Sri Venkateswara University, Tirupati-517502, India

Presenting author optoelec@rs.noda.tus.ac.jp, phone/ fax number +81-4-7121-1585 (M. Sugiyama)

Binary IV-chalcogenide orthorhombic semiconductor tin sulfide (SnS) has a direct energy band gap of 1.3 eV with a high absorption coefficient and involves elements that are more abundant, economic and safe to handle. These properties made SnS as a promising candidate for light absorption in the development of next generation solar cells. SnS films have been deposited by different physical and chemical methods. Sulfurization of metal precursors has many advantages in the fabrication of solar cells as it is a simple and dry process that can be scaled up for large area deposition.

Investigation on the band discontinuities is important for device design and development as these band offsets determine the junction transport and other interface related properties. SnS is one of the potential materials for solar cell application and the reported data on SnS related junctions is very meager. In this work, the growth of SnS films by sulfurization of 'Sn' layers deposited by sputtering and evaporation. The precursors were sulfurized at different temperatures and times, and the structural characterization of the synthesized layers was carried out. Moreover, the band discontinuities of a typical SnS-based solar cell with the configuration, glass/SnO_2/SnS/CdS/ZnO will be presented.

Sputtered 'Sn' precursors sulfurized at 330 °C, for time periods < 60 min indicated various phases of Sn and S that led to the development of SnS at a sulfurization time of 90 min. However, evaporated 'Sn' precursors needed lower sulfurization times of 20 - 30 min to develop SnS phase. Longer sulfurization times made the layers to be 'S' rich. The X-ray diffraction data indicated that the orientation and density of 'Sn' precursor is crucial in developing SnS films by sulfurization. These results were analyzed to identify the different phases present in SnS layers synthesized using both evaporated and sputtered precursors in order to evaluate the possible growth mechanism.

The valence band offsets were determined to be approximately 1.5 eV for SnS/CdS and 3.5 eV for SnO_2/SnS interfaces by using the X-ray Photoelectron Spectroscopy (XPS). Using these values and the energy band gaps of the corresponding layers, the energy band diagram was developed and considered to be TYPE-II form of the heterostructure. The Fermi level was found to be much closer to the valence band maximum for SnS while it was present in the upper half of the band gap for both CdS and SnO_2. The qualitative behavior of the junction in relation to the band offsets will be reported and discussed.

Acknowledgments: This work was supported in part by the Advanced Device Laboratories, Research Institute for Science and Technology, Tokyo University of Science.

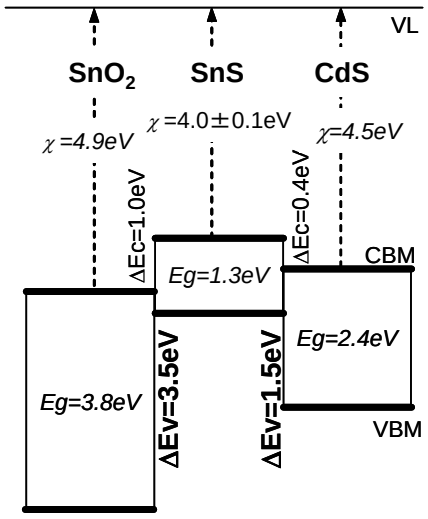

Fig. 1. Band diagram of SnS/CdS heterojunction

P7-19

Comparison of the valence band structure peculiarities in the $Bi_{1-0.84}$-$Sb_{0.16}$-$Sn_{0.01}$ and pure semiconducting $Bi_{1-x}Sb_x$ alloys

Bakir Tairov[1] and Eltaj Yuzbashov[1]

[1] Institute of Physics of Azerbaijan National Academy of Sciences, H.Javid pr., 33, Baku, AZ 1143, Azerbaijan ; btairov@physics.ab.az, 994-12-439-7211

The investigation of Bi-Sb alloys has a great importance both theoretically and practically. Due to high mobility of the charge carriers the semiconducting alloys are one of the best materials for thermoelectric and galvanomagnetic devices. Complexity of the band structure, easily reconstruction of the band structure by small variation of Sb concentration, temperature, pressure resulting in transition between semimetallic, gapless, semiconducting states and other peculiarities of these alloys are of great value to theoretical investigations too. That is why these materials are still being investigated as bulk materials, thin films and nanoscale structures [1,4].

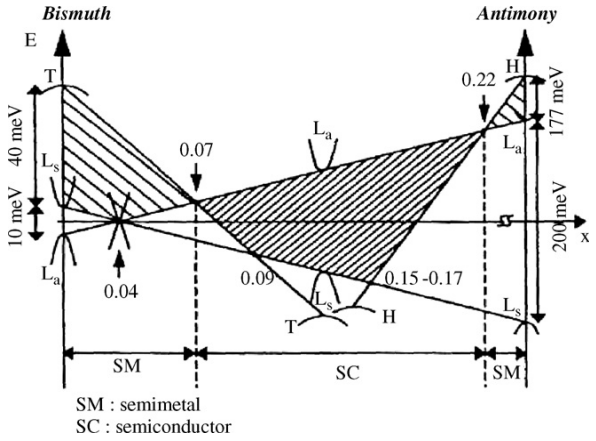

Fig. 1. Band diagram of $Bi_{1-x}Sb_x$ alloys as a function of x at T=0K.

In the present work specific electrical resistance, Hall coefficient, and low magnetic field magnetoresistance tensor components have been measured in n-$Bi_{1-x}Sb_x$ single crystals ($0.16 \le x \le 0.25$) and in $Bi_{1-0.84}$-$Sb_{0.16}$-$Sn_{0.01}$ at the temperature range of 77-300 K. On the basis of these measurements, calculations of the kinetic parameters of charge carriers for the $Bi_{1-x}Sb_x$ were conducted by using 9 formulas connecting kinetic and energetic band parameters with independent coefficients of the low field galvanomagnetic tensor. As it is seen from Fig.1 for semiconducting $Bi_{1-x}Sb_x$ ($0.16 \le x \le 0.25$) alloys there is a region, where all hole valleys (T, H and L_s) may contribute to the transport phenomena. Calculations of kinetic parameters (N, P, – concentration of electrons and holes, respectively; μ_i , ν_i – mobilities of electrons and holes, respectively) for these undoped semiconducting alloys were carried out by using many ellipsoidal model for Fermi surface of corresponding charge carriers. Particularly the following results concerning hole ellipsoid parameters have been obtained at nitrogen temperatures: ν_2/ν_1=0.05, ν_3/ν_1=0.5. But these parameters for a hole ellipsoid don't correspond to any of the L, T, H ellipsoids. To clarify this situation, analogical calculations were performed for $Bi_{1-0.84}$-$Sb_{0.16}$-$Sn_{0.01}$, where Fermi level lies below conduction band extremum and we deal solely with valence band extremes. The obtained results for the previously mentioned hole mobility ratios within experimental errors were the same. It is shown that the hole ellipsoids corresponding to the obtained results less anisotropic in comparison with L-hole ellipsoids, where ν_2/ν_1=0.009, ν_3/ν_1=0.7 and their slope is significantly larger than and L-hole (and L-electron) ones.

Such behavior of hole charge carriers may be explained either by assuming existence of a new type of hole ellipsoids located in some point of the Brioullin band or by introducing an effecttive hole ellipsoid combined from all contributions of lighthole L band and heavyhole T&H bands. The final decision about the peculiarities of the valence band requires the knowledge of the precious values of effective masses of the carriers (their temperature dependence too) in all the three bands under consideration, and the temperature dependence of the band gap and consideration of scattering mechanisms of current carriers in Bi–Sb alloys.

[1]. S. Dutta, V. Shubhaa and T.G. Ramesha, *Physica B: Condensed Matter*, **v.405,** N**o 5**, (2010), p.1239.
[2]. J. Heremans, D. L. Parlin, and et.al. *Physical Review B*, **v.48**, No 15, (1993), p. 11329.
[3]. D.Choi. A.Balandin, and et.al. Appl. Phys. Lett. 89, (2006), p.1415.
[4]. S.Dutta, V. Shubha, T.G. Ramesh, Florita D'Sa. *Journal of Alloys and Compounds,* **467,** (2009), p. 305.

P7-20

Intermediate structural phase of Sm-substituted $BiFeO_3$: multiferroic properties

V.A. Khomchenko[1], J.A. Paixão[1], B.F.O. Costa[1], I.O. Troyanchuk[2], D.V. Karpinsky[3] and A.L. Kholkin[3]

[1] CEMDRX/ Department of Physics, University of Coimbra, 3004-516 Coimbra, Portugal
[2] SSPA "Scientific-Practical Materials Research Centre of NAS of Belarus", P. Brovka str. 19, 220072 Minsk, Belarus
[3] CICECO/ Department of Ceramics and Glass Engineering, University of Aveiro, 3810-193 Aveiro, Portugal

E-mail address: uladzimir@fis.uc.pt, phone: +351-239410637, fax: +351-239829158

In recent years, there has been a revival of interest in developing multiferroic materials possessing ferroelectric polarization and magnetic ordering in the same phase [1]. Coupling between the corresponding order parameters gives rise to a magnetoelectric effect, which might be used in technological applications [2]. However, single phase magnetic ferroelectrics with a large polarization and magnetization coexisted near room temperature have hitherto not been identified. The scarcity of the materials results from the contradiction between the conventional mechanism for cation off-centering in ferroelectrics and the formation of magnetic order (so called "d^0 vs. d^n problem") [1]. Accordingly, to combine ferroelectricity and magnetism in a single phase, the atoms that move off centre to form an electric dipole moment should be different from those that carry a magnetic moment. This approach is realized in case of the multiferroic perovskite $BiFeO_3$ [2], which is known as a unique material possessing spontaneous polarization and magnetic ordering at room temperature. Taking into account that the crystal structure of bismuth ferrite cannot accommodate any other transition metal ions in an amount sufficient to compete with the dominant antiferromagnetic superexchange interactions Fe^{3+}-O-Fe^{3+}, Bi substitution by magnetically-active rare-earth ions (which suppress the spiral spin modulation to give rise to weak ferromagnetism and whose magnetic moments contribute to the resulting magnetization through the *f-d* exchange coupling) has been considered as an effective way to improve multiferroic properties of the parent compound [3].

An overview of the crystal chemistry of lanthanum and rare-earth substituted $BiFeO_3$ was presented in recent article of *Karimi et al.* [4]. The authors proposed the preliminary phase diagrams of the $Bi_{1-x}Ln_xFeO_3$ (Ln= La, Nd, Sm, Gd) systems. One of the most interesting findings of the work was the discovery of the intermediate structural form, existing between the polar *R3c* and the nonpolar *Pnma* phases, characteristic of the end members of the series $(BiFeO_3)_{1-x}$-$(LnFeO_3)_x$. The intermediate form tends to coexist with the $BiFeO_3$-type and $LnFeO_3$-type structures, becoming dominant only in a very narrow concentrational range near x~ 0.15 (for Nd and Sm-doped systems). The phase was claimed to have a structure closely related to that characteristic of antiferroelectric perovskite $PbZrO_3$ (space group *Pbam*). In order to investigate multiferroic properties of this phase, we carried out solid-state synthesis and X-ray diffraction, piezoresponse force microscopy (PFM), SQUID-magnetometry, and Mössbauer spectroscopy measurements of $Bi_{0.85}Sm_{0.15}FeO_3$ samples. In contrast to macroscopic ferroelectric investigations demonstrating the behavior typical of antiferroelectrics, PFM measurements revealed some features characteristic of ferroelectric materials. It was found that Sm substitution suppressed the spiral spin modulation peculiar to pure $BiFeO_3$ to give rise to the appearance of a weak ferromagnetic moment. The results are important for understanding the evolution of crystal structure and physical properties of $BiFeO_3$ upon Sm substitution and constructing the phase diagram of $Bi_{1-x}Sm_xFeO_3$ multiferroics.

[1]. D. Khomskii, *Physics* **2** (2009), p. 20.
[2]. G. Catalan and J.F. Scott, *Adv. Mater.* **21** (2009), p. 2463.
[3]. V.A. Khomchenko, V.V. Shvartsman, P. Borisov, W. Kleemann, D.A. Kiselev, I.K. Bdikin, J.M. Vieira and A.L. Kholkin, *Acta Mater.* **57** (2009), p. 5137.
[4]. S. Karimi, I. M. Reaney, Y. Han, J. Pokorny and I. Sterianou, *J. Mater. Sci.* **44** (2009), p. 5102.

P7-21

Studies on $ZnIn_2Se_4$ nano crystallites synthesized by chemical precipitation

P. Babu[1], N. Revathi[1], T.Sato[2], M. Sugiyama[2] and K.T. Ramakrishna Reddy[1a]

[1]Thin Film Laboratory, Department of Physics, Sri Venkateswara University, Tirupati – 517 502, India.
[2]Department of Electrical Engineering, Tokyo University of Sciences, Noda, Japan.

[1a]Corresponding author: Email: ktrkreddy@rediffmail.com Tel: +918772289472; Fax: +91 877 2289555

Recently, much interest has been paid in the preparation and characterization of ternary semiconductors due to its potential applications in various fields [1-3]. $ZnIn_2Se_4$ (ZIS) is one among them that belongs to the $A^{II}B_2^{III}X_4^{IV}$ defect chalcopyrite family. $ZnIn_2Se_4$ (ZIS) has been used as a buffer layer in the fabrication of $CuInGaSe_2$ based solar cells [4, 5]. In the present work, nano-crystalline powders of ZIS have been synthesized by simple and economic chemical precipitation method at different reaction temperatures (T_R) that vary in the range, 60 – 100 ^oC for a fixed reaction time of 60 min. The chemical and physical properties of the synthesized powders were analyzed using appropriate techniques. The XRD analysis revealed that the synthesized powders were nanocrystalline and showed (112) plane as the preferred orientation. The grain size of the powder samples were varied in the range, 10 - 25 nm. SEM micrographs revealed that the samples had a cauliflower like structure. The optical transmittance of these samples was found to be >70% in the visible region and the evaluated energy band gap was 2.85 eV for the powder synthesized at a reaction temperature of 100 ^oC. The detailed study of these results were presented and discussed.

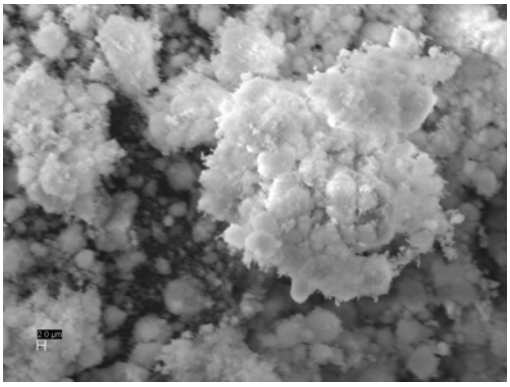

Figure 1. SEM micrograph of bulk ZIS synthesized at T_R = 100 ^oC.

[1]. I.M. Dharmadasa, R.P. Burton, M. Simmonds, Sol. Energy Mater. Sol. Cells, 90 (2006) 2191.
[2]. V.M. Nikale, N.S. Gaikwad, K.Y. Rajpure, C.H. Bhosale, Mater. Chem. Phys., 78 (2002) 363.
[3]. V.L. Mathe, K.Y. rajpure, C.H. Bhosale, Bull. Mater. Sci., 22 (1999) 927.
[4]. J. Luenga, N. V. Joshi, Material Latters, 47 (1996) 26.
[5]. E Fortin and F.Raga, Solid State Commun., 847 (1974) 14.

P7-22

Preparation and properties of co-evaporated Cu_4SnS_4 layers.

V.P. Geethavani[1], N. Revathi[1], T. Sato[2], M.Sugiyama[2] and K.T. Ramakrishna Reddy[1a]

[1]Thin Film Laboratory, Department of Physics, Sri Venkateswara University, Tirupati – 517 502, India
[2]Department of Electrical Engineering, Tokyo University of Sciences, Noda, Japan.
[1a]Corresponding author: Email: ktrkreddy@gmail.com, Tel: +918772289472; Fax: +91 877 2289555,

The ternary chalcopyrite semiconductors, particularly the Cu-III-VI_2 compounds are the most potential absorber materials for heterojunction solar cell application in terms of conversion efficiency and long-term stability. Among the various combinations of ternary as well as quaternary compounds, $CuInSe_2$ and $CuInGaSe_2$ proved to be the successful absorbers and electrical conversion efficiencies higher than 16 % and 19.2 % [1, 2] at the laboratory level have been respectively obtained on these materials. However these materials involve In and Ga, which are less abundant and costly. In recent years new and novel alternative materials that offer low cost and better photovoltaic properties have been suggested. Copper tin sulfide (Cu_4SnS_4) is one such material that has been used as an absorber layer for solar photovoltaic application due to its optimum physical properties [3]. In this study, we have prepared Cu_4SnS_4 thin films by co-evaporation technique on Corning 7059 glass substrates at different substrate temperatures (T_s) that varied in the range, 200 - 350^{o}C. The effect of substrate temperature on composition, structure, morphology and optical properties of the as-grown Cu_4SnS_4 films has been studied. All the layers exhibited orthorhombic crystal structure with the (121) crystal plane as the preferred orientation. The evaluated grain size of the films varied from 18 nm to 37 nm. The films were highly absorbing with the absorption coefficient > 10^5 cm^{-1}. The layers prepared at a substrate temperature of 300 ^{o}C showed an optical energy band gap of 1.9 eV. The details of physical properties were reported and discussed.

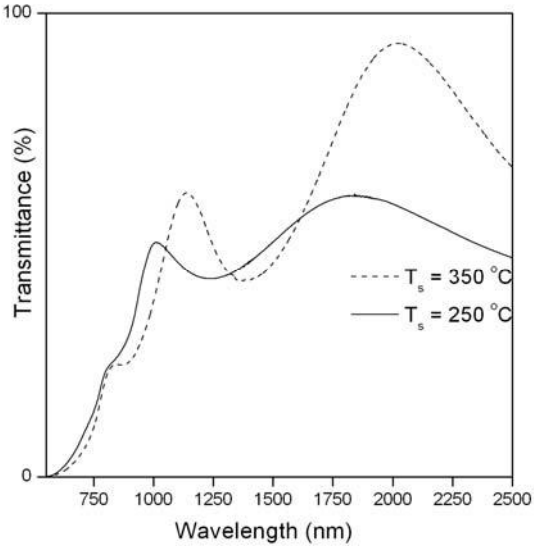

Figure 1: Transmission versus wavelength spectra of Cu_4SnS_4 films.

[1]. D. Braunger, D. Hatiskos, T. Walter, H.W. Schoock, Sol. Energy Mater. Sol. Cells, 40 (1996) 97.
[2]. I. Repins, M.A. Contreras, B. Egaas, C. Dehart, J. Scharf, C.L. Perkins, B. To, R. Noufi, Prog. Photovoltaic.: Res. Appl., 16 (2008) 235.
[3]. A. Kassim, S.Nagalingam, T. W. Tee, A.M. Sharif, D. K. Abdullah, Md. J. Elas and H. S. Min, Philippine Journal of Science 138(2009) p.161.

P7-23
Preparation of $Cu(In,Ga)Se_2$ thin films with Ga content of around 0.8 and their solar cell application

Toshiyuki Yamaguchi[1], Yasutaka Asai[1] and Tooru Tanaka[2]

[1] Wakayama National College of Technology, 77 Noshima, Nada-cho, Gobo-shi 644-0023, Japan
[2] Saga University, 1 Honjo, Saga-shi 840-8502, Japan

yamaguchi@wakayama-nct.ac.jp, +81-738-29-8367/+81-738-29-8216

$Cu(In,Ga)Se_2$ thin films are promising candidates as absorber layers of single- and multi-junction solar cells. Conversion efficiencies for $Cu(In,Ga)Se_2$ based solar cells with Ga/(In+Ga) ratio of around 0.3 have been significantly improved using three-stage process from elemental Cu, In, Ga and Se sources [1]. The conversion efficiencies of $Cu(In,Ga)Se_2$ thin film solar cells decreased with increasing a Ga/(In+Ga) mole ratio above 0.3 [2]. We have reported the process using a vacuum deposition apparatus with three evaporation boats which was the sequential evaporation technology from $CuGaSe_2$ and $CuInSe_2$ ternary compounds [3]. In this study, we have fabricated $Cu(In,Ga)Se_2$ thin films with high Ga/(In+Ga) mole ratio and their solar cells by sequential evaporation process and their properties have been investigated.

Our sequential evaporation process consisted of three steps. In the first step, Cu-In-Ga-Se layer was evaporated from $CuInSe_2$ and $CuGaSe_2$ compounds onto the Mo/soda-lime glass substrate. In this study, the $CuGaSe_2/(CuGaSe_2+CuInSe_2)$ mole ratio of 0.8 was used for fabrication of $Cu(In,Ga)Se_2$ thin films with a high Ga content. In the second step, In-Ga-Se layer was deposited from In_2Se_3 and Ga_2Se_3 compounds at 490°C. The $Ga_2Se_3/(In_2Se_3+Ga_2Se_3)$ mole ratio was varied from 0 to 0.8 in this experiment. Finally, only Se was effused at the same substrate temperature. We fabricated the solar cells with a configuration of ZnO:Al/i-ZnO/CdS/$Cu(In,Ga)Se_2$/Mo/SLG substrate.

The Ga/(In+Ga) mole ratio in the thin films was within the range from 0.83 to 0.92. XRD studies showed that the prepared thin films had a chalcopyrite $Cu(In,Ga)Se_2$ structure. The best solar cell using $Cu(In,Ga)Se_2$ thin film prepared at $Ga_2Se_3/(In_2Se_3+Ga_2Se_3)=0.8$ demonstrated V_{oc}=550mV, I_{sc}=23.8mA/cm^2, FF=0.55 and efficiency=7.25% without AR-coating.

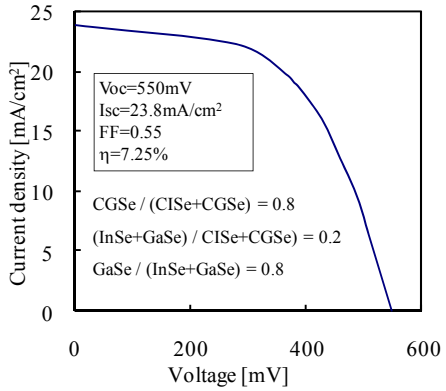

Figure 1. I-V characteristics of $Cu(In,Ga)Se_2$ thin film solar cell prepared at $Ga_2Se_3/(In_2Se_3+Ga_2Se_3)$ =0.8.

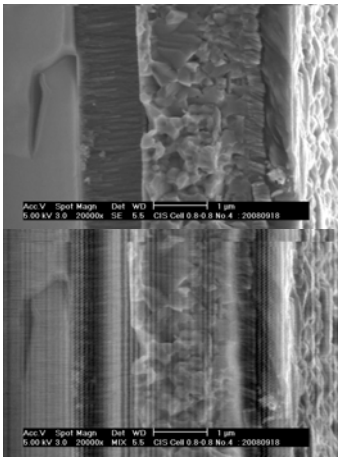

Figure 2. SEM image and EBIC signal of $Cu(In,Ga)Se_2$ thin film solar cell.

Acknowledgments: This study was supported in part by a Grant-in-Aid for Scientific Research from the Ministry of Education, Culture, Sports, Science and Technology in Japan.

[1]. I. Repins, M. A. Contreras, B. Egaas, C. DeHart, J. Scharf, C.L. Perkins, B. To and R. Noufi: Prog. Photovolt. Res. Appl. 16 (2008), p.235.
[2]. M. A. Contreras, K. Ramanathan, J. AbuShama, F. Hasoon, D. L. Young, B. Egaas and R. Noufi: Prog. Photovolt. Res. Appl. 13 (2005), p.209.
[3]. T. Yamaguchi, M. Naka, S. Niiyama and T. Imanishi: J. Physics and Chemistry of Solids 66 (2005) Issue 11, p.2000.

P7-24

Photoelectric properties of Ox/$Cd_{1-x}Mn_xTe$ heterostructures

R.Yu.Petrus'[1], V.Yu.Rud'[2], Yu.V.Rud'G.A.Il'chuk[1], V.V.Kusnezh[1],

Ioffe Physicotechnical Institute, Russia Academy of Sciences, 194021 St.Petersburg, Russia
[1] National University „L'vivska Politekhnika", 79013, L'viv, Ukraine
[2] St. Petersburg State Polytechnic University, 195251, St. Petersburg, Russia

petrus@polynet.lviv.ua, phone: +38 (032) 258-23-42

The Ox/$Cd_{1-x}Mn_xTe$ photosensitive heterojunctions with rectifying properties were fabricated by a thermal treatment of $Cd_{1-x}Mn_xTe$ solid solutions crystals in air conditions. The plane-parallel single crystal wafer, ~2 mm thick with mirror-smooth surface prepared by cleaving from middle part of bulk ingot, were used for thermal treatment. The ohmic contacts were fabricated by indium soldering of thin wire (Pt or Ag, diameter ~20 μm) to self oxide (Ox) films, while to free surface of $Cd_{1-x}Mn_xTe$ by deposition of Au film. Measurement of stationary current-voltage characteristics confirms fabrication of rectifying heterostructures by $Cd_{1-x}Mn_xTe$ wafer thermal treatment at chosen conditions for composition range x=0÷0.6 of $Cd_{1-x}Mn_xTe$ solid solution. The conducting directions correspond to negative polarity of external bias on Ox film. The photovoltaic effect was observed in Ox/$Cd_{1-x}Mn_xTe$ heterostructures under illumination from side of oxide film. In all fabricated structures the Ox film was negatively charged. In best structures the U_{oc}=0.2 V, $I_{sc}=5\cdot10^{-6}$ A and volt sensitivity 30 V/W at T=300 K was reached. Spectra of relative quantum efficiency dependences η(ħω) for two hetorostructures fabricated on $Cd_{1-x}Mn_xTe$ single crystal wafers with different composition were investigated, **Figure. 1.** It can be seen that with x increase the maximum of η(ħω) curve is shifting to short wave region of spectra. The long wave edge of relative quantum efficiency curve can be approximated by line in $(\eta\hbar\omega)^2=f(\hbar\omega)$ coordinates, **Figure. 1. b**. This indicate [1, 2] direct optical band transitions for structures with compositions x=0.4 (curve 1) and x = 0.6 (curve 2). The energy of direct band transitions E_g=1.47 and 2.2 eV at T = 300 K for solid solution compositions x = 0.4 and 0.6 was calculated from the $(\eta\hbar\omega)^2\rightarrow0$ extrapolation.

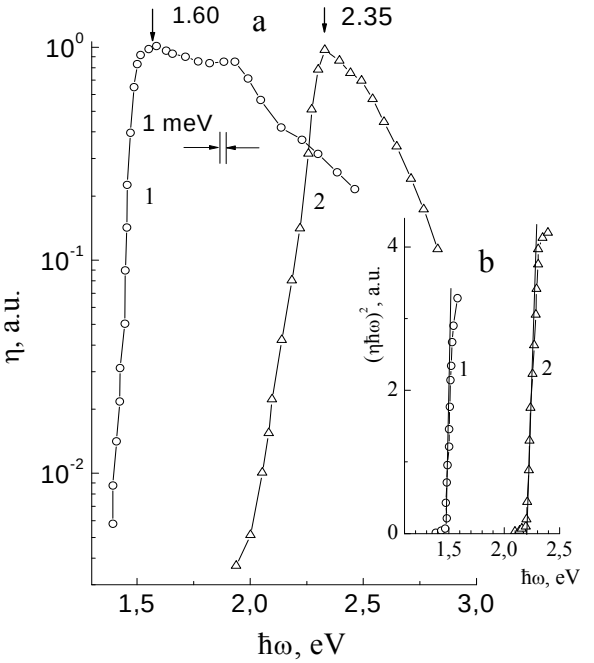

Figure. 1. The relative quantum efficiency of photoconversion η(ħω) – a and $(\eta\hbar\omega)^2=f(\hbar\omega)$ – b of Ox/$Cd_{1-x}Mn_xTe$ (x=0.4 – 1, x=0.6 – 2) structures.

The obtained material allows to make the conclusion about possibility of application of Ox/$Cd_{1-x}Mn_xTe$ heterostructure, created by the method of surface oxidization, as new generation of sensors with photosensitivity to external magnetic fields.

[1]. C.M. Sze. Physics of semiconductor devices (John Wiley and Sons, New York, London, Sydney, Toronto, 1969).
[2]. Jacques I. Pankove. Optical processes in semiconductors (Courier Dover Publications, 1975).

P7-25

The phonons scattering mechanisms in $Ga_xIn_{1-x}As$ solid solutions

M.I.Aliyev, I.X.Mammadov[1], D.H.Arasly, R.N.Rahimov, A.A.Khalilova

Institute of Physics of the Azerbaijan National Academy of Sciences,
33 H.Javid, Az-1143, Baku, Azerbaijan
E-mail: rashad@physics.ab.az ; phone: +(99412)4393315; Fax: +(99412) 447 04 56;

[1]National Academy of Aviation, Bina, Baku, Azerbaijan

In the present work the thermal conductivity of InAs-rich ($0 \le x \le 0.08$) and GaAs-rich ($0.97 \le x \le 1$) $In_{1-x}Ga_xAs$ single solid solutions in the temperature range between of 80 and 300K has been investigated. The samples were prepared by the Czochralski method and had the identical charge carrier concentration of $2\text{-}4 \times 10^{17} cm^{-3}$ and the dislocation density of $10^3 \div 10^4$ cm^{-2}. The thermal conductivity was measured by the absolute stationary method.

The thermal conductivity of $In_{1-x}Ga_xAs$ single solid solutions decreases depending on the second component, and its temperature dependence in the range 80 to 300K weakens. In the temperature dependence of the thermal conductivity the obvious dip within the narrow interval of 95 to115K is observed for InAs-rich single solid solution up to x=0.04, which disappears with x>0,04. The dip in the rich- GaAS single solid solution in the dependence K(T) was not observed.

The experimental results of thermal conductivity as a function of temperature and the alloy composition have been analyzed on the base of the various theoretical models [1-5]. It is obtained that the intensity of normal phonon- phonon scattering processes (N- process) is greater than umklapp processes (U- processes) and they jointly with U- processes play more essential role in phonon scattering in the lattice thermal conductivity of the $In_{1-x}Ga_xAs$ solid solutions. It has been established that the Herring processes - interactions of different polarized phonons - are dominated in the three-phonon N- processes.

The temperature dependence of the thermal conductivity is analyzed in the framework of the Callaway relaxation model [1] and Holland [6] approximation for the phonon spectrum with allowance for phonon–phonon scattering processes and Rayleigh scattering by point defects, vacancies and complexes regarding to the local change of density and elastic properties of crystals. Intensities of all these processes have been determined.

The analyze of the temperature dependence of phonon thermal conductivity within the framework of the Holland's two-parametric approximation showed that the contribution of transverse acoustic phonons in K(T) at temperatures higher than 200K is main.

The revealed dip in the temperature dependence of the thermal conductivity was explained by the phonon resonance scattering by localized acoustic mode produced by impurities.

To describe the anomaly in the dependence K(T) the relaxation time of phonon resonance scattering was included in the complex relaxation times. The frequency of the phonons resonance scattering has been determined. It is assumed that the centers of the phonons resonance scattering can be complexes, connected with the nonequivalence of the neighboring environment of atoms in the crystal lattice.

[1]. J.Callaway and H.C.von Bayer, *Phys.Rev.* 1960, **120,** 1149.
[2]. F.Szmulowicz, F.L.Madarasz, P.G.Klemens, J.Diller, *J.Appl.Phys.* 1989, **66**, (1) p252.
[3]. B.Abeles *Phys.Rev.* 1963, **131,** 1906.
[4]. S.Adachi, *J.Appl.Phys*. 2007, **102**, p063502(1 -7).
[5]. S. Adachi, *Physical Properties of III-V Semiconductor compounds.* Wiley-Interscience, New York, 1992, 296p.
[6]. M.G.Holland, *Phys.Rev*., **134 (**1964) 2, A471-480.

P7-26

Deep centers in single crystals $(TlGaS_2)_{1-x}(TlInSe_2)_x$

E.M. Kerimova, F.I. Ismayilov, S.S. Abdinbekov, A.B. Magerramov, P.Y. Ismayilova,
X. Sh. Valibayov, N.A. Aliyeva, A.A. Isayeva

Institute of Physics, Azerbaijan National Academy of Sciences, Az-1143, Baku, Azerbaijan
e-mail: ekerimova@physics.ab.az, tel. +99412 4395913

A^3B^6 –typed single crystals of semiconductive compounds and solid solutions on their base are promising materials for creating various functional elements of micro-and optoelectronics. In particular single crystals $(TlGaS_2)_{1-x}(TlInSe_2)_x$ have already found use as good-quality materials to produce quick-response photodetectors (PD) of near infrared band of spectrum. Besides investigation of influence of solid state composition continious substitution on their photoelectric properties can give valuable information on the nature and spectrum of energy levels localized in band gap of semiconductor under investigation, also the mechanism of recombination processes in them.

In given paper with the aim of revealing pecularities and clearing up the mechanism of recombination processes dependence in deep centers in single crystals$(TlGaS_2)_{1-x}(TlInSe_2)_x$ on the composition of double substitution there have been studied basic characteristics of dark, photo-and thermostimulated conduction (TSC) at different values x, too.

Single crystals $(TlGaS_2)_{1-x}(TlInSe_2)_x$ of composition x=0÷0.1 have been synthesized in graphitizated quartz ampoules then they have been grown by Bridgemen-Stochbarger modified method. They appear to be rather high-ohmic and photosensitive (at T 77K specific dark resistance is $10^7 \div 10^8$ Ohm/cm).Current contacts have been created by sealing metal indium out of doors and are ohmic ones under all investigated conditions.

There have been investigated distinctive curves of PD spectral characteristics of single crystals $(TlGaS_2)_{1-x}(TlInSe_2)_x$. To find out intrinsic and impurity photoconductivities appears to make this spectrum rather wide-band. With increase of double substation content in single crystal composition long - wave boundary of photoconductivity shifts to the side of relatively low energies (to the side of long waves). It is expected that the change of photoconductivity spectrum maximum position with increase of x in $(TlGaS_2)_{1-x}(TlInSe_2)_x$ is due to the change of their band gap but obtained impurity photoconductivity is related to the presence of sensitivity r-centers in band gap of discussed films. Both assumptions are well in agreement with reference data. At rather low temperatures in photoconductivity spectrum there has been prevailed maximum related to intrinsic photoconductivity. At lower temperatures within the maximum display the thermal activation of photoconductivity has been observed. In doing so with light intensity growth activation ratio has been decreased but dependence extremum $Y_p(T)$ shifts to the side of higher temperatures.

In samples under investigation at T 300K and higher temperatures there has been observed thermal etching of photoconductivity. In TSC curves T=200-250K which maximum with the second component content increase shifts to the side of relatively low temperatures.

With the increase of incident light intensity on the sample also illumination duration and heating rate TSC peak amplitude has been increased, and its maximum shifts to the side of relatively higher temperatures. Energy depth of occurring trapping centers defined by Bube method in single crystals $(TlGaS_2)_{1-x}(TlInSe_2)_x$ is 0.27-0.30eV depending on the composition.

Temperature dependence of photocurrent indicates that it is related to recombination and thermal exchange of trapping a-centers with conduction band. At heating concentration of captured charge carriers decreases but free nonequilibrium ones increases.

Optic recharging between a-and r-centers ensuring within low temperatures (T=80-140K) strong emptiness of photoconduction centers reduces sharply the efficiency of recombination through them. There has been started prevailing hole recombination through another channel (S).

As a result impurity photoeffect disappears and intrinsic photoconductivity prevails. Photocurrent decrease at T≥300K can be explained by decrease of recombination flow passing through r-centers.

SECTION EIGHT

Misscellaneous

P8-1

Conversion of the chemical energy into the electric energy on the surface of semiconductor – catalyst

A.M.Pashayev, M.A.Talibi, G.A.Mamedova

Institute of Physics, Azerbaijan National Academy of Sciences,
H.Javid av., 33, AZ1143, Baku, Azerbaijan

magulnar@mail.ru, +994 50 348 31 87

In the selenium heterojunctions under the action of the expiratory air low the phenomenon of the advent of the short-circuit current is found. In the regime of diod, if to the p-n junction even few inverse voltage up to 1V was impressed, the short-circuit current will rise 10 times in comparison with the regime when the external condition is equal to zero $U_{inv.}= 0$. Rise of the short-circuit current occurs proportionally to the inverse voltage. With enough load resistance R in the external circuit the voltage drop across the load IR serves as the recording working signal. In the regime of diod, with rise of the inverse voltage the current across the load and respectively the voltage drop across the load rise 100 times in comparison with condition when the external voltage is equal to zero. In order to find out the nature of the current and procedural mechanisms leading to generation of the current, the special experiments were carried out. It was found out that that is the analogue of photo effect on p-n junction. The short-circuit current is generated by the non-equilibrium electron-hole pairs. The last mentioned are generated on the surface of the semiconductor under the effect of the flow at a distance of the length of diffuse shift from the p-n junction. Energy for generation of electrons develops across as a result of chemical heterogenetic radicalo-recombinational exothermic reactions without destruction of the semiconductor-catalyst. By this means in the result of the direct conversion of the chemical energy into the electric energy in the selenium heterojunctions under the action of the expiratory air low in the diod regime, the effect of strengthening of the recording working signal is observed. Thus the latter was an electronic enhancer managed by the external signal.

This provides an opportunity for creation of indicators of new type for registration of molecule flow with small intensiveness. The effect discovered is called effect of Pashayev-Talibi-Mamedova.

P8-2

Effects of cathode microstructure on the Performance of electrolyte supported solid oxide fuel cells

Mahmut D. Mat[1], Yüksel Kaplan[1], Beycan İbrahimoğlu[2]

[1] *Nigde University, Mechanical Engineering Department, Nigde, Turkiye*
[2]*Gazi University, Mechanical Engineering Department, Ankara, Turkiye*

ykaplan@nigde.edu.tr

In this study, effects of particle size at cathode functional and current collector layers, sintering temperature and cathode thickness on the performance of electrolyte supported solid oxide fuel cell are experimentally investigated. A mixture of LSF40 and ScSZ is used as cathode materials for the functional layer and LSF40 for the current collecting layer. The particle size is controlled by calcination temperature and the effect of calcination temperature is investigated in a temperature range of 600-800°C. The sintering temperature is also varied between 900-1200°C. It is found that the microstructure and thickness of cathode functional layer is a major factor affecting the performance of an electrolyte supported SOFC. By optimizing the cathode microstructure it is shown that the performance of the SOFC increased from 0.425 W/cm^2 to 0.706 W/cm^2.

P8-3

High performance anode supported solid oxide fuel cells by ion conductor phase impregnation

Mahmut D. Mat[1], Yüksel Kaplan[1], Beycan İbrahimoğlu[2]

[1] *Nigde University, Mechanical Engineering Department, Nigde, Turkiye*
[2] *Gazi University, Mechanical Engineering Department, Ankara, Turkiye*

ykaplan@nigde.edu.tr

A high performance anode supported solid oxide fuel cell (SOFC) is developed by low-cost tape casting, co-sintering and nano-ion conductor infiltration techniques. The mixture of gadolinium and cerium nitrate solution is infiltrated into both anode and cathode layers and fired at a temperature that gadolinium nitrate and cerium nitrate undergoes a solid state reaction and forms nano ion conductor phase in both electrodes. The effect of molar concentrations and firing temperature of nano ion conductor phase on the cell performance are investigated. The measurements show that nano-sized ion conductor infiltration significantly improves the cell performance. The cell provides 1.718Wcm^{-2} maximum power density at an operation temperature of 750°C. The high performance is attributed to increase in the oxide ion conductivity and three phase boundaries of both anode and cathode layers by nano ion-conductor infiltration.

P7-4

Plasma application in fuel cells and hydrogen technologies

[1]Beycan Ibrahimoglu, [2]Ibrahim Ibrahimoglu, [3]Sadig Kuliyev

1-Gazi university,Faculty of Engineering 06570 Maltepe,Ankara/Turkey
2- Anadolu Plasma Teknolojileri Merkezi ,Gazi Ünversitesi Gölbaşı Yerleşkesi Teknoplaza Binası A-B Blok Geçişi 1.Kat N0 G103-G104 Gölbaşı/Ankara /Turkey
3- Vestel Defence Industry Tashpinar Mah.Serpmeleri Kume Evleri N0:87/1-2 06830 Gölbashi-Ankara/Turkey
i.ibrahimoglu@gmail.com +90312 484 79 +90312 484 79 34

Plasma Technologies are widely used in different branches of modern industry. Among these applications, low-calorie coal processing, conversion of various organic fuels to hydrogen–reach fuel and electrochemical electrolysis of water by plasma are more popular.
Nowadays, solid oxide fuel cell (SOFC) system is one of the usage area of plasma technology. SOFC is generally active at high temperature -650-1000 ^{0}C. So corrosion problems of current collector materials, contact problems between ceramic membrane and current collectors and leakage problems can be solved by plasma application.
One of the biggest problems of SOFC is the activation of cathode reaction. The present study deals with plasma application for the fuel preparation, the cathode reactions and the solid oxide ceramic membrane.

AUTHORS INDEX

Arif PASHAYEV

Nazim MAMEDOV

Chingiz QAJAR

Oktay ALEKPEROV

Katsuaki SATO

Kazuki WAKITA

Elena ROGACHEVA

Daniel LINCOT

Ayaz BAYRAMOV

Emil HUSEYNOV

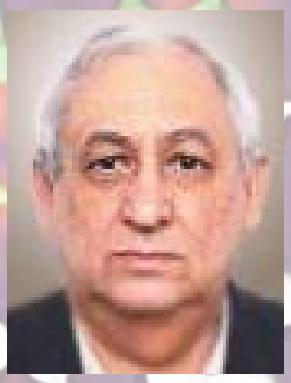

Tofig MAMMADOV

Talat MEHDIYEV

Eldar MAMMADOV

Ismail YUSIFOV

www.science.gov.az/physics